U.PORTO

FEUP FACULDADE DE ENGENHARIA
UNIVERSIDADE DO PORTO

INTEGRATED MASTER IN ENVIRONMENTAL ENGINEERING 2019/2020

LIFE CYCLE ASSESSMENT OF A NOVEL CO_2 CAPTURE TECHNOLOGY (HGTS) ON RETROFITTING COAL AND NATURAL GAS POWER PLANTS: PORTUGAL CASE STUDY

ANA RITA M. MARTINHO

Dissertation submitted for the degree of

MASTER ON ENVIRONMENTAL ENGINEERING

President of the jury:
Prof. Dr. Cidália Botelho

Supervisor at the University:
Prof. Dr. Ricardo Santos

Supervisor at Foreigner University (or company):
Dr. Marcelo Costa
Prof. Dr. Aleksandra Zieminska-Stolarska

July 2020

Integrated Master in Environmental Engineering 2019/2020

LIFE CYCLE ASSESSMENT OF A NOVEL CO_2 CAPTURE TECHNOLOGY (HGTS) ON RETROFITTING COAL AND NATURAL GAS POWER PLANTS: PORTUGAL CASE STUDY

ANA RITA M. MARTINHO

Dissertation submitted for the degree of

MASTER ON ENVIRONMENTAL ENGINEERING

President of the jury:
Prof. Dr. Cidália Botelho

Supervisor at the University:
Prof. Dr. Ricardo Santos

Supervisor at Foreigner University (or company):
Dr. Marcelo Costa
Prof. Dr. Aleksandra Zieminska-Stolarska

July 2020

To my parents and sister.

Agradecimentos

Após o culminar de uma das mais intensas etapas da minha vida, não posso deixar de agradecer às pessoas que me acompanharam e contribuíram para o enriquecimento desta experiência.

Aos meus amigos e companheiros de curso por todos os momentos de partilha, amizade e aprendizagem: Gustavo Rangel, Miguel Ribeiro, Fábio Barbosa, João Duarte, Ricardo Correia, Leonardo Sampaio, Rita Moreira, Bruno Vale, Sara Rodrigues, Maria Isabel Silva e Filipa Faria.

À minha família por todo o apoio e amor: Catarina Martinho, Fátima Martinho, Manuel Martinho e Violeta.

Às minhas amigas Carolina Ventura, Cláudia Loureiro, Sara Monteiro e Maria Vaz por serem quem são e por estarem ao meu lado a tornarem fáceis até os momentos mais difíceis.

Ao corpo docente que integra o Mestrado Integrado em Engenharia do Ambiente pelo excelente trabalho que têm desempenhado neste árduo processo de nos tornarem pré-profissionais capazes.

Deixo também um agradecimento a toda à equipa do Net4CO2, em especial, ao Dr. Marcelo Costa por me ter acompanhado neste projeto e ao professor José Carlos Lopes por me ter possibilitado este primeiro e tão interessante contacto com a Engenharia.

Ao professor Ricardo Santos, por me ter acompanhado nesta última e mais importante etapa do meu percurso académico.

I must also thank professor Aleksandra Ziemińska, for all the support and guidance on this project. It was a great pleasure for me to meet her and her colleagues.

A todos, muito obrigada.

Doctor Ricardo J. Santos, supervisor of this work, is member of the Associate Laboratory LSRE-LCM funded by national funds through FCT/MCTES (PIDDAC): Base Funding UIDB/50020/2020. Ricardo J. Santos was supported by Project PTDC/EQU-EPQ/30445/2017 - POCI-01-0145-FEDER-030445 - funded by FEDER funds through COMPETE2020 - Programa Operacional Competitividade e Internacionalização (POCI) and by national funds (PIDDAC) through FCT/MCTES.

Resumo

O presente trabalho foi solicitado pelo laboratório colaborativo Net4CO2 e tem como principal objetivo a avaliação da performance ambiental da implementação de uma tecnologia inovadora de captura de CO_2 – *Hydra Gas-to-Solid* - em centrais termoelétricas, num contexto nacional. Esta tecnologia insere-se no leque de soluções para Captura, Armazenamento e/ou Utilização do Carbono – ação estratégica global para mitigação do Aquecimento Global e Alterações Climáticas.

Com o propósito de incluir todas as etapas da cadeia de captura, transporte e armazenamento do CO_2, foi desenvolvida a Avaliação do Ciclo de Vida do aprovisionamento à rede nacional de um 1 MWh de eletricidade produzida por duas centrais termoelétricas em Portugal – Sines (central a carvão) e Ribatejo (ciclo combinado de gás natural) – para um ano genérico de operação. A performance da operação da unidade de captura do CO_2 é avaliada por comparação com o cenário de referência de operação das centrais. É feita uma análise comparativa entre as duas centrais e entre meios de transporte diferentes. Foram simulados diversos cenários que permitiram a análise de sensibilidade a alguns dos parâmetros que podem influenciar os resultados, como a qualidade da energia utilizada para o transporte e a profundidade de injeção.

Numa abordagem de 'berço à porta', a redução do Potencial de Aquecimento Global foi de 79 % para a central a gás natural, e de 89 % para a central a carvão. Com a inclusão dos processos de transporte e armazenamento, a redução de CO_2eq foi de 50-69 % para a central a carvão e 74-79 % para a central a gás natural. As restantes categorias de impacte, à exceção da 'depleção abiótica', são penalizadas com aumentos entre 5-393 %. Em termos absolutos, as categorias de impacte que são significativamente afetadas (com ordens de grandeza iguais ou superiores à unidade) estão relacionadas com a toxicidade humana e a ecotoxicidade terrestre e dos meios aquáticos. O transporte por conduta revelou-se como o único meio ambientalmente sustentável num contexto nacional e para fontes emissoras de larga-escala.

Os resultados obtidos revelam que a implementação desta tecnologia a centrais termoelétricas é uma medida eficaz para reduzir o Potencial de Aquecimento Global associado ao setor e que pode ser bastante competitiva no mercado, uma vez que compreende a captura total das emissões atmosféricas das centrais e que a penalidade energética associada à sua operação é baixa (cerca de 3.7 % para a central a gás natural e 9.3 % para a central a carvão).

Palavras-chave: Captura e Armazenamento de Carbono; Avaliação de Ciclo de Vida; Hidratos; Centrais termoelétricas.

Abstract

The present study was commissioned by the collaborative laboratory Net4CO_2 and has the main goal of evaluating the environmental performance of a novel carbon capture technology – Hydra Gas-to-Solid – on retrofitting thermal powerplants, in a national context. This technology is part of the range of solutions for Carbon Capture Utilisation and Storage of CO_2 – a strategy for Global Warming mitigation pathways.

With the aim of including all stages within Carbon Capture and Storage chain, the study is based on a Life Cycle Assessment of the production of 1 MWh for supply the grid, by two power plants in Portugal – Sines (coal based) and Ribatejo (natural gas based) – considering an year of operation. Scenarios of reference operation are the baselines for evaluating the performance of the HGtS operation. A comparative analysis is made between the two plants and between different means of transport. Several scenarios were simulated enabling the sensitivity analysis to some parameters that can influence the results, such as the quality of the energy used for transport and the injection depth.

In a 'cradle to gate' approach, the mitigation of Global Warming Potential was 79 % for the natural gas power plant, and 89 % for the coal power plant. With the inclusion of transport and storage processes the reduction of CO_2eq was 50-69 % for the coal-fired power plant and 74-79 % for the natural gas-fired power plant. The remaining impact categories, disregarding 'abiotic depletion', are penalised with load increases varying between 5-393 %. In absolute terms, the impact categories that are significantly affected (with orders of magnitude equal to or greater than the unit) are related to human toxicity and terrestrial and aquatic ecotoxicity. Pipeline transport has proven to be the only environmentally sustainable transportation mean in a national context and for large-scale emitting sources.

The results obtained show that the retrofitting of this technology on thermal power plants is an effective measure to reduce the Global Warming Potential associated with the sector and that it can be quite competitive in the market, since it enables the total capture of atmospheric emissions from the plants and that the energy penalty associated with its operation is quite low (about 3.7 % for the natural gas power plant and 9.3 % for the coal power plant).

Keywords: Carbon Capture and Storage; Life Cycle Assessment; Hydrates; Thermal Power Plants.

Index

1. Introduction 1
1.1. Understanding Global Warming: trends and the role of Carbon Capture and Storage (CCS) in mitigation pathways 1
1.1.1 Climate change and Paris Agreement 1
1.1.1. Emission trends and mitigation pathways 2
1.2. Global status of CCS worldwide 4
2. State of art of CCS technologies 7
2.1. Capture processes 7
2.1.1. Post-combustion 8
2.1.2. Pre-combustion 8
2.1.3. Oxyfuel-combustion 9
2.2. Separation technologies 9
2.2.1. Membranes 9
2.2.2. Absorption 10
2.2.3. Adsorption 10
2.2.4. Chemical looping 11
2.2.5. Calcium Looping 11
2.2.6. Cryogenic separation 12
2.2.7. Hydrates-based 13
2.3. Transport 16
2.3.1. Pipelines 16
2.3.2. Ship 17
2.4. Storage 18
2.4.1. Geological formations 18
2.4.2. Deep ocean storage 20
2.4.3. Hydrate storage 20
3. Case study: Net4CO_2 capture technology on power generation sector in Portugal. 21
3.1 Energy and electricity generation in Portugal – emissions and trends 21
3.1.1 Energy production and consumption per energy source 21
3.1.2 Carbon intensity and National Plan for Energy and Climate 23
3.1.3 CCS retrofiring on Sines and Ribatejo power plants 24
3.2 HGtS separation technology by Net4CO2 25
3.2 CO_2 fate 26
4. Life Cycle Assessment methodology 27
4.1 Previous studies review 28
4.2 The goal and scope definition 30

4.2.1 Functional unit and reference flow 31
4.2.2 System description and boundaries 32
4.2.3 Allocation 36
4.2.4 Time Horizon 36
4.2.5 Impact categories and impact assessment method 36
4.2.6 Data quality and availability 38
4.2.7 Limitations and uncertainty management 39
4.3 Life cycle inventory 40
4.3.1 Natural gas supply chain 40
4.3.2 Ribatejo NGCC Powerplant 45
4.3.3 Coal supply chain 49
4.3.4 Sines Pulverized Coal Powerplant 50
4.3.5 HGtS retrofitting: CO2 capture process 60
4.3.6 Transportation 62
4.3.7 Storage 69
4.4. Results 75
4.4.1. Coal vs. Natural Gas supply chain 75
4.4.2. Reference operation scenarios 77
4.4.3 Powerplants operation with HGtS – approach 'cradle to gate' 81
4.4.4. Full LCA results: CPP 85
4.4.5 Full LCA: NGPP 89
4.4.6 CPP vs NGPP: 'cradle to grave' 94
4.4.7 Uncertainty analysis: Monte Carlo simulations 96
5. Conclusions 98
Recommendations 98
References 100
Appendixes 108
Appendix I – Pedigree Matrix 109
Appendix II – Natural gas imports by Portugal 110
Appendix III – Natural gas supply chain sub-processes 111
Appendix IV – Distances for natural gas transportation 118
Appendix V – Natural gas powerplant data processing 121
Appendix VI – Sines powerplant data processing 128
Appendix VII – Coal composition 137
Appendix VIII – Artificial Neural Network for predicting emissions on Sines powerplant 141
Appendix IX – HGtS operation data provided by Net4CO_2 149

Appendix X – Materials requirement of pipeline commissioning for transportation of hydrate slurry 150

Appendix XI – Raw results 152

List of Figures

Figure 1 – Energy related emissions evolution from 1990 to 2018. Source: IEA, 2020 [33]. 2
Figure 2 - "CO2 emissions reductions by measure in the Sustainable Development Scenario relative to the Stated Policies Scenario, 2010-2050". Source: Global CCS Institute, 2019 [16]. 3
Figure 3 - Number of projects in different stages of development from 2010 to 2017. Source: IEA, 2017 [10]. 5
Figure 4 - Investment risk curve of CCS technologies and integrated plants. Source: [21]. 7
Figure 5 – CO_2 capture processes. Source: [23]. 8
Figure 6 - CO_2-HO_2 phase diagram. Source: Costa, M. [51]. 14
Figure 7 - Global storage resource estimates in gigatons around the world. Source: Global Status Report 2019 [16]. 18
Figure 8 - Storage security as a function of the trapping mechanisms. Source: IPCC, [11]. 19
Figure 9 - Primary energy consumption evolution at left and final energy consumption evolution at right. Source: DGEG [63]. 21
Figure 10 – Electricity generation by primary source [63]. 22
Figure 11 - Transformation for electricity production. Source: DGEG [63]. 22
Figure 12 - GHG emissions evolution in Portugal. Source: APA [42]. 23
Figure 13 - Evolution of the installed capacity by 2030. Source: PNEC [64]. 23
Figure 14 - Evolution of electricity generation by 2030. Source: PNEC [64]. 24
Figure 15 - NETmix's network with 5 rows and 2 collumns. Source: LSRE-LCM, FEUP [71]. At right, the fluid mixture within the network. Source: Lopes, José et. al., 2013 [72]. 25
Figure 16 - Gas volume reduction due hydrates formation. 26
Figure 17 – Location of potential storage areas and feasible paths for pipeline construction for CO_2 transport. 26
Figure 18 - LCA stages according to ISO 14040:2006. Source: ISO14040:2006(E) [73]. 27
Figure 19 - Scenarios performed for coal powerplant (Sines). 31
Figure 20 - Scenarios performed for natural gas powerplant (Ribatejo). 31
Figure 21 - System boundaries set for CPP. The downstream processes at yellow are only applied to CCS scenarios. 33
Figure 22 - System boundaries set for NGPP. The downstream process at yellow are only applied for CCS scenarios. 33
Figure 23 - Flowchart of the Sines powerplant operation. 34
Figure 24 - Flowchart of RIbatejo (NGPP) operations powerplant. 35
Figure 25 - Flowchart of HydraGtS CO2 capture process. Legend: 1 – water pump; 2 - water heat exchanger; 3 - gas pre-cooler heat exchanger; 4 - gas compressor; 5 - gas intercooler heat exchanger; 6 - gas after-cooler heat exchanger; 7 - CO_2 pump; 8 - NETmix reactor; 9 - transport pump; 10,12 - refrigeration chiller; 11,13 - refrigeration pump. 35
Figure 26 – On the left, the chart represents the share of the most important NG producers for Europe modelled in Ecoinvent database, which is deduced based on

trade movements provided in the BP Statistical Review of World Energy in 2011 report [83]. Most recent updates have been performed for specific countries processes [84] but no updates to European region have been reported. On the right, the share of most relevant NG producers for Portugal modelled fro the current assessment is displayed. The data is based on DGEG annual reports [87]. 40
Figure 27 - Main process steps in NG supply chains. 41
Figure 28 - Hard coal imports for Portugal by country of origin. Source: DGEG [87] (2011-2016), Eurostat [102] (2009-2010, 2017-2018). 50
Figure 29 - EU hard coal imports by country of origin. Source: Eurostat [103]. 50
Figure 30 - Diagram representing the architecture of the developed ANN for predicting emissions and waste generation in Sines powerplant.....56
Figure 31 - Transport scenarios considered for CO2 hydrates of both powerplants. ..63
Figure 32 - Transport scenarios considered for CO2 hydrates of both powerplants. ..63
Figure 33 - Cross section of onshore pipeline. 64
Figure 34 - Characterized results obtained for 1 MJ of natural gas supplied to Portugal trough the model simulated in the current assessment and for 1 MJ of hard coal supply to Portugal by using an Ecoinvent 3.3 process. 76
Figure 35 - NGPP and CPP reference operation scenarios.....77
Figure 36 - Sensitivity analysis to the electricity generated by NGPP (Ribatejo).....79
Figure 37 - Monte Carlo analysis to the standard errors inherent to data for CPP reference operation scenario.....80
Figure 38 - Monte Carlo analysis to the standard errors inherent to data for CPP reference scenario operation.....80
Figure 39 - Monte Carlo analysis to the standard errors inherent to data for NGPP reference scenario operation.....81
Figure 40 - Results of characterization of each impact category for reference and capture scenarios under an approach of 'cradle to gate' on Sines powerplant (CPP). The results are normalized to the functional unit. 82
Figure 41 - Results of characterization of each impact category for reference and capture scenarios under an approach of 'cradle to gate' on Ribatejo powerplant (NGPP). The results are normalized to the functional unit. 82
Figure 42 - Impact characterization for each category between NGPP and CPP with HGtS operation and without grid's compensation. 85
Figure 43 – Relativized results of the LCA for CPP with HGtS retrofitting, pipeline transportation of hydrates slurry for onshore and offshore injection at different depths (800 m, 1650 m and 2500 m) with the energy required being feed by Portuguese electricity supply mix and burning of diesel. 85
Figure 44 - Relativized results of the LCA for CPP with HGtS retrofitting with different means of transportation: bulk ship transportation without cooling system (ship); bulk ship transportation with cooling system (ship w/cooling) and pipeline (both onshore and offshore). The model comprises offshore injection for ship transportation and onshore and offshore injection for pipeline scenario. The injection depth is at 1650 m for the three scenarios.....87
Figure 45 - Relativized results of the LCA modelled for three scenarios of CPP operation. Two CCS scenarios with pipeline transportation for onshore and offshore injection at 1650 m with a sensitivity analysis to the quality of the grid used for transport and onshore injection – Norwegian (NO) and Portuguese (PT) – and another scenario without HGtS retrofitting – reference scenario (Ref). 87

Figure 46 - Loads for best and worst CCS scenario with pipeline transportation and the reference scenario for: GWP, human toxicity, fresh water toxicity and marine aquatic ecotoxicity. 88
Figure 47 - Relativized results of the LCA for NGPP with HGtS retrofitting, pipeline transportation of hydrates slurry for offshore injection at different depths (800 m, 1650 m and 2500 m) with the energy required being feed by Portuguese electricity. 89
Figure 48 - Relativized results of the LCA for NGPP with HGtS retrofitting with different means of transportation: bulk ship transportation without cooling system (ship); bulk ship transportation with cooling system (ship w/cooling) and pipeline (both onshore and offshore). The model comprises offshore injection for ship transportation and onshore and offshore injection for pipeline scenario. The injection depth is at 1650 m for the three scenarios.....90
Figure 49 - Relativized results of the LCA modelled for three scenarios of NGPP operation. Two CCS scenarios with pipeline transportation for offshore injection at 1650 m with a sensitivity analysis to the quality of the grid used for transport and offshore storage.....90
Figure 50 - Loads for best and worst CCS scenario with pipeline transportation and the reference scenario for: GWP, and marine aquatic ecotoxicity. 91
Figure 51 - Results of the LCA for NGPP with HGtS retrofiting, pipeline ransportation and offshore storage for several utilization rates of Ribatejo powerplant. 92
Figure 52 - Relativized results of the LCA for NGPP with HGtS retrofitting, pipeline transportation of hydrates slurry for onshore injection at different depths (800 m, 1650 m and 2500 m) with the energy required being feed by Portuguese electricity. 93
Figure 53 - Relativized results of the LCA modelled for three scenarios of NGPP operation. Two CCS scenarios with pipeline transportation for onshore injection at 1650 m with a sensitivity analysis to the quality of the grid used onshore storage. ..94
Figure 54 - Relativization of impact loads for CPP and NGPP for the scenarios with pipeline transportation and offshore injection at 1650 (using PT grid as electricity source for downstream processes).....94
Figure 55 - Monte Carlo results for the 95 % confidence interval of each impact category, for CPP. These results were obtained for the CCS scenario with pipeline transportation to onshore and offshore storage at 1650 m using PT grid.....96
Figure 56 - Monte Carlo results for the 95 % confidence interval of each impact category, for NGPP. These results were obtained for the CCS scenario with pipeline transportation to offshore storage at 1650 m using PT grid. 97

List of Tables

Table 1 - Main advantages and disadvantages of different separation technologies. .15
Table 2 - Follow-up of table 1 'Main advantages and disadvantages of different separation technologies'. 16
Table 3 - Example of cost studies for different types of transport in China, in 2011. Source: Leung D. [4]. 18
Table 4 - Main parameters related to the modelling of the studies aforementioned. 29
Table 5 - Summarize table regarding uncertainties sources of LC models and the methods applied in the current assessment to control and characterize them. 39
Table 6 - Life cycle inventory for imported natural gas and its transportation until Ribatejo's powerplant. 44
Table 7 - LCI results for each production scenario for Ribatejo Powerplant. 47
Table 8 - Life cycle inventory for each operation scenario simulated for Ribatejo powerplant. 47
Table 9 - Follow-up of Table 8. 47
Table 10 - Raw materials consumption. 51
Table 11 - Summary table of wastewater treatment operations and discharge. The arrows represent effluent fluxes until the discharge points. Depending on the resulting quality, the effluent from TL4 can be directly discharged in EH2 or redirected to TL7.....53
Table 12 - Life cyle inventory for Sines operation without HGtS.....58
Table 13 - Follow-up of Table 12. 59
Table 14 - Follow-up of table 12 and 13. 60
Table 15 - Life cycle inventory of powerlan0st operation with HGtS retrofitting. The materials required for equipment and their dismantling were disregarded from the study. The entries are presented on table 16 for each operation scenario performed. 61
Table 16 - Entries for each scenario, on the processes describing powerplants operation with HGtS retrofitting.....62
Table 17 - CO2 hydrate characterization for maintaining its stabilization during pipeline transportation.....65
Table 18 - Pipeline parameters and distances estimated. 65
Table 19 - Follow-up of Table 18. 66
Table 20 - LCI for pipelines construction and decommissioning for hydrate slurry transport for both powerplants. The uncertainties were defined by Pedigree Matrix for an entry of (3,na,na,na,na). 66
Table 21 - Leakage rates for the transport scenarios by pipeline simulated. 67
Table 22 - Process architecture for pipeline transport of hydrates in slurry state. The entries depend on powerplant operation and transport scenario.....67
Table 23 - CO2 pellets characterization for ship transport. 68
Table 24 - Calculation method to determine the tonnes-km for each operation scenario.....68
Table 25 - General criteria for storage selection. Source: [66]. 69
Table 26 - Storaae site characterization.....70
Table 27 - CO2 hydrates characterization at the end of pipeline.....70

Table 28 - Mass fluxes of CO2 hydrates. 71
Table 29 - Number of wells needed and the ratio between the injection rate with the cluster injection rate in % for diferent operation scenarios. 71
Table 30 - LCI for the drilling activity for both onshore and offshore deep wells. 72
Table 31 - Follow-up of Table 30. 73
Table 32 - Pressures at different stages of injection process....74
Table 33 - Process architecture for modelling hydrate slurry stored into the deep saline aquifers. 74
Table 34 - Power required for each operation scenario, assuming an efficiency of 85 %. 75
Table 35 - Load of each impact category for reference operation scenario of both powerplants. 78
Table 36 - Results obtained for capture and reference scenarios operation on both powerplants under an approach of 'cradle to gate'. The results are normalized for the functional unit: 1 MWh of electricity produced for supplying to the grid. 84
Table 37 - Relation between the load of each impact category within the different scenarios and with the reference operation (without HGtS). 84
Table 38 - Load for reference operation scenario, worst and best CCS scenarios for CPP, and the variation between these and the reference scenario. 88
Table 39 - Load for reference operation scenario, worst and best CCS scenarios (NGPP with offshore injection), and the variation between these and the reference scenario. 91
Table 40 – Environmental loads for reference operation scenario, worst and best CCS scenarios (NGPP with onshore injection), and the variation between these and the reference scenario. 93
Table 41 - Results obtained from pipeline transport step normalized to the mass of CO_2 transported and distance travelled. 95
Table 42 - Results obtained for storage step normalized to the mass of CO2 injected. 95
Table III-543 - Life cycle inventory for the natural gas transportation by onshore pipelines in western Europe. 115
Table 44 - Scores for each impact category of NG supply chain. 116
Table 45 - Emissions for ocean by desulphurisation, chemical and domestic effluents in tonnes. 134

Nomenclature

ANN – Artificial Neural Networks

BECCS – Bioenergy with carbon capture and storage

BECCS – Bioenergy with carbon capture and storage

CaL – Calcium Looping

CCS – Carbon Capture and Storage

CCU – Carbon Capture and Utilisation

CCUS – Carbon Capture Utilisation and Storage

CG – Climate Change

CLC – Chemical Looping Combustion

CPP – Coal power plant

DAC – Direct Air Capture

EII – Energy Intensive Industries

EOR – Enhanced Oil Recovery

EWC – European Waste Codes

GHG – Green House Gases

GWP – Global Warming Potential

HGtS – Hydra Gas-to-Solid (carbon capture technology)

IC – Impact Category

IEA – International Energy Agency

IPCC – Intergovernmental Panel on Climate Change

LCI – Life Cycle Inventory

LCIA – Life Cycle Impact Assessment

LHV – Low Heating Value

NG – Natural gas

NGPP – Natural gas power plant

PCC – Post-combustion capture

PP – Power Plant

SDS – Sustainable Development Scenario

STEPS – Stated Policies Scenario

toe – Tonne of Oil Equivalent

UN SDG –Sustainable Development Goals of United Nations

WEO – World Energy Outlook

Chapter 1

Introduction

The current project has the main goal of evaluating the environmental performance of a novel carbon dioxide capture technology - *Hydrate Gas-to-Solid* (HGtS) - on retrofitting two Portuguese thermal power plants: one using coal and another using natural gas as the main fuel. This study was commissioned by Net4CO_2, the collaborative laboratory that developed the technology. The tool applied was Life Cycle Assessment as it can address the environmental benefits and trade-offs related to the all CCS chain stages. Chapter 1 introduced the overall role of CCS technologies on Global Warming mitigation pathways. Chapter 2 presents the most relevant insights of the state of the art of CCS technologies among all chain stages: capture, transport and storage phases. Chapter 3 introduces the scope of the project, by presenting an overview of the energy sector in Portugal, introducing the *Hydrate Gas-to-Solid* technology and possible fates for CO_2 captured in the country. Chapter 4 presents the methodology applied to develop a Life Cycle Assessment of HGtS on retrofitting the two Portuguese power plants - Sines and Ribatejo – and the results obtained. Chapter 5 presents the conclusions and recommendations for further research work.

1.1. Understanding Global Warming: trends and the role of Carbon Capture and Storage (CCS) in mitigation pathways

1.1.1 Climate change and Paris Agreement

In the past decades, changes in climate patterns and ecosystems have been affecting biophysical and biogeochemical interactions between land and climate and causing changes in cryosphere [1]. Although, those interaction are of great complexity, it is consensually accepted that global warming (the continuous increase of global average temperatures associated with the intensification of *greenhouse effect*) is a major driver of Climate Change (CG) and sets a relation of positive feedback to it [1].

To avoid harmful climate impacts, world's societies will need to mitigate global warming and adapt to climate change [2]. Paris Agreement is considered a milestone for the global transformation to a low-carbon and climate-resilient society [3]. Ratified by 55 countries (54 nowadays with the 'exit' of USA), accounting for at least 55 % of global emissions, the agreement comprises both mitigation and adaption actions considering the following main goals [3]:

- Keep the global average temperature well below 2ºC above pre-industrial levels;
- Pursue efforts to limit the temperature increase to 1.5 ºC above pre-industrial levels;
- The need for global emissions to peak as soon as possible;
- Undertake rapid reductions thereafter, in accordance with best available science.

European Union has established the goal of reducing 80-95% of GHGs emissions compared to 1990 levels in industrial countries until 2050 and achieve the neutrality over the 2nd half of the century [4].

IPCC conducted a series of scenarios relating complex climate interactions with the evolution of the atmospheric concentration of CO_2 and concluded that the range of concentrations for which the likelihood of the temperature change (relative to 1850-1900) being lower than 2 ºC and 1.5 ºC over the 21st century is higher than 66% is from <430 to 480 parts per million (ppm) CO_2eq[1] [2]. Such scenarios are characterized by achieving carbon neutrality in the 2nd half of century [2].

1.1.1. Emission trends and mitigation pathways

From 2014 to 2017 was reported a global stabilization of CO_2 emissions [3,5], followed by annual increases of 2.7% and 0.6% in 2018 and 2019, respectively [5]. However, in advanced economies the tendency for stabilization and decrease was maintained (see Figure 1), especially because of the decreases in energy related emissions: 85% of the total decrease [7, 8]. Therefore, it has been observed a partial decoupling between CO_2 emissions and Gross Domestic Product, due to a transformation into a paradigm of energy efficiency and a less carbon intensive energy mixes [3,7].

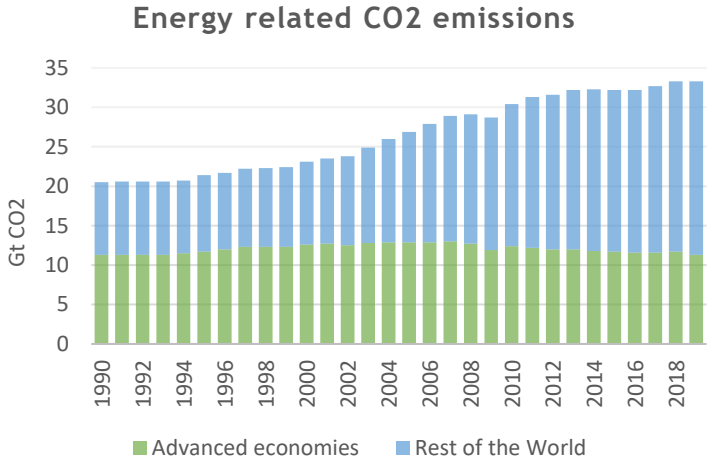

Figure 1 - Energy related emissions evolution from 1990 to 2018. Source: IEA, 2020 [33].

Energy and industrial sectors together contribute to about 54-55% of the total GHG emissions (data from 2010) [2,5]. Energy Intensive Industries (EII) such as cement, iron and steel production account for 25% of the total emissions [9]. Thus, both sectors are strategic to achieve the decarbonization goals. IEA have estimated that industrial emissions must be reduced by at least 50%, depending on the strategic pathways adopted [10].

Energy efficiency improvements and the decarbonisation of the electricity mixes are crucial on mitigation actions for stabilization of the atmospheric GHG concentration [2]. Regarding the second, besides switching to less carbon-intensive fuels, nuclear power, renewable energy sources, Carbon (CO_2) Capture and Storage (CCS) technologies are essential to fully achieve close to zero net CO_2 emissions, especially for power generation and EIIs [11,12,9,13].
IPCC defines CCS as a 'process consisting of the separation of CO_2 from industrial and energy related sources, transport to storage location and long-term isolation from the atmosphere (…) in geological formations, in the ocean, in mineral carbonates or for use in industrial processes' [11]. As both capture and cost efficiencies improve for carbon intensive activities, these

[1] In 2018, the global average atmospheric CO_2eq concentration was 407.4±0.1 parts per million (ppm), reaching the higher ever record concentration [6].

technologies are more likely to be applied at large point sources: fossil fuel power plants, fuel processing plants and the industries of iron, steel, cement and bulk chemicals [11]. For the power sector, these strategies are especially promising because considering the fluctuating and, sometimes inaccurate, forecasted feed-in of renewable power, CCS technologies ensure electricity supply during peak loads. Besides, the complete replacement of progressively phased out nuclear power by renewables within the foreseen timeframe is highly unlikely [14]. While renewable sources and energy storage capacity is insufficient for substitution of base-load technologies, CCS contributes actively for less carbon intensive electricity grids during the transition period. Moreover, when applied to bio-energy production, CSS solutions offer the opportunity to achieving negative emissions (BECCS) [13].
For carbon intensive industries, such as iron, steel and cement production, CCS technologies may represent the ultimate solution to decarbonize their activities.

The analysis of simulated scenarios of Climate Change (CG) mitigation pathways performed by IPCC and IEA confirms the key role of CCS technologies for limiting the global average temperature increase to not more than 1.5 – 2 ºC in relation to pre-industrial age, in a cost effective way and without compromising the trends for energy demand [15,1,2]. In fact, 'excluding CCS from the portfolio of measures used to reduce emissions would lead to a doubling in cost – the largest cost increase from the exclusion of any technology' [16].

The most recent data related to CG mitigation pathways simulations was released in the IEA's World Energy Outlooks (WEO) 2019 report, where two main scenarios are displayed (see Figure 2):

- Stated Policies Scenario (STEPS) – based on existing and announced policies, this scenario is poorly managed to achieve the UN SDGs related to energy[2] [15];
- Sustainable Development Scenario (SDS) – 'outlines a major transformation of the global energy system in a realistic and cost-effective way in order to achieve the UN SDGs related to energy'. It also meets the Paris Agreement conditions: 'holding the temperature rise below 1.8 ºC with a 66% probability (which is equivalent to limiting the temperature rise to 1.65 ºC with a 50% probability)' [15].

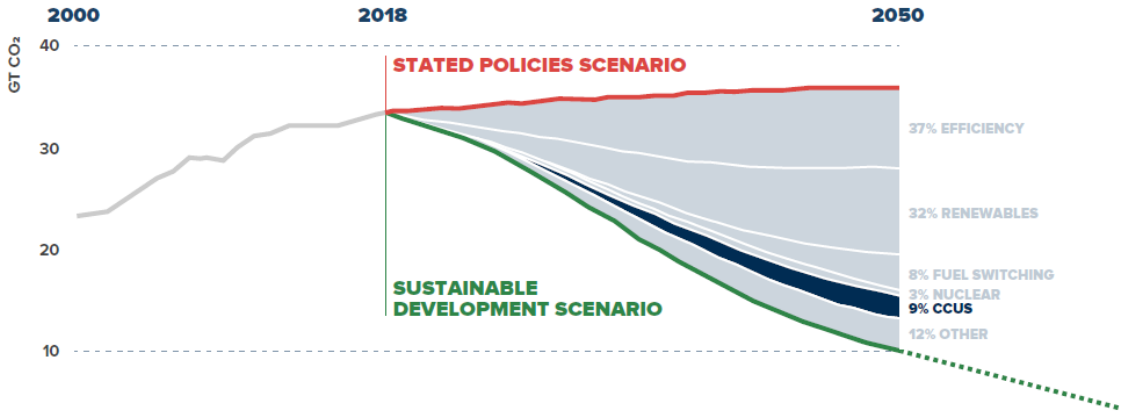

Figure 2 - "CO2 emissions reductions by measure in the Sustainable Development Scenario relative to the Stated Policies Scenario, 2010-2050". Source: Global CCS Institute, 2019 [16].

Despite the continuing demand for energy consumption worldwide, the simulation of SDS accounts for a global 'CO_2 emissions decrease from 33 billion tonnes in 2018 to less than 10

[2] IEA refers that the UN SDGs most related to energy are: the reduction of the impacts of air pollution in human health (SDG 3); affordable and clean energy (SDG 7); action to promote the climate change mitigation (SDG 13).

billion tonnes by 2050' and the probable achievement of net zero emissions by 2070 [15]. Figure 2 shows the CO_2 emissions reductions in the SDS for different mitigation strategies.

Under SDS, one may conclude the following topics:

- 9% of the cumulative emissions reduction between 2018 and 2050 are attributed to CCUS [16];
- The average mass of CO_2 captured and permanently stored each year between 2019 and 2050 is 1.5 billion tonnes per annum (46.5 billion tonnes of CO_2 stored in 2050), comprising almost equally both power and industrial sectors [16];
- Due to technological progress in renewable energy, especially solar and wind, the SDS's reliance on CCUS and nuclear energy have fall down when comparing to previous scenarios, currently accounting for 3900 TWh of the electricity [16, 17, 18];
- Besides the lack of reliance on global net-negative GHG emissions, SDS trajectory is well within the envelope of the 90 scenarios presented in IPCC Special Report on Global Warming of 1.5 ºC [15,1];
- For the overall investment over 2050, SDS requires about 25% more than the STEPS, that can be partially counter balanced by reduced fuel costs [15].

Regarding the analysis of such scenarios and studies conducted by Dr Niall Mac Dowell and Mr Yoga Pratama [19], it is possible to conclude that:

- The exclusion of CCS strategies from the 'portfolio of available options has the effect of increasing the cost of delivering a net zero system by between a factor of two and seven' [15,19];
- They are a key point to achieve the decarbonisation goals without compromising the increasing demand for power [19].

Therefore, policymakers should promote conditions for the support and expansion of such measures to overcome the delay of their deployment situation over the scenario's predictions.

1.2. Global status of CCS worldwide

Currently there are over 150 CCUS related projects undergoing worldwide [20]. However, there has been relatively limited investment (approximately USD 12.3 billion from 2005 until 2016, with a private share of 77 % [21]) and support for implementation of large-scale CSS projects for various reasons: the early stage of development of some of the technologies [11]; the absence of policy frameworks; projects can be capital intensive and profitably poor; the management of the risk of future CO_2 leakage as well as the allocation of responsibilities among the different stakeholders in this matter [21]. Figure 3 shows the number of projects undergoing at different stages of development from 2010 to 2017.

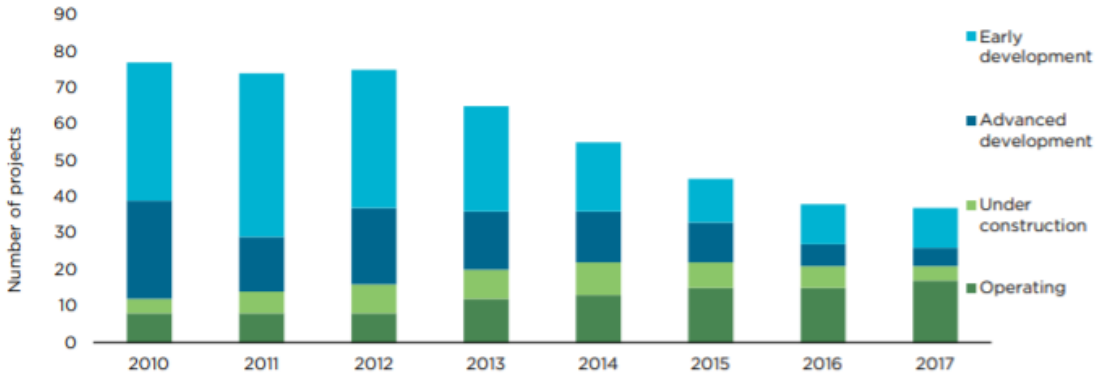

Figure 3 - Number of projects in different stages of development from 2010 to 2017. Source: IEA, 2017 [10].

Despite the facts, the global portfolio of large-scale CCS projects in operation continues to expand [10,21,20], even though a higher large-scale deployment is needed to deliver further costs reductions [22] and to meet the previsions by IEA's Sustainable Development Scenario.

Sleipner was the first large-scale CO_2 capture project, operating in a natural gas production facility, with permanent and dedicated CO_2 injection and storage under monitoring [23]. In 2016, this project completed 20 years of successful operation, have safely stored close to 17 million tonnes (Mt) of CO2 [10] in a saline aquifer some 800-1100 metres beneath North Sea [21] into the Utsira Formation – a massive sandstone with 200-250 meters of thickness with an estimated storage capacity of 600 billions tons of CO_2 [23]. No leakage incidents have been notified.

In 2019, the number of large-scale facilities reached 51, with more than 25 million tonnes of CO_2 from the power and industrial sectors permanently stored [16,20]:

- 19 in operation;
- 4 under construction;
- 28 are in current development.

Global CCS Institute affirms that 'to achieve the levels outlined in the SDS, the number of industrial scale facilities needs to increase from 19 in operation now to more than 2000 by 2040' [16].

1.2.1. Policy framework and major drivers for CCS deployment

There is a range of conditions and policies applied worldwide to contribute for the economic feasibility of large-scaling facilities. Some are climate-based regulation, others are CCS-targeted policy incentives that go along with some external aspects driving the CCS deployment [16,21]:

- Financial framework: carbon taxes (Norway), tax credits or emissions credits (US and Canada) and grant support (US, Canada and Australia);
- Political framework: public financial support (Canada, Brazil, Norway, UAE and China) and regulation of CCS operations (US, Canada, EU and Australia).
- Power and industrial cooperation featuring hubs and clusters (15 out 19 operating large-scale facilities) which can 'reduce the unit cost of CO_2 storage through economies of scale, offering synergies that reduce the risk of investment'.
- Enhanced oil recovery (EOR) is applied for 14 out 19 large scale facilities.

Whilst, the purpose of carbon taxes is to reduce GHG emissions form large emission sources, carbon prices may not be enough to accelerate a total transition for renewable energy generation. In Europe, there are still fossil fuel based powerplants under construction planning. Bloomberg New Energy Finance stated that on way of preventing a 'lock-in' for European power sector to high carbon emitting technologies would be to ban the construction of those new powerplants without CCS [22].

Although being less effective in GHG emission reductions, CO_2 utilisation (CCU) for derived products is consider to be attracting for investors as it could contribute to increased profits by dynamizing CO_2's market and it can engage this product into a circular economy [16]. It is a crucial alternative for locations where pipeline transportation is unfeasible [16]. However, its future is difficult to predict due to the 'early stage technology deployment for many applications and the reliance on supporting policy frameworks' [24]. Moreover, carbon markets are unlikely to evolve fast enough to support the investments needed in the near term [21].

The emerging market opportunities for CO_2 usage are summarized in the following topics [24]:

- CO_2 derived fuels including methane, methanol gasoline and aviation fuels, in combination with hydrogen, providing less carbon intensive production routes;
- CO_2 derived chemicals such as plastics, fibres and synthetic rubber, which production also represents some potential climate benefits;
- Using CO_2 to replace water in concrete is the most mature and promising application;
- CO_2 can also react with waste materials from power plants or industrial processes to produce construction aggregates;
- Crop yield boosting with CO_2 has already been happening naturally, the so-called greening effect of climate change on land [25]. When well-managed, it can increase yields by 25% to 30%, as it also can promote algae production. Netherlands estimated annual consumption for this matter is between 5 to 6.3 $MtCO_2$.

It should be mentioned that, with the exception for concrete bounding, these options do not correspond to long-term sequestration of CO_2. 'Mac Dowell et al estimates that up to 700 million tonnes per year of CO_2 could be utilized by 2050' [16,26]. However, considering that 'only about 25% of the products correspond to sequestering CO_2 for any significant duration', the contribution of CCU to the expected mitigation emissions for CCUS share[3] remains about 0.5% [26].

1.2.2. Regulatory framework

In contrast to CO_2 capture and transport phases, which regulation follows already existent legislation for other similar activities (covering aspects as environmental impacts, occupational health and safety, emissions control and reporting), the storage of CO_2 will involve specific regulation covering topics as: ensuring a legal basis for CCS, site selection, safe operation, responsibilities allocation over time, the leakage risk management and potential adverse impacts assessment [21]. Some aspects however could be governed by existing natural resource extraction and mining. In UE, the directive 2009/31/EC regulates the geological storage of carbon dioxide.

[3] Mac Dowell et al have considered previous IEA's scenarios, expecting CCS for reducing 14-20% of mitigation emissions, which corresponds to a cumulative CO_2 storage of 120-160 Gt_{CO2} until 2050 [26].

Chapter 2

State of art of CCS technologies

CCS solutions comprise a diverse range of technologies with the main purpose of capturing CO_2 from different sources depending on its partial pressure, operating conditions and composition of the gas mixture [27]. CCS chains can be grouped in 4 main sectors regarding technological and application specifications: carbon capture and storage (CCS), carbon capture utilisation and storage (CCUS), bioenergy with carbon capture and storage (BECCS) and direct air capture (DAC) [16]. Direct air capture (DAC) is out of the scope of the project and it will not be subject of further review. Both BECCS and CCUS share some of the individual components of CCS chains.

2.1. Capture processes

The type of combustion and/or industrial process directly affects the suitability of the different types of capture technologies and processes [4]. The key points for each technology are capture efficiency, energy penalty and operating costs. As these are energy intensive processes, contributing to around 70-90% of the total operating cost of the three-stage carbon capture and storage system [28], enormous R&D studies have been conducted to improve energy penalties without compromising CO_2 recovery rates and operating costs.

Through such studies, all the chain stages (capture, separation, transport and storage) have been tested at or close to industrial scale [13]. Some technologies however are found at a more mature stage, *i.e.* post-combustion CO_2 separation by absorption using MEA (monoethanolamine) (see Figure 4). There are three main classes of capture processes: post-combustion, pre-combustion, oxyfuel combustion. The separation technologies comprise a wider range of solutions.

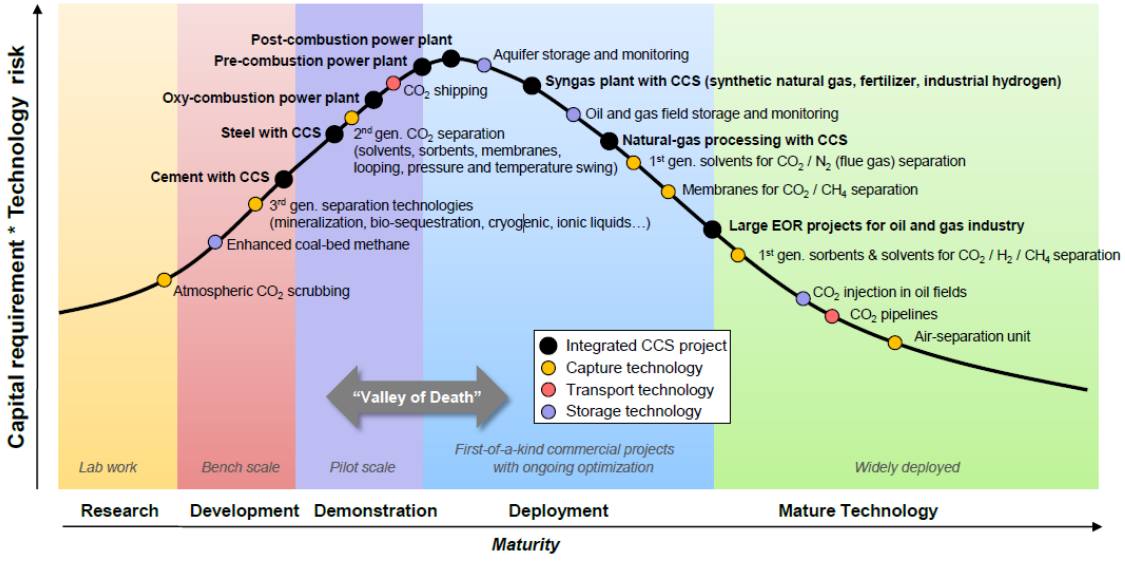

Figure 4 - Investment risk curve of CCS technologies and integrated plants. Source: [21].

Figure 5 presents an additional capture process, chemical oxidation which will be considered as a separation technology in further review.

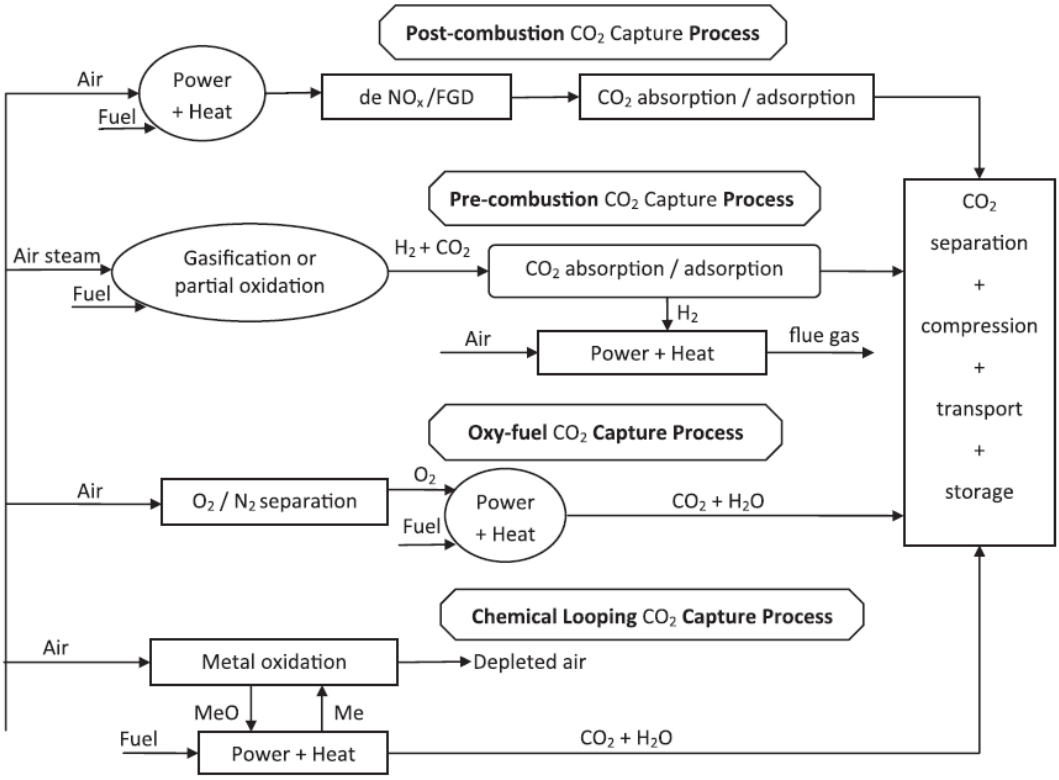

Figure 5 – CO_2 capture processes. Source: [23].

2.1.1. Post-combustion

In post-combustion processes the CO_2 is removed from the flue gas, composed mainly by N_2 and CO_2, after combustion has taken place – 'end of pipe' technology [29-30]. This technology is the most feasible on a short time scale due the possibility of retrofitting existing PP [4-30]. The major challenge regarding post-combustion capture (PCC) is related to the energy penalty[4] to enrich the fraction of CO_2 to levels that are suitable for transport and storage [4,30].

The reference systems for PCC are industrial processes and thermal power generation [11], which accounts for a total capacity of about 1531 MWe worldwide [31].

Several separation technologies can be applied to a PCC process. The most mature technology is amine-based chemical absorption (see Figure 4) [21,13,30] and it was first applied at scale at Boundary Dam Unit 3 PP in 2014 (first-generation solvents developed by Cansolv Technology). Energy penalty associated with amine regeneration has been reduced by 50% approaching the thermodynamic limit [21,13]. Further reductions must come from the deployment of novel technologies.

2.1.2. Pre-combustion

In this process, the fuel (typically coal or natural gas) reacts with oxygen or air and/or steam to produce syngas, composed mainly by H_2 and CO, which further reacts with steam in a catalytic reactor (water gas shift converter) forming more H_2 and the CO reduces to CO_2. The result is a H_2/CO_2 fuel gas with a CO_2 concentration over 20% [4], which facilitates the separation process. After CO_2 capture, the hydrogen-rich fuel can be applied in boilers,

[4] 'Energy penalty' refers to the fraction of fuel or energy content dedicated to the operation of the capture unit for a fixed quantity of work output.

furnaces, gas turbines, engines and fuels cells [11]. Its combustion releases mainly N_2 and water vapor [4].

These processes can be applied to integrated gasification combined cycles (IGCC) power plants [11,13,4]. The reference separation technology is the physical absorption. At large-scale, two solvents are used: Selexol at Kemper Country IGCC project (USA) and Rectisol at Dakota Gasification facility (USA) [21].

2.1.3. Oxyfuel-combustion

In oxyfuel-combustion, the fuel is burned in an enriched mixture of O_2 and recycled flue gas (RFG – to moderate the extremely high flame temperature) [11,13]. The exhaust gas will then be composed mainly by CO_2, water vapour, particulate matter and SO_2 [4]. The substantial reduction of NO_x is a great advantage, turning the selective catalytic reduction (SCR) unit sometimes obsolete for the flue gas treatment. After particles and SO_2 remove, the flue gas contains a CO_2 concentration of 80-98% (depending on the fuels), that can be compressed for further transportation [4]. However, the energy penalty associated with the O_2 enrichment for combustion oxidant mixture is significant and when combined to CO_2 compression process results in overall plant efficiency reduction of 8-12% [13]. Oxygen is usually produced by cryogenic distillation methods or membranes and chemical looping cycles that reduces energy consumption [13]. Another disadvantage regarding this process is the higher risks for equipment corrosion due the higher concentration of SO_2 caused by the volumetric flow reduction of the flue gas. This can be mitigated using 'low sulphur and/or high calcium coals, wall soot blowing, limestone injection and sulphur scrubbing prior to recycle' [13].

The power plants suitable for oxyfuel-combustion capture processes are the same as for PCC [11,21]. The technology has been successfully tested at pilot and small scale (30-35 MW) worldwide. However, with the cancellation of the FutureGen 2.0 and White Rose projects, there are no large-scale undergoing projects [21].

2.2. Separation technologies

2.2.1. Membranes

Membranes can be used to separate only CO_2 from the flue gas in a continuous way at ambient temperatures without the need for additional chemical substances.

There are various materials used for CO_2 separation membranes: silica (high selectivity and medium high cost), zeolite (very high selectivity, high permeability, good stability however high costs), carbon molecular sieve with polymers (good thermal and chemical stability but costs can be very high), metal (high selectivity, high temperature tolerance but very high costs) and ceramic (high selectivity, high temperature tolerance but costs can be very high) [4].

The capture of more than 90% of CO_2 from the flue gas is unlikely to be achieved by a single-stage membrane process, but a multi-stage would do [32]. The development of ceramic and metallic and polymeric membranes can increase the current capture efficiencies [4]. The performance is mainly affected by low CO_2 concentration and pressures [4].

These technologies have significant energy penalties associated to compression equipment and face some scale-up challenges. The compression of the flue gas can be provided either by compressing the feed gas or by drawing a vacuum on the permeate. The second, despite being less energy intensive, is commercially unavailable and requires a wider membrane area [32]. A turboexpander allows the recovery of a portion of the energy needed but the energy penalty is still more than 20% [32]. Recent studies have concluded that energy penalty and costs performance of membrane technologies do not overcome amine-based chemical absorption technologies performances [30].

2.2.2. Absorption

Depending on the processes and the solvents used, absorption separation can be classified as chemical or physical. As already aforementioned, Rectisol and Selexol are the most used separation processes. They are low and high temperature physical absorbers, respectively. Rectisol process makes use of methanol and its wash enables the removal of H_2S, CO and CO_2 as well as other impurities, such as HCN and NH_3. 'Most of the solvent can be regenerated by a simple pressure let down or by inert gas stripping' [32].

Chemical absorption with amine solvents is the most mature and cost-effective technology (Figure 4) and the most applied to commercial and large-scale facilities (both natural gas and flue gas treatment) including industrial processes (*e.g.* ammonia production) [33]. The capture efficiencies reach about 90 %.

After the absorption of CO_2 from the flue gas, the liquid sorbent become a CO_2-rich fluid which can be regenerated through a stripping or regeneration process by heating and/or depressurization [4,31].The solubility of CO_2 in the solvent, the cyclic capacity, the heat of absorption and the kinetics of the reaction are the main optimizable variables [35,36] and the main challenge is how to reduce the energy consumption related to sorbent regeneration. The sorbents are mainly amine-based, alkaline solvents (*e.g.* NaOH and $Ca(OH)_2$) and ionic liquids [37].

Significant progress has been achieved on the development of amine-base solvents. The general trend of amines in order of loading capacity is primary amines (*e.g.* monoethanolamine or MEA) < hindered amines (*e.g.* KS-1) < secondary amines (e.g. diethanolamine or DEA) < tertiary amines (*e.g.* methylodietyloamine or MDEA) < diamines [33,35]. The energy penalty in the firstgeneration technologies related to amine regeneration is already close to thermodynamic limit and further improvements must come from the development of new solvents generations. Conventional amine (e.g. MEA) requires a significant amount of energy, about 4.1 GJ per tonne of CO_2. Second generation of amines has reduced this energy penalty to about 2.6 GJ per tonne of CO_2 and with the development of new chemicals and mixed solvents (third generation) the energy penalty can be further reduced to 2.0 GJ per tonne of CO_2 [35]. Some studies present even lower prospects, but those technologies have not been tested at pilot scale yet. Those new solvents generations face some new challenges such as long-term efficiency and the maintenance of constant compositions in mixed solvents [35]. Other operational aspects as corrosion, solvent degradation, solvent management, solvent emissions, process monitoring, and system-optimization are common issues for full-scale among all chemical absorption technologies.

Despite their mature stage and the good separation performances, there are environmental issues regarding the toxicity level emissions associated to amines production and degradation, increasing the potential harm of other environmental burdens besides Global Warming Potential [34].

2.2.3. Adsorption

Sorbents are solid substances with high specific surface area and high selectivity in which CO_2 stays bind. As in absorption, solid's regeneration ability is a key criterion for sorbents selection. Typical sorbents include molecular sieves, activated carbon, zeolites, calcium oxides, hydrotalcites and lithium zirconate [4]. While metal framework and amine-functionalized adsorbents are still under development, zeolites are currently the most favourable choice [38]. Sorbents regeneration can be processed by swinging the pressure (PSA) or temperature (TSA) of the system. In TSA, the adsorbed CO_2 is released by increasing system temperature by hot air or steam injection and the resulted CO_2 purity can be higher than 95% [4]. However, PSA, in which the regeneration is performed by the swing from high to low pressures (usually atmospheric pressure), is considered the most promising alternative, with potential for

reducing energy penalty, environmental impacts and operational costs [38]. Its CO_2 recovery efficiencies can vary between 85 to 90% [38].

Besides the good capture efficiencies and operability, both energy penalty and costs are still not competitive with chemical absorption [38]. As an alternative for costs abatement, agriculture and industrial residues are being tested for sorbents development [4]. In pre-combustion applications, adsorption processes have the plus advantage of being able to simultaneously retrofit hydrogen production [38].

2.2.4. Chemical looping

In chemical looping combustion (CLC), a metal oxide is used as an oxygen carrier (instead of air) and is reduced to metal during combustion while the fuel is oxidized to CO_2 and water. The metal is then oxidized and reused. This process offers the advantage of getting a total CO_2 recovery by conducting the flue gas to a simple condensation process for water removal. The effectiveness of different metal oxides has been studied. The most used carriers include Fe, Ni, Cu, Mn and Co [4]. Support inert material can be used to optimize the process performance but the overall results depend on the combination between inert material and oxide metal used [4]. Chemical looping technologies comprise a wide range of alternative pathways for combustion, and it can also address H_2 production.

Based on simulations performed by Jing Li et al., an NG-CLC plant can achieve efficiencies up to 52-60% (LHV[5]) including CO_2 compression, which represents an increase of 3-5% comparing with conventional NGCC with CO_2 capture [39]. For IGCC, the implementation of multi-stage CLC can highly increase net plant efficiency [40]. For coal combustions, efficiencies of 42% have been reported, which is about 2% lower than a reference case and higher energy penalties were reported for pre-combustion and oxyfuel-combustion [40]. The integration of interconnected fluidized beds is very promising for CLC application. Erlach et al. have compared this technology in a pre-combustion process of an IGCC plant with a conventional CLC scenario and had concluded that net plant efficiency of the first was 2.8% higher [41].

The main disadvantage is related to the impossibility of retrofitting existent PP, but the technology is yet at relatively early stage of development regarding reactivity, thermal stability, mechanical strength, oxygen transport capacity, and toxicity [39]. The overall costs can be higher than existing technologies [39] and it mainly depends on the metal used as an oxygen-carrier and particles lifetime. Juan Adanez et al. have however concluded that considering makeup flow of the particles as the main cost, a lifetime of about 300 hours would represent the same cost of makeup of amine in a conventional MEA absorption technology [40]. Besides, particles with lifetimes under 100 hours can fulfil the target range of 20-30$ per tonne of CO_2 avoided [40]. Thus, particles costs may not be a limitation. However, little information regarding environmental aspects relating to particles emissions have been reported. There are potential risks associated with carcinogenic properties of some of used metals and more studies should be carried out.

2.2.5. Calcium Looping

Calcium Looping is suitable for pre-combustion, oxy-fuel and post-combustion integration [19]. The process is based on the multi-cyclic carbonation/calcination of CaO at high temperatures. CO_2 reacts with solid sorbent (CaO) at 500-650 ºC leading to calcium carbonate formation, which is further decomposed into CaO and CO_2 stream at 800-950 ºC [36]. Then CaO is recycled and the process is then repeated. The level of conversion decreases when the number of carbonation-calcination cycles is increased, due to drop in internal surface area and associated increase in pore size [19].

[5] Low heating value.

This technology is competitive for its thermodynamic advantages. In literature, energy penalties ranges between 6 and 8 % with respect to reference plants without the CO_2 capture [19]. Moreover, when integrated on a pre-combustion system, although its increased complexity, calcium looping offers the possibility of being combined with reforming and/or gasification processes to produce syngas, high fuel conversions and minimal CO formation [19].

2.2.6. Cryogenic separation

Cryogenic separation technologies take advantage of the different condensation and desublimation properties of the different flue gases to isolate CO_2, with high purity levels (99%) and high recovery rates (99%) [43]. The most common method is cryogenic distillation in which flue gas is cooled to desublimation temperature (-100 to -135 ºC) and then solid CO_2 is separated from other light gases and compressed to a high pressure of 100-200 atmospheres (atm) [4]. These technologies face the challenge of reducing their high energy load associated with cold energy consumption. 'The coefficient of performance of a typical refrigerator that cools to -140ºC is typically 0.5, which means the consumed electricity would be equal to twice the thermal energy' [43]. An effective approach is to reuse waste cold energy from industrial or powerplants sources by an inertial carbon extraction system, a thermal swing process or an external cool looping. Song et al. presented some of interesting studies on the matter [43], which are summarized below.

Tuinier et al. studied dynamically operated packed beds, a steel monolith structure, using liquified natural gas (LNG) as the cold energy source, which had decrease operating costs relating to the refrigeration to keep temperatures around -150ºC [43,44]. The process separates simultaneously CO_2 and H_2O and it does not require chemical absorbent and elevated pressure. It can also be used to upgrade biogas with better performance that vacuum pressure swing adsorption: 94.3% recovery rate and a productivity of 350.2 kg CH_4 h^{-1} $m_{packing}^{-3}$.

Baxter et al. presented a hybrid cryogenic carbon capture system via an external cooling loop: the formed solid CO_2 and residual flue gas are re-heated via incoming gases [51,53]. The result is a liquid CO_2 phase and a N_2-rich stream. The capability to store energy in LNG offers the possibility of managing the energy penalty by using a 'stored refrigerant to drive the process during peak demand and regenerating the refrigerant during low-demand periods' [43,45]. This process is less energy intensive (an average of 0.98 MJ/kg CO_2) than other more conventional [43].

Clodic and Younes have designed and test an anti-sublimation CO_2 capture process (AnSU) in a 660 MW_e boiler with a CO_2 concentration of 15.47% at 60ºC and 120 kPa. The energy penalty was about 3.8-7.2% of the power plant efficiency, much lower than first generation chemical sorbents [46]. In the process, the latent heat of fusion, release from CO_2 defrosting, is used to cool down the liquid blend of refrigerants before evaporation [46]. This process however implies moisture removal from the flue gas to prevent clogging and pressure rise during operation [43]. However, a decrease CO_2 partial pressure would affect adversely both energy penalty and capture efficiency. Some operational issues, as the growing frosted CO_2 layer would also reduce efficiency [43].

Song et al. designed a Stirling cooler system at low temperature and by waste sensible and latent heat recoveries, the process can be controlled to values below 0.55 $MJ_{electrical}$/kg CO_2 [43]. However, this technology has been tested only at laboratory scale with a CO_2/N_2 binary gas and further studies for scale-up are needed.

Cryogenic processes are also being intensively studied for oxyfuel combustion and for natural gas refining. The captured CO_2 can achieve high purity levels which increase its industrial market value, as it becomes more efficiently converted into valuable chemicals by catalytic or biologic reactions (e.g. steam methane reforming and artificial photosynthesis) [43]. Another advantage is related to the possibility of avoiding a final compression, as CO_2 can be captured in different phases. Regarding Baxter's studies, CO_2 product can also be used as a cold energy

source for other industrial processes as natural gas liquefaction (energy stored for cryogenic carbon capture – CCC-ES) [43,47]. This is currently applied in a process with an open natural gas refrigeration loop by Baxter's group. The costs can be lower than other competitors technologies as these are less equipment intensive. The great disadvantage is related to the operational vulnerability to different flue gas qualities and impurities presence.

Regarding the transportation advantages and high purity of their final products, cryogenic technologies have been increasing attentions to integrate conventional capture processes: cryogenic-based hybrid processes [48]. Song et al. have reviewed the status and development of such processes [48]. Most of the ongoing studies are at laboratory scale and it can be divided in 4 groups: absorption-based (60%), followed by adsorption (20%), membrane-based (16%) and cryogenic-based (4%). It was concluded that hybrid processes show potential improvements regarding CO_2 recovery, energy penalty and installation investments [48].

2.2.7. Hydrates-based

Hydrate-based carbon capture (HBCC) technologies have been increasing attentions due its unique separation mechanism and mild operation conditions [49,50].

Concept of hydrate-based separation processes

Gas hydrates or clathrates are nonstoichiometric solid crystalline compounds formed by a network of cavities of hydrogen-bonded water molecules which block gas molecules (guests), such as CH_4, CO_2, N_2 and H_2. Those gas molecules form strong van der Waals forces with water molecules, resulting in a polyhedral crystalline structure. They form under favourable thermodynamic conditions of low temperature and high pressure and depending on guests' molecules, they can assume three different structures [50]: cubic structure I (S_I), cubic structure II (S_{II}) and hexahedral structure (S_H). Typically, small molecules such as CO_2, methane, ethane or xenon form S_I structures. However, for N_2/CO_2 mixtures, when CO_2 molar concentrations are lower than 15%, hydrates will form S_{II} structure [51]. It is also worth mention that theoretically, hydrates formation is not a chemical reaction, as there are no creation and destruction of chemical bonding and the conceptualized reaction is not stoichiometric, as n is not necessarily integer [51]:

$$G + n\,H_2O \leftrightarrow G \cdot n\,H_2O \quad (1)$$

Theoretically, the concentration of guest compounds must be higher than their solubility in water for the crystallization process to occur. Hydrates can only form at temperatures lower than the equilibrium temperature at a given pressure, or at pressures higher than the equilibrium pressure, at a given temperature (see Figure 6).

Hydrate based separation processes are based on the different affinities for the guest molecules to crystallize hydrates and they have been applied for separate CO_2 from flue gas, methane from nitrogen, hydrogen purification and many others [51]. HBCC technologies are still at early stage of development and the performance of processes has been studied on two major fronts: phase equilibrium of pure CO_2 hydrates and the enhancement of recovery rates of CO_2 while optimizing energy consumption either by using chemical additives or by improving mechanical processes. Therefore, the main demands are high hydrate formation rates, low hydrate pressure, as well as the prevention for agglomeration to occur in downstream processes as pipeline transportation [50,52,54].

The efficiency of HBCC technologies is described by the following parameters [50]:

- hydrates induction time, representing the time taken for a crystal nuclei to form, is determined by the time that gas consumption becomes observable;
- gas consumption, which is the maximum amount of gas trapped and is determined by the subtracting to total number of moles prior to process the number of moles at the end through the application of ideal gas law;

- hydrate equilibrium pressure;
- CO_2 recovery or split fraction (S.Fr.) is the ratio between the moles of CO_2 in hydrate phase and the moles of CO_2 in the feed gas;
- separation factor (S.F) for a flue gas containing CO_2 and other gas (A) is calculated by the following equation:

$$S.F. = \frac{n_{CO_2}^{H} \times n_A^{gas}}{n_{CO_2}^{gas} \times n_A^{H}},$$

Where $n_{CO_2}^{H}$ and $n_{CO_2}^{gas}$ are the moles of CO_2 present in hydrate phase and in residual gas phase, respectively and n_A^{H}, the moles of the other gas (A) in hydrate phase and n_A^{gas} the moles of the later in residual gas.

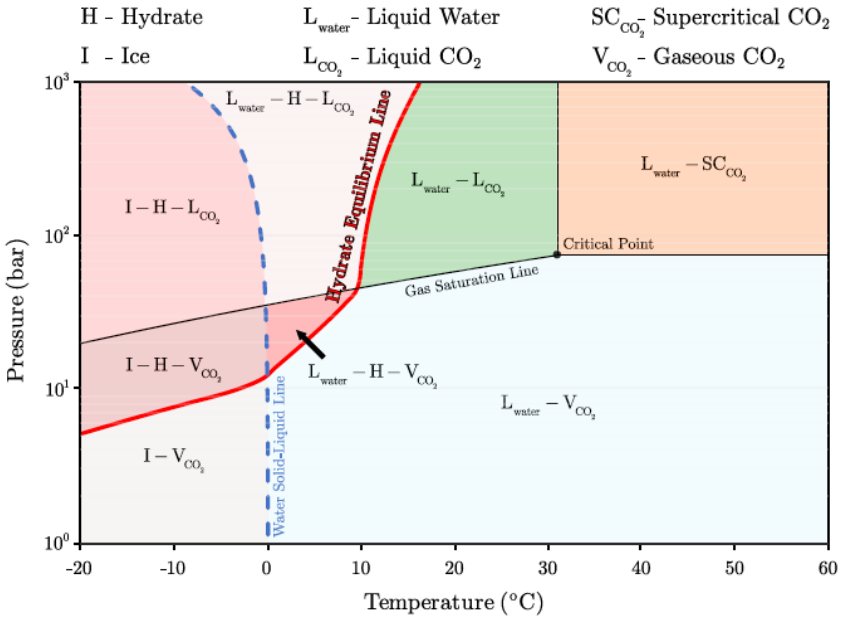

Figure 6 - CO_2-HO_2 phase diagram. Source: Costa, M. [51].

Chemical additives

Chemical additives are generally divided in two groups: thermodynamic promoters (THF, TBAB, TBAF, CP, C_3H_8) and kinetic promoters (SDS, DTAC) [49]. These additives can change the natural tendency of structures formation, increase the number of caged molecules and enhance hydrates stability [51].

Thermodynamic promoters are small molecules that take part in the construction of structures enhancing their stabilization at moderate conditions of temperature and pressure. The most significant results are the reduction of hydrate equilibrium pressure and the increased CO_2 selectivity [49,50]. The most tested promoters for HBCC are TBAB (tetra-n-butyl ammonium bromide) and THF (tetrahydrofuran) [52]. According to Linga et al. studies, the addiction of THB to a CO_2/H_2 flue gas mixture decrease induction time, switch hydrate structure from S_I to S_{II} and lower hydrate formation pressure (from 8.4 to 0.5 MPa for a 17%CO_2/83% N_2 mixture with 1 mol% of THB in the water at 275.15 K) [53]. However, because THF molecules compete with CO_2 for large cavities, it cannot remarkably improve gas consumption and CO_2 separation factor [52]. The addiction of TBAB shifts the phase equilibrium to even lower boundary resulting in shorter induction times, but both gas consumption and hydrate growth rate decrease with increasing TBAB concentration (for a 16.9%CO_2/83.1%N_2 mixture at 11.0 MPa, S.Fr. and S.F. were 36.7% and 5.3 respectively and 42.1% and 13.2 at 10.0 MPa according to Linga et al.) [53]. The mixture of these additives can improve separation processes. Yang et al. have tested different additive mixtures compositions with THF and TBAB and found that with the increase

in THF and/or TBAB mass fraction, both gas consumption and S.Fr. increased substantially. The mixture with 5% of THB and 10% of TBAB was considered the most efficient for separation [54].

Kinetic promoters are mostly surfactants that do not alter thermodynamic equilibrium, instead they reduce induction time by improving hydrate formation rates, possibly due an increase of the gas solubility in water [49, 51]. Among kinetic promoters, the most used are T-80, DTAC and SDS [51].

Other substances can act as inhibitors of hydrate formation, either by lowering the equilibrium temperature or increasing the equilibrium pressure [51]. Thermodynamic inhibitors, such as alcohols, glycols and salts, are considerably soluble in aqueous solutions and increase competition with the original guest molecules for water cages and ion through hydrogen bonding [51]. Kinetic inhibitors are low molecular weight polymers which are frequently used for pipeline transportation to prevent plug formation. Regarding pipelines blockage, Rong Li et al. proposed the use of an anti-aglomerant composed of 90% cocamidopropyl dimthylamine and 10% glycerol (6-8 wt. % in solution), which can prevent TBAB hydrate from agglomerating in a 19.3-29 wt. % stable state of slurry solution over 72h [52]. Besides, they also conclude that the addition of AA can improve S.Fr. and S.F. to 70.3% and 42.8%, respectively, and it can reduce particles size, which enhances storage capacity [52].

Carbon capture processes

Besides chemical additives, studies of different mechanical processes have been carried out with the aim of reducing energy consumption and improve CO_2 recovery. The most tested processes include stirred tank reactors, fixed bed crystalliser, bubble tower and spray tower [49]. In stirred tank reactors, agglomeration of crystals can occur reducing hydrate formation rate [52]. Fixed bed crystalliser has been studied as an alternative to overcome this problem. Silica as a cheap resource and its porous nature is a promising material to be used in these processes. The dispersed water in silica pores promotes water and gas mixture which eliminates the need for intensive mechanical agitation and water excess [50]. Both silica gel and silica sand bed have been tested, and results of these studies suggest that silica sand bed have better performance [50]. In a gas bubble tower, a bubble plate is displaced at the bottom of the reactor, from which CO_2 is introduced in the reactor. Bubbles of CO_2 arise, and hydrates forms firstly from the gas-liquid boundary around the bubble and then grows in the inner side of the bubble to form a hydrate particle [55].

These technologies have the advantage of small energy penalty (6–8%) [4]. US DOE considers this technology to be the most promising long-term CO2 separation technology [4].

Table 1 summarizes the main advantages and disadvantages related to each separation technology reviewed.

Table 1 - Main advantages and disadvantages of different separation technologies.

Type	Advantages	Disadvantages
Membranes	Capture efficiencies can achieve more than 90% in multi-stage systems Work continuously and at ambient temperatures Do not require additional chemicals Relatively low installation costs	Huge energy penalties Depending on the processes, active deposits can be frequent, affecting efficiency.
Absorption	Most mature process for CO2 separation High separation efficiencies (>90%)	Separation efficiencies are dependent on CO2 concentration. Significant amounts of heat for absorbent degradation are required. Environmental impacts related to absorbent degradation need to be better understood.

Table 2 - Follow-up of table 1 'Main advantages and disadvantages of different separation technologies'.

Type	Advantages	Disadvantages
Adsorption	Capture efficiencies from 85 to 90%.	Energy penalties and costs are still not competitive.
	CO2 purity can achieve 95% in some processes.	
	Possible hydrogen co-production.	
Chemical Looping combustion	Avoids energy intensive air separation processes.	There are no large-scale operation.
		Impossibility of retrofitting existing power plants.
		Environmental aspects related to particles emissions
Calcium Looping	Energy penalties are competitive with other technologies.	Under developing technologies.
	It provides the possibility for a co-production wof syngas.	
Cryogenic	CO2 can be captured in different phases and so, an additional compression stage can be avoided	The required cold energy consumption can increase energy penalties
	Possibility for recovering high purity CO2, which is more valuable for industrial market.	Some technologies performance is highly depend on flue gas conditions.
		Under developing technologies: most have been tested at laboratory scale only.
Hydrates	Operation at mild pressures and temperatures	Under developing technologies.
	Easy to regenerate	
	Capable of separating gas mixtures	

2.3. Transport

After separation, CO_2 needs to be transported to the storage sites or industrial facilities. The mean of transportation will depend on the quantity of CO_2, the distances, territory specifications and CO_2 properties. Pipelines are the most explored alternative, due to its feasibility for long distances, for long-term sources and specially for onshore transportation [4]. For moving CO_2 on small scale, transportation via rail or road is more cost-effective. Ship will be the best option for long distances or when there's the need to move over large bodies of water [13]. An important parameter to optimize in transport stage is the mass/volume ratio. For that reason, CO_2 is mostly transported as a dense phase, either in liquid, supercritical or solid phase.

2.3.1. Pipelines

The most efficient phase for transportation is either as at a liquid state or as a supercritical fluid (above its critical point: 31.2 ºC and 73.8 bar [56]), since in both cases the volume is ordrs of magnitude smaller but materials are still flowable [13]. Thus, when conventional absorption, adsorption or membrane separation technologies are used, there is an additional need for compressing the gas. The typical range of pressures and temperatures for transporting CO_2 supercrititical via pipeline are 85-135 bar and 13-44 ºC, respectively [21].

Hydrate formation and corrosion

As aforementioned, hydrate formation can occur during transport by pipeline, in the presence of water. When the hydrates concentration increases, the transport fluid does not have enough momentum to drag the solids which can lead to pipeline blockage [51]. High levels of water and other hydrate-formed compounds as sulphurs increase the risk of hydrate formation [13,51]. Another problem concerning pipeline transportation is corrosion caused by the presence of some compounds as H_2S, amines, NH_3, methanol and glycols. Despite, alloyed steel being more resistant to corrosion the most used material is carbon steel as it is much cheaper. The estimated corrosion values of carbon steel for transport CO_2 supercritical are 10 mm/year [13].

Therefore, the level of impurities is an important variable to consider. Mitigation of hydrate formation and corrosion risk often requires pre-treatment units and it can be expensive. In the literature, values suggested for limiting the water content for supercritical CO_2 transport can be found (from 250 ppm to 640 ppm [57, 58]). The development of more-resistant polymers to cover pipeline components is also a work front.

Pressure drop

Another important technical issue regarding pipelines transportation is pressure drop management. As temperatures are not easily controlled along the pipeline, the vapour-liquid equilibrium should be mostly controlled upon pressures [13]. Thus, pipelines design, based on hydrodynamic properties of CO_2, which depend on temperature, pressure, flow rate and composition, is an important step to avoid hydrate formation, corrosion and other operational problems.

Hydrate slurry transportation

Transportation of CO_2 in a hydrate slurry phase has been little mentioned in literature, as HBCC technologies are still at early stage of development. The CO_2 transportation under these conditions would eliminate the need for gas compression and/or liquification which is an energy intensive step on CCS chains. Moreover, the risk for hydrates to block pipelines could be reduced as the drag force in a slurry phase is higher than in a gaseous phase. Volume reduction is also a potential economic advantage: when comparing to supercritical gas, hydrates transportation, even using a 30% in weight slurry, lead to a 60 times volume reduction [51]. On the other hand, a pre-treatment unit for removing undesirable compounds and injection of anti-agglomeration compounds could be needed, as well as pipeline insulation for temperature control as temperatures needed (about 2 ^oC) are lower than the typical range [51]. Hence, more studies should be developed in order to accurate the technical and economic feasibility for hydrate slurry transportation.

Infrastructure

Despite being a mature technology, only a few pipelines are currently used to carry CO_2 being almost entirely used for EOR projects in United States. One recent offshore underwater pipeline has been developed in Barents Sea for the Snøhvit project.

The number of accidents reported in the period of 2002 to 2008 was about 0.76/year for every 1000 km over an overall pipeline length of 5800 km, much lower than the incidents involving gas/oil pipelines. However, the statistical significance is uncertain, as those networks differs some orders of magnitude from CO_2 pipelines [4]. Regarding this topic, the transport of CO_2 in a slurry state phase could also improve the safety associated with the process as the gasification rates is much slower than for supercritical state [51].

Integrated networks for CO_2 transportation could lead to costs reduction, and has been studied by European Union under projects such as COMET, which purpose was to study an optimal network for CO_2 transportation via pipeline, involving the study of potential storage sites in West Mediterranean (Portugal, Spain and Morocco) [59].

2.3.2. Ship

Transportation by ship is more flexible than by pipelines as it is not so dependent on design conditions and can better adapt to fluctuations of CO_2 production. The most efficient phase for ship transportation is cryogenic liquid or hydrates due their volume reduction. Although some losses are expected to occur, they can be minimized by utilising a refrigerated container ship [13]. In CCS projects in regions as Norway, Baltic Sea, Japan and South Korea, ship transportation has grown in recent years, but a network has not yet been developed [21].

Transportation cost are highly dependent on regional paradigms. A case study in North Sea reveal that transport by ship tanker in LPG is cost competitive with pipelines with costs ranging

20 to 30 USD/tonne when more than 2 $MtCO_2$/year are transported [4]. A case study for China comparing costs of the 3 mean of transportation is presented in the table below.

Table 3 - Example of cost studies for different types of transport in China, in 2011. Source: Leung D. [4].

China - Transportation of 4000 ton CO2/day

Transport by ship tankers	Transport by railway and road tankers	Pipelines
7.48 USD/ton CO2	12.64 USD/ton CO2	7.05 USD/ton CO2

2.4. Storage

From the results of IPCC climate pathways models, multi-gigatonnes annual CO_2 storage rates are expected for the next decades [1], leading to the need of characterise, appraise and develop thousands of individual storage sites [16]. Several projects have been implemented worldwide to estimate and characterise potential storage sites. In Europe, the GeoCapacity project has initiated the assessment of European capacity for geological storage of CO_2 in deep saline aquifers, oil and gas structures and coal beds. The results claimed that storage in deep saline aquifers is the most promising in Europe, as both hydrocarbon and coal fields together accounted for just 31.500 mega tonnes of storage capacity, while annual CO_2 emissions from large sources were by that time (2009) 2000 mega tonnes [60]. Figure 7 shows the global storage resources worldwide in Gtonnes.

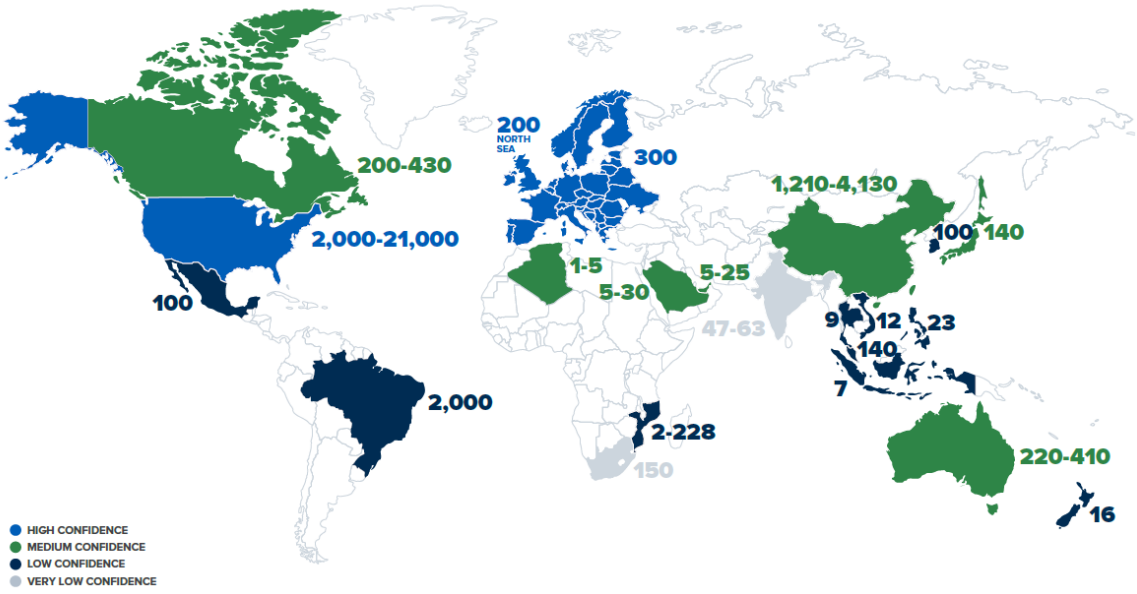

Figure 7 - Global storage resource estimates in gigatons around the world. Source: Global Status Report 2019 [16].

2.4.1. Geological formations

Geological storage of CO_2 is not a novel technology, it has been performed for several years in United States for Enhanced Oil Recovery (EOR) and in CCS dedicated projects as Sleipner, Weyburn and In Salah [11]. Information and experience gained through these projects indicate the feasibility of this option for CO_2 emissions mitigation strategies. The key issues relating to storage areas that have been investigated are the understanding of different trapping mechanisms and the likelihood of CO_2 migration and detailed assessments of safe storage sites capacity [13].

Leakage risk is the most controversial issue regarding CO_2 storage because if significant leakage rates are verified in relatively short time periods, the feasibility of all CCS chains become compromised. It could also cause groundwater degradation and ecotoxicological risks for in situ ecosystems. Leakage can occur when a site is poorly characterised and monitored as it can be caused by leaking injection wells, abandoned wells, leakage across faults and ineffective confining layers [11]. For sites characterization, general requirements must be considered, including appropriate porosity, thickness and permeability of the reservoir rock, sealing capacity of cap rocks and stabilization of geological formation [4]. To ensure the site stability, injection pressures must be kept to as low as necessary to avoid caprock damaging and wells must be properly sealed [11]. The likelihood for leakage to occur have been decreasing while monitoring technologies have been improved and regulatory frameworks became tighter. It is considered likely that 99% or more of the injected CO_2 will be retained for 1000 years [11]. However, Boot-Handford et al. stated that it is wrong to associate a leakage rate over time has the 'low risk of leakage occurs mainly during the injection period and declines with time as pressure dissipates and the CO_2 becomes less mobile' [13].

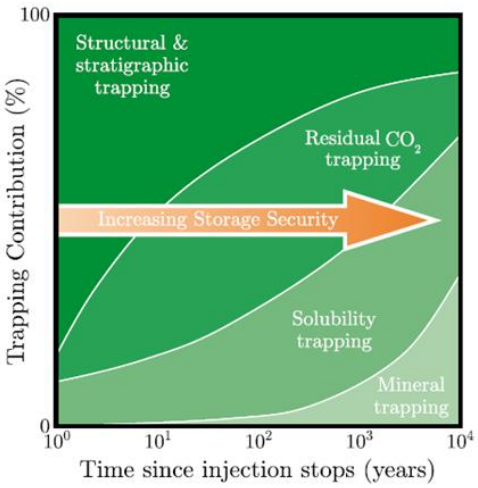

Figure 8 - Storage security as a function of the trapping mechanisms. Source: IPCC, [11].

Depending on site specific characteristics, there are four main mechanisms through which CO_2 can remain underground: physical trapping bellow an impermeable, confining layer (cap rock); capillary trapping as an immobile phase within pore spaces of the storage formation; dissolved in the in situ fluids which tends to slowly sink through saline aquifer; adsorbed onto organic matter in coal and shale; and by reacting with host rock precipitating carbonate minerals (see Figure 8) [11,13].

CO_2 can be injected into depleted oil and gas reservoirs, coal bed formations, saline formations and applied for EOR.

When stored in depleted oil and gas reservoirs, previous infrastructures can be used, and the information already obtained regarding geologic formation can represent an advantage to mitigate leakage risks [11].

CO_2 can be injected into deep coal beds for methane recovery (CO_2-ECBM). Successful projects have been carried out in New Mexico (USA) and Alberta (Canada) [4]. This technology has been increasing interest as methane is the cleanest of the fossil fuels, and several projects have been recently started worldwide [4].

Saline aquifers have no commercial value but represent an enormous potential capacity for CO_2 storage. Besides, some studies have suggested that CO_2 storage in deep saline aquifers have little or insignificant environmental impacts [4]. However, more data regarding post-injection behaviour inside the reservoir need to be assessed for leading plume stabilization and long-term trapping. Regarding the widespread availability of such sites, it is likely that they will be highly used for CO_2 storage, located in the same region as world's emissions sources [11].

In Enhanced Oil Recovery, the injected CO_2 fluid provide pressure to drive the extraction of residual oil and gases for further energy valorisation. Due their profitability, EOR projects are important to accelerate the development of pipelines network and thus CO_2 storage projects in general. However, they contribute little to CO_2 net reduction.

The costs of geological storage depend on site specification as depth of storage formation, the number of wells needed for injection and whether the project is onshore or offshore. In CCS special report released by IPCC, storage costs, including monitoring were presented within a range of 0.6-8.3 US$/tonne of CO_2 stored with the possibility of negative costs of 10-16 US$/tonne of CO_2 if an Enhanced Oil Recovery system is applied [11].

2.4.2. Deep ocean storage

At depths greater than 3 km, CO_2 liquefies and becomes denser than the surrounding water which will make it sunk to the bottom [4]. In this way, CO2 can be kept into the ocean for several hundreds of years. Although, IPCC has recognised the great potential of ocean storage of CO_2 [11], this option is rather disregarded due to acidification problems and the potentially CO_2 leakages in short-time period. Indeed, the European directive related to geological storage of CO_2 states the prohibition of the 'placement of CO_2 into the water-column of the sea and on the seabed, because of the potential negative effects' [61].

2.4.3. Hydrate storage

The storage of CO_2 hydrates can add some advantages compared to supercritical CO_2, as it requires similar high pressures but can stabilize at lower temperatures, thus offering a wider range of possible storage sites comprising the so-called 'cool storage' sites [62]. Moreover, its 'lower buoyancy and higher viscosity would also help reduce the rate of vertical mitigation from the storage horizon' [62]. Rochelle et al. identifies the possibility of using CO_2 hydrates as cap rocks, however they mention the need for a deep understanding of the small-scale interactions between hydrates and the sediment grains and their influences on the overall physical properties of the sediment and trapping mechanisms.

Chapter 3

Case study: Net4CO_2 capture technology on power generation sector in Portugal

3.1 Energy and electricity generation in Portugal – emissions and trends

3.1.1 Energy production and consumption per energy source

In the past two decades, Portugal have increased its production share of the total primary energy from 15 % in 2000 to 29 % in 2018 [63]: for one hand the installed capacity for electricity generation in the country has been increasing (from 15 GW in 2007 to 22 GW in 2018) mainly due to the Renewable Energy (RE) sources (from 7.4 GW in 2007 to 14 GW in 2018); for another hand, the primary and final energy consumption have decreased. Figure 9 shows primary (at left) and final energy consumption (at right), and the shares among energy sources. It is possible to conclude that Portugal is still highly dependent on fossil fuels.

Oil's consumption as primary energy has been decreasing over the last two decades however it is still the main source (40.2%), followed by natural gas (24.2%), renewables (21.3%) and coal (14.4%) [63]. In 2017, the consumption of final energy was 15 613 ktoe[6] with the following shares: 48.4% of oil, 25.7% of electricity, 11.1% of natural gas, 7.3% of heat and 6.8% of renewables [63]. Besides being the second more contributor activity (following transports), industry sector accounted for the higher consumption decrease (-2.4% during the period of 2007-2017).

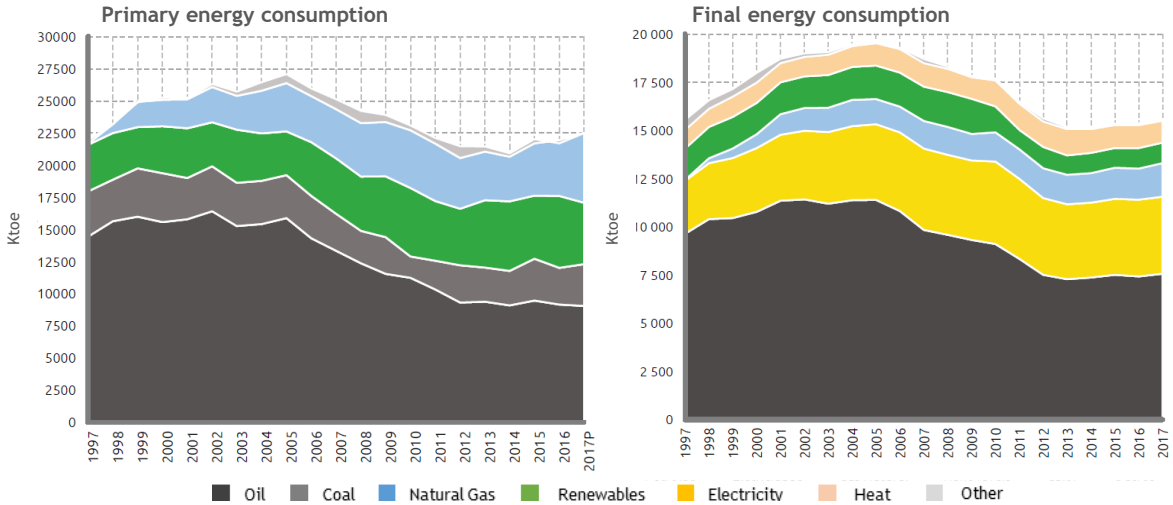

Figure 9 - Primary energy consumption evolution at left and final energy consumption evolution at right. Source: DGEG [63].

The domestic production – supported on endogenous sources – is dominated by biomass (54% in 2017) and electricity (35%). About 95% of the electricity comes from hydroelectric and wind parks, and only 5% on solar sources. Most of the biomass is used for heat and electricity production although a very significant amount is for direct consumption (34%) [63].

Figure 10 represent the share of each energy source (endogenous and non-endogenous) for the electricity generation in Portugal from 2007 until 2017. The production of electricity in plants

[6] Toe means tonne of equivalent oil.

over the last ten years has fluctuated between 44% and 71% of gross production. Figure 11 shows the consumption of several energy sources on their transformation[7]. The intensity of use of these energy forms depends on the hydrological years, as this source represents more than half of the installed capacity of Renewable Energy (RE). The use of oil for electricity is in decline, while the use of biomass on thermal powerplants and co-generation has increased in 34 %.

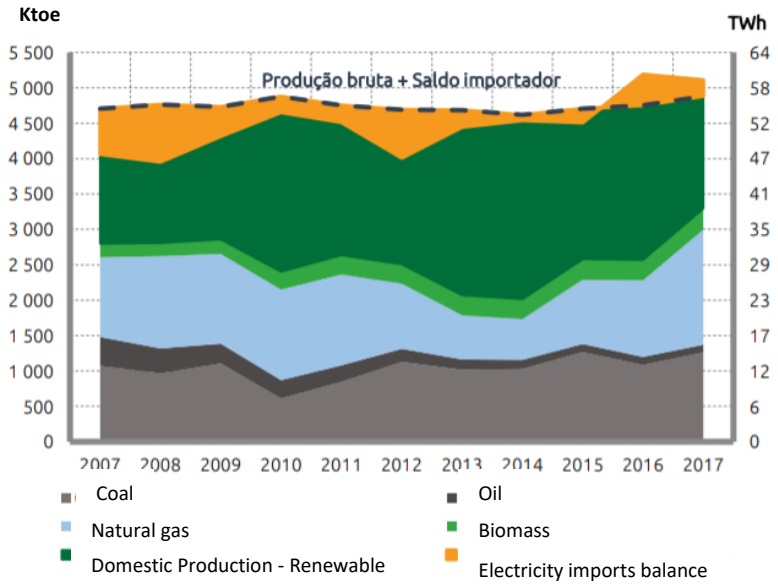

Figure 10 – Electricity generation by primary source [63].

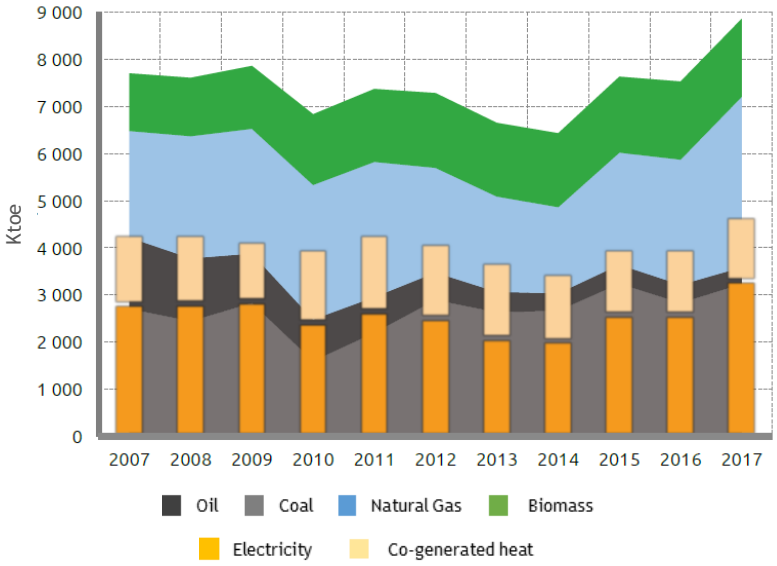

Figure 11 - Transformation for electricity production. Source: DGEG [63].

The primary energy consumption per capita has been decreasing since 2005, achieving the value of 2.2 toe/inhabitant in 2017, while consumption of electricity has been slightly increasing to 4.6 MWh/inhabitant.

[7] The transformation of energy takes place mainly in two major industrial processes: refining and electricity production in thermal power plants, including cogeneration [63].

3.1.2 Carbon intensity and National Plan for Energy and Climate

After a few years of economic prosperity, GHG emissions dropped following a global tendency that was marked by the global economic crisis [3]. Besides the increase in 2017, emissions per capita were about 21% lower than the average in UE-28 (8.7 ton CO_{2eq}/capita). The 'carbon intensity of energy consumption'[8] in 2017 was 2.27 ton CO_2/toe (-7.7% and +4.5% comparing to 1995 and 2016, respectively).

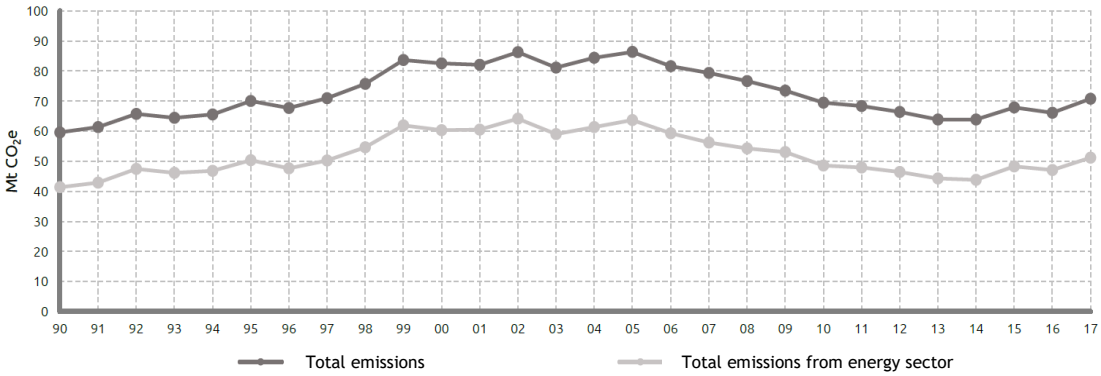

Figure 12 - GHG emissions evolution in Portugal. Source: APA [42].

Under Paris Agreement goals, Portugal has defined strategic targets, by the so-called 'National Plan for Energy and Climate', for the next decades towards carbonic neutrality achievement: GHG emissions reduction of 45-55% until 2030, 65-75% until 2040 and 85-90% until 2050. The sectors accounting for a more significant CO_{2eq} emissions reduction are energy and transportation.

Figure 13 shows the expected evolution for installed power and Figure 14 represents the expected evolution of the electricity production mix by 2030.

Evolution of the installed capacity by 2030

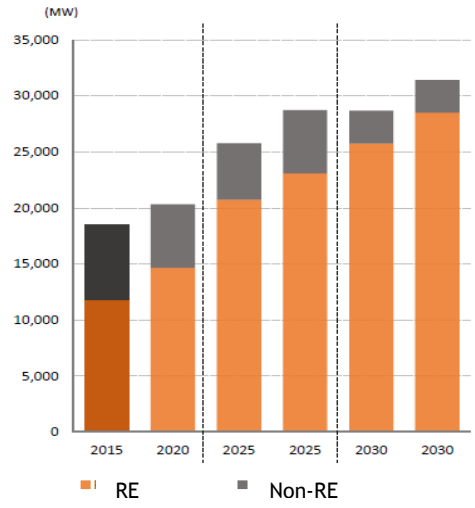

	2015	2030
Fossil Fuel	6,7 GW	2,9 GW
Hydropower	6,0 GW	9,0 GW
Fossil	5,0 GW	8,0 - 9,2 GW
Solar	0,5 GW	8,1 - 9,9 GW
Other RE	0,3 GW	0,6 - 0,7 GW
TOTAL	**18,5 GW**	**28,6 – 31,7 GW**
TOTAL RE	**11,8 GW**	**25,7 – 28,8 GW**

Figure 13 - Evolution of the installed capacity by 2030. Source: PNEC [64].

[8] It results from the ratio between total GHG emissions related to energy consumption and primary energy consumption [63].

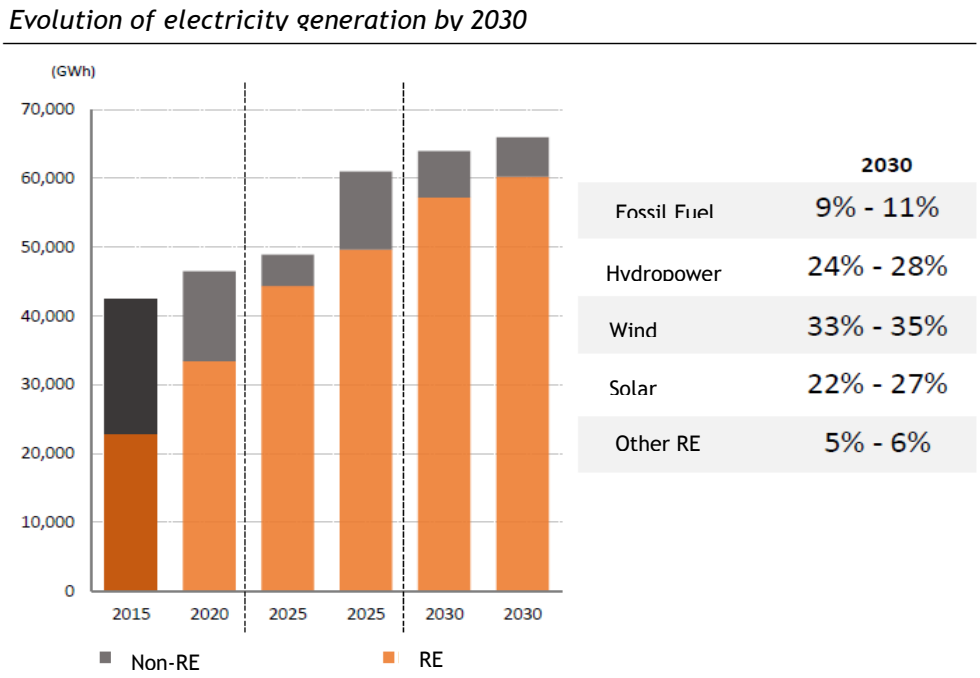

Figure 14 - Evolution of electricity generation by 2030. Source: PNEC [64].

In 2030, the electrical generating system is expected to have an installed capacity of about 30 GW (+10 GW than 2015), for which the share of RE would achieve 80 %.

3.1.3 CCS retrofiring on Sines and Ribatejo power plants

CCS technologies are included on the agenda for the innovation fund, under a perspective of support the national transition to a decarbonised economy [65]. On a study developed by National Laboratory of Energy and Geology (LNEG) with the aim of defining a roadmap for CCS technologies in Portugal [66], an econometric analysis regarding the CO_2 capture technologies implementation in both power plants and cement industries, in the country, for the next decades, indicates cement production industries as serious candidates to be first movers in adopting these technologies, as carbon capture technologies may represent the only solution for emissions reduction associated with the sector [66]. Yet, the purpose of the current study will be the analysis of environmental performance through Life Cycle perspective of a novel CO_2 capture technology on two thermal power plants in Portugal: one using coal as its main fuel – Sines – and another using natural gas – Ribatejo. These power plants have similar and the higher installed capacities among national thermal power plants (1176 MW on Ribatejo and 1256 MW on Sines). Sines power plant emits about 0.84 tonnes of CO_2 per MW generated (average value from 2009 to 2018) [67], while Ribatejo powerplant emits about 0.36 tonnes per MWh (average value from 2008 to 2018) [68]. The transition of both powerplants to produce hydrogen has being studied.

3.2 HGtS separation technology by Net4CO2

$Net4CO_2$ is a non-profit collaborative laboratory (CoLAB) which mission relies on developing processes and products which provide competitive solutions for the CO_2 capture, separation and valorisation. Moreover, as a CoLAB, it has the specific long-term goals of strengthening synergies between industry, academic and scientific communities, develop scientific human resources, in particular young graduates and develop Portuguese-based technologies to foster the evolution of the energy mix of the future in a sustainable global environment [69].

HGtS (Hydrate Gas-to-Solid) is a novel technology developed by $Net4CO_2$ for capturing CO_2 by mixing the flue gas with water to continuously produce gas hydrates – 'crystalline solid materials, wherein non-polar small molecules, such as CO_2, CH_4, N_2, H_2 and other small hydrocarbons are trapped in water molecules (cages) linked by hydrogen bonds' [70].

To overcome typical difficulties regarding mixing and crystallization by improving mass transfer rate without compromising energy penalties, as well as, improving heat transfer as hydrates precipitation is a strong exothermic process (hydrates fusion heat of 152 kWh p/tonne of H_2O), this process makes use of the NETmix technology – a novel static mixer and chemical micro-reactor characterised for its high efficiency for mass transfer processes, control of fluid mixture and energy consumption. NETmix 'has been successfully tested for: fast precipitation/crystallization reactions; liquid-liquid reactions; photocatalytic reactions; and the production of gas hydrates' and it's been used by *Fluidinova SA* to produce nanocrystalline hydroxyapatite [71].

The device 'consists on a 2D network of mixing chambers (zones of complete mixing) interconnected by transport channels' [71]. Each chamber is linked with two inlets and two outlet channels forming a unit cell, which is replicated within the network (Figure 15) [71]. Proper mixing is achieved above the critical Reynolds number at the channels that enables flow to evolve from a steady flow to a self-sustained dynamic and chaotic oscillatory flow regime inducing laminar mixing [71]. Hence, NETmix is particularly efficient for complex and fast kinetics reactions which mixing quality and intensity are critical [51]. Different designs enable a vast range of selectivities for complex reactions due the possibility to set different mixing rates combined with different reactant injection schemes [71].

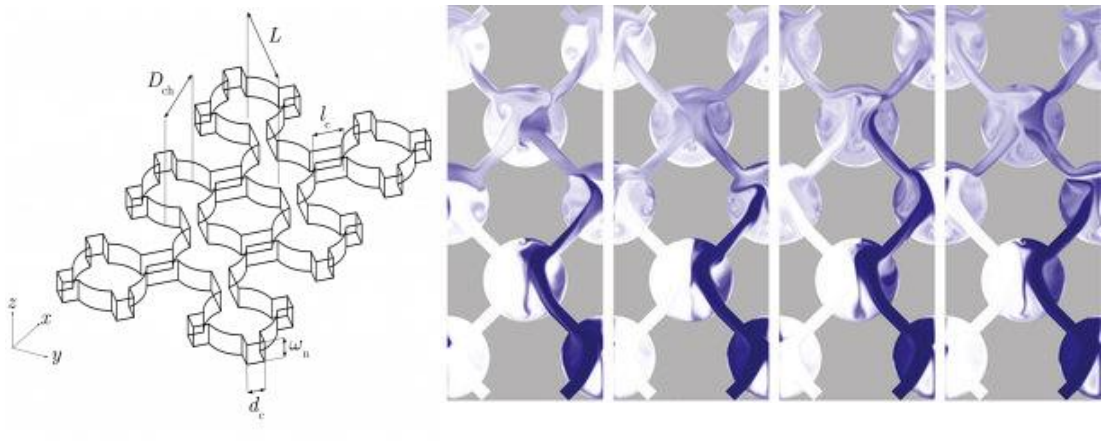

Figure 15 - NETmix's network with 5 rows and 2 collumns. Source: LSRE-LCM, FEUP [71]. At right, the fluid mixture within the network. Source: Lopes, José et. al., 2013 [72].

HGtS technology for CO_2 capture has been successfully demonstrated at lab (1 kg CO_2/h) and pilot scale (10 kg CO_2/h). Separation tests from a N_2/CO_2 flue gas composition are currently at demonstration and the installation of a unit for capturing 1 ton CO_2/h is being planned [70]. It is a continuous counter-current process between water and the flue gas and makes use of THF to reduce equilibrium pressure [51]. The mastery behind this process consists in optimizing both mass and heat transfer rates to promote crystallization under favourable conditions of

temperature and pressure. When isolated from thermal energy sources, hydrates can be stable at ambient pressure and cold temperatures (-20 ºC) [70]. The gas suffers a drastic volume reduction which facilitates further transport and storage (see Figure 16). The post-combustion process has proven to be technically feasible to capture CO_2: about 85 % is captured into hydrate cages while the remaining emissions are dissolved in the water. The result is a slurry with water and hydrates containing all the flue gas emissions. The process is described in more detail on section 4.

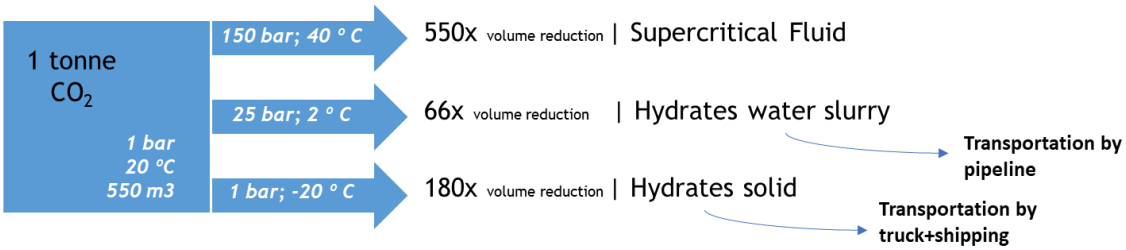

Figure 16 - Gas volume reduction due hydrates formation.

3.2 CO_2 fate

After captured, CO_2 can follow directly to a pipeline for further storage or remain temporarily deposited in a downstream unit for further shipping to long-term storage or industry use.

In this study, the fate of CO_2 will be long-term storage, and the used data is based on a study developed by a National Laboratory of Energy and Geology (LNEG) et al. with the aim of defining a roadmap for carbon dioxide transport and storage in Portugal [66]. In the Figure 17 the circular clusters represent the potential locations for CO_2 storage and the lines represent potential future pipelines interconnecting the main sources of CO_2 emissions in Portugal Mainland, *i.e.* fossil fuel-based power plants and cement industries. For each storage basin is presented an estimation of the storage capacity and a qualitative risk evaluation. The study also presents an economic analysis to evaluate the feasibility of each storage cluster and mean of transportation depending on the amount of captured CO_2 and the distance between source and storage location. By crossing variables such as storage capacity, risk and costs, it was concluded which are the most feasible clusters – S03 and S04 – although, clusters S01, S02 and S05 also presenting good preliminary results in terms of security.

An economic analysis to the mean of transport indicates that for CO_2 sources close to Lisbon and Sines ports, pipelines are more feasible than ship when the amounts of CO_2 produced annually are higher than 4 Mtonnes to 15 Mt, depending on the offshore cluster considered [66].

In the Figure 17, the stars represent the locations of the power plants object of study. From the north to the south: Ribatejo and Sines.

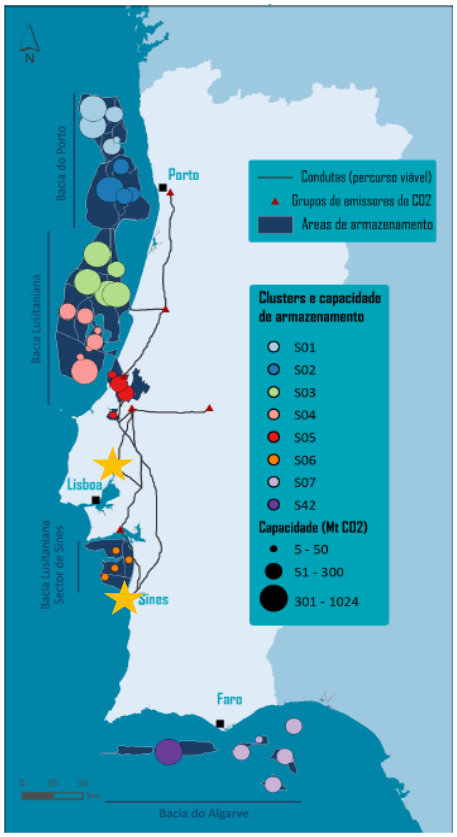

Figure 17 – Location of potential storage areas and feasible paths for pipeline construction for CO_2 transport.

Chapter 4

Life Cycle Assessment methodology

The main goal of this study is to evaluate the environmental performance of the implementation of HGtS carbon capture technology in some of the Portuguese fossil-fuel based power plants followed by long term storage. To conduct a proper study, overall implications in power generation processes must be taken into account. Besides the fraction of CO_2 captured: the potential increase of CO_2 production resulting from loss in overall efficiency of power plants or industrial processes due the additional energy penalty and the impacts of CO_2 transport and storage, and the possible leakage that may occur during both transport and long-term storage [11, p.16]. For this reason, Life Cycle Assessment was the tool chosen to conduct the study, as it addresses the potential environmental impacts considering all the inputs, outputs and other relevant environmental aspects throughout the entire life cycle of a technology or a product [73, 74, 75]. The methodology applied is framed by ISO 14040:2006 and ISO 14044:2006 and follows the approach of 'cradle to grave'. The stages of a LCA performing according to the methodology applied are presented in Figure 18.

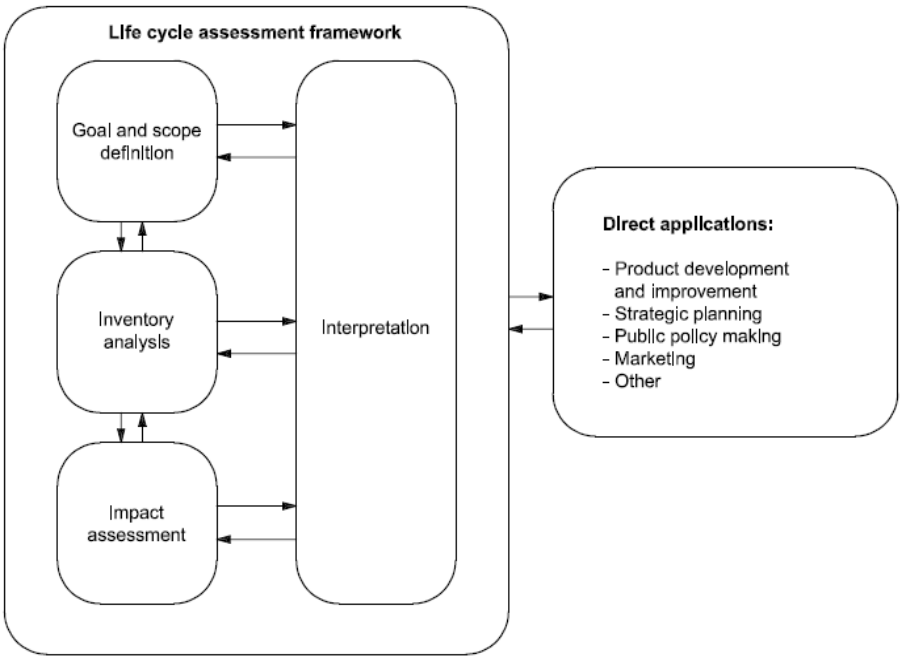

Figure 18 - LCA stages according to ISO 14040:2006. Source: ISO14040:2006(E) [73].

Goal and scope definition describe the purpose of the study, the intended audience, the object of study, functional unit, spatial and technical system boundaries, allocation procedures, impact categories considered, data source and quality as well as the limitations of the study [73, 74]. Inventory analysis quantifies the inputs and outputs within system boundaries, which are related to the functional unit [73-76]. In order to make an attributional analysis to each life cycle stage, one must develop a process with inputs and outputs for each stage. 'Impact assessment characterizes the effects of these inputs and outputs considering resource depletion, human health, ecosystem quality and climate change' [76]. During the interpretation of the results, the main conclusions regarding impacts weight, attributional analysis and comparison between different scenarios are taken into account to develop a set of 'recommendations and implications for decision making' [76].

4.1 Previous studies review

Life Cycle Assessment is a powerful tool to evaluate the performance of CCS technologies as an attempt to quantify the benefits and the trade-offs that occur from their application on industry and energy sector, as well as comparing different technologies. Numerous studies concerning LCA of electricity production and CCS technologies have been conducted.

Petrescu L. et al. [14] simulate and compare three novel separation technologies on supercritical pulverized coal power plant with a benchmark option (without CCS), under a 'cradle to grave' approach – MDEA and aqueous ammonia adsorption as well as Calcium Looping (CaL). They concluded that these are more favourable than the traditional amine-based CO_2. For a capture rate higher than 85 % for CCS scenarios, the Global Warming Potential (GWP) achieved overall reductions from 41 % to 52 %, however all other impact categories are highly penalized, with loads that increase over 100 % for most of them. While aqueous ammonia usage proved better performances for some impact categories as GWP, abiotic depletion and eutrophication potential, CaL achieved the best results for the remaining.

Schreiber A. et al. [77] combined an existing projection of the development of electricity production with CCS environmental assessment. The technology modelled was post-combustion with amine (MEA) scrubbing. The authors concluded that the implementation of CCS leads to a considerable loss of efficiency causing an additional requirement of about 50 million t of lignite in 2030 in comparison to the reference scenario in 2010. The GWP on its turn, can be reduced up to 70%. Other environmental burdens increased in part considerably. The study revealed the coal composition and origin have a significant role on the overall performance, affecting both CCS and reference scenarios, pipeline transport and storage score a minor contribution.

Volkart K. et al. [78] conducted a systematic comparison of LCA-based environmental performances of fossil and wood power plants (considering reforming of syngas) as well as cement production in Europe for 2025 and 2050 with and without CCS technologies (post-comb. with chemical absorption, pre-comb. with physical absorption and oxy-fuel comb. with cryogenic air separation). The results indicate GHG emissions reductions of 68-92 % for fossil fuel power generation, 39-78 % for cement production, and negative emissions for wood power generation. The life cycle GHG emissions resulting from power generated from coal and natural gas with CCS are very similar. The cement industry can potentially benefit from CCS technologies, but on-site power and heat sources on the scale installed at cement plants are expected to be insufficient to meet the energy demands. The environmental burdens are highly influenced by the source of heat and power.

There are some studies focusing on downstream processes of CCS chains. Wildboz C. [79] described the logistics for pipeline transport and CO_2 injection into gas fields and saline aquifers. IEA have published an external study [80], which describes the logistics for the transport of CO_2 hydrates for deep ocean storage via bulk and container ship. However, for transporting supercritical CO_2 the most common approach regarding ship transportation considers liquefied natural gas logistics [75,76,79].

Table 4 shows the most important parameters regarding the modelling of these projects.

The comparison of technologies between studies is unveiled because of different reference system and different assumptions. However, based on these studies and some other review papers [75, 76] of older studies, some highlights are following described:

- Although some studies use the mass of CO_2 captured as the functional unit, the most common one is a unit of electricity produced when power plants are the reference systems or a unit of product for industry.

- The most frequently chosen impact categories, besides GWP are: acidification potential, eutrophication potential, photochemical oxidation, human toxicity potential, abiotic depletion potential [75].
- The choice of the reference system is one of the most important parameters: 'the improvement potential of today's technologies is much higher than of enhanced future systems' [75].
- There is a consensus regarding the general trade-offs of CCS technologies: while reducing GWP, all other environmental categories increase with the respect to reference case scenarios (without CCS).
- Several studies point that the source of fuels can highly influence the results. Moreover, it plays an important role for the overall performance when the compensation of energy is performed by an over consumption of fuel by the plant.
- The energy penalty and capture efficiency are determining for the overall performance of the system. The compensation of the energy penalty can be modelled by different approaches: either in fuel input per unit of delivered electricity, or as the decrease in electricity output for a given fuel input [76] or compensated by the grid [81].
- The net-life cycle CO_2 emission reduction between cases with and without CCS is lower than the capture efficiency, especially when the energy penalty compensation is supported on an over consumption of fuel [76].
- The construction and dismantling of capture unit, powerplants and pipelines score rather residual impacts with respect to systems operation. The transport and storage phases are not so significant as the plants or industry operation for the overall performance.

Table 4 - Main parameters related to the modelling of the studies aforementioned.

Study	Scope	LCIA	Functional Unit	LCA	Facility	Capture tech	Separation tech	Transport	Fate
[14]	Comparison: post combustion technologies; PP with and without CCS	CML 2001	MWh of net energy produced	craddle to grave'	Coal PP	Post-comb.	Absorption with MDEA, aqueous ammonia and CaL	Pipeline	Deep saline
[77]	Evaluate the environmental effects of CCS implementation strategies at a national level..	CML 2001	kwh of energy produced	craddle to grave'	Hard coal PP	Post-comb.	MEA scrubbing	Pipeline	Deep saline
[78]	Systematic comparison of LCA-based environmental performances of fossil and wood power plants as well as cement production in Europe for 2025 and 2050 with and without CCS.	ReCiPe v. 1.07	KWh of electric. at busbar (for power plants); kg cement (at the factory gate)	craddle to grave'	Hard coal, lignite, natural gas and biomass power plants and cement industry	Post-comb.; pre-combustion and oxy-fuel combustion	MEA scrubbing for post-combustion; cryogenic air separation for oxy-fuel combustion; physical absorption with Selexol for pre-combustion.	Pipeline	Deep saline

The most prominent open question related to the application of LCA to CCS technologies is associated to the modelling of leakage rates of stored CO_2. On one hand, the prediction of leakage rates is a difficult task, requiring a deep understanding of site-specific characteristics. On the another hand, there is a methodological hurdle in 'dealing with long-term emissions in relation to emission reduction today' [75] as they depend on the total amount deposited and LCA is used to describe environmental aspects in a steady-state situation. Therefore, the timeframe of the study and the time horizon selected for GWP assessment are important parameters.

To guarantee the comparability of the studies, it is helpful to have a set of background or benchmark information about considered technologies.

4.2 The goal and scope definition

The present study was commissioned by Net4CO_2 with the main goal of evaluating the overall environmental performance of retrofitting the HGtS capture technology in Portuguese fossil fuel-based powerplants for CO_2 long term storage as well as identifying and quantifying key trade-offs (related to energy penalty, transport and storage emissions) and potential benefits (associated to the reductions of CO_2 emissions in the source). This is an internal LCA study with the main purpose of support decision making for strategic planning and create a basis for further external communication, in particular, for product declarations and benchmarking. Therefore, all the procedures, choices, data gaps will be deeply described, and uncertainties will be analysed.

The obtained results are expected to attend to the following questions:

- How much benefit would the HGtS retrofitting on powerplants bring to the overall environmental performance of their power generation processes? And for which fuel combustion process, the technology is more effective?
- What are the dominating causes for the environmental burdens associated: capture operation, transport or storage phase?
- Which mean of transportation will be potentially more environmentally sustainable in a Portuguese scenario?

In order to allocate the benefits and the trade-offs of retrofitting HGtS on powerplants, a comparative analysis between CCS scenarios (comprising both electricity generation and CCS chain processes) with reference operation scenarios (without considering the operation of the capture unit) was conducted. As reference cases, one NGCC powerplant – Ribatejo - and one pulverized coal powerplant – Sines - were chosen based on their installed power. In one hand, they correspond to the thermal plants with major installed power capacity verified in Portugal, and in another hand, as they have similar capacities, the same utilization rate of the plant produces similar amounts of electricity per year. The comparison basis is the functional unit, which is discussed in the next section.

Moreover, different sensitivity analysis are performed in order to characterize the operation of HGtS under several possible scenarios based on variables as: fuel used for the combustion process in the plants, plant's utilization rates, the compensation of energy penalty of the capture unit, the mean of transporting the hydrate slurry, the location of the storage field, the quality of the grid used along the CCS chain and to the injection depth. Figure 19 and 20 summarizes the main scenarios performed for each powerplant.

Systems modelling, data processing, classification and characterization were performed in SimaPro 8.5 software. Emissions and resource consumption related to the operation of both powerplants are based on site-specific historical data, which were correlated to energy generation as an attempt to create an LCA that is more robust by conducting a sensitivity analysis to the electricity generated in each powerplant i.e. to the utilization rate of the powerplants. More sensitivity analyses were performed, along with scenario analysis and parameters uncertainty analysis to assess the variability and feasibility of results. Background data relating to resources supply chain and waste management were taken from Ecoinvent 3.3 database, with some adjustments and updating. For scenarios considering the retrofit of a HGtS capture unit, the energy penalty compensation by an over operation of the powerplants was not modelled, as it would result in an over production of CO_2 emissions and by consequence an over energy consumption by the capture unit. Energy compensation in literature was generally modelled when thermodynamic data of combustion process is known which enables their simulation on process integration tools, such as Aspen, to find a reference flow equilibrium. NETL introduced a method for modelling energy penalty compensation by the electricity grid – 'make-up power' effect' [81], supported on the principle that the consumption of an under production of electricity on both powerplants would be compensated by the grid in downstream

processes. Although, being out of the frontiers of the study, this compensation was also modelled and analysed for a 'cradle to gate' approach.

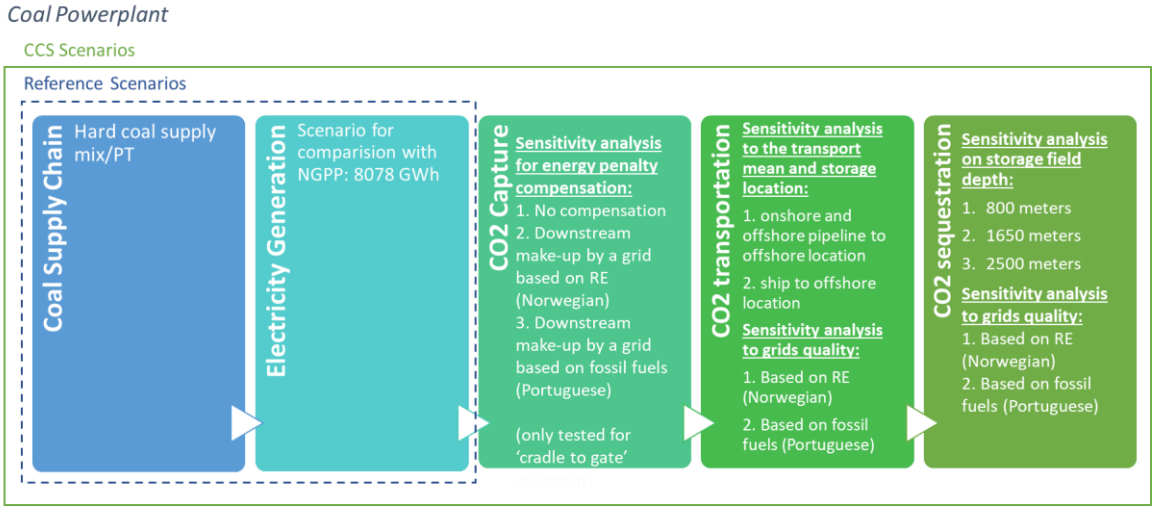

Figure 19 - Scenarios performed for coal powerplant (Sines).

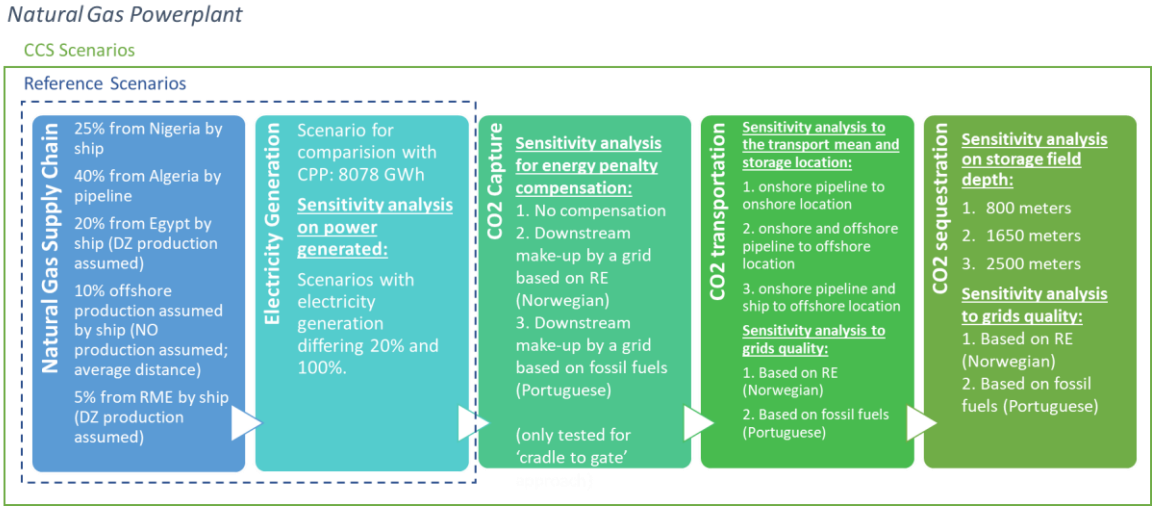

Figure 20 - Scenarios performed for natural gas powerplant (Ribatejo).

4.2.1 Functional unit and reference flow

All the impacts are allocated to the functional unit, which is a comparison basis between assessments of different alternatives within a system, different related systems or different related products. However, comparison between studies with the same functional unit can be unfeasible when studies are based on different assumptions and different system boundaries.

As the aim of the study is to determine the performance of power generation by fossil fuels combustion with HGtS carbon capture, transport and storage, the functional unit chosen for the study is 1 MWh of electricity produced by each power plant and provided to the network grid (without the energy penalty of plants operation). Besides being the typical functional unit on LCA of CCS technologies, CO_2 could also be considered, as a by-product of the system. However, it would be even more difficult to cross results from different studies, because the gas is produced in different compositions, purities and pressures depending on each system and technology [75]. The two reference flows are: the electricity produced through which all inputs and outputs are correlated based on historical data for each facility; and the slurry of CO_2 hydrates produced. The timeframe for plants operation is one year.

4.2.2 System description and boundaries

The approach for conducting LCA scenarios are 'cradle to grave', starting with raw materials extraction and supply chains and ending with the disposal of the final products, with exception for electricity, which downstream processes were not considered. The system boundaries are presented in Figure 21 for coal PP and in Figure 22 for NGCC PP. The following issues were excluded from the system boundaries: construction of some infrastructure and vehicles for fuel transportation; power plants construction and decommissioning; construction and decommissioning of capture unit; the electricity transmissions and distribution network; consumer use of electricity; indirect land use; low-frequency, high-magnitude, non-predictable environmental events; social and economic aspects.

The construction and dismantling of infrastructure and vehicles was indirectly addressed: in Ecoinvent libraries, the processes modelling the extraction, production and transportation of natural gas and coal provide an allocation of the infrastructures to the unit of fuel extracted or produced, assuming a lifetime for the infrastructure and an exploration rate. The exception is for the transport of liquefied natural gas (LNG), coal and CO_2 hydrates via transoceanic ship, as the allocation impacts is extremely difficult to estimate though the fact that such infrastructure serves multiple purposes, which would contribute for an increase of the results uncertainty.

The construction and dismantling of the powerplants and the quantification of associated impacts is also out of the scope of the present study. The evaluation of environmental performance of retrofitting existing powerplants with CCS technologies by comparison with a reference scenario with current operations, can exclude such variables, as they would be accounted in both scenarios. Moreover, in several previous studies, these processes often score low environmental load within different impact categories [14,75-78], which unveils the effort required for gather the data regarding powerplants construction and dismantling. However, the relative contributions of CCS processes for the overall impact's loads can be somewhat penalized with this simplification.

The construction and dismantling of the capture unit was not addressed as the process is adapted to each powerplant and the sizing of the equipment was not performed.

The inclusion of all sustainability dimensions in LCA has been argued, as it would result into a more holistic study and the results would have added-value for decision-makers. However, the projects would become more time and financially intensives and the increased complexity could in turn increase uncertainties. Moreover, software is not fully adapted to integrate social and economic aspects into modelling. Economic aspects are especially difficult to integrate on a LCA simulation as economical models depend on a wide range of factors and the lack of a time perspective inhibits the possibility of modelling interest or discount rates, taxes and prices fluctuation (in this particular case, CO_2 taxes fluctuation) [82]. For the current study, the most relevant social aspects are related to environmental aspects such as air and water quality. However, if results show that fossil fuel based powerplants can be competitive with RES, the dismantling of Sines powerplant (pointed out until 2030) could be delayed which would represent social benefits among working class. However, such estimates were not performed. To account such dimensions, other tools can be applied instead such as multi-criteria decision analysis.

In this CCS chain study, the spatial representation is highly specific, from the combustion process to storage injection of CO_2. Due to this fact, fuels have high mass inflows for power generation processes and the specifications of their supply chain and/or composition highly - influence LCA results, especially for coal PP [14,75-79], it is convenient to avoid global averages and, work with site specific LCI instead. Besides, their supply chain can be easily simulated as both NG and coal physical flows correspond well to the contractual relations, in opposition to electricity supply [83].

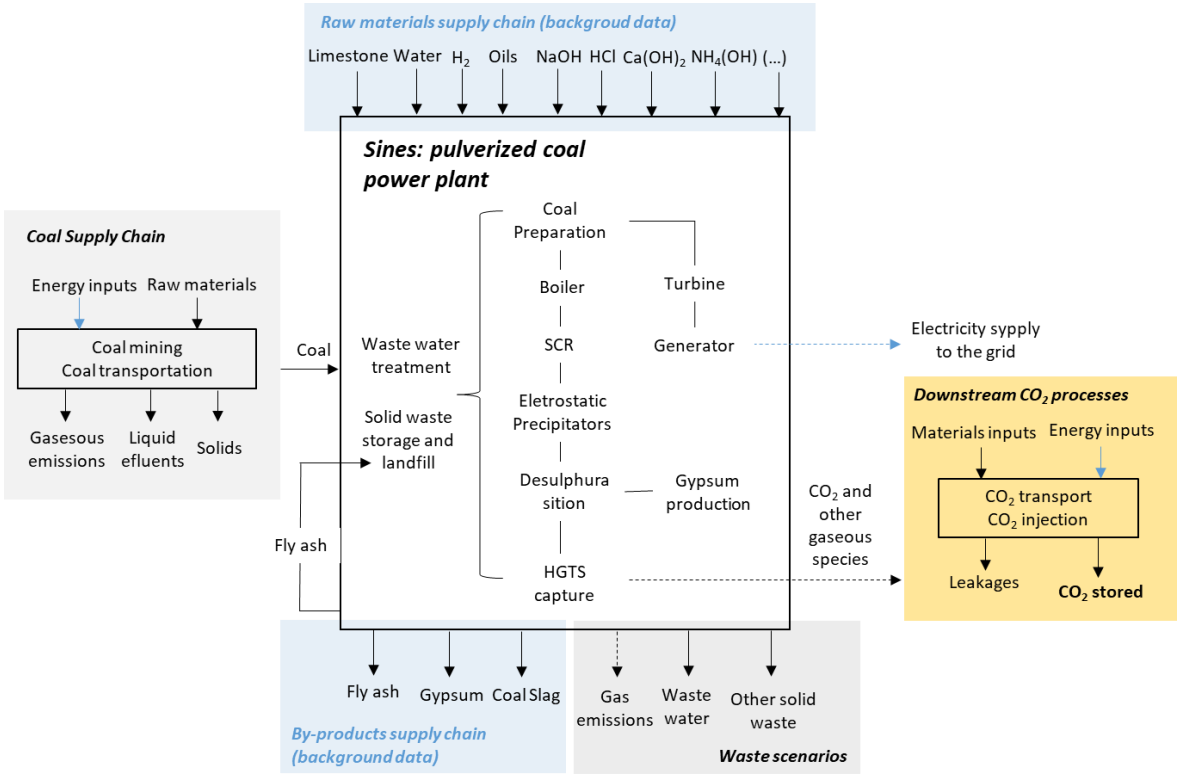

Figure 21 - System boundaries set for CPP. The downstream processes at yellow are only applied to CCS scenarios.

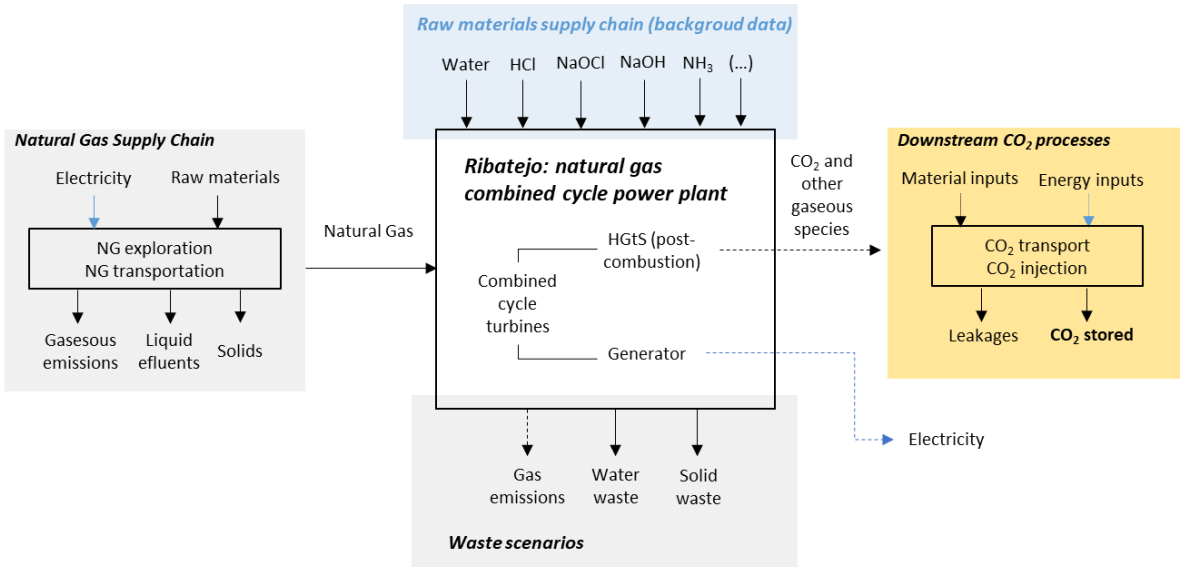

Figure 22 - System boundaries set for NGPP. The downstream process at yellow are only applied for CCS scenarios.

Power generation processes are real case studies and as a result the inventory data regarding all inputs and outputs of these processes come from the processing of historical measured data.

4.2.2.1 Coal Powerplant (Sines)

Sines pulverized coal PP (CPP) is located in the coastal south of Portugal and it is the largest electricity producing centre in the country with an installed power of 1256 MW (four generator groups of 314 MW each). It has started operation in 1995 and since then some units had been added (for flue gas treatment) and adjustments have been performed to improve thermal efficiency. Figure 23 shows a simplified flow chart of the operations. The source of coal is mainly from Colombia and it is transported by ship to Sines port and then by automatic rolled carpets (3.5 km) to Sines Park to be pulverized before combustion [84]. Storage park capacity

gives the plant autonomy for five months of full operational load [85]. Fuel oil, used for boilers ignition, is supplied by tanker trucks and stored in 4 reservoirs. Its pre-processing consists in filtration and heating with auxiliary steam. The water used for coal pre-processing is treated afterwards and the rainwater is collected for further treatment if its quality so requires.

The water used to generate steam is from Atlantic Ocean and after heat exchanger is rejected back to the Ocean passing through a mini-hydroelectric system to recover potential energy. After combustion, the flue gas passes through a selective catalytic reactor (SCR) installed in 2011 for NO_x removal by using NH_3 as a reduction agent. Its removal efficiency is greater than 80%. After, flue gas follows to an electric precipitators unit for capturing particles with an efficiency greater than 99.5%. Then, it follows to a desulphurization unit with an efficiency of 95% for SO_2 removal. In this unit is also verified the reduction of fine particles and chlorinated and fluorinated organic compounds. Along the installation, there are several units to measure emissions and other physical parameters such as temperature of water in the ocean where the water steam is released.

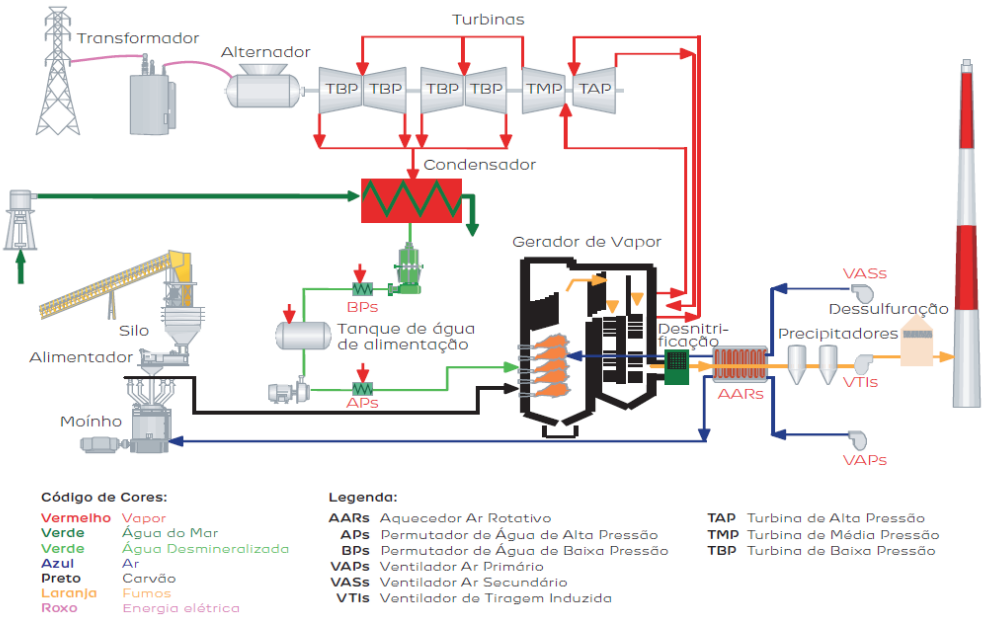

Figure 23 - Flowchart of the Sines powerplant operation.

4.2.2.2 Natural gas powerplant (Ribatejo)

The process in Ribatejo PP (NGPP) is a natural gas combined cycle, with an installed power of 1176 MW (three generator groups of 392 MW each). It is located in Carregado, Lisbon and it was commissioned in 2001. Figure 24 shows a simplified operations flow sheet. Each group has a gas turbine and a vapour turbine connected to the same shaft. The gas turbine is responsible for 2/3 of the total generated power. Gas cycle comprises the gas turbine, air compressor, combustion chamber, the recovery boiler through which flue gas outflows. The water-vapour cycle comprises the turbine, the steam condenser and the recovery boiler. The alternator is attached to the rotating shaft and the global efficiency is about 57%. The flue gas from NGCC powerplants are much cleaner than the ones resulting from CPP operation. Ribatejo does not

have any air treatment unit. A wastewater plant treats the water contaminated and potentially contaminated before being discharged to Tejo River.

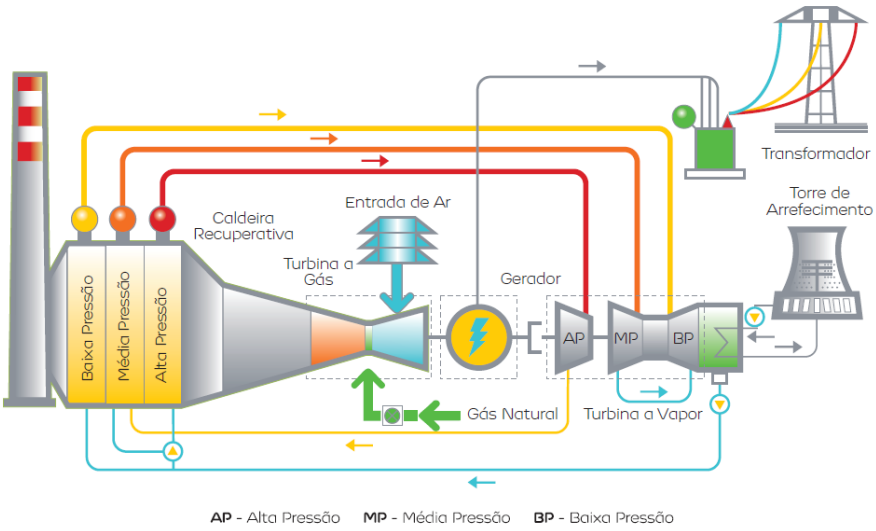

Figure 24 - Flowchart of RIbatejo (NGPP) operations powerplant.

4.2.2.3 HGtS capture unit

The HGtS CO_2 capture unit has been modelled for separation of N_2/CO_2 mixtures as so it is a PCC process. Thus, it would retrofit the processes at the end line of flue gas treatment processes and its installation is based on NETmix technology unit and two parallel cooling circuits. The flowchart is presented in Figure 25. The flue gas enters in pre-cooler heat exchanger (3) and follows to heat exchanger 5 and 6 crossing the two parallel cooling circuits: one coming from chiller 12 with an aqueous solution with 27% of ethylene glycol (~ -20 °C) and another one coming from chiller 10 with an aqueous solution with 35% of ethylene glycol (-50 ºC). The first circuit is also used to cool the water flow and the second one to cool down NETmix unit, where capture occurs. The water consumption is about 2.5 tonnes per tonne of CO_2.

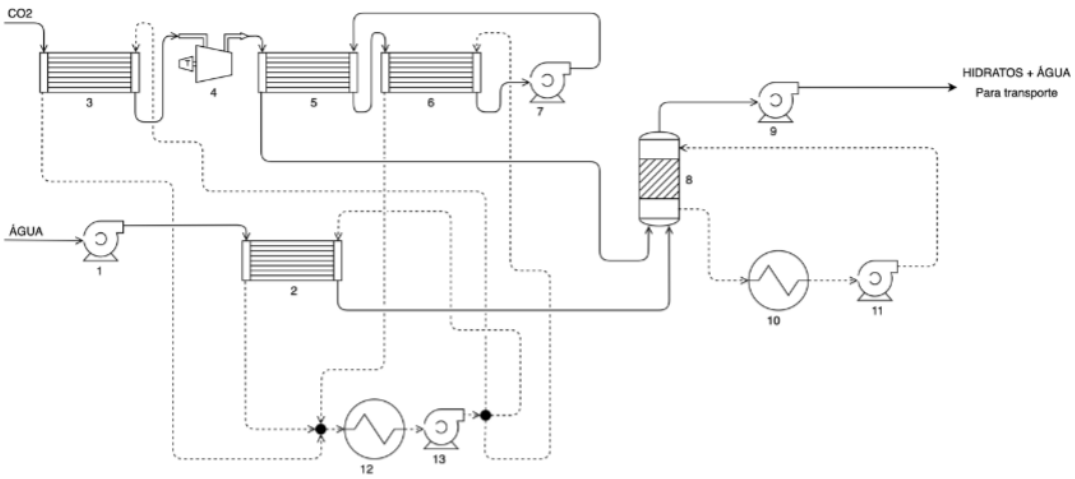

Figure 25 - Flowchart of HydraGtS CO2 capture process. Legend: 1 – water pump; 2 - water heat exchanger; 3 - gas pre-cooler heat exchanger; 4 - gas compressor; 5 - gas intercooler heat exchanger; 6 - gas after-cooler heat exchanger; 7 - CO_2 pump; 8 - NETmix reactor; 9 - transport pump; 10,12 - refrigeration chiller; 11,13 - refrigeration pump.

4.2.2.4 Transport and Storage of CO_2

For CO2 transportation, the simulated processes are averaged processes with distances based on the right trajectories defined in COMET and QTejo projects. Regarding storage sites, although storage capacity is not explicitly addressed in LCA formulation, the choice of the site interferes with possible means of transportation and distances. The site chosen was based on the results of the economic feasibility study performed by LNEG [66] and on the storage capacity for CO_2 mass flows.

4.2.3 Allocation

For power generation studies 'the partitioning and relating of inputs and outputs' (allocation) between products and by-products [39] is usually done considering heating value or exergy. Besides CO_2, other by-products can be considered as gypsum and ash for cement industry. However, in this project, these products will not be allocated to impacts as their trading is merely an attempt to minimize and valorise waste as their profit is residual when comparing to electricity supply. For the current study, historical data regarding plants operation is used as its veracity overcomes thermodynamic and simulations data. However, the lack of it unveils the allocation of HGtS retrofitting based on exergy. Therefore, its allocation will be related to the difference between reference scenarios and capture scenarios. Therefore, reference scenarios act as baselines for allocating the impacts associated with HGtS capture technology.

4.2.4 Time Horizon

Although GWP impact category is not affected by the choice of different time horizons[9], as CO_2 characterisation factor is always 1 kg_{eq} [75], it is generally accepted that studies with different time horizons cannot be compared, especially when other impact categories are analysed. Therefore, for the present study, it was considered a time horizon of 100 years as it is typically used.

Time horizon is a particularly important assumption to simulate the leakage rate [75]. According to Boot-Handford et al. [13], over time storage becomes more secure and CO_2 less likely to escape which avoids the typical assumptions of leakage rate and storage time [13]. Due to this, a time horizon of 100 years is assumed to reasonably represent the total leakage that may occur.

4.2.5 Impact categories and impact assessment method

The collection of inputs and outputs build the basis for the subsequent impact assessment [75], in which emissions and materials exploitation are 'assigned to the impacts categories according to the substance's ability to contribute to different environmental problems' [82]. According to ISO 14040/44, for Life Cycle Impact Assessment (LCIA) must at least include classification and characterization, while elements such as normalization, ranking, grouping and weighting are optional [74]. Normalization and weighting are based on aggregate scores of each impact category to have an overall evaluation in terms of human health, ecotoxicity and resources depletion or instead a single score. These steps have the advantage of simplifying the results, especially in cases where alternative studies present better performances in different impact categories, and it can be particularly useful to communicate results for product/systems managers. However, these two steps are highly subjective, and it makes comparison within different scenarios and studies even more difficult. Hence, these two steps were disregarded.

The effects of some impact categories are embedded on a global scale, such as climate change and ozone depletion. As the most directly affected environmental compartment is the atmosphere, the effects are rapidly spread and the time horizon for these impact mechanisms is long. Other impact categories, related to soils and water contamination, ecotoxicity and human toxicity have more regional or even local effects, and their risk magnitude is highly

[9] In this context, the veracity of the sentence must be considered only in practical terms, when simulating LCA with impact characterization model.

dependent on ecosystems morphology and sensitivity. The cause-effect chain comprises four main steps: fate, exposure, effect and damage. Depending on local environment, a stress may not even cause an actual effect or damage.

The selection of impact categories often implies the selection of impact assessment methods. The methodology framework of Life Cycle Impact Assessment (LCIA) is still under discussion and there are not standardised methods, although some as CML and ReCiPe are referred as the most widely used [82]. The methodologies may differ in terms of impact categories, category indicators and characterization factors. To better understand the relation between those variables: Life Cycle Inventory (LCI) results are assigned to the impact categories through category indicators and the conversion is performed via characterisation factors.

There are two characterization approaches, depending on what point of the cause-effect chain the assessment is performed: midpoint method and endpoint method [82,33]. At midpoint method the quantitative modelling is performed at a point before the exposure/effect stages and the potential impacts are assessed by using midpoint indicators (*e.g.* global warming potential, eutrophication, etc.). The endpoint method also includes the last stages of cause-effect chain and endpoint indicators are more extensive, as they refer to a final outcome of a complex environmental mechanism: potential environmental damages to human health, ecosystems and resources exploitation. Taking global warming as an impact category example, the midpoint indicator would be the mass of CO_2 equivalents, and the characterisation factor for each substance express the radiative forcing and an endpoint indicator could be the increased on global average temperature or seawater level.

As International Organisation for Standardization (ISO) has not yet defined 'endpoint indicator' and its characterisation factors modelling are more sensitive to formulated assumptions, the impact assessment methods applied to the present study is based on midpoint characterisation - CML baseline. As the applied approach is 'cradle to grave' and the system reveals interaction with all environmental compartments, among population, all the impact categories inherent to CML baseline were considered.

Furthermore, ecotoxicological impact categories are important to evaluate as they may address for distinguish advantage of HGtS when comparing to other PCC technologies such as amine-based absorption. Considering that CCS implementation causes additional material requirement for pipeline construction and wells drilling as well as additional raw materials consumption either for energy penalty compensation either for HGtS operation, abiotic depletion potential (ADP) must also be analysed.

- **Abiotic resources depletion potential** can be a regional to global IC and refers to the depletion of natural resources (with focus on coal, natural gas, limestone and water). The characterisation factor is the ratio of quantity of resource used versus quantity of resource left in reserve and the indicator is commonly a kg of minerals, or MJ of fossil fuels or m^3 of water, depending on the model. The LCI data relevant for this impact is the quantity of minerals used, fossil fuels and water used.
- **Acidification potential** is a regional and local scale IC and refers to the reduction of the pH due to the acidifying effects of anthropogenic emissions in soil and water systems. The characterisation factor is hydrogen (H^+) ion equivalent and the indicator factor is typically kg SO_2 equivalent.
- **Ecotoxicity potential** is a local scale IC and it depends on the toxicological responses of different species and the nature of the chemicals in the ecosystems. The characterisation factor is LC_{50} equivalents and the common units are kg 1,4-DB equivalent. The LCI data relevant for this impact are toxic chemicals with a reported lethal concentration to rodents or to fish.
- **Eutrophication potential** is a local scale IC and it refers to the increase of nutrients (nitrogen and phosphorus concentration) in water systems which causes formation of

biomass (*e.g.* algae). The characterisation factor and units are either kg PO_4^{3-} equivalent or kg N equivalent. The LCI data relevant for this impact is PO_4^{3-}, NOx and NH3.

- **Human toxicity potential** is a local scale IC and is 'a calculated index that reflect the potential harm of a unit of chemical released into the environment'. The characterisation factor is LC_{50} and the units are commonly kg of 1.4-DB equivalent.
- **Global Warming potential** refers to the global scale impact of anthropogenic GHG emissions, which enhance the radiative forcing of the atmosphere, causing an increase in global average temperature. The characterisation factor is kg CO_2 equivalents. The LCI data relevant for this impact is: CO_2, CH_4, NO_2.
- **Photochemical oxidant creation potential** is a local scale IC that refers to the formation of reactive chemical compounds such as ozone, by the action of sunlight on certain primary air pollutants. The characterisation factor is ethane (C_2H_6) equivalents.
- **Stratospheric ozone depletion potential** is a global scale IC and it refers to the anthropogenic emissions of ozone depleting substances which causes the thinning of ozone layer in which a greater fraction of UB-B radiation is absorbed. The characterization factor is kg CFC-11 equivalents.

Land use could be an interesting impact category to analyse, especially regarding pipelines construction. However, average data found in literature does not add significant value to the study, attending to its geographical specificity. Therefore, it will not be addressed. Noise impacts was also disregard, attending to the lack of high valued data.

Effects relating to the underground storage of CO_2 are not well represented in the current range of standard impacts [75] and besides more information have been released and more accurate monitoring technologies have been developed and used, there is still lack of confidence regarding the risks of long-term underground CO_2 storage.

To forecast impacts regarding human and ecotoxicity with more accuracy and other site-specific aspects like noise impacts, LCA can be combined with other environmental decision tools, like Environmental Impact Assessment (EIA) and Risk Assessment for providing a more comprehensive picture of the actual regional and local impacts. However, such studies were not performed.

4.2.6 Data quality and availability

The sources of data used for LCI varies among the processes. For upstream processes such as fuels supply chain, the data is literature based. Some other background data as other resources supply chain and waste management is based on Ecoinvent database. The data regarding power generation processes (all inputs and outputs within the white rectangle in Figures 21 and 22) is based on historical data processing. Historical data was taken from environmental reports for both PP under ISO 14001 and EMAS certifications framework and all the inputs and outputs of the processes were correlated to energy generated through simple regressions for the NGPP and through an Artificial Neural Network (ANN) for CPP, tested by machine learning on Python. As further explained, the sensitivity analysis to the electricity generated on CPP was disregard, as the results from the ANN were not satisfactory. Data related to capture unit was provided by Net4CO2: energy penalty, auxiliary materials for the process and hydrates properties. For downstream process (transportation and storage of CO2), some data is calculated (injection power required), other obtained from simulations on Aspen (power required for the transport along pipelines and pipelines sizing), and also literature based (as the commissioning and dismantling of pipelines and drilling activities). The main assumptions are related to the transportation distances, measured in Google Earth and supported on the results from Ktejo and COMET project – an international cooperation study to evaluate the 'techno-economic feasibility of integrating CO_2 transport and storage infrastructures in the West Mediterranean area (Portugal, Spain and Morocco)' [59].

4.2.7 Limitations and uncertainty management

The model applied in SimaPro must be developed in a way that simplifications and distortions do not influence the results to a large extent [82]. However, the complexity of the model designed for the current assessment increases the likelihood of assumptions influencing too much the results. In fact, several sources of uncertainty can be found in all phases of LCA [86]. Table 5 shows the nature of different uncertainty types and the methods used to measure, characterize and control those. Along the Life Cycle Inventory (LCI) phase, those uncertainty sources and assumptions – associated to the limitations of the study – are described in detail.

Table 5 - Summarize table regarding uncertainties sources of LC models and the methods applied in the current assessment to control and characterize them.

Parameter Uncertainty
Related to missing data, incomplete data and errors in measured data. Methods applied: Probability distributions describing data variation either obtained by sampling data processing or by using Pedigree Matrix in SimaPro for Monte Carlo simulations.
Scenario Uncertainty
Related to normative choices for constructing LC models, besides some assumptions and structural scenarios choices, functional unit, impact assessment methods and the selection of characterization factor. Methods applied: Sensitivity analysis to some important parameters, such as the plant's utilization rate, mean of transportation, the quality of the grid used for transport and injection depth of storage reservoir. The study did not take into account more than one impact assessment method, although being a good practise, as mismatches between data and the characterization factors can conduct to underestimation of impacts.
Method Uncertainty
Related to the variability in structure and mathematical relationship between model inputs and outputs in LC models. This type of uncertainty was not considered. The time frame of the study is one year of operation, therefore the inventory of energy and materials balances are annual, regarding different plants operation scenarios. The materials related to the infrastructure is allocated to one year of operation through the amount of their use rates and estimated lifetime. Other mathematical relations are inherent to the SimaPro operation.

The most relevant limitations are related to the storage scenarios, which are based on injection rates determined for CO_2 supercritical regarding data of shallower sediments, and for which no leakage rates were assumed.

4.3 Life cycle inventory

4.3.1 Natural gas supply chain

Previous studies of LCA of CCS technologies on retrofitting powerplants show that fuels supply chains have a major influence on the impact assessment results. Hence, for geography specific studies, these processes should be thoroughly modelled.

In Ecoinvent database, a specific process for modelling NG imports by Portugal is not available and the average processes for European region are unreasonable to use, due to significant differences between supply chains as shown in Figure 26. Unlike electricity supply, both coal and NG physical flows correspond well to the contractual relations [83], which eases their modelling. For the purpose of the current study the natural gas supply chain was modelled, based on the main following assumptions:

1. NG consumption share at Ribatejo powerplant was based on the average of importing shares of NG by the country for the period between 2011 and 2018 with some simplifications. Portugal has no NG production of its own;
   1.1. It was applied a cut off criteria of 5 % to exclude some irregular exporters from the study, i.e., countries from which the importing share was lower than 5 % were disregarded;
   1.2. The rounding up and down for the remaining has taken into account the average between 2016 and 2018, which resulted in a smooth reduction of the shares for Algeria, Nigeria, unspecified countries offshore production and Qatar and a steep increase of the share for Egypt (which represented 50% of the total NG imported in 2018);
2. The NG imported from Algeria is transported via pipeline (both onshore and offshore). From Qatar, Egypt, Nigeria and the offshore production, liquefied natural gas is transported via ship. This assumption will be further explained.

Some other assumptions to design transportation scenarios are presented in Appendixes II to IV. Only direct imports were considered based on data from annual reports by Directorate General for Energy and Geology (DGEG), which can be consulted in Appendix II.

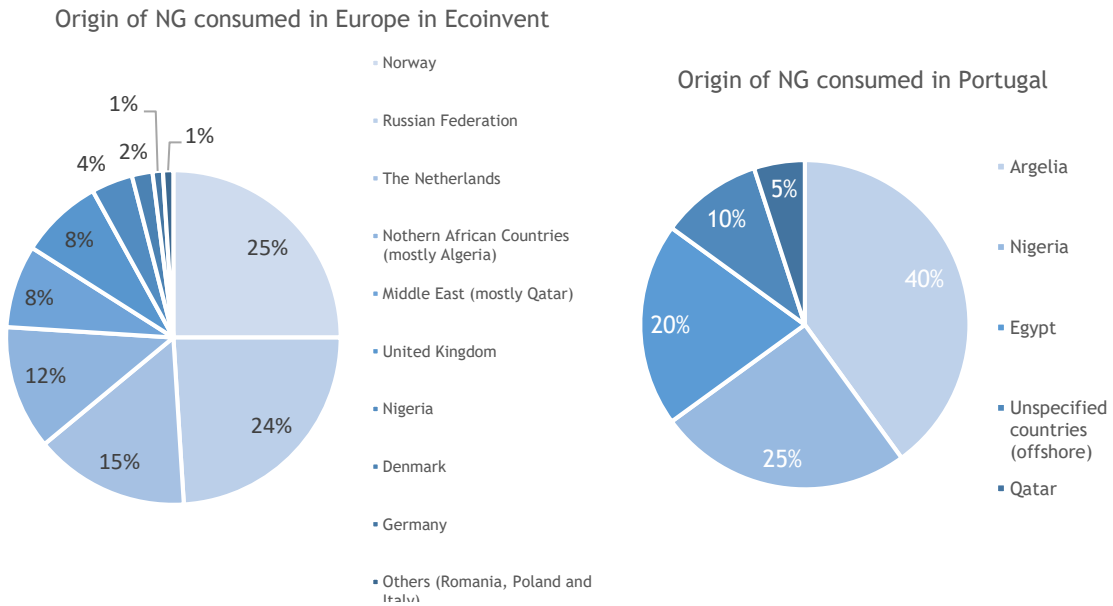

Figure 26 – On the left, the chart represents the share of the most important NG producers for Europe modelled in Ecoinvent database, which is deduced based on trade movements provided in the BP Statistical Review of World Energy in 2011 report [83]. Most recent updates have been performed for specific countries processes [84] but no updates to European region have been reported. On the right, the share of most relevant NG producers for Portugal modelled fro the current assessment is displayed. The data is based on DGEG annual reports [87].

The source of NG is part of the reference case scenario systems boundaries and it does not interfere with the HGtS retrofitting NGPP and downstream processes performance. Hence, a sensitivity analysis for NG supply chain could only be interesting if a comparison between HGtS retrofitting thermal PP with RE were performed. However, as that study is out of the scope of the current assessment, only one case scenario was modelled.

4.3.1.1 Natural gas production and trading: processes description

Figure 27 shows the main stages of NG supply chain: exploration, processing and in case of LNG imports, liquification/regasification, the long-distance transport and the regional distribution to the final consumer. After exploration drilling, different processing stages can take place depending on the quality of the gas [83]:

- Separation of free water and oil;
- Separation of higher hydrocarbons;
- Natural gas drying, desulphurisation and recovery of elementary sulphur (sweetening);
- Additional drying of higher hydrocarbons.

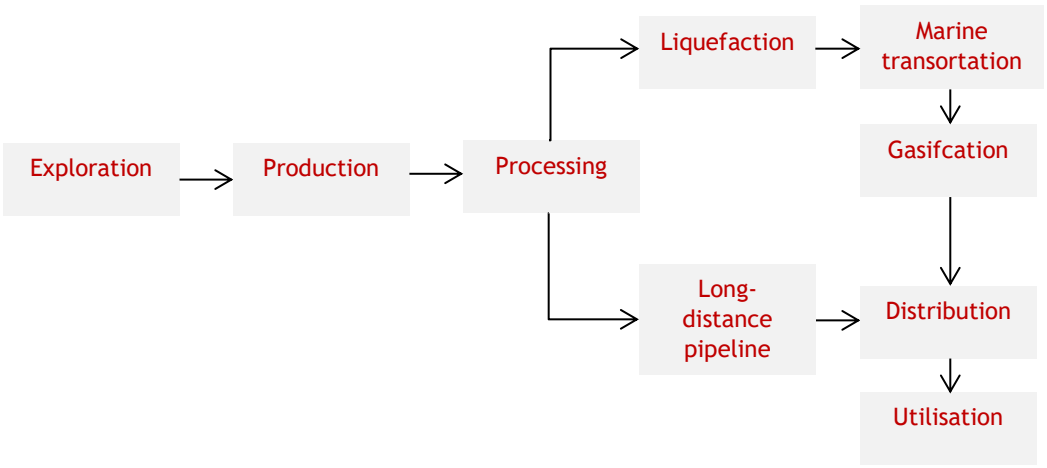

Figure 27 - Main process steps in NG supply chains.

In general, sour gas requires more complex processing steps. The gas from Algeria and Nigeria is mostly sweet so that desulphurisation does not occur [83]. In Nigeria, a share of the natural gas is produced in combination with crude oil. The overall impacts are typically allocated to each product in terms of energy content (low heating value), and water consumption and discharge just as by-products trading (mixture of ethane, propane, butane and pentane) are attributed to the oil production [83]. In Algeria, Egypt and Qatar, natural gas is produced in onshore plants; for Nigeria, the production of natural gas occurs in both onshore and offshore processing plants.

The energy consumption is mostly associated to gas turbines compression for pipeline transportation, especially for increased age gas fields and a small share of waste heat is used for in-field gas processing [83]. Process related emissions to air are related to:

- Gas flaring, i.e. deliberate burning of NG that is associated with combined oil and gas production;
- Gas venting, i.e. direct (deliberate or not) release of NG into the environment;
- Gas leakages of the plants.

Gas flaring and venting are the main contributors for upstream GHG emissions on NG supply chains and may compromise the overall performance of NG relative to other fuels as coal or oil [88], especially when CCS technologies are applied in downstream combustion processes. Gas flaring is the combustion of gas (without energy recovery) in an open flame and is practised in oil production sites [89]. The resulting emissions are mainly CO_2, sulphur dioxide (SO_2) and nitrous oxides (NOx), although there are also significant amounts of CFCs equivalent emissions,

e.g., halon 1301, which is traditionally used on suppression systems, for gas turbine fire control [90]. In Nigeria, a significant part of Natural Gas is explored in combination with crude oil, thus flaring occurs and may be responsible for an increase of environmental load of the overall process when comparing to other sources. Gas venting is the discharge of unburned gases into the atmosphere, often carried out in order to maintain safety condition during processing and supply chain of NG. Related emissions depend on NG quality, and are mainly methane (CH_4), CO_2, volatile organic compounds (VOCs), sulphur compounds and other gas impurities. These activities can be more impactful than flaring, as the methane is not reduced. Hence, sometimes, gases are burnt rather than being simply dispersed [89], which in turn increases CFC equivalent emissions, due the use of halon 1301 for fire control.

Most important process related emissions of water are:

- Emissions from discharge of produced water:
  Onshore: injection into oil/natural gas reservoirs or discharged into surface water;
  Offshore: direct discharge into the sea, injection into oil/natural gas reservoirs or transport and disposal on the mainland;
- Pollution to the soil or sea water via lubricating oil, fats or detergents;
- Emissions from sludge disposal or other pollutants that are separated from the process water.

For pipeline transportation, compression units may be required depending on the length of the pipeline and the age of the field. Seasonal storage of natural gas during the summer period is also an important part of the natural gas supply system [83]. For freight ship transportation, NG needs to be liquified to reduce its volume (liquified natural gas – LNG) and evaporated on the landing terminals to be transported to the consumers via onshore pipelines and local distribution networks. Along distribution networks, NG is depressurized on stations which can produce energy for being distributed on low pressure networks for the final consumer. This step was disregarded, as NG supply to powerplants is given at high pressure.

4.3.1.2 Life cycle Inventory

Most of the sub-processes among NG supply chains are available on Ecoinvent 3.3 for different geographies and most of them are reported on Schori et al. 2012 [83]. This data refers mostly to 2010 and sources for technical data may date back a few decades. An important assumption is that the material and service inputs from a time far away is modelled with respect to recent technology (2010). Some updates have been published since then (Faist Emmenegger M. et al. [84,91], and an ESU-services report in 2018 [92]) and were used to model some processes which were not available or outdated on Ecoinvent 3.3. The input-output inventories for liquefication and evaporation processes were also adjusted to account proper updated production processes and exclude upstream natural gas production and transportation, respectively.

Production and liquefication

Production processes modelled in Ecoinvent libraries include energy use, infrastructure and emissions.

For the Northern African countries few specific data is available. In Ecoinvent database, Algeria's NG production activities are supported on data from Russian Federation, as in both countries, it is produced from NG fields instead of oil and gas combined production. Some adjustments are however performed such as flaring, venting and recovery rates, fugitive emissions and processing modifications (the desulphurization process is not performed in Algeria as the natural gas is sweet). ESU-services and Ecoinvent recommended the use of Algeria's processes for modelling other Northern African countries and the Region of Middle East [83, 84]. However, an update for liquified natural gas production in the Region of Middle East was reported in Ecoinvent 3.6 dataset documentation [93] and its input-output inventory was reproduced to model the production of LNG in Qatar. Therefore, Algeria's data was only used to model NG liquification processes in Egypt and Nigeria.

As a result of methane halons emissions, the ozone depletion potential for the process modelling NG production in Nigeria available in the database of Ecoinvent 3.3 was greater than the production processes in the remaining geographies in 4 orders of magnitude (with the production shares presented in Figure 26 (right). Niels Jungbluth informed the dataset was outdated and the LCI reported by Meili et al. 2018 [92] for combined oil and gas production in Nigeria was modelled and used instead with allocation based on the low heating value of each product. The inventory data corresponds to an average process considering 75 % onshore and 25 % onshore production [92]. The direct emissions for methane halon (1301) and methane HFC-23 to produce 1 Nm^3 of natural gas were lower than the ones reported on the previous dataset by 13 orders of magnitude. To model the unspecified LNG production offshore a process describing the same activity for Norway was assumed.

Transport and Evaporation plant

In 2018, about 44% of the total gas was imported via pipeline (from Spain) and the remaining 56% by ship to Sines in liquid phase [94]. For the supply chain model, it was assumed that NG from Algeria comes from pipeline and the NG coming from Nigeria, Egypt and Qatar comes in a liquified state by freight ship. This assumption is supported on the following points:

- available trading data for Spain shows that the country imports only LNG from Nigeria and Qatar and only a residual proportion of NG imported from Algeria is transported by ship [84, data from BP];
- available data of pipeline structures in Egypt reveal no direct connection with Europe or with Algeria [95];
- Ouki M. reported that the export made from Algeria to Portugal is mainly by pipeline [96].

In Ecoinvent database, processes for NG transportation in Western Europe and Algeria are available for both onshore and offshore pipelines. For Western Europe, Middle East and North Africa the natural gas use of the compressor stations per 1000 km of pipeline transport is 1.8 % (m^3 natural gas / m^3 natural gas transported), as an average value of data reported in literature [83]. 'In the European natural gas networks losses occur mostly at barriers where venting is necessary' and the losses per 1000 km of transmissions pipelines (including compressor stations) are estimated in 0.026 % by ESU-services [83]. This value was updated to 0.019 % for Western European countries ('{RER w/o DE+NL+NO}') on Ecoinvent 3.6 [84, 91] and the updated LCI was taken to model NG pipeline transportation in Spain and Portugal. For Nigeria and Middle East, the European leakage rates are used [83]. As the report on greenhouse gas emissions for Algeria does not give any specific figures for natural gas transmission in the country, the leakage rates used to model pipeline transport is from Russian Federation (0.2 % per 1000 km) [83]. Ecoinvent 3.6 accounts however with an updated value of 0.026 % (30 % higher) [91]. Freons and halons are used for cooling systems in the compression stations and, in Ecoinvent libraries, their emissions, which have a significant impact on ozone depletion, are estimated based on data reported in environmental reports of a Dutch company [83]. Seasonal storage during the summer period and the infrastructure needed is also accounted in the processes modelled by Ecoinvent.

The distances were based on pipelines length [95] assuming the following trajectory: Hassi R'Mel – Arzwe – Beni Saf – Almeria – Cordoba – Campo Maior – Leiria – Lisbon (Carregado). Some missing data was estimated through google maps distance measuring tool. A standard distance of 100 km was assumed for pipeline transport between production and liquefication plants in Nigeria, Egypt and Qatar. The process for onshore pipeline transport on Algeria was extrapolated for the three mentioned countries.

The imported LNG lands in Sines Port [88]. The transportation for freight ship is also modelled in the database. The distances between Nigeria, Egypt and Qatar ports with Sines port were estimated through google maps distance measuring tool based on the maritime route's information available in [97].

Table 6 - Life cycle inventory for imported natural gas and its transportation until Ribatejo's powerplant.

Natural gas for use at powerplant	**1**	**m^3**		
Inputs for technosphere			***Distribution***	***2*SD***
Liquefied natural gas (Qatar)	0.05	m^3	Lognormal	1.08
Comments: Production in Qatar. Data gathered from ecoinvent 3.6 dataset documentation [93]. Pedigree Matrix: (2,2,2,1,1,na).				
Liquefied natural gas (Nigeria)	0.25	m3	Lognormal	1.08
Comments: The production of natural gas was based on the LCI reported on ESU-services database [92] and the liquefication process was based on the same process for Algeria. Pedigree Matrix: (2,2,2,1,1,na).				
Liquefied natural gas (Egypt)	0.2	m3	Lognormal	1.09
Comments: The process is based on the liquefication process for Algeria, with some adjustments, e.g. the production process used in the one for Algeria, as suggested in [73]. Pedigree Matrix: (2,2,2,1,1,na).				
Natural gas, at production offshore/NO S	0.1	m^3	Lognormal	1.08
Comments: It was assumed to model the LNG production from unspecified offshore sources. Pedigree Matrix: (2,2,2,1,1,na).				
Transport, liquefied natural gas, freight ship/OCE S	10.5	Tkm	Lognormal	1.12
Comments: The ton-km was calculated by the multiplication of the estimated distance with NG density (0.78 kg/m3 – reference value for ecoinvent database [98]) and the share of the corresponding volume of the NG (60 %). Pedigree Matrix: (3,2,2,1,1,na).				
Evaporation of liquefied natural gas	0.6	m^3	Lognormal	1.08
Comments: This process was modelled based on the input-output of 'Natural gas, high pressure {RER}| evaporation of natural gas' available on ecoinvent 3.5 documentation. However the grid selected is for PT and the processes of LNG production and transportation were excluded. Pedigree Matrix: (2,2,2,1,1,na).				
Transport, pipeline, long distance, natural gas {RER w/o DE+NL+RU}	0.0978	m^3	Lognormal	1.12
Comments: This process describes the transport from evaporation plant in Sines until Ribatejo powerplant. The ton-km was calculated by the multiplication of the estimated distance with NG density (0.78 kg/m3 – reference value for ecoinvent database [98]) and the share of the corresponding volume of the NG (60 %). Pedigree Matrix: (3,2,2,1,1,na).				
Natural gas, at production onshore/DZ S	0.4	m^3	Lognormal	1.08
Comment: NG production in Algeria. Pedigree Matrix: (2,2,2,1,1,na).				
Transport, natural gas, offshore pipeline, long distance/DZ S	0.0624	Tkm	Lognormal	1.12
Comments: The process describes the transportation of NG from Beni Saf until Almeria. Besides being reported a standard distance of 100 km on ecoinvent libraries for this trajectory, the distance for this process was based on the pipeline length reported in [95] of 200 km. The ton-km was calculated by the multiplication of the estimated distance with NG density (0.78 kg/m3 – reference value for ecoinvent database [98]) and the share of the corresponding volume of the NG (40 %). Pedigree Matrix: (3,2,2,1,1,na).				
Transport, natural gas, onshore pipeline, long distance/DZ S	0.172	Tkm	Lognormal	1.12
Comments: The process describes the transportation of NG in Algeria. Pipelines lengths were taken from [95] and some missing data was estimated with google maps tools. The ton-km was calculated by the multiplication of the estimated distance with NG density (0.78 kg/m3 – reference value for ecoinvent database) and the share of the corresponding volume of the NG (40 %). Pedigree Matrix: (3,2,2,1,1,na).				
Transport, pipeline, long distance, natural gas {RER w/o DE+NL+RU}	0.242	Tkm	Lognormal	1.12
Comments: The process describes the transportation of NG in Spain and Portugal. Pipelines lengths were taken from [95] and some missing data was estimated with google maps tools. The ton-km was calculated by the multiplication of the estimated distance with NG density (0.78 kg/m3 – reference value for ecoinvent database [98]) and the share of the corresponding volume of the NG (40 %). Pedigree Matrix: (3,2,2,1,1,na).				

The evaporation process available in Ecoinvent libraries were readjusted to exclude the production of LNG and the transportation process from its input-output inventory, as they were based on average data. This process takes place in Sines [88] and the NG follows to Ribatejo's powerplant by pipeline.

Table 6 shows the resulting LCI for NG supply chain. More details about data gathering, background information and adjustments performed to processes available on Ecoinvent libraries are reported in Appendix III. The distances estimated for NG transport are presented in Appendix IV. It must be mentioned that the processes describing LNG production are normalized on gaseous form of gas, which allows the modelling in terms of volume.

Appendix III shows the results and analysis of the supply of 1 m^3 of natural gas through the LCI modelled in the current study and through an average process for Europe, available in Ecoinvent.

Uncertainties and error propagation on Monte Carlo analysis

As for this process, data does not result directly from the processing of a sample, the standard errors (geometric standard deviations) were estimated using Pedigree Matrix, by considering lognormal distributions. The six criteria selection is shown in the comments below each sub-process.

4.3.2 Ribatejo NGCC Powerplant

The data used to estimate raw materials consumption and emissions was supported on a series of annual historical data (from 2008 to 2018) taken from environmental reports published by EDP, SA under EMAS industrial ecology certification program [68].

4.3.2.1 Processes description

Among raw materials consumption are fuels, both NG and diesel, surface water from Tejo River, groundwater and some other chemical agents used for water pre- and post-treatment: hydrochloric acid (HCl), sodium hypochlorite (NaOCl), ammonia (NH_3), sodium hydroxide (NaOH).

Although natural gas represents the main source of fuel, diesel is also used for emergency generator and fire control pump. Its consumption is not correlated with power generation as its use is somewhat random, as it will be further discussed.

The water used in the plant is supplied from two abstractions: one of surface water from Tejo River and another from groundwater. The surface water enters the industrial water system after a screening process and acid-base treatment. The groundwater undergoes only a screening process and it is used for fire control and demineralised water production. When groundwater capture is unable, surface water is used instead requiring some additional treatment processes: flocculation, settling and further filtration. In the demineralisation unit, pre-treated water undergoes a reverse osmosis process, followed by an ion exchange resins process (mixed beds), being finally stored. This water is used on water-vapour circuit of the main and auxiliary boilers, on the chiller circuit and on the demineralisation unit. The water-vapour circuit is close and has a purge on the cooling towers to avoid any excessive increase of solid matter.

Along operation processes, described in the previous section, different air and water emissions sources are continuously monitored:

- Air emissions – steam generators chimneys which emit combustion flue gas after passing the recovery boilers; chimney of auxiliary boiler which uses NG as fuel; chimney of emergency diesel group; chimney of fire system group also feed with diesel;
- Liquid emissions – washing of gravimetric filters; reverse osmosis concentrate; purges from cooling towers; oily, chemical, domestic and rainwater effluent from places susceptible to some contamination.

On the reports, besides a disinfection process on cooling towers to prevent *legionella* emissions, other air treatment units are not mentioned. However, Dry Low NOx burners were implemented allowing a reduction of carbon monoxide (CO) emissions [99]. Emissions of nitrogen oxides (NOx) and CO and continuously monitored in each generator group. Suspended particles and volatile organic compounds (VOCs) are monitored two times a year in each generator group. Emissions results are annually reported on [68]. Particles and VOCs emissions were calculated based on the average of emissions flows obtained from the sampling trials (kg/h) and the utilization rate of the powerplant (hours of operation) for each year. For the purpose of legal compliance, the plant has several air quality monitoring units on its surroundings.

Diffuse emissions from loading, unloading, transport and storage of raw materials are not reported. Their estimation is rather difficult to perform, as part of them end up being gathered in wastewater collectors, following for further treatment and/or water discharge. Hence, these emissions were not account in LCI for NGPP operation.

Liquid effluents pass by a wastewater treatment plant before being discharged to Tejo River.

As a result of the plant activities, different types of waste are produced, which are separated, classified according to the European Waste Codes (EWC) and forwarded to authorised consignees for recovery, treatment or disposal. Their storage site is conditioned to minimize material and/or substances losses that could lead to soil and water contamination [99].

4.3.2.2 Life Cycle Inventory: data processing and forecasting method

Raw data collected and its processing is reported in detail in Appendix V. All parameters were correlated to the generated electricity in MS Excel and all the regressions obtained with coefficient of determination (R-squared) above 0.80 were used to estimate raw materials consumption and emissions to perform a robust sensitivity analysis to different utilization rates of the powerplant. Parameters as diesel consumption and detergents concentration in the final effluent were almost constant along the time series, so that an average value was used equally for all operation scenarios instead. Using simple regressions, total waste generation has an unpredictable behaviour, thus an average value was also used. Its classification into 'hazardous' and 'non-hazardous' and management mechanisms was split based on average rates:

- In average, about 85 % of the total produced waste is non-hazardous and the remaining 15 % is classified as hazardous;
- In average, about 70 % of the total produced waste is valorised through recycling and recovery, and the remaining is landfilled.
- It was assumed that 5 % of the total produced waste was hazardous and the remaining 65 % (from the total valorised waste) is non-hazardous. This assumption is based on the fact that for some years the amount of valorise waste exceeds the amount of non-hazardous waste which suggests that a small fraction of the hazardous waste is also valorised.

The regressions obtained for NOx, suspended particles and VOCs have a range of negative predicted emissions for electricity generation (annually) below $1E10^6$ MWh for NOx and $2{,}5E10^6$ MWh for particles and VOCs. For the scenarios simulated with electricity below $2{,}5E10^6$ MWh, the minimum values for particles and VOCs reported in the period considered (0.08 and 2.90 kg, respectively) were used instead.

Table 7 shows the reference scenarios of electricity generation tested for the NGPP (Ribatejo). The scenario '8k' provides the comparison basis with CPP. Table 8 shows the LCI for the operation of the Ribatejo powerplant without the capture unit and the method used to predict the different parameters. The last column shows the interval of 95 % around the best estimate, considering that the variation of the values for each parameter describes a normal distribution. The entries given for each scenario for the parameters showed in LCI are presented in Table IV-5 (Appendix V).

Table 7 - LCI results for each production scenario for Ribatejo Powerplant.

Scenarios		Av-20%	Av.	Av+20%	Av+40%	Av+60%	Av+80%	Av+100%	Av+200%	8k
Electricity generated	**GWh**	**1804**	**2255**	**2706**	**3157**	**3608**	**4059**	**4510**	**6764**	**8268**
Electricity supplied	**GWh**	**2186**	**1747**	**2706**	**3066**	**3507**	**3949**	**4392**	**6618**	**8078**
Utilization rate	%	18%	22%	26%	31%	35%	39%	44%	66%	80%
Operation hours (full load)	h	1534	1917	2301	2684	3068	3451	3835	5752	7031
Carbon dioxide	ton	654067	817584	981101	1144618	1308135	1471651	1635168	2452752	2998144
Carbon dioxide	ton/h	426.4	426.4	426.4	426.4	426.4	426.4	426.4	426.4	426.4

Table 8 - Life cycle inventory for each operation scenario simulated for Ribatejo powerplant.

Electricity produced in NGPP (reference operation)		ref_E	**MWh**			
Resources from environment	**Sub. Comp.**	**Entry**	**Unit**	***Prediction method***	***R^2 (reg.)***	***2*SEE / 2*SD***
Water, river, PT	in water	(-8*10^(-8)*ref_E^2+1,2828*ref_E)*0,95	m3	Polynomial regression	0.9265	337250
Water, well, in ground, PT	land	(-8*10^(-8)*ref_E^2+1,2828*ref_E)*0,05	m3	Polynomial regression	0.9265	17750
Inputs from technosphere: Materials/Fuels						
Natural gas at use on powerplant		164,67*ref_E	Nm3	Linear regression	0.9996	10395
Diesel {RER}| market group for		5.08	ton	Average		1.88
Hydrochloric acid, without water, in 30% solution state {RER}| market for		8*10^-9*ref_E^2+0,1697*ref_E	kg	Polynomial regression	0.9801	56961
Sodium hypochlorite, without water, in 15% solution state {GLO}| market for		-1*10^-8*ref_E^2+0,2224*ref_E	kg	Polynomial regression	0.9235	87380
Ammonia, liquid {RER}| market for		-2*10^-10*ref_E^2+0,0031*ref_E	kg	Polynomial regression	0.8716	1049
Sodium hydroxide, without water, in 50% solution state {GLO}| market for		1,26*10^4	kg	Average		16881

Table 9 - Follow-up of Table 8.

Emissions to air

Nitrogen oxides, PT	high. pop.	9*10^-11*ref_E^2-7*10^-5*ref_E	ton	Polynomial regression	0.9795	131
Carbon monoxide, fossil	high. pop.	1*10^-12*ref_E^2+1*10^-5*ref_E	kg	Polynomial regression	0.8491	12.6
VOC, volatile organic compounds	high. pop.	6*10^-9*ref_E^2-0,0138*ref_E	kg	Polynomial regression	0.9874	835
Carbon dioxide, fossil	high. pop.	0,3626*ref_E	ton	Polynomial regression	0.9864	1.86E+05
Suspended particles	high. pop.	4*10^-10*ref_E^2-0.0011*ref_E	kg	Linear regression	0.9874	587

Emissions to water

Ammoniacal nitrogen	river			Polynomial regression	0.9643	525
Nitrogen	river	10^-10*ref_E^2+0,002*ref_E	kg	Polynomial regression	0.9931	1071
BOD5, Biological Oxygen Demand	river	0,0041*ref_E	kg	Linear regression	0.8408	3473
COD, Chemical Oxygen Demand	river	10^-9*ref_E^2+0,0143*ref_E	kg	Polynomial regression	0.994	7534
Chlorine	river	23,311*EXP(6*10^-7*ref_E)	kg	Exponential regression	0.9161	104
Phosphorus, total	river	87,171*EXP(6*10^-7*ref_E)	kg	Exponential regression	0.9364	373
Oils, unspecified	river	-2*10^-11*ref_E^2+0,0006*ref_E	kg	Polynomial regression	0.9616	207
Hydrocarbons, unspecified	river	0,0003*ref_E	kg	Linear regression	0.9607	1.38
Detergents, unspecified	river	3,67*10^-2*(6*10^-8*ref_E^2+0,5347*ref_E)*10^-3	kg	Average of conc. and polynomial reg. effluent volume	0.9933	18
Suspended solids, unspecified	river	(5*10^-13*ref_E^2-1*10^-6*ref_E+7,9284)*(6*10^-8*ref_E^2+0,5347*ref_E)*10^-3	kg	Polynomial regression of conc. and effluent volume	0.8919; 0.9933	8
Hazardous waste, unspecified treatment		11718	kg	10 % of total prod. waste (average)		135142
Hazardous waste, recovery		5859	kg	5 % of total prod. waste (average)		6757
Non-hazardous waste, unspecified treatment		23436	kg	20 % of total prod. waste (average)		27028
Non-hazardous waste, recovery		76169	kg	65 % of total prod. waste (average)		87842

Uncertainties and confidence intervals

To estimate models' uncertainties, the variation of the data was assumed to be described by a normal distribution, for which the input value for each parameter is the 'best guess' acting as the mean value of the distribution and the 95 % confidence interval is found between two times the standard deviation above and below the mean. The results are presented in the last column in Tables 8 and 9.

For parameters predicted by regressions, the standard error of the estimate (SEE) calculated to each regression through its definition:

$$SEE = \sqrt{\frac{\sum(\hat{y} - y)^2}{n - 2}}$$

Where variable *y* is the dependent variable on the regression, with $\hat{y}$ being the estimate value i.e. obtained from the regression, and *y* being the actual values from the dataset; variable n is the sample size. This statistical parameter measures the standard distance between the observations and the regression line i.e. the precision of the model's predictions. It was used to obtain a rough estimate of the 95 % predication interval. For parameters resulting from average values and regressions ('detergents') and others resulting from two regressions ('suspended solids'), the standard error derivates from the propagation of the standard error of each regression and average value.

4.3.3 Coal supply chain

The source for the coal used in Sines powerplant was assumed to correspond to the share of coal imports in Portugal. Figure 28 shows hard coal imports by country of origin. As for natural gas, Portuguese imports are highly different from the average in European region (see Figure 29). However, Ecoinvent database 3.3 provides a process that model hard coal supply mix for Portugal. The process includes all transport from the storage in producing regions to power plants in Portugal. Transport distances and exporting regions are specifically estimated for each country, other parameters are generic such as: average coal losses and average emissions to water due to leaching from coal heaps at storage at receiving terminal. This process was designed by Paul Scherrer Institute (PSI) and it was used in this assessment to model coal supply chain to Sines powerplant.

During coal mining the methane (CH_4) formed during coal formation that remains trapped in the strata is released and it is the main contributor for the emissions of the activity. The amount of CH_4 released depends on several factors, 'the most important of which are coal rank, coal seam depth, and method of mining' [100]. The emissions increase for increased coal rank and depth as deeper coal seams generally contain more methane. Furthermore, underground mining releases more methane than surface mining or open-pit mining because of the higher gas content of deeper seams and because of activities related to explosions and broken up of underground strata [100]. Colombia is the main exporter to Portugal, therefore, its coal mining process have a major influence on the overall performance of the coal supply. The country holds significant volumes of coal mine and coalbed methane utilization potential [101]. Thirteen of Colombia's fifteen largest coal mines are at surface [101], contributing to a less carbon emissions intensive supply.

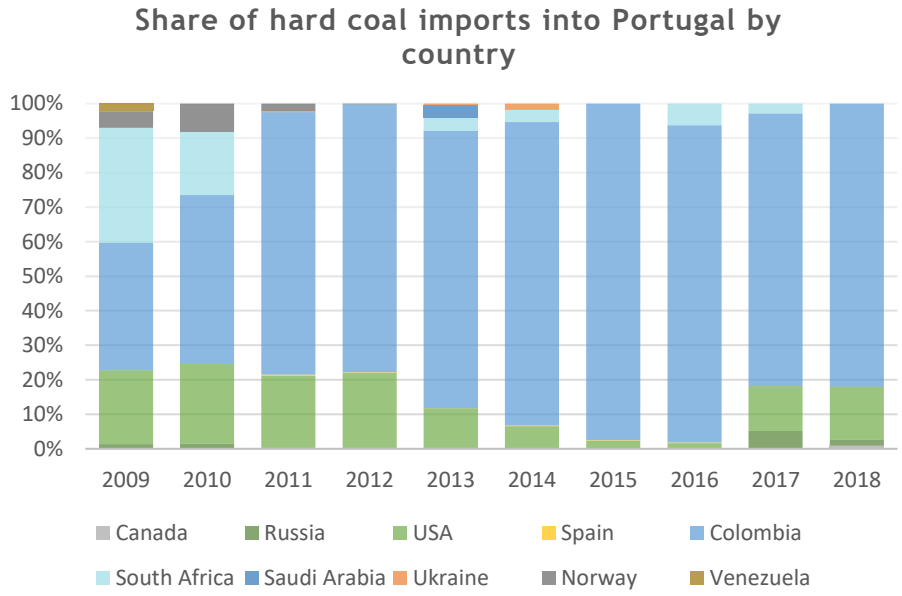

Figure 28 - Hard coal imports for Portugal by country of origin. Source: DGEG [87] (2011-2016), Eurostat [102] (2009-2010, 2017-2018).

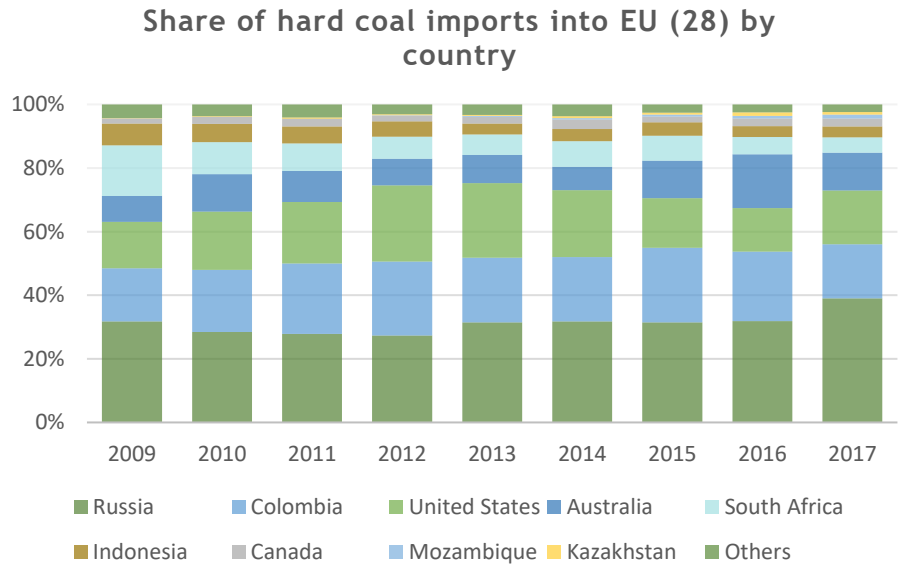

Figure 29 - EU hard coal imports by country of origin. Source: Eurostat [103].

4.3.4 Sines Pulverized Coal Powerplant

The data used to estimate raw materials consumption and emissions was supported on a series of annual historical data (from 2009 to 2018) taken from environmental reports published by EDP, SA under EMAS industrial ecology certification program [67].

4.3.4.1 Raw materials consumption

Coal is the main raw material used to produce electricity in Sines PP. The only parameter regarding its composition reported is the content in sulphur (%), which needs to comply with the legal maximum limit of 1.2 %. As coal composition highly influence operations emissions [14,75-78], its estimation was necessary for giving as an input for the predicting model designed. The method for estimating coal composition was based on the supply mix for each

year and country specific composition data. The estimation method is described in Appendix VI. A sensitivity analysis to coal supply chain was not performed.

Table 10 - Raw materials consumption.

Raw Material	*Use*
Fuel oil	Boilers ignition
Diesel	Auxiliary boilers, emergency situations and fire pumps
Propane[10]	Boilers ignition
Limestone	Desulphurisation of flue gases
Hydrochloric acid	Resin regeneration and wastewater treatment
Ammonia hydroxide	Boiler conditioning and wastewater treatment
Calcium hydroxide	Wastewater treatment
Sodium hydroxide	Resin regeneration
Iron (III) chloride	Wastewater treatment
TMT-15 (2,4,6 – Trimercapto – s – triazine)	Wastewater treatment
Polyelectrolyte[11] (Sodium hypochlorite)	Water treatment
Aluminum sulfate	Wastewater treatment
Hydrazine hydrate	Wastewater treatment
Carbohydrazide	Boiler conditioning
Hidrogen	Alternator cooling
Oils	Lubrification and hydraulic systems
Carbon Dioxide	Firefighting and wastewater treatment
Solvents	Cleaning
Industrial water	Operations use
Drinkable water	Personal use

Besides coal, other raw materials are used. Operations in Sines PP is more complex than in Ribatejo PP: besides water pre-treatment, it comprises flue gas treatment units, wastewater treatment units and two landfills. Therefore, much more raw materials are used. Table 10 shows all those raw materials, apart from coal, and its use purpose.

The water used for chiller circuit is captured from the ocean and is not considered as a raw material as it circulates in an open system. Nonetheless, its chlorine emissions are accounted.

4.3.4.2 Atmospheric emissions

The powerplant has nine fixe sources of atmospheric emissions associated to the main chimneys (FF1 and FF2), auxiliary boilers (FF3), emergency generators (FF4, FF5 and FF6), diesel pumps

[10] Propane use was discontinued in 2017.

[11] These compounds were not clearly defined. For the assessment, it was assumed to be sodium hypochlorite, electrolyte used to control the growth of marine organisms in the ocean water used in the main cooling circuit, as reported in [88].

used for firefighting (FF7 and FF8) and diesel generator on desulphurisation unit (FF9). Emissions are periodically monitored in sources FF1 and FF2 with exception for CO_2 which emissions are continuously monitored. For the other sources, functioning hours and fuel consumption are reported [87].

Diffuse emissions from loading, unloading, transport and storage of raw materials are not reported. The estimation of these emissions as well as the ones from emission sources FF4 to FF9 was not performed, to avoid the increase of uncertainty in the model. Therefore, only emissions from the main chimneys are accounted for the LCA, which results in an underestimation.

Selective Catalytic Reduction (SCR)

In 2011, denitrification systems were installed in each generator group. The process is based on Selective Catalytic Reactor (SCR) through which the high dust flue gas follows after the combustion chamber, reducing some compounds as nitrogen monoxide (NO), nitrogen dioxide (NO_2), nitrogen molecular (N_2) and water vapour (H_2O) through the action of ammonia (NH_3) [87]. These SCR are just upstream of electrostatic precipitators and their removal efficiency for nitrogen oxides exceeds 80 % [87].

Electrostatic precipitators

Each steam generator group is furnished with electrostatic precipitators which removes coarse and fine particles with an efficiency of 99.5 %. The retained particles fall into the hoppers and are transported pneumatically into a storage site [88], where their classification according ISO is proceeding. Collected fly ash can be classified as a by-product and sold to cement industry or, in case of poor quality it follows into the landfill of non-hazardous wastes in Sines Park, which use is exclusive for fly ash and coal slag.

Desulphurisation unit

After combustion, the flue gas is treated in a desulphurisation unit to reduce its content of sulphur dioxide (SO_2). The gases pass through a limestone slurry solution in counter-flow, which absorb SO_2, fine particles, fluorinated and chlorinated compounds. From the process two flows are generated: flue gas with low content of SO_2 (95 % of efficiency) and gypsum. Limestone is supplied in crashed stone and its pre-treatment comprises a grinding and humid process. Gypsum produced is recirculated into pulverisers and reused, another part is dehydrated and temporarily stored until sent to final destination. The small fraction of purged water follows to a treatment unit.

4.3.4.3 Water treatment unit

The industrial water used for the compensation of the steam-water circuit and for the desulphurisation unit is supplied by Água de Sto. André (AdSA) [87, 88]. The process to which the surface water is subjected to in Morgavel water treatment plant comprises: pre-oxidation with chlorine; chemical coagulation with aluminium sulphate; flocculation and settling, filtration and sludge treatment [89]. Although the water is classified as industrial by AdSA, in Ecoinvent database, the process for water supply describing the most similar treatment process is classified as potable water. The inventory is based on an average between 9 different water plants in Canada and the treatment process is rather similar to the process described by AdSA with the exception for an additional unit for disinfection with ultraviolet radiation for one out nine plants [104].

At Sines Park, the water is pre-treated in to reach the required quality to be used on steam-water circuit. The main processes occurred in the ion exchange demineralisation facility are:

- Filtration through activated carbon adsorption process;
- Degasifiers;
- Demineralisation by ion exchange in a cationic resin, further anion exchanger and a final mixed bed;

4.3.4.4 Wastewater treatment and discharge

Sines powerplant produces different types of effluents that can be grouped into four main networks: potentially contaminated rainfall water, oily wastewater, chemical wastewater and domestic wastewater. Those effluents are subjected to a totally of nine independent treatment lines (TL). The main operations are summarized in Table 11.

Table 11 - Summary table of wastewater treatment operations and discharge. The arrows represent effluent fluxes until the discharge points. Depending on the resulting quality, the effluent from TL4 can be directly discharged in EH2 or redirected to TL7.

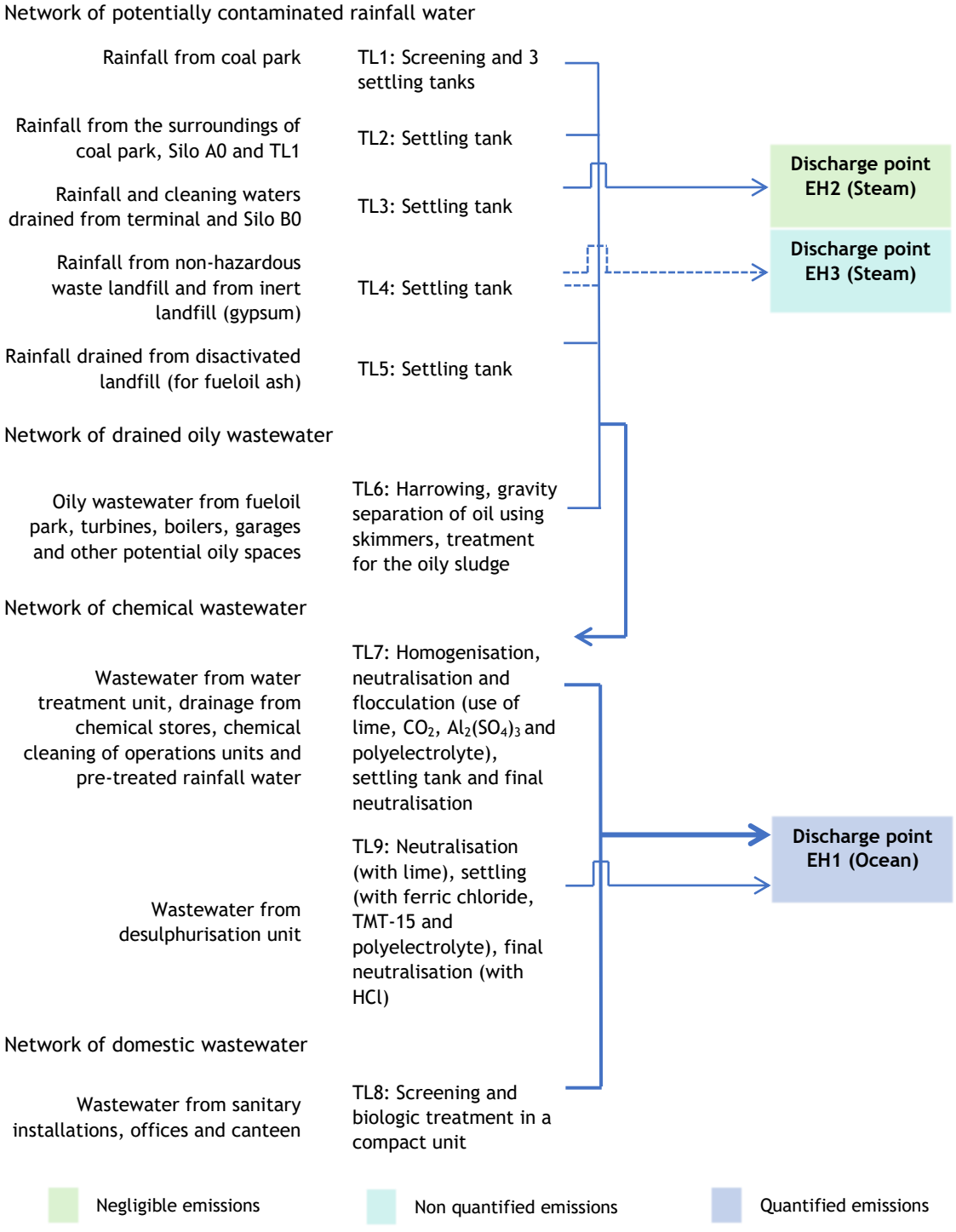

The decanted solids on settling tanks are collected, stored and classified into by-products or waste. The produced waste is either landfilled or forwarded to authorised consignors. The oil and the oily sludge produced in TL6 is collected by authorised operators.

The effluent that results from the settling treatment in TL3 is considered clean and is directly discharged on a steam (Junqueira). The effluent that results from the settling treatment in TL4 is either redirected to TL7 or discharged in another steam (Esteveira), depending on its quality. Esteveira is periodically monitored. Physical and chemical parameters are quantified at an upstream point and a downstream point in relation to the discharge EH3. However, as there is no available information regarding the steam flow, those emissions cannot be estimated.

The effluent from TL7 and TL8 are discharged together to the Ocean. The effluent from TL9 is also discharged to the ocean, however from a different outlet. The emissions from these two final effluents are reported on [87] and presented in Appendix VI already converted into a single effluent discharge.

4.3.4.5 Solid waste

As a result of activities in the plant, different types of wastes are produced, mostly non-hazardous, which are separated, classified according to the European Waste Codes (EWC) and routed to the site customised for temporary storage (two parks). Finally, they follow to authorised consignees for recovery, treatment or disposal. The amounts of waste which is produced and valorised are reported and presented in Appendix VI.

As aforementioned, Sines park has one disactivated landfill, used for fuel oil ash, one landfill of non-hazardous wastes, for fly ash and coal slag, and another landfill for inert waste, for gypsum.

4.3.4.6 By-products

The fly ash that is collected in the electrostatic precipitators are almost entirely valorised to cement and concrete industries. They are transported by tanker trucks or tanker in railways wagons. Ash quality is characterized according to NP EN 196 and NP EN 450 and the noncompliant share is either reused for combustion process or landfilled.

As a result of coal combustion, coal slag is produced and collected through mechanic drag equipment (dry method) from boilers ashtrays. After collected, coal slag used to be landfilled. In 2017, the landfill was exceeding its projected capacity, which enhanced the valorisation of this waste. In the same year, APA (Environmental Portuguese Agency) declared coal slag produced in Sines PP as a by-product. Since then, it has been almost entirely valorised, mainly for the cement industry. In 2018, the amount of sold slag was higher than the amount that was produced which suggests that some previously landfilled slag was already carried off.

From 85 to 95% of total produced gypsum (in the desulphurisation unit) is valorised as a raw material according to the norm EUROGYPSUM and the remaining goes to the landfill of inert waste. During the period of economic crisis in Portugal, the sales decreased, and a significant share of gypsum was temporarily stored in a closed cell of the same landfill.

Sales volumes and the inputs and outputs of each by-product/waste in landfill/storage is reported on [87] and presented in Appendix VI. The amounts of their annually production were obtained by an indirect relation of reported variables.

4.3.4.7 Life cycle inventory

The historical dataset collected from a total of 10 environmental reports (from 2009-2018) were used to estimate the entries for the operation scenarios. Unlike data from natural gas powerplant, almost any parameters could be related to generated power with simple excel regressions (linear, polynomial, exponential, logarithmic, moving-average, power). The reason for this could be linked with the greater complexity of Sines plant operation and to the variability of coal composition within the years, factor of major influence on emissions [14,75-

78]. Unlike natural gas[12], coal composition can vary widely depending on its source. For that reason, an Artificial Neural Network was designed for predicting atmospheric emissions, effluent emissions, waste and by-products generation giving coal composition, and the electricity generated as inputs.

Raw materials consumption was not considered as targets for the ANN model as their causality relation with coal composition is null and the same relation with electricity generated was already proved poor through regressions results. To model such parameters average values could be used.

Artificial Neural Network

'Artificial Neural Networks (ANN) is an information processing paradigm that is inspired by the way biological nervous systems, such as brain, process information' [104]. The structure of the information is composed of interconnected processing elements (neurons), which are 'configured for a specific application, such as pattern recognition or data classification, through a learning process' [104].

There are two main approaches to train an ANN: supervised and unsupervised learning. The supervised learning provides both inputs and outputs. Typically, the original dataset is divided into training, validation and test. 'The network then processes the inputs and compares its resulting outputs against the desired outputs (validation set). Errors are then propagated back through the system, causing the system to adjust the weights which control the network. This process occurs over and over as the weights are continually tweaked' [104]. To evaluate the accuracy (for classification) or relative and absolute errors (for regression problems), the model is tested with the test dataset, through the comparison of resulting outputs against the original ones. The bigger the dataset the more accurate will be the predicting model and lower is the chance of overfitting to occur. Networks don't learn when 'input data does not contain the specific information from which the desired output is derived'; and 'don't converge if there is not enough data to enable complete learning' [104]. In unsupervised learning, the outputs are not provided and the 'system itself must then decide what features it will use to group the input data'. It is used for a narrower range of applications and its mathematical modelling is not yet fully understood [104].

ANN can be modelled with different architectures, depending on the number of hidden layers, the number of neurons, connections between layers, summation, transfer and training functions and even the initial weights [104, 105].

Two ANN were designed in Python 3 using Jupyter Notebook. The tools used were from Keras Models, available in Tensorflow, which is an open source machine learning library that provides tools and other resources that enhance the build-up of models. The first ANN designed was a non-deep feedforward neural network trained with supervised learning with the dataset split into training, validation and test. The second one was a K-fold model, typically used for small datasets, as it does not require the split into training, validation and test. In K-fold models, a cross validation is performed: the dataset is divided into K groups and then the model takes each group as a test dataset and set the remaining groups as a training set [106]. Although, the first model achieved a better performance (measured in terms of mean squared error), both

[12] Natural gas composition is more stable within each type. Table below shows typical values of the composition of five natural gas fuels of distinguished qualities [83] (data from 2008).

(% vol.)	H_2	CO	CH_4	C_2H_6	C_3H_8	C_4H_{10}	Other C_xH_y	CO_2	N_2	O_2
Blast furnace gas	4.1	21.4						22	52.5	
Coke oven gas	54.5	5.5	25.3				2.3	2.3	9.6	0.5
Low calorific NG			81.8	2.8	0.4	0.2		0.8	14	
High calorific NG			93	3	1.3	0.6		1	1.1	
Biomethane			>97					< 2	< 0.8	

models were used for predicting emissions. Figure 30 is a graphical representation of the architecture of the feedforward ANN designed. The algorithm is presented in Appendix VII.

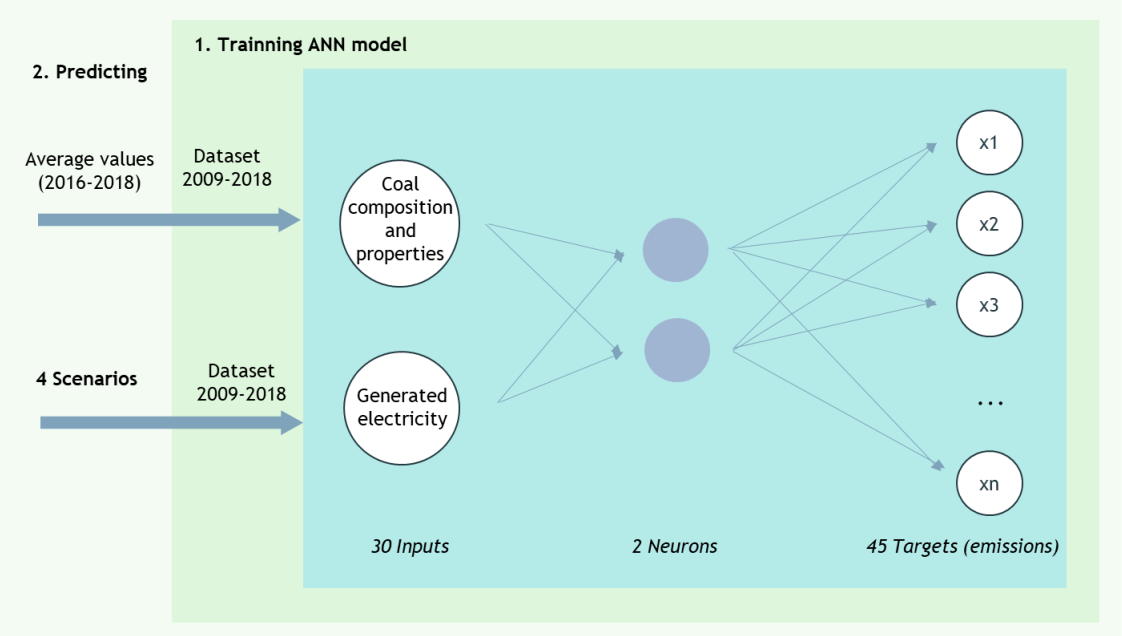

Figure 30 - Diagram representing the architecture of the developed ANN for predicting emissions and waste generation in Sines powerplant.

One of the main important design aspects is the activation function. The activation function is a mathematical gate between the input feeding the current neuron and its output going to the next layer [98]. The basic process carried out by a neuron is represented above:

$$Y = \sum(weight \times input) + bias$$

Th weight in each neuron can range between -inf and +inf. Activation functions are the mathematical operators that decide if the output of each neuron should be activated or not. The most recommended activation function for regression problems found in literature and data science forums is the non-linear ReLU function (Rectified Linear Unit). This function was used in the model for the input layer and the neurons hidden layer. For the outputs layer the linear function was chosen. The loss function (optimization method) was the mean absolute error. An early stooping mechanism was modelled to avoid overfitting ('EarlyStopping' with a patience of 3 epochs). Regarding other design features, a sensitivity analysis was performed to determine which number of neurons, hidden neurons layers, optimizer (Stochastic Gradient Descent (SGD) and Adam) and split of samples into 60 % training/ 20 % validation/ 20% test or 50 %/30 %/20 % (for feed-forward model) provided best results. The best achieved performance with a mean absolute error of 0.7011 and mean squared error of 0.7525 was achieved by feed-forward model with:

- Number of epochs: 7
- Number of neurons: 2
- Number of neurons hidden layers: 1
- Optimizer: 'adam'
- Sample split: 60 % training; 20 % validation; 20 % test

The first step consisted in training the ANN by importing a dataset with both inputs (average coal composition for each year and the electricity it generated in each year from 2009 to 2018)

and targets (atmospheric emissions, wastewater emissions[13] and generated waste in each year from 2009 to 2018, in a mass basis). The annual average of coal composition was estimated based on national hard coal imports by country and on data found in literature regarding hard coal composition in main exporters. As the original dataset presented a wide range of numerical values within the different variables/parameters, the data was standardized through Z-score's definition to improve model's convergence:

$$Z = \frac{(x - \mu)}{\sigma}$$

For prediction (second step), the inputs dataset was based on an average coal composition between 2016 and 2018 and 4 different operation scenarios were set: 5000 GWh (5K); 7338 GWh (AVminus – average between 2016 and 2018 minus 20 %); 9172 GWh (AV – average between 2016 and 2018); 11006 GWh (AVplus - average between 2016 and 2018 plus 20 %). The amount of coal consumed for each scenario was calculated through the linear regression of energy generated vs. coal consumption. The amount of coal was multiplied by the content of each component, to obtain the content input on a mass basis. Then, all inputs were standardized with the mean and standard deviation of the original input's dataset. The obtained results were subjected to an inverse process to standardization, through the operation of the mean and standard deviation of the original targets dataset.

The datasets and the results obtained are presented in Appendix VIII.

For all scenarios the same coal composition was given as input, thus it was expected a slight increase or even decrease of emissions with the increase of electricity generated by the plant, in a regular behaviour. However, results describe irregular and hyperbolic behaviours for most of the emissions. The reason may be linked to an overfitting of the models to the original dataset, which is common for models trained with small sample sizes (with less than 100 samples). While overfitting, the model will reduce the loss function, improving its precision and accuracy but compromising its predictive power for other input datasets. None of the models were good enough for predicting emissions. Hence, their use was disregard and the sensitivity analysis to different operation scenarios (corresponding to different utilization rates or electricity produced) was not performed for Sines powerplant.

Conclusion

Instead of predicting input/output inventories, the LCA was based on the historical data. The amount of electricity generated in the years of 2014, 2016 and 2018 were almost equivalent with an average value of 8713 GWh and a standard deviation of 23 GWh (about 0.27 %). However, as expected from the results of regressions, raw materials consumption and emissions can vary significantly. An average scenario using data from these three years was used to model powerplants operation and the standard deviation of each parameter was used to estimate the uncertainties on the results by considering that the variation within the data for each parameter is described by a normal distribution. The operation scenario initially defined to serve the comparison between coal powerplant and natural gas powerplant of 5 GWh was, by consequence, redefined for 8078 GWh (the amount provided to the grid for an average year producing 8713 GWh).

Table 12 shows the life cycle inventory for Sines powerplant operation. In the environmental reports, data is not divided per sub-process, thus a single process describing the overall input/output of plant's operation was designed.

[13] Hexavalent chromium (Cr (VI)) was disregarded, as the data reported on environmental assessments show range within 4 orders of magnitude which could be explain for different complexation processes used for measuring. Therefore, the inclusion of Cr (VI) in the dataset could increase noise into the learning process.

Table 12 - Life cyle inventory for Sines operation without HGtS.

Electricity produced at Sines powerplant		**8.078E6**	**MWh**		
Inputs from technosphere: Materials/fuels	*Sub-compartiment*	*Atribution*	*Unit*	*Distribution*	*2*SD*
Hard coal supply mix/PT S		3207110	ton	Normal	37841
Heavy fuel oil {Europe without Switzerland}| market for		5982	ton	Normal	1554
Diesel {Europe without Switzerland}| market for		573	ton	Normal	1642
Limestone, crushed, for mill {RoW}| market for limestone, crushed, for mill **Comments:** No transportation accounted. Easily justified as Portugal produces much more limestone than it imports and production spots are in south. Should CH represent a better approximation than RoW?		66474	ton	Normal	13181
Hydrochloric acid, without water, in 30% solution state {RER}| market for | Alloc Def, S		1330	ton	Normal	1571
Ammonia, liquid {RER}| market for **Comments:** Used as a simple approximation to ammonia hydroxide		17832	ton	Normal	2520
Quicklime, milled, loose {CH}| market for quicklime, milled, loose		257	ton	Normal	182
Sodium hydroxide, without water, in 50% solution state {GLO}| market for		825	ton	Normal	1406
Iron (III) chloride, without water, in 40% solution state {GLO}| market for		23	ton	Normal	17
Sodium hypochlorite, without water, in 15% solution state {GLO}| market for		15	ton	Normal	15
Aluminium sulfate, without water, in 4.33% aluminium solution state {GLO}| market for		6	ton	Normal	7
Hydrogen, liquid {RER}| market for		18181	ton	Normal	13352
Lubricating oil {GLO}| market for		34	ton	Normal	16
Carbon dioxide, liquid {RER}| market for		21	ton	Normal	12
Solvents, organic, unspecified, at plant/GLO S		1	ton	Normal	1
Tap water {Europe without Switzerland}| water production with conventional treatment **Comments:** Tap water with conventional treatment has the most similar process to the one described by ADsa for industrial water. It does not account for transport or losses, which does not represent a significant underestimation as the water supply by pipeline from Morgavel water treatment plant to final user is gravitational.		2194952	ton	Normal	177693
Tap water {RER}| market group for		13585	ton	Normal	4615
Emissions to air					
Sulfur dioxide, PT	low. pop.[14]	3719	ton	Normal	428
Nitrogen oxides, PT	low. pop.	4365	ton	Normal	522
Particulates, < 2.5 um **Comments:** Eletrostatic precipitators are highly efficient for fine particles.	low. pop.	41	ton	Normal	52
Fluoride compounds, unspecified	low. pop.	39	ton	Normal	12
Chlorinated solvents, unspecified	low. pop.	48	ton	Normal	40
Carbon monoxide	low. pop.	493	ton	Normal	342
Carbon dioxide, fóssil	low. pop.	7382804	ton	Normal	119093
VOC, volatile organic compounds	low. pop.	111	ton	Normal	127
Heavy metals, unspecified	low. pop.	8	ton	Normal	2

[14] Sines is a city with 14238 inhabitants (Censos 2011 – INE) which returns a population density of 70 inh/km^2 [107], lower than the criteria of 400 inh/km^2 to classify the area with high population density.

Table 13 - Follow-up of Table 12.

Electricity produced at Sines powerplant		**8.078E6**	**MWh**		
Emissions to water	*Sub-compartiment*	*Atribution*	*Unit*	*Distribution*	*2*SD*
BOD5, Biological Oxygen Demand	ocean	798	ton	Normal	939
COD, Chemical Oxygen Demand	ocean	26198	ton	Normal	3386
Suspended solids, unspecified	ocean	7960	ton	Normal	2283
Mineral oil	ocean	72	ton	Normal	64
Ammonia	ocean	901	ton	Normal	1188
Nitrogen	ocean	590	ton	Normal	844
Iron	ocean	85	ton	Normal	105
Mercury	ocean	4	ton	Normal	6
Vanadium	ocean	172	ton	Normal	97
Zinc	ocean	12	ton	Normal	19
Aluminium	ocean	197	ton	Normal	146
Arsenic	ocean	2	ton	Normal	1
Copper	ocean	5	ton	Normal	12
Manganese	ocean	30	ton	Normal	32
Nickel	ocean	29	ton	Normal	27
Cadmium	ocean	2	ton	Normal	5
Lead	ocean	48	ton	Normal	145
Magnesium	ocean	162440	ton	Normal	65050
Potassium	ocean	10280	ton	Normal	6612
Sulfate	ocean	558645	ton	Normal	498476
Sulfide	ocean	2	ton	Normal	3
Sulfite	ocean	99	ton	Normal	53
Nitrate	ocean	1824	ton	Normal	2492
Phosphorus	ocean	80	ton	Normal	72
Chromium VI	ocean	1769	ton	Normal	6122
Chromium	ocean	4	ton	Normal	6
Oils, unspecified	ocean	107	ton	Normal	86
Chlorine **Comments:** Emitted on recirculated water from ocean used for steam.	ocean	110	ton	Normal	164
Final waste flows					
Hazardous waste, unspecified treatment		2267	ton	Normal	1735
Non-hazardous waste, unspecified treatment		5499	ton	Normal	17226
Non-hazardous waste, recovery		5916	ton	Normal	8733
Waste to treatment					
Waste gypsum {Europe without Switzerland}| treatment of waste gypsum, inert material landfill **Comments:** No direct emissions (leachate) are inventoried as deemed negligible. Module contains only exchanges to process-specific burdens and infrastructure. Renaturation after closer. 50% of the sites feature a base seal and leachate collection system.'		1303	ton	Normal	4511
Waste gypsum {Europe without Switzerland}| market for waste gypsum **Comments:** The same transport distances as in the global market are used.'		136324	ton	Normal	72824
Hard coal ash {PT}| treatment of, residual material landfill **Comments:** 'Waste-specific short-term emissions to water from leachate. Long-term emissions from landfill to ground water. Waste composition as given in literature reference, theoretical data or other source. Transfer coefficients from prospective model.'		5532	ton	Normal	17493

Table 14 - Follow-up of table 12 and 13.

Electricity produced at Sines powerplant		**8.078E6**	**MWh**		
Waste to treatment	*Sub-compartiment*	*Atribution*	*Unit*	*Distribution*	*2*SD*
Hard coal ash {GLO}| market for **Comments:** It only accounts for transportation by freight train (0,0112 ton*km) and lorry (0,0193ton*km)		254725	ton	Normal	244575
Blast furnace slag {GLO}| market for **Comments:** It only accounts for transportation. As the market for blast furnance slag is the same as for coal slag, the distances should be the standard ones for coal slag market.		28144	ton	Normal	23462
Waste gypsum {Europe without Switzerland}| treatment of waste gypsum, inert material landfill		1303	ton	Normal	4511

Uncertainties and confidence intervals

To estimate models' uncertainties, the variation of the data was assumed to be described by a normal distribution, for which the input value for each parameter is the 'best guess' acting as the mean value of the distribution and the 95 % confidence interval is found between two times the standard deviation above and below the mean. The results are presented in the last column in Table 12, 13 and 14.

4.3.5 HGtS retrofitting: CO2 capture process

The process describing HGtS retrofitting was based on adjustments of the reference operation processes of the powerplants by:

- including the two raw materials used - industrial water or tap water and two ethylene glycol aqueous solutions, one with a concentration of 27 % and other with 35 %;
- reducing the electricity produced in each scenario to account the energy penalty;
- eliminating air emissions as the flue gas is completed trapped into the water cages of CO_2 hydrates or dissolved in the water within the hydrates are flowing;
- adding hydrates slurry production to the reference products;
- eliminating the consumption of CO_2 liquid by Sines powerplant for fire extinguishers, as the amount needed can be suppressed through the valorisation of CO_2 hydrates.

In SimaPro the processes chosen from Ecoinvent libraries to describe the use and supply of water was the one used for the industrial water for CPP's operation which comprises conventional treatment [108]. In NGPP, the water required for HGtS could also be sourced in the surface and groundwater capturing units, however, as it would be necessary to estimate an over consumption of raw materials for the pre-treatment, the same process was used. The ethylene glycol solutions were modelled using the same process form Ecoinvent libraries is a rough approximation.

The data for HGtS capture process was provided by Net4CO2 (see Appendix IX) and was obtained through simulations and scaling calculations considering a continuous flow of flue gas. As the equipment was not dimensioned, the materials required (mainly aluminium) for NETmix reactor plates, structure and pipes was not estimated. According to results of LCA with attributional analysis to CCS technologies retrofitting powerplants found in literature [75,76], the underestimation resultant is assumed to be negligible.

The thermal fluids recirculate in a close loop. However, as a result from the simulations its mass is obtained as a continuous flow (ton/h). Since, the equipment is not dimensioned, an accurate estimate for the exact mass of ethylene glycol solution in circulation is not possible. Due the fact that HGtS units result from the encapsulation of several micro-reactor plates – NETmix – the structures do not tend to be large nor the tubes to be long. Thus, it is assumed that the residence time of the fluid in the circuit is 30 minutes and consequently, the mass of fluid in circulation corresponds to 50 % of the flow obtained by the simulations. Furthermore,

a make-up of 5 % per year of the fluid is assumed, which combined with a lifetime of 20 years for the installation returns an average value of the mass of the fluid subjected to a year of operation.

After conducting experimental tests, Hatakeyama et al. [109] concluded that CO_2 hydrate can be used to extinguish fire. The dissociation of the hydrates decreases the temperature in the flame base, and the non-flammable gases released prevent the supply of oxygen to the flame. They have concluded that CO_2 hydrate require less water compared to ordinary ice and to dry ice. Therefore, it was assumed that part of the hydrate formed is used to supress the CO_2 consumed by the plant to extinguish fires.

The results for the LCI of both powerplant's operation with HGtS capture unit is showed in Table 16. Table 15 presents the structure of the LCI on the software. The products avoided: emissions to air and the liquid CO_2 used in the process to provide a direct comparison with the reference operation without HGtS.

Table 15 - Life cycle inventory of powerlan0st operation with HGtS retrofitting. The materials required for equipment and their dismantling were disregarded from the study. The entries are presented on table 16 for each operation scenario performed.

Electricity produced at Sines powerplant with HGtS retrofitting	**A**	**MWh**	**Allocation:**	**100 %**
Comment: To electricity generated without the operation of HGtS it was subtracted the energy penalty associated with its operation. The overall impacts are then divided to the functional unit to provide a direct comparison between these operation scenarios and the reference ones. The allocation of the impacts to HGtS retrofitting will be provided by that comparison.				
Slurry of CO_2 hydrate	**B**	**ton**		**0%**
CO_2 used in the process for fire extinguishers	**C**	**ton**		**0%**

Products avoided	*Entry*	*Unit*	*Distribution*	*2*SD*
(The total amount of **air emissions** is avoided for each plant, as the gases and particles are either caged in hydrate or dissolved in the water.)				
Carbon dioxide, liquid {RER}| market for **Comments:** CO_2 hydrates can be used for fire extinguisher.	**D**	ton	Normal	12

Inputs from technosphere:
Materials/fuels

(The materials and fuels consumed remained the same with exception for the carbon dioxide liquid consumed in Sines powerplant)				
Tap water {Europe without Switzerland}| water production with conventional treatment	**E**	ton	Normal	8.215E5
Ethylene glycol {GLO}| market for **Comments:** It circulates in close cycle. It was assumed, that the total mass in circulation on the equipment was 50% of the mass calculated for 1 hour of operation assuming continuous flow. It was assumed an annual make-up of 5% and a lifetime of 20 years.	**F**	ton	Lognormal	1.5

Emissions to water

(The emissions to water remained the same with or without CO2 capture unit.)

Final waste flows

(The final waste flows remained the same with or without CO2 capture unit.)

Waste to treatment

(The waste to treatment remained the same with or without CO2 capture unit.)

Table 16 - Entries for each scenario, on the processes describing powerplants operation with HGtS retrofitting.

	Ribatejo									
	Av-20%	**Av.**	**Av+20%**	**Av+40%**	**Av+60%**	**Av+80%**	**Av+100 %**	**Av+200 %**	**8k**	**Sines**
Total work (MWh)	66797	83474	100195	116872	133593	150271	166991	250465	322618	753902
Energy penalty (%)	4%	4%	4%	3.70%	3.70%	3.70%	3.70%	3.70%	3.70%	9%
(a)	1646824	2102546	2588839	2932529	3357124	3782489	4141914	6295469	7771842	7324431
(b)	6456161	5166276	7749414	9039299	10332552	11622437	12915690	19371851	24952373	58309892
(C)	0	0	0	0	0	0	0	0	0	21
(d)	0	0	0	0	0	0	0	0	0	21
(e)	4512151	5638719	6768227	7894794	9024303	10150870	11280379	16919097	21793045	50926580
(f)					6078					7421

Moreover, scenarios with a compensation of the energy penalty caused by HGtS operation on the grid was simulated, considering two different quality mix production: Portuguese grid, based on fossil fuel combustion and with the RER mostly supported on hydroelectric generation; and Norwegian grid, less carbon intensive, representing therefore a cleaner mix production. The processes are from Ecoinvent libraries.

Uncertainties and confidence interval

The variation of the data for the water consumption was assumed to be described by a normal distribution, for which the entries describe presented in table above act as the mean value of the distribution and the 95 % confidence interval is found between two times the standard deviation above and below the mean. The standard deviation was calculated from the water input obtained for the three different operation scenarios of Sines powerplant. Ethyelene glycol consumption is highly uncertain with the data being obtained by an assumption. Therefore, the distribution is considered to be lognormal, and the confidence interval was estimated using Pedigree Matrix. The results are presented in the last column in Table 15.

4.3.6 Transportation

The scenarios formulated for CO_2 transport and storage were based on the report mentioned in section 3.3 which defines some guidelines for a roadmap for CCUS industrial paradigm in Portugal. Under the COMMET project, preliminary studies were developed to acquire the geological feasibility to store CO_2 in Portuguese territory. The results provided in the report points three storage clusters as the most economical and technically feasible: S03, S04 (offshore) and S05 (onshore). However, other storage clusters were also considered to respect the maximum injection rates indicated by the same study. Transport scenarios are presented in Figures 31 and 32. They were developed based on storage sites characterization, discussed on the next section.

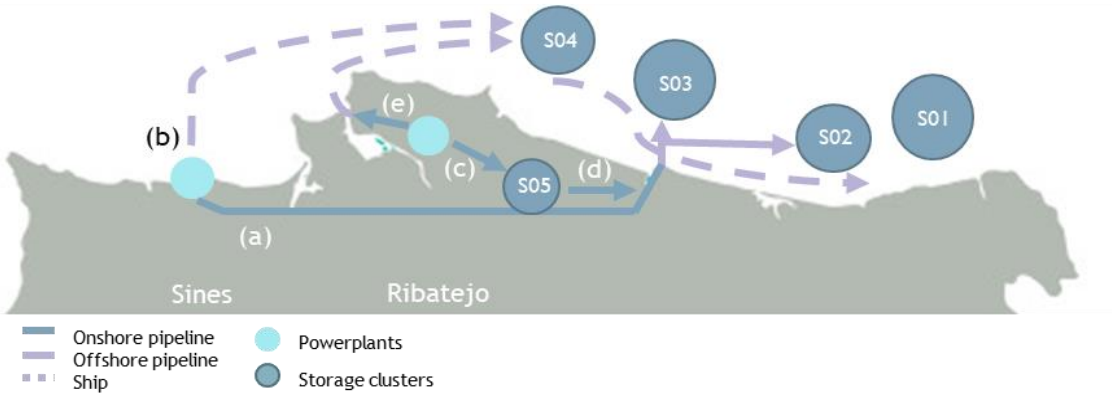

Figure 31 - Transport scenarios considered for CO2 hydrates of both powerplants.

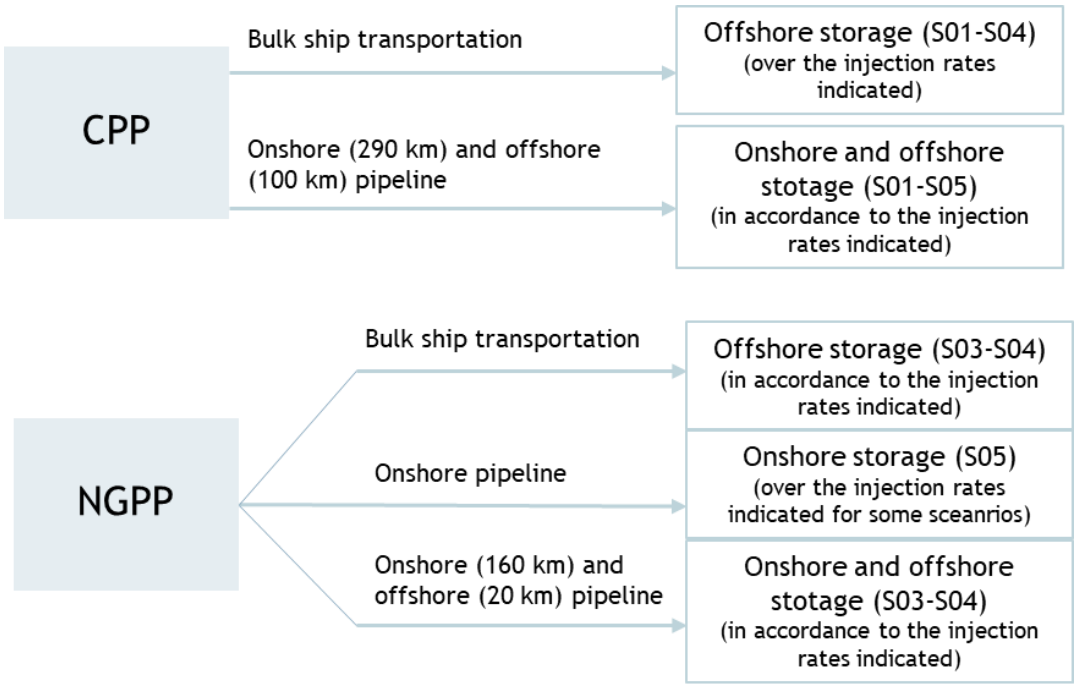

Figure 32 - Transport scenarios considered for CO2 hydrates of both powerplants.

4.3.6.1 Life cycle inventory for pipeline transportation

For modelling offshore pipeline commissioning and decommissioning, the process available in Ecoinvent libraries for natural gas was used. The data is calculated for pipelines in the North Sea (capacity: 1.6 Nm^3 gas per hour). 'The quantity of steel and concrete is calculated for an average Norwegian North Sea pipeline (diameter 1000mm, thickness steel 25mm, thickness concrete 100mm)' [117].

The process for onshore pipelines was adapted:

- the materials requirement was calculated based on pipelines diameters by considering the structure designed in Figure 33;
- the type of steel used was changed from reinforcing steel to low-alloyed steel, as a better approximation of the carbon steel;
- Some processes as water consumption and electricity grid used was changed from an average process into Portuguese specific processes;

- Leakage rates for CO_2 were considered to be half of the ones estimated for natural gas [91] and commonly attributed to CO_2 transportation in supercritical state [79], due the fact that as long as favourable thermodynamic conditions are maintained, CO_2 gasification is unlikely and the process is slow.
- For the remaining species, the leakage rate is assumed to be the same as for natural gas;
- The waste management scenarios were maintained: sand, steel and polyurethane disposal in inert landfill.

The material requirement calculations are presented on Appendix X. The process for offshore pipelines was not adapted, as the diameter of the pipeline assumed in the process provided by Ecoinvent differs only 17 % and 7 % for Ribatejo and Sine's pipelines, respectively, and it is convenient to use reinforcing steel in a marine environment to avoid high corrosion rates.

The pipeline is assumed to be buried in a trench in a minimum depth of 1 m, as a standard distance from the top of the pipe to the surface [110]. The lifetime assumed is 25 years, following reference values found in literature [79].

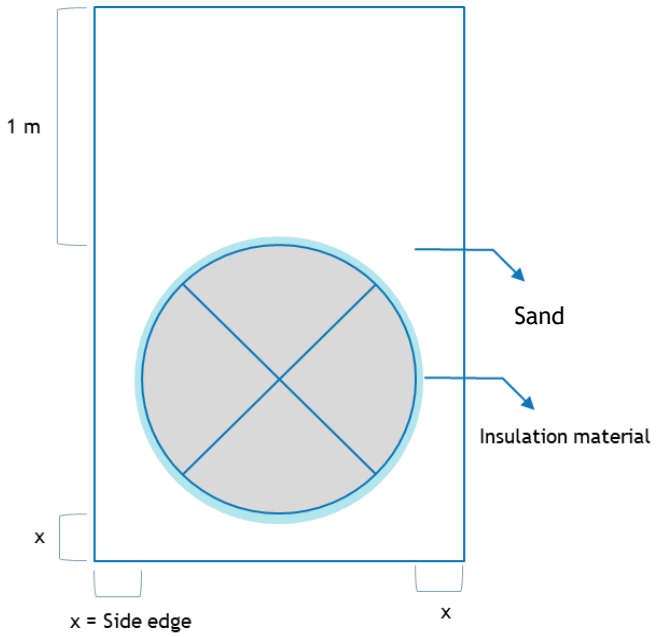

Figure 33 - Cross section of onshore pipeline.

Unlike CO_2 transport in supercritical conditions, hydrate transport in a slurry state do not require any initially compression of the gas, being less energy intensive, however giving the distances and the considerably high amounts of the hydrate fluxes the pressure drops along the pipeline network are significant. Thus, an initial boosting was admitted fed by plants itself, and an iterative method was studied to acquire the need for recompression while defining some pipeline parameters.

Network design and distances estimate

The distances for pipeline networks (see Tables 18 and 19) were estimated using Google Earth tools, and its design was followed by the pipeline's map represented in Figure 17 (section 3.3) taken from [66].

To simplify, it was assumed a constant CO_2 mass flow rate of 3122 and 1279 ton/h for CPP and NGPP, respectively. This assumption implies that each plant was assumed to operate at full load for a period correspondent to the annual utilization capacity simulated (82.6 % for Sines and from 18 % to 80 % for Ribatejo). Therefore, besides the mass of CO_2 transported within

different operation scenarios for Ribatejo powerplant being different, the flow rate is the same.

To provide stabilisation for hydrates and avoid CO_2 gasification the temperatures on the pipeline should not exceed 8 ºC for a pressure range between 5 to 60 bar. The thermodynamic conditions are set in the table below. For the region crossed by pipelines network soils temperature at a depth of 5 cm vary between 10 and 20 ºC [111], which implies the need for insulation material.

Table 17 - CO2 hydrate characterization for maintaining its stabilization during pipeline transportation.

CO_2 hydrates characterization for pipeline transport		
max. temperature	ºC	8
min. temperature	ºC	2
average density	kg/m3	1050
max. pressure	bar	60
min. pressure	bar	5

To attend to pipelines dimensioning, the thickness required of insulation material and to accurate the need for recompression, an unidimensional model was simulated on Aspen by the Net4CO2 team. The inputs given to the model are: heat exchange coefficients (it was assumed constant along the pipeline length); the initial pressure; the initial flow rate (and its composition/concentrations); initial temperature; environment temperature; pipeline diameter; and pipeline length. It returns the pressures and temperature profiles along the pipeline and the heat exchanged. The heat transfer coefficients are manually calculated attending to the heat transfer resistances of carbon-steel and polyurethane, the insulation material considered. Carbon steel is the most common material used for CO_2 pipelines is carbon steel. Although it has higher corrosion rates, its price makes up for the need of an increased thickness. Land's slope and local pressure drops were not taken into account. An average environment temperature of 14 ºC was assumed. Additionally, as a result from the recompression process a little increase in temperature may occur [79].

Based on the pressure and temperature profile, several sensitivity analyses to pipeline diameter and polyurethane thickness were made to accurate the most favourable scenario. The processed and most important results are shown in Tables 18 and 19.

Table 20 shows the LCI for onshore pipelines commissioning and decommissioning with the entries for the hydrates produced in NGPP and CPP and Table 22 shows the structure of the LCI for hydrate slurry transport by pipeline.

Table 18 - Pipeline parameters and distances estimated.

			Sines (CPP)	***Ribatejo (NGPP)***
CO2 hydrate slurry flux		ton/h	8224	3368
Onshore storage	onshore	Km	210	80
Diameter		mm	-	762
Pressure drop (p/100 km)		Bar	-	46.6
Boosting needed		kW	-	1398
Recompression needed		kW	-	0
Insulation material thickness		Mm	-	76

Table 19 - Follow-up of Table 18.

			Sines (CPP)	***Ribatejo (NGPP)***	
CO2 hydrate slurry flux		ton/h	8224	3368	
Offshore storage	onshore	Km	290	160	50
	offshore	Km	100	20	0
	total	Km	290	180	50
Diameter		mm	1066.8	762	762
Pressure drop (p/100 km)		m/m (m)	48.0	46.6	23.3
Boosting needed		kW	6385	2456	0
Recompression 1 needed		kW	5343	4232	0
Insulation material thickness		Mm	76	76	76

The second column for NGPP is related to a pipeline required for transporting the hydrates from the plant facility until Lisbon Port for scenarios with ship transportation.

The leakage rates were recalculated for each scenario attending to their distance. The results are shown in the Table 21.

Table 20 - LCI for pipelines construction and decommissioning for hydrate slurry transport for both powerplants. The uncertainties were defined by Pedigree Matrix for an entry of (3,na,na,na,na,na).

Pipeline onshore for hydrates slurry transportation	**1**	**1**	**km**		
Resources inputs	*Entry for CPP*	*Entry for NGPP*	*Unit*	*Distribution*	*2*SD*
Water, unspecified natural origin, PT	187	187	M3		
Inputs from technosphere: Materials/fuels/electricity					
Sand, at mine/CH U	5371	4152	ton	Lognormal	1.12
Steel, low-alloyed, at plant/RER	472638	336414	Kg	Lognormal	1.11
Polyurethane, flexible foam {GLO} market for	352	261	Kg	Lognormal	1.11
Transport, lorry 16-32t, EURO3/RER	650988	488944	tkm	Lognormal	1.21
Comments: Standard distances for materials supply chain taken from [112]: 72 km for 'gravel and crushed stone'; 193 km for 'plastic and rubbers'; 559 km for 'articles of base metal'. Densities were taken from literature.					
Diesel, burned in building machine/GLO	3.31E6	3.31E6	MJ	Lognormal	1.21
Electricity grid mix 1kV-60kV, AC, consumption mix, at consumer PT	540	540	Wh	Lognormal	1.21
Comments: For pipeline monitoring. Details shown in appendix 'Materials requirement of pipeline commissioning for transportation of hydrate slurry'.					
Waste to treatment					
Disposal, polyurethane, 0.2% water, to inert material ladfill/CH	352	261	ton	Lognormal	1.11
Disposal, inert waste, 5% water, to inert material ladfill/CH	5371	4152	Kg	Lognormal	1.11
Disposal, steel, 0% water, to inert material ladfill/CH	472638	336414	kg	Lognormal	1.11

Table 21 - Leakage rates for the transport scenarios by pipeline simulated.

	Distances among transport scenarios (km)				
	1000	290	160	80	50
	Leakage rates (%)				
CO_2 and CO emissions	9.50E-05	2.76E-05	1.52E-05	7.60E-06	4.75E-06
Other emissions	1.90E-04	5.51E-05	3.04E-05	1.52E-05	9.50E-06

Table 22 - Process architecture for pipeline transport of hydrates in slurry state. The entries depend on powerplant operation and transport scenario.

Hydrate slurry transported by pipeline	**ton**		
Inputs from technosphere: Materials/fuels/electricity	*Unit*	*Distribution*	*2*SD*
Pipeline, natural gas, long distance, high capacity, offshore/GLO	km	Lognormal	1.07
Comment: this entry equals zero for transportation between Ribatejo and Lisbon Port and Leiria and equals to 20 km for the remaining scenarios (a) and (d).			
Pipeline onshore for hydrate slurry transportation	km	Lognormal	1.07
Comments: Distances divided by pipeline lifetime (25 years).			
Electricity, medium voltage, at grid/PT	kWh	Lognormal	1.56
Comments: Used for recompression. This entry equals zero for some transporting hydrate slurry from Ribatejo to Leiria (onshore storage) and from Ribatejo to Lisbon Port. To calculate the other the remaining entries, the total 'recompression needed' in Table 18 and 19 was multiplied by the number of hours of operation for each simulated scenario for both powerplants.			
Electricity produced by powerplants with the operation of the capture unit	kWh	Lognormal	1.56
Comments: Used for initial boosting. This entry equals to zero for transportation between Ribatejo and Lisbon Port. The remaining entries were calculated by the multiplication of the 'boosting needed' in Tables 18 and 19 for the number of hours of operation for each scenario simulated for both powerplants.			
Emissions to air			
***Comment**: the emissions were calculated for a leakage rate of 0.019 % per 1000 km for all species, except for carbon monoxide and dioxide, with a leakage rate of 0.0085 % per 1000 km.*			
Sulfur dioxide, PT	kg	Lognormal	2.24
Nitrogen dioxide, PT	kg	Lognormal	2.24
VOC, volatile organic compounds	kg	Lognormal	2.24
Fluoride compounds, unspecified	kg	Lognormal	2.24
Chlorinated solvents, unspecified	kg	Lognormal	2.24
Carbon dioxide, fossil	kg	Lognormal	2.24
Carbon monoxide, fossil	kg	Lognormal	2.24

Uncertainties and confidence intervals

The confidence intervals were determined using Pedigree Matrix assuming that data variation is described by a lognormal distribution. The entries on Pedigree Matrix were:

- Pipelines attributes – 'data partially verified in hypothesis or data not verified with measures' for fidelity;
- Energy inputs – 'qualified estimate' for fidelity and 'data from processes and materials related' for technology correlation;
- Leakage emissions – 'non-qualified estimate' for fidelity and 'data from processes with different technology' for technology correlation.

The results are presented in the last column of the table representing the LCI.

4.3.6.2 Life cycle inventory for ship transportation

The transportation by ship was modelled based on the study presented by Aker Kvaerner [80] to assess feasible mechanisms for transport and storage of CO_2 hydrates. Transport by bulk type vessel was found to be more desirable than container type, in terms of logistics. Therefore, to model LCI for ship transportation a process available in European reference Life Cycle Database (ELCD) library (v.3.2) modelling 'Bulk carrier ocean, technology mix, 100.000-200.000 dwt RER'. The entry in tkm[15] was estimated by the method described in Table 24, following the logistic presented in [80], for CO_2 hydrates transport by a bulk ship 169.400 dwt, with the characteristics presented in Table 23.

The transport of the hydrates in form of pellets optimizes the volume occupied by a reduction factor of 180 times. The thermodynamic conditions to ensure their stabilization are shown in table below. The transport by ship implies an intermediate unit for store the cumulative volume of pellets formed. As a first estimation, it was assumed that the use of a heat insulated tank could ensure the maintenance of the thermodynamic conditions required. However, a sensitivity analysis to include the operation of a cooling reefer was performed in SimaPro, through the use of an average process found in Ecoinvent libraries; 'Operation, reefer, cooling {GLO}', giving entry of the amount of mass chilled per year.

Table 23 - CO2 pellets characterization for ship transport.

CO_2 pellets characterization for ship transport			**Source**
average density	kg/m3	1070	Net4CO2
Bulk ship parameters			
Volume capacity	m^3	185000	[122]
Mass capacity for transporting hydrates	Ton	197950	Calculated
Velocity	Knots	15	[122]
Time to travel 400 km (CPP)	D	0.64	Calculated
Time to travel 200 km (NGPP)	D	0.32	Calculated
Time for onloading (full cargo)	D	0.75	50% of the value presented in 2004 [122]
Time for offloading	D	0.35	50% of the value presented in 2004 [122]
Time required for a round trip (CPP)	d	2.4	Calculated
Time required for a round trip (NGPP)	d	1.7	Calculated

To estimate the number of travels needed for the time period simulated (a year), it was necessary to account for the number of roundabouts required for each production scenario, assuming a constant flow rate (powerplants operation at full load). Giving the time required for onloading and the time required for the whole round trip is then possible to use 3 carriers for CPP and 2 for NGPP for not having the need of storing CO_2 hydrates, over a period of 5 hours for CPP and 8 hours for NGPP. However, it was merely assumed that the cargos were travelling at full load resulting in the use of 2 carries for CPP and 1 carrier for NGPP. The number of roundabouts was obtained from the ratio between the volume produced per year by the carrier capacity. The distances were also estimated on Google Earth.

Table 24 - Calculation method to determine the tonnes-km for each operation scenario.

[15] Tonne-kilometre (tkm) is a unit of measure for transporting tonnes of mass of a product by a given transport mode over a distance in kilometres.

I. Determination of tkm	Sines	Rib. Av-20	Rib. Av.	Rib. Av+20	Rib. Av+40	Rib. Av+60	Rib. Av+80	Rib. Av+100	Rib. Av+200	Rib. 8K
Volume produced per year	54625838	4828295	6033795	7242443	8447943	9656591	10862091	12070739	18104534	23319974
Number of roundabouts needed	295	26	33	39	46	52	59	65	98	126
km travelled p/year	236220	10440	13046	15659	18266	20879	23486	26099	39145	50422
Mass produced per year (kg)	5.84E+10	5.166E+09	6.456E+09	7.749E+09	9.039E+09	1.033E+10	1.162E+10	1.292E+10	1.937E+10	2.495E+10
tkm p/year	6.90E+12	2.70E+10	4.21E+10	6.07E+10	8.26E+10	1.08E+11	1.36E+11	1.69E+11	3.79E+11	6.29E+11
Volume produced per year	54625838	4828295	6033795	7242443	8447943	9656591	10862091	12070739	18104534	23319974
Number of roundabouts needed	295	26	33	39	46	52	59	65	98	126

4.3.7 Storage

Due to the fact that productive reservoirs of hydrocarbon reservoirs do not yet exist, the opportunities for CO_2 storage in Portugal are restricted to deep saline reservoirs in sedimentary basins [66]. Those cover about one third of the of the onshore territory along the coastline and extend into the submerged zone (offshore) [66]. The assessment of CO_2 storage capacity was developed under COMMET and KTejo EU projects and considered three national Meso-Cenozoic basins: the Porto Basin, the Lusitanian Basin, and the Algarve Basin.

Table 25 - General criteria for storage selection. Source: [66].

Storage Capacity	
Porosity	Ideally: >15 %; Acceptable depending on other criteria: 6% to 15%
Type of trap	Local traps and regional reservoirs.
Porous effective volume	Capacity > 3Mt
Reservoir depth	Top of the reservoir: 800 to 2500 m of depth
Injection rate	
Type of trap	Reservoirs with lateral continuity
Permeability	Ideally > 200 mD
Rock mechanics	Depending on the geomechanical parameters, the maximum pressure induced should be 20 % of the initial pressure.
Sealant integrity	
Permeability	< 10^{-2} mD
Sealant thickness	Ideally > 50 m
Tectonic activity and faults	Less fractured formations are favoured. Seismic activities are relevant. Disregard traps with activate faults.
Sealant consistency	Formations homogenous and with lateral continuity are

The criteria for characterization of storage clusters, defined by Directive 2009/31/EC, were transposed into Portuguese law in DL60/2012. The general criteria to select storage clusters are showed in Table 25.

Technical and economical preliminary studies were developed by the consortium [66] to accurate the most feasible clusters for storage the captured CO_2. The site characterization parameters for the clusters of most interest and studied in the current assessment are shown in Table 26.

Table 26 - Storaae site characterization.

		S01 offshore	**S02 offshore**	**S03 offshore**	**S04 offshore**	**S05 onshore**
Cluster Areas		5	4	5	8	4
Capacity	Mt	1230	870	2200	1590	340
Depth	m	800-2500	800-2500	800-2500	800-2500	800-2500
Cluster maximum injection rate	Mt/y	16.1	3.8	11.8	11.4	10.7
Well maximum injection rate	Mt/y	<0.8	<0.5	<0.8	<0.6	<0.8
Well injection rate (safety factor: 5%)	Mt/y	0.76	0.48	0.76	0.57	0.76
Reservoir pressure		Subject to assumptions, further discussed.				
Reservoir temperature		It was not modelled in the current assessment.				

The temperature on reservoir is not relevant for this study as storage mechanisms are not modelled. Yet it may be an important parameter to estimate leakage rates, by quantifying the probability for CO_2 gasification and its dispersion. The injection rates were determined assuming the density and viscosity of CO_2 supercritical and they must be somehow different for hydrates injection. However, a study for adapting the reference values reported on [66] for injection rate was not performed.

As the range for depths is considerably wide and it may highly influence the energy required for injection, a sensitivity analysis will be performed by simulating the processes for the minimum, average and maximum depth.

The characterization of CO_2 hydrate at the end of the pipe are shown in the following table. The pressure and temperature were set up on Aspen simulations, the density is assumed to be approximately the density of water under the same thermodynamic conditions.

Table 27 - CO2 hydrates characterization at the end of pipeline.

Pressure	bar	5
Temperature	ºC	2-8
Density	kg/m^3	1050

Storage scenarios are highly dependent on annual maximum injection rates of each storage cluster and the hydrates fluxes resultant from CPP and NGPP. Table 28 shows the annual fluxes of CO_2 produced by the operational scenarios performed for NGPP and for the only operational scenario of CPP. At dark grey are the results of combining the fluxes produced by both powerplants. Table 29 shows the number of wells required for each possible storage scenario, by considering the flux of CO_2 and the maximum well injection rate. It is also presented the

ratio between the annually injection rate and the maximum injection rate for the cluster. The simultaneous injection of CO_2 hydrates from both powerplants in the same cluster is rather impractical, thus it was not modelled.

Table 28 - Mass fluxes of CO2 hydrates.

			Sines 8078 GWh	
		Mt/y	5.84E+01	id
Ribatejo	Av-20%	5.17E+00	6.36E+01	1
	Average (16-18)	6.46E+00	6.49E+01	2
	Av+20%	7.75E+00	6.62E+01	3
	Av+40%	9.04E+00	6.75E+01	4
	Av+60%	1.03E+01	6.88E+01	5
	Av+80%	1.16E+01	7.01E+01	6
	Av+100%	1.29E+01	7.14E+01	7
	Av+200%	1.94E+01	7.78E+01	8
	8078 GWh	2.50E+01	8.34E+01	9

Table 29 - Number of wells needed and the ratio between the injection rate with the cluster injection rate in % for diferent operation scenarios.

	Ribatejo (NGPP)					
	S03 (50 % of the hydrates)		S04 (50 % of the hydrates)		S05	
id	Nr wells	%	Nr wells	%	Nr wells	%
1	3	22%	5	23%	7	48%
2	4	27%	6	28%	8	60%
3	5	33%	7	34%	10	72%
4	6	38%	8	40%	12	84%
5	7	44%	9	45%	14	97%
6	8	49%	10	51%	15	109%
7	8	55%	11	57%	17	121%
8	13	82%	17	85%	25	181%
9	16	106%	22	109%	33	233%

Sines for pipeline scenarios			
	Nr wells	%	% hydrates injected
S01	22	109%	30%
S02	9	154%	10%
S03	16	100%	100%
S04	20	100%	20%
S05	15	109%	20%
Sines for ship scenarios			
S01	22	109%	30%
S02	9	154%	10%
S03	23	149%	30%
S04	31	154%	30%

Therefore, the storage scenarios simulated are:

- The injection of hydrates from Sines (CPP) in the 5 clusters considered (both offshore and onshore) for pipeline transportation scenarios;
- The injection of hydrates from Sines (CPP) in S01, S02, S03 and S04 (offshore clusters) for ship transportation scenarios;
- The injection of hydrates from Ribatejo (NGPP) in cluster S05, as it is far closer to the facility than the offshore clusters, however, according to the data available regarding injection rates, this storage scenario is not feasible for plants utilization rates over 40 %;
- The injection of hydrates from Ribatejo in clusters S03 and S04.

4.3.7.1 Life cycle inventory

Infrastructure: material and drilling

Already existing facilities could be considered if its reuse for CO2 injection prove itself feasible. In this way a decrease in the material and energy consumption for the storage process would be achieved. However, this assumption was not considered for the study as there are no previous similar infrastructures in Portugal.

The LCI for drilling was based on the Ecoinvent process 'deep well drilling, for deep geothermal power - PT' reported by [112], yet with some adjustments:

- For onshore drilling, the reinforcing steel was changed for low-alloyed steel as a better approximation to carbon-steel, cement was modelled with unspecified quality instead of Portland and particles emissions to air were added based on the LCI for 'onshore well production, oil/gas - GLO' of Ecoinvent 3.6 libraries.
- For offshore drilling, the cement remained of Portland type, as it is impermeable and hydraulically isolate [112], reinforcing steel was selected as it outperforms carbon steel in terms of corrosion; instead of electricity, 'diesel burned in diesel-electric generating set, 10 MW' was considered the main source of energy; lastly, wastewater and particles were modelled being emitted into the ocean.
- The attributes related to the land use were disregarded as that impact category was not analysed in this study.
- An additional amount of cement was modelled as reported in [79].

The number of wells needed were calculated based on the well injection rate for each cluster. Horizontal and extended wells can be good options to improve injection rates, thus the wells length is assumed to equal 150% of the storage aquifer depth [113]. Moreover, additional wells for monitoring are also important to account for. The amount of monitoring wells assumed are one fifth of the injection wells, if each of them can monitor five of the injection wells by being alongside them. Wells diameters are average values and correspond to the ones assumed for the inventory of the 'deep well drilling, for deep geothermal power'. The length of monitoring wells is assumed to be half of the injection ones [79] and their diameter should be thickener, however the same process was used to model both wells. Although in literature [79], lifetime of 15 years is reported, for allocating construction and drilling impacts for a timeline of operation, the lifetime considered is 20 years, equivalent of the one assumed for capture unit.

Table 30 - LCI for the drilling activity for both onshore and offshore deep wells.

Deep well, drilling and construction (adapted from geothermal powerplants)	**1**	**1**	**m**		
Inputs from technosphere: Materials/fuels/electricity	*Entry for onshore well*	*Entry for offshore well*	*Unit*	*Distribution*	*2*SD*
Barite {GLO}| market for	20	20	kg	Lognormal	1.37
Bentonite {GLO}| market for	20	20	kg	Lognormal	1.37
Cellulose fibre, inclusive blowing in {GLO}| market for	17.5	17.5	kg	Lognormal	1.37
Cement, unspecified {Europe without Switzerland}| market for cement, unspecified	246	0	kg	Lognormal	1.38
Comments: It accounts surplus 35 kg for construction of the well, data taken from [106].					

Table 31 - Follow-up of Table 30.

Deep well, drilling and construction (adapted from geothermal powerplants)	**1**	**1**	**m**		
Inputs from technosphere: Materials/fuels/electricity	*Entry for onshore well*	*Entry for offshore well*	*Unit*	*Distribution*	*2*SD*
Portland cement {Europe without Switzerland}| market for **Comments:** It accounts surplus 35 kg for construction of the well, data taken from [106].	0	246	kg	Lognormal	1.38
Potassium carbonate {GLO}| market for	15	15	kg	Lognormal	1.37
Chemical, organic {GLO}| market for	20	20	kg	Lognormal	1.37
Sodium chloride, powder {GLO}| market for	6	6	kg	Lognormal	1.38
Sodium hydroxide, without water, in 50% solution state {GLO}| market for	1	1	kg	Lognormal	1.37
Electricity grid mix 1kV-60kV, AC, consumption mix, at consumer, 1kV - 60kV PT	3930	0	MJ	Lognormal	1.37
Diesel, burned in diesel-electric generating set, 10MW {GLO}| diesel, burned in diesel-electric generating set, 10MW	111	4041	MJ	Lognormal	1.37
Steel, low-alloyed {GLO}| market for	309.5	0	kg	Lognormal	1.37
Reinforcing steel {GLO}| market for	0	309.5	kg	Lognormal	1.37
Waste to treatment					
Particulates, > 10 um (low population)	0.0148	0	kg	Lognormal	1.46
Emissions to water					
Waste water	0.6	0.6	kg	Lognormal	1.38
Final Waste flows					
Waste, from drilling, unspecified	466	466	kg	Lognormal	1.37

Energy requirements for injection of CO_2 hydrate

The energy required for the injection of CO_2 hydrate depends on the injection rate ($\dot{m}_{hydrates}$) and the pressure difference required to be suppressed (ΔP). It was calculated by the following equation, assuming an efficiency (η) of 85% for the pump.

$$P = \frac{\Delta P \times \dot{m}_{hydrates} \times \rho_{hydrates}}{\eta}$$

'The injection pressure results from the actual reservoir pressure and the overpressure required for injection' [79]. The overpressure depends upon several factors besides the underground pressure profile, such as permeability and the injection rate, which turns the modelling for the injection process quite complex [79]. Indeed, the pressures in the reservoir can vary widely; in literature different values can be found, approximately between 200 and 1000 bar [79]. For this study, the same assumption made by Wildboz [79] for modelling the hydrostatic pressure gradient of 9.8 kP/m was considered and an overpressure of 8.5 bar is assumed, as a rough approximation to the overpressure resulted from simulations performed by Tian L. et al. for a Sweden case study, on South Scania site [114]. The depth for the reservoirs studied in [114] vary between 1613 and 1783, with the primary trap being at 1673 m. The basin is also sedimentary with sandstones as sealing units and clays as cap rocks. It should the mentioned yet that sedimentary basins can have abnormal pressure systems i.e. outside the common gradient of 9.8 kPa/m [79]. Assuming a sea depth about 250 m (estimated by using Google

Earth), with water volumetric weight of 9810 N/m^3 and a pressure of 5 bar at the end of onshore pipeline, the surface pressure of CO_2 at the well head of offshore clusters was estimated to be about 30 bar. As a matter of simplification, the same pressure of 5 bar was assumed for the end of the pipeline of the freight ship. The pressure drop in the wells over the injection depth is negligible in comparison to the required pressure to overtake for injection and not considered in this study.

Table 32 - Pressures at different stages of injection process.

Parameter	Offshore			Onshore			Unit	Source
Depth	800 (min)	1650 (av.)	2500 (ma)	800 (min)	1650 (av.)	2500 (ma)	m	[29]
Surface pressure of CO_2 at the well head	30	30	30	5	5	5	bar	Calculated and assuming a sea depth of 250 m for offshore wells.
Hydrostatic pressure in the reservoir	105	186	270	78	162	245	bar	Calculated assuming a pressure profile of 9.8kPa/m and sea depth of 250 m for offshore wells.
Overpressure	8.5						bar	Assumed based on [114].
Pressure required at bottom hole	113.5	194.5	278.5	86.5	170.5	253.5	bar	Calculated (hydrostatic pressure in the reservoir + overpressure).
ΔP required for injection	83.5	164.5	248.5	81.5	165.5	248.5	bar	Calculated (pressure required - pressure at the well head).

The pressure difference that is to overtake for injection results from the delivery pressure at the end of the pipeline and the required pressure for injection at the bottom hole. The results are shown in Table 34. Table 33 shows the structure of the LCI modelled in the software. The energy supply in the offshore storage site is provided by burning diesel.

Table 33 - Process architecture for modelling hydrate slurry stored into the deep saline aquifers.

Hydrate slurry stored	**Ton**		
Inputs from technosphere: Materials/fuels/electricity	*Unit*	*Distribution*	*2*SD*
Deep well, drilled (adapted from geothermal powerplants) **Comment:** this entry equals zero for transportation between Ribatejo and Lisbon Port and Leiria and equals to 20 km for the remaining scenarios (a) and (d).	Km	Lognormal	1.52
Electricity, medium voltage, at grid/PT S **Comments:** Used for injecting slurry on the onshore site.	kWh	Lognormal	1.52
Diesel burned in diesel-electric generating set/GLO S **Comments:** Used to inject slurry on the offshore site.	kWh	Lognormal	1.52

Leakage rates were not considered. As the time frame of the assessment performed is for one year of operation, leakage rates would add low meaning, as the amount of CO_2 in stored clusters is continuously increasing.

Table 34 - Power required for each operation scenario, assuming an efficiency of 85 %.

	Sines	Rib. Av-20	Rib. Av.	Rib. Av+20	Rib. Av+40	Rib. Av+60	Rib. Av+80	Rib. Av+100	Rib. Av+200	Rib. 8K
Hours of funtioning	7107	7107	1534	1917	2301	2684	3068	3451	3835	5752
Slurry flow (ton/h)	8224	6579	3368	3368	3368	3368	3368	3368	3368	3368
Slurry flow (m3/h)	8635	6908	3536	3536	3536	3536	3536	3536	3536	3536
Power required for inject hydrates in offshore site (MJ)										
Power required Offshore 800 m	6.029E+08	4.823E+08	5.329E+07	6.659E+07	7.993E+07	9.324E+07	1.066E+08	1.199E+08	1.332E+08	1.998E+08
Power required Offshore 1650 m	1.188E+09	9.502E+08	1.050E+08	1.312E+08	1.575E+08	1.837E+08	2.100E+08	9.983E+04	2.625E+08	3.936E+08
Power required Offshore 2500 m	1.794E+09	1.435E+09	1.586E+08	1.982E+08	2.379E+08	2.775E+08	3.172E+08	3.568E+08	3.965E+08	5.947E+08
Power required for inject hydrates in onshore site (MJ)										
Power required Onshore 800 m	-	1.18E+08	5.20E+07	3.39E+05	3.39E+05	3.39E+05	3.39E+05	3.39E+05	3.39E+05	3.39E+05
Power required Onshore 1650 m	-	2.39E+08	1.06E+08	1.32E+08	1.58E+08	1.85E+08	2.11E+08	2.38E+08	2.64E+08	3.96E+08
Power required Onshore 2500 m	-	2.87E+08	1.59E+08	1.98E+08	2.38E+08	2.77E+08	3.17E+08	3.57E+08	3.96E+08	5.95E+08

Uncertainties and confidence intervals

The confidence intervals were determined using Pedigree Matrix assuming that data variation is described by a lognormal distribution. The entries on Pedigree Matrix were:

- Deep well and energy inputs – 'data partially verified in hypothesis or data not verified with measures' for fidelity and 'data from related processes or materials' for technology correlation;
- Leakage emissions – 'non-qualified estimate' for fidelity and 'data from processes with different technology' for technology correlation.

The results are presented in the last column of the table representing the LCI.

4.4. Results

4.4.1. Coal vs. Natural Gas supply chain

Figure 34 presents the obtained results characterized to each impact category by comparing coal and natural gas supply chains. The functional unit or comparison basis is 1 MJ, thus the results are subjected to 0.03973 kg of hard coal (calorific value of 25.17 MJ/kg, weighted average data based on results for coal composition presented in Appendix VII) and 0.02624 m^3 of natural gas (weighted average between calorific value or low heating value (LHV) for RME (5 %), NAC (85 %) and Europe (10 %) of 37.5 [93], 38.5 [83] and 35.1 [115] MJ/m^3, respectively, resulting in 38.11 MJ/m^3).

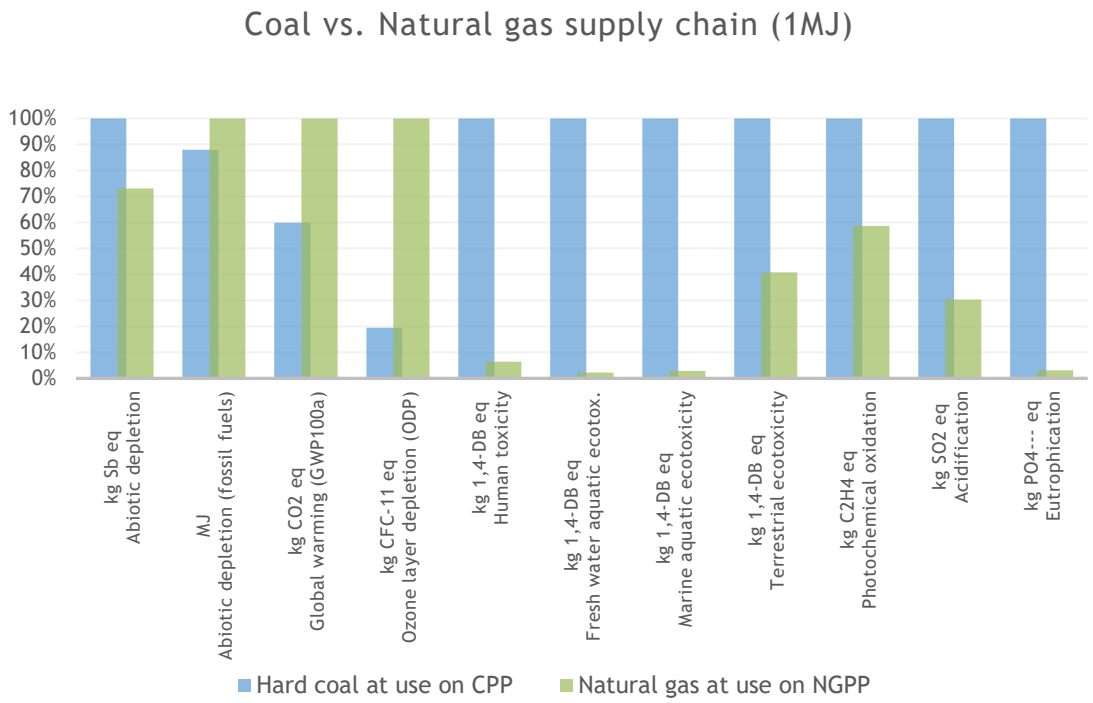

Figure 34 - Characterized results obtained for 1 MJ of natural gas supplied to Portugal trough the model simulated in the current assessment and for 1 MJ of hard coal supply to Portugal by using an Ecoinvent 3.3 process.

As it was already expected the hard coal supply scores higher environmental loads than natural gas, for the great majority of the impact categories. The difference obtained for 'Abiotic depletion (fossil fuels)' is in part related to fuels leakages and use during the fuels processing and trading and in part related to different characterization factors[16].

The higher load of GWP for NG supply can be related to flaring and venting activities, which occur during the whole process with higher weight on NG production. Those processes can be responsible for the emission of huge amounts of methane, even higher than the ones inherent to coal mining, as predicted by Freire F. [88], especially for surface mining, the most frequent on Colombia, which is the most significant exporter to Portugal.

The higher load of ODP for NG supply is related to methane halons 1301 and 1211 and HCFC-22 emissions (see Figure III-2 in Appendix III), which occur due to leakages on refrigeration systems [83] and the use of those substances for control combustion of natural gas in flaring processes [90]. Flaring can occur during NG production, but also during pipeline transportation, when venting is needed due to safety reasons, and the gases are burnt as an attempt to reduce methane to carbon dioxide, to reduce the GWP [89].

Appendix III presents with more detail the results of impacts characterization for NG supply chain, including a comparison with an average process of NG consumption in Europe, available in Ecoinvent libraries.

Impacts related to ecotoxicity and human toxicity are much higher for coal supply chain as their process can release higher amounts of particles and heavy metals resulting in soil contamination. On the other hand, marine ecotoxicity gets more penalized due to the fact the maritime routes for coal transportation being more extensive, as it is mainly sourced on Colombia and United States.

[16] Characterization factors for fossil fuels depletion can differ within fuels types due to resource scarcity, function of extraction and recovery [116].

4.4.2. Reference operation scenarios

4.4.2.1. Coal versus Natural gas powerplant

Figure 35 shows impacts characterization for NGPP and CPP respectively under reference operation scenarios. The comparison basis is therefore the same amount of electricity produced and supplied to the grid (without the energy penalty of powerplants operation) – 8704 GWh. PP's operation impacts (mid green for NGPP and yellow for CPP) are reflected mainly through the emissions, as the supply chain of raw materials and by-products downstream processes appears apart. The overall system of CPP operation scores more impacts than NGPP, with exception for ODP, for which, natural gas supply chain (mid blue) has a major contribute, due gas flaring and venting, as aforementioned.

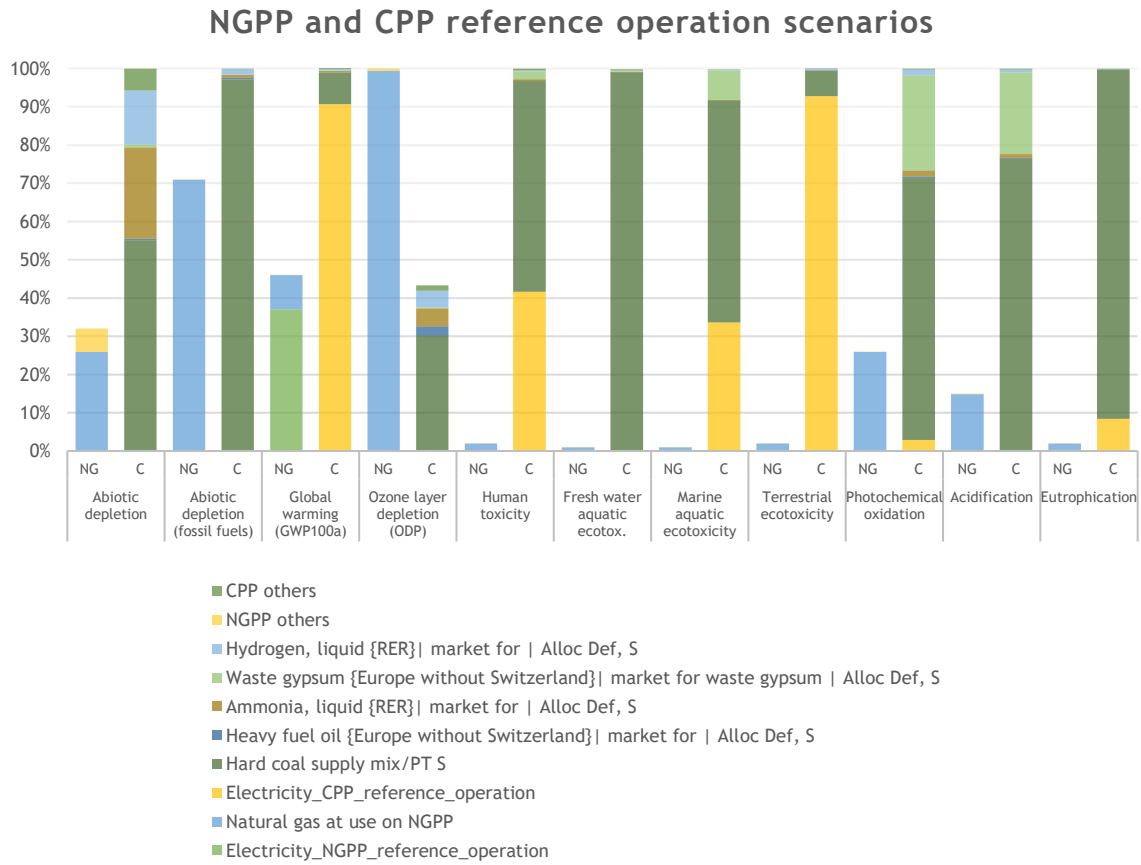

Figure 35 - NGPP and CPP reference operation scenarios.

Table 35 shows the absolute environmental loads associated to each impact category, for the operation scenarios simulated and per functional unit. As one may conclude, the most significant impact categories are: abiotic depletion of fossil fuels, representing the depletion of global fossil fuels resources due the exploration of natural gas and coal and other auxiliary fuels used on both powerplants; GWP related to emissions of CO_2, NOx and fluorinated gases (for CPP); human toxicity, for which, wastewater emissions with potential for soil contamination are most responsible for; fresh water ecotoxicity related to fuels supply chain (97 % for NGPP and 99 % for CPP), with coal supply chain being significantly more impactful; marine ecotoxicity, related to wastewater emissions for CPP (34 %) and fuels supply chain for both powerplants.

Table 35 - Load of each impact category for reference operation scenario of both powerplants.

Product: 8704000 MWh of electricity supplied to the grid					
		NGPP		**CPP**	
Impact Category	**Unit**	**total**	**per MWh**	**total**	**per MWh**
Abiotic depletion	kg Sb eq	1.19E+02	1.37E-05	3.73E+02	4.28E-05
Abiotic depletion (fossil fuels)	MJ	6.32E+10	7260	8.90E+10	10230
Global warming (GWP100a)	kg CO2 eq	3.72E+09	427	8.14E+09	935
Ozone layer depletion (ODP)	kg CFC-11 eq	1.61E+02	1.85E-05	6.92E+01	7.95E-06
Human toxicity	kg 1,4-DB eq	6.60E+07	7.58	2.79E+09	321
Fresh water aquatic ecotox.	kg 1,4-DB eq	3.93E+07	4.51	2.65E+09	304.5
Marine aquatic ecotoxicity	kg 1,4-DB eq	1.10E+11	12612	1.01E+13	1161236
Terrestrial ecotoxicity	kg 1,4-DB eq	5.82E+05	0.0668	3.29E+07	3.78
Photochemical oxidation	kg C2H4 eq	1.18E+05	0.0135	4.55E+05	0.0522
Acidification	kg SO2 eq	1.98E+06	0.228	1.32E+07	1.52
Eutrophication	kg PO4--- eq	3.98E+05	0.0457	1.85E+07	2.13

Regarding CPP, hard coal supply, at dark green, and electricity generation represents the major contributors to most of the impact categories. Electricity generation scores high environmental loads for: GWP, human toxicity, and marine ecotoxicity, due to the emissions mentioned above. The processes describing downstream gypsum trading ('market for waste gypsum' at light green), has a significant contribution for photochemical oxidation and acidification. However, the process only accounts standard distances and means of transportation for gypsum trading. The contribution is in fact residual, as load for both impacts is not very significant.

The same occurs for hydrogen supply chain in relation to ODP for CPP operation.

Besides, being less intensive for almost every impact category, the major contributor for NGPP impacts is the NG supply chain, scoring between 81 and 99 % for all categories, with exception of 100 % contribution for fossil fuels depletion and 19 % for GWP. The process of electricity generation (gate-to-gate) scores 81 % of the emissions with GWP (CO_2 and NOx) and 13 % of the emissions related to eutrophication, through wastewater.

4.4.2.2. Natural Gas powerplant – sensitivity analysis

Figure 36 shows the results obtained for NGPP operation under several utilization rates. The bars at blue represent steps of 20 % in terms of electricity generated and bars at blue represents steps of 100 %. As already expected through the regressions obtained for LCI articles, the environmental load of each impact category acts almost linearly to the electricity that is generated. The only exception is for eutrophication that has a subtle exponential behaviour: for higher utilization rates, the eutrophication load increases faster. This is due to the fact that historical data of phosphorus emissions fitted an exponential regression.

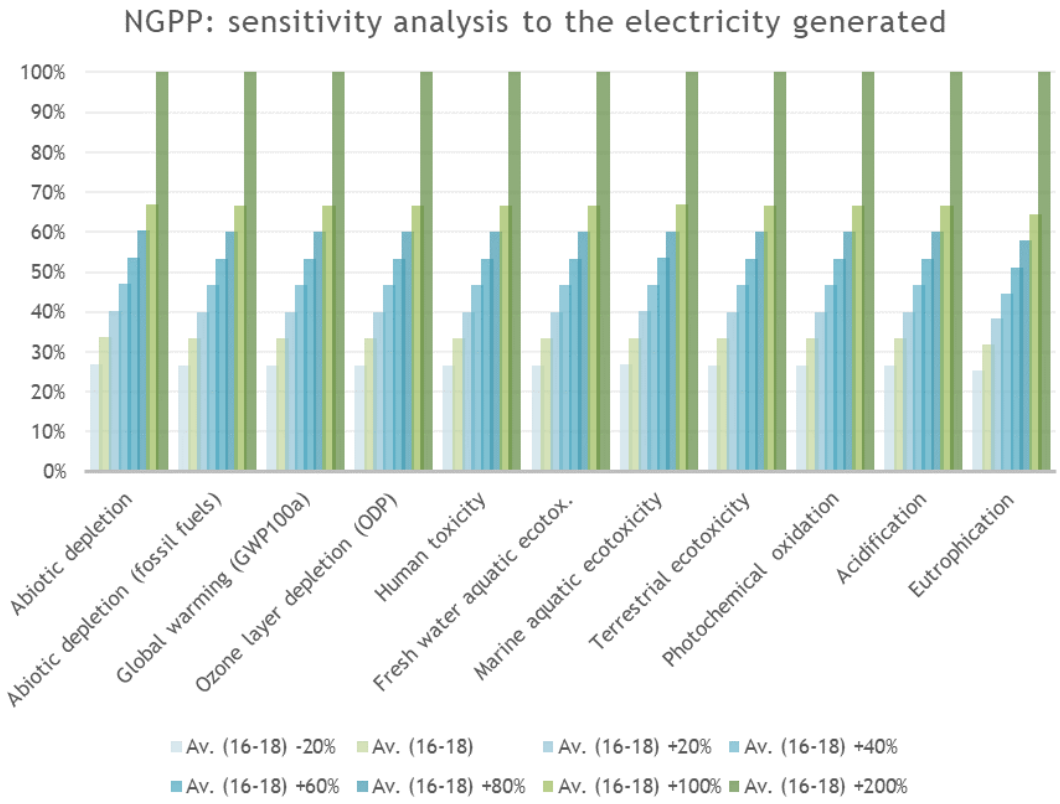

Figure 36 - Sensitivity analysis to the electricity generated by NGPP (Ribatejo).

4.4.2.3. Uncertainty analysis: Monte Carlo simulation

The following charts show the 95 % confidence intervals for CPP (Figures 37 and 8) and NGPP (Figure 39) reference operation scenarios, for each impact category. The variation on the confidence intervals results from the standard errors inherent to the background data, often determined through the use of Pedigree Matrix, and to data given as entry on the models, determined based on the standard deviation for CPP sample size and on the regression fitting to NGPP data, assuming that a normal distribution could describe data's variation. Figure 37 shows however the confidence intervals of 95 % without considering the uncertainties of background data.

Figure 38 shows that the CPP model owns significant uncertainties ranges, and for most of the impact categories is related to background data, as suggested by the difference between the charts presented in Figures 37 and 38. Despite, nullifying the exact characterization of all environmental burdens, as the uncertainties are mostly sourced in background data, it is still possible to analyse the evolution of the mean value between reference scenarios and CCS scenarios. As suggested by Heijungs and Kleijn [117], while uncertainty propagation yields the probability distribution of the LCA results for each scenario, discernibility analysis provides the distribution of the difference between the scenarios. Thus, some uncertainties may have the same influence on the scenarios but no influence on the differences between them [86].

However, 'terrestrial ecotoxicity' reveals a high uncertainty level even without considering background data errors. Thus, this impact category was disregarded from further analysis of CPP scenarios. The negative range of values is merely a mathematical result considering that the confidence interval is equally dispersed around the mean value (normal distribution), but does not have a physical significance, as there are no avoided products or emissions for this model. This high uncertainty is associated to the high standard deviations verified for wastewater emissions of some high toxic chemical species, such as hexavalent chromium, zinc, copper and chlorine, besides, solid waste management scenarios uncertainty.

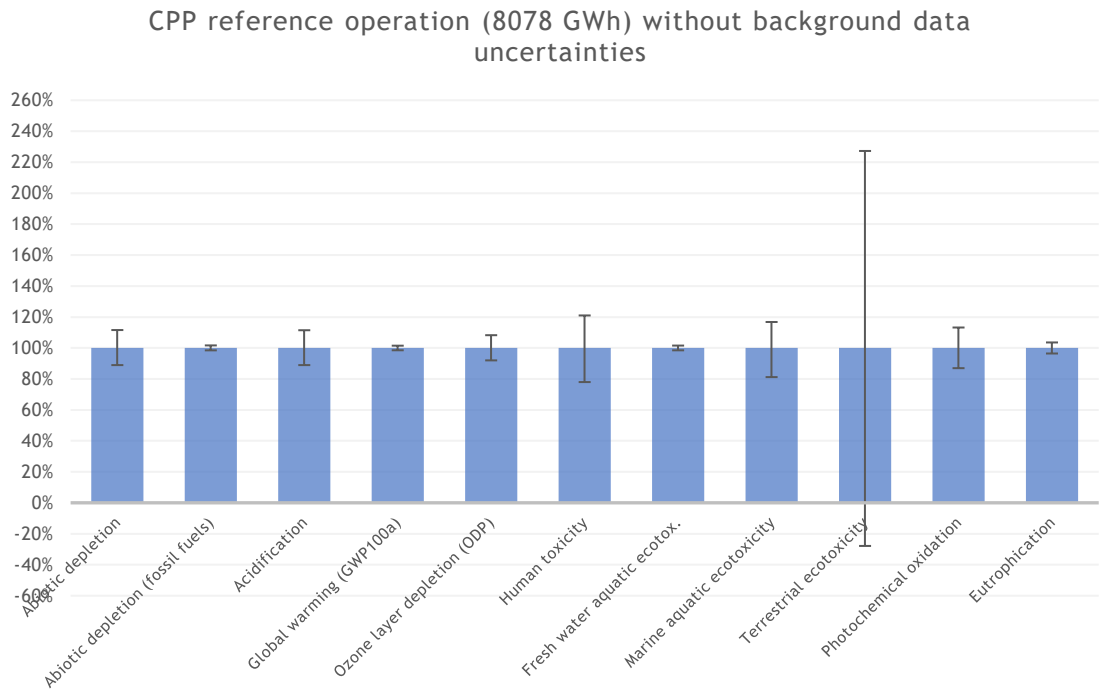

Figure 37 - Monte Carlo analysis to the standard errors inherent to data for CPP reference operation scenario.

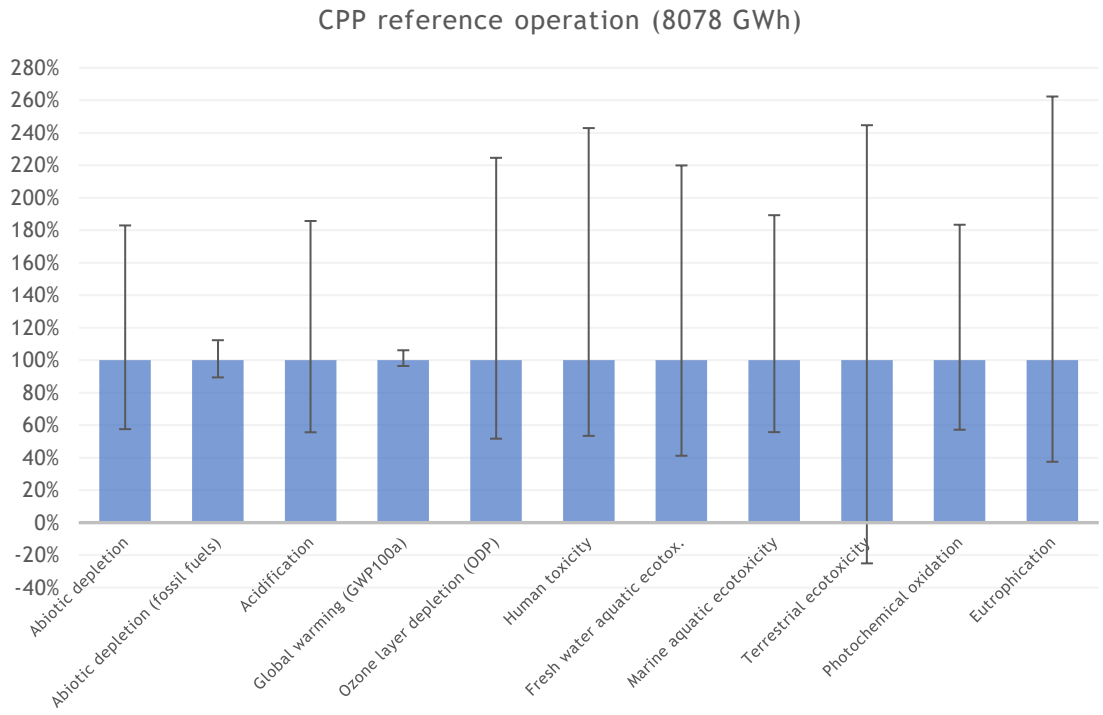

Figure 38 - Monte Carlo analysis to the standard errors inherent to data for CPP reference scenario operation.

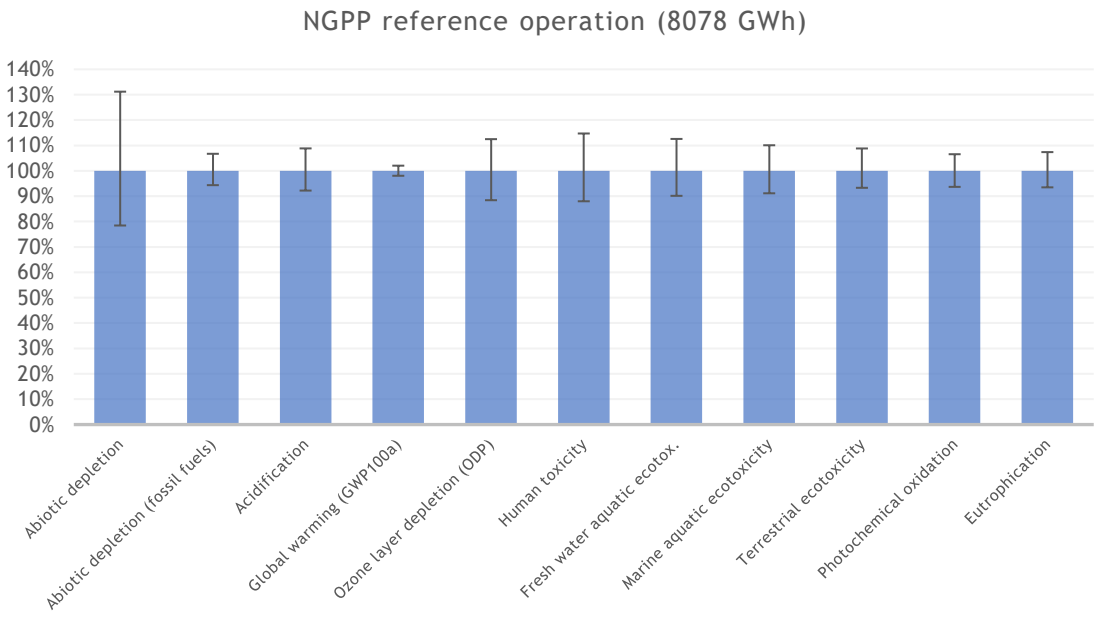

Figure 39 - Monte Carlo analysis to the standard errors inherent to data for NGPP reference scenario operation.

4.4.3 Powerplants operation with HGtS – approach 'cradle to gate'

Figure 40 and figure 41 show the results obtained from the characterization of each impact category, for CPP and NGPP, respectively, under an approach of 'cradle to gate' and for four different scenarios. The results were obtained for powerplants operating at 80 % of full load for Ribatejo (NGPP) and 82.6 % for Sines (CPP), thus providing a supply of 8078 GWh to the grid without the operation of HGtS capture unit (reference scenario). Capture scenarios are divided into three: two scenarios with a compensation of the energy penalty resulting from HGtS operation with a Portuguese mix production (PT) and another with a Norwegian mix production (NO); and yet, the only one restricted to the frontiers of both powerplants, without any compensation (W/o), but providing only 7772 GWh and 7324 GWh, from Ribatejo and Sines, respectively. The results were then normalized to the functional unit (1 MWh of electricity produced and supplied to the grid).

Each bar is characterized within the processes that comprise the reference operation of the powerplant ('others') and the ones related to the operation of HGtS.

The abiotic depletion results reveal the additional raw materials needed. The increase of blue proportion - 'reference' processes – for the scenario without grid compensation on abiotic depletion, as well, as for other impact categories, is a consequence of the reduction of the amount of electricity supplied to the grid. Fossil fuels depletion confirms that the Norwegian grid is mainly supported on non-fossil fuel-based sources.

Regarding CPP, the consumption of ethylene glycol is almost imperceptible among other processes, and the water consumption causes more impacts on ODP, due to pre-treatment processes and raw materials consumption. The major differences between capture and the reference scenario are related to the grid's compensation, especially when the grid is mainly supported on fossil fuels, as the case of the Portuguese grid back in 2011[17], and on the air avoided emissions, which mitigate GWP and photochemical oxidation loads.

[17] Ecoinvent reports the last update on 2016, but the original dataset dates back from 2011.

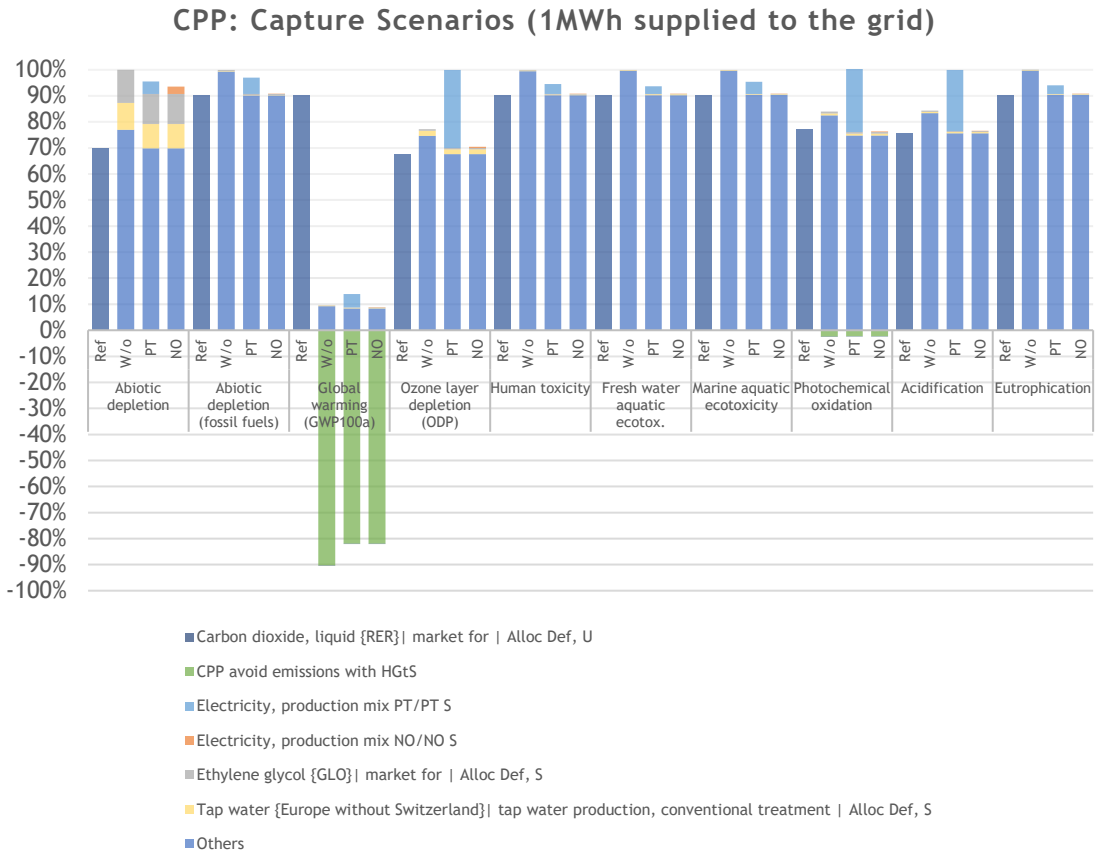

Figure 40 - Results of characterization of each impact category for reference and capture scenarios under an approach of 'cradle to gate' on Sines powerplant (CPP). The results are normalized to the functional unit.

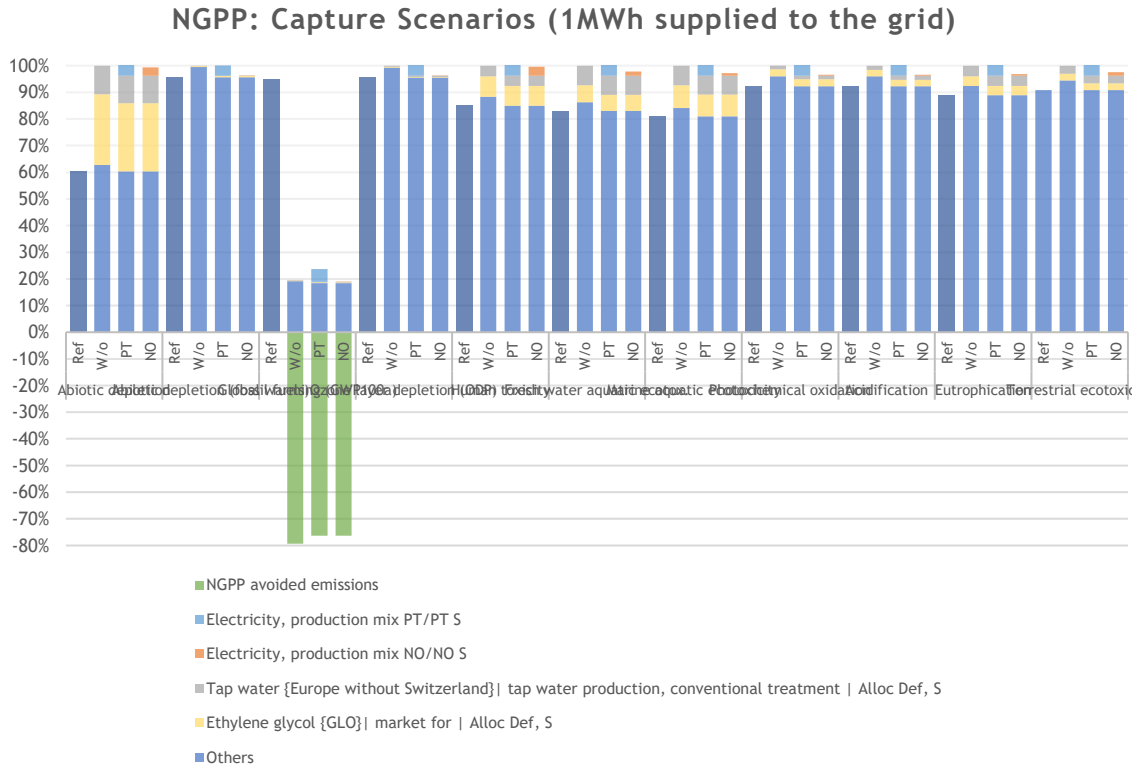

Figure 41 - Results of characterization of each impact category for reference and capture scenarios under an approach of 'cradle to gate' on Ribatejo powerplant (NGPP). The results are normalized to the functional unit.

Even though, the amount of ethylene glycol estimated for HGtS retrofitting on NGPP being lower than the amount required for CPP, as the overall load of impact categories is much less significantly for NGPP, the relative weight of both ethylene glycol and water used are more significant than for CPP.

The energy penalty of HGtS operation is 9.3 % and 3.7 % on CPP and NGPP, respectively. Therefore, the normalized impacts of electricity compensation between the two differ, being more significant for CPP with the Portuguese (fossil fuel-based) grid.

If considering that the Portuguese production mix could be described by the operation of Sines powerplant, the overloads scored for each impact category should be proportioned to the energy penalty of 9 %. For most of the impact categories, they range between 2% and 7 %, however for ODP, photochemical oxidation and eutrophication overloads of 44, 34 and 31 % are respectively achieved. The increase in terms of photochemical oxidation can be explained by the fact that in 2011, the emissions of NO_x were not mitigated, i.e., in Sines the unit for NOx removal (denitrification unit) was implemented on 2011 [67]. Increased eutrophication loads could be related to the lack of advanced methods of wastewater treatment, and the ODP might be related to the use of more impactful raw materials. Therefore, it is likely that the current situation of Portuguese electricity sector does not result into such characterization. For full LCA studies, the capture scenario was modelled without electricity compensation on the grid, respecting the frontiers of the study.

Despite the relative reduction of the GWP for the scenarios with electricity compensation being lower, the mass of avoided emissions is the same in the three capture scenarios. Simply, in the scenario without energy compensation, the impacts are normalized by a lower value, meaning that the positive impacts worsens while the GWP impact improves, in proportion to the energy penalty, since CO2 emissions and the electricity generated are directly proportional to the historical data of the plants. Either way, the balance for GWP is negative for both powerplants, as the overall CO_2eq emissions are 21 % and 11 % of the ones obtained in reference operations of Ribatejo and Sines powerplant, respectively. These proportions justify the difference for HGtS potential for reducing GWP between both powerplants: 79 % for NGPP and 89 % for CPP (without considering any make-up of the energy penalty). The absolute difference of these reduction potential is even sharper, as CPP's GHGs intensity is heavier in emissions (see Figure 35).

Besides, GWP, photochemical oxidation is another impact category with mitigation potential due to HGtS retrofitting. Without compensation, the consequent normalization of impacts to the functional unit counterbalances its reduction. With a compensation provided by a grid supported on fossil fuels and without CCS, the mitigation can be exceed resulting in a subtle increase of the overall impact. For NGPP, as NOx emissions are negligible, photochemical oxidation mitigation is imperceptible.

Table 36 shows the results (without considering the avoided emissions) normalized to the functional unit for each operation scenario for both powerplants and table 37 shows the relation between loads of each capture scenario with the reference operation. Figure 42 presents the relation between the impacts of HGtS retrofitting NGPP and CPP without grid's compensation.

Lastly, it is possible to conclude that under an approach of 'cradle to gate', HGtS retrofitting on both powerplants results in a significantly decrease of GWP, without significantly compromising the other impact categories, especially when a compensation of the energy penalty is set by a decarbonised grid as the Norwegian, which is mainly supported on RER.

Table 36 - Results obtained for capture and reference scenarios operation on both powerplants under an approach of 'cradle to gate'. The results are normalized for the functional unit: 1 MWh of electricity produced for supplying to the grid.

		Product: 1 MWh of electricity supplied to the grid							
		NGPP				**CPP**			
Impact category	**Unit**	**NO**	**PT**	**Without**	**Ref**	**NO**	**PT**	**Without**	**ref**
Abiotic depletion	kg Sb eq	2.52E-05	2.58E-05	2.44E-05	1.48E-05	6.18E-05	6.31E-05	6.59E-05	4.61E-05
Abiotic depletion (fossil fuels)	MJ	8.18E+03	8.50E+03	8.18E+03	7.82E+03	1.11E+04	1.19E+04	1.22E+04	1.10E+04
Global warming (GWP100a)	kg CO2 eq	9.56E+01	1.19E+02	9.53E+01	4.61E+02	9.86E+01	1.55E+02	1.08E+02	1.01E+03
Ozone layer depletion (ODP)	kg CFC-11 eq	2.08E-05	2.24E-05	2.08E-05	2.00E-05	8.92E-06	1.27E-05	9.76E-06	8.56E-06
Human toxicity	kg 1,4-DB eq	9.96E+00	1.59E+01	9.62E+00	8.17E+00	3.48E+02	3.62E+02	3.83E+02	3.46E+02
Fresh water aquatic ecotox.	kg 1,4-DB eq	5.96E+00	1.05E+01	5.86E+00	4.86E+00	3.30E+02	3.41E+02	3.63E+02	3.28E+02
Marine aquatic ecotoxicity	kg 1,4-DB eq	1.70E+04	4.47E+04	1.68E+04	1.36E+04	1.26E+06	1.32E+06	1.38E+06	1.25E+06
Terrestrial ecotoxicity	kg 1,4-DB eq	8.04E-02	1.06E-01	7.93E-02	7.20E-02	4.09E+00	4.15E+00	4.51E+00	4.08E+00
Photochemical oxidation	kg C2H4 eq	1.59E-02	2.39E-02	1.58E-02	1.46E-02	5.58E-02	7.47E-02	6.13E-02	5.63E-02
Acidification	kg SO2 eq	2.67E-01	4.82E-01	2.66E-01	2.46E-01	1.66E+00	2.17E+00	1.83E+00	1.64E+00
Eutrophication	kg PO4--- eq	5.58E-02	9.23E-02	5.54E-02	4.93E-02	2.30E+00	2.39E+00	2.54E+00	2.30E+00

Table 37 - Relation between the load of each impact category within the different scenarios and with the reference operation (without HGtS).

		NGPP			**CPP**		
Impact category	**Unit**	**NO**	**PT**	**Without**	**NO**	**PT**	**Without**
Abiotic depletion	kg Sb eq	+42%	+43%	+40%	+25%	+27%	+30%
Abiotic depletion (fossil fuels)	MJ	+4%	+8%	+4%	+1%	+7%	+10%
Global warming (GWP100a)	kg CO2 eq	-79%	-74%	-79%	-90%	-85%	-89%
Ozone layer depletion (ODP)	kg CFC-11 eq	+5%	+11%	+5%	+4%	+32%	+12%
Human toxicity	kg 1,4-DB eq	+18%	+49%	+15%	+1%	+5%	+10%
Fresh water aquatic ecotox.	kg 1,4-DB eq	+18%	+54%	+17%	+1%	+4%	+10%
Marine aquatic ecotoxicity	kg 1,4-DB eq	+20%	+70%	+19%	0%	+5%	+10%
Terrestrial ecotoxicity	kg 1,4-DB eq	+10%	+32%	+9%	0%	+2%	+10%
Photochemical oxidation	kg C2H4 eq	+8%	+39%	+8%	-1%	+25%	+8%
Acidification	kg SO2 eq	+8%	+49%	+8%	+1%	+24%	+10%
Eutrophication	kg PO4--- eq	+12%	+47%	+11%	0%	+4%	+10%

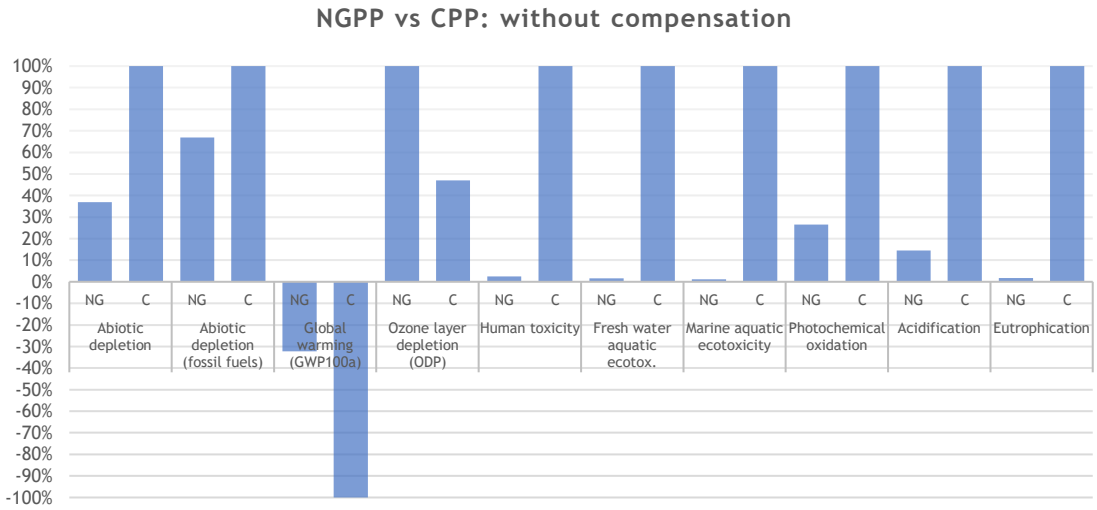

Figure 42 - Impact characterization for each category between NGPP and CPP with HGtS operation and without grid's compensation.

4.4.4. Full LCA results: CPP

Figure 43 shows the relativization of impacts loads for the scenarios with pipeline transport with a sensitivity analysis to the injection depth. The electricity supply used to model these scenarios was the electricity mix in Portugal.

The impact categories for which powerplants operation scores low loads, the share for the transportation and injection phase are higher, even though, those scores are lower than others such as for Human Toxicity or Marine Aquatic Ecotoxicity.

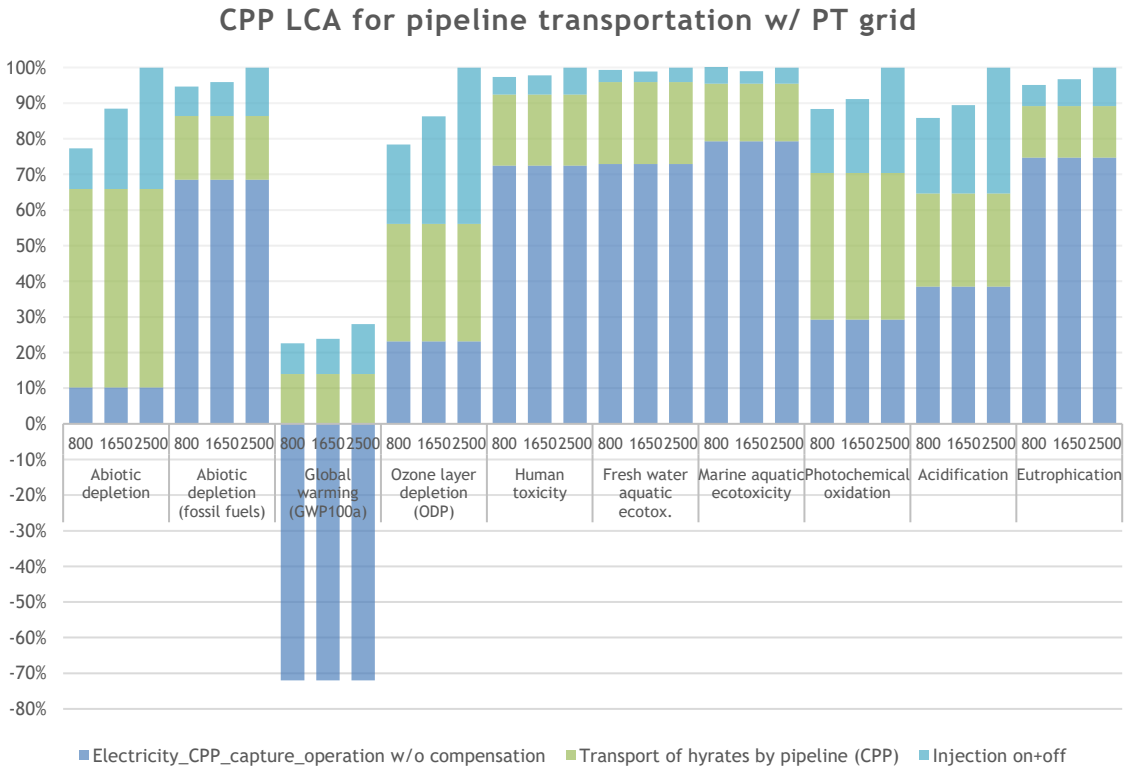

Figure 43 – Relativized results of the LCA for CPP with HGtS retrofitting, pipeline transportation of hydrates slurry for onshore and offshore injection at different depths (800 m, 1650 m and 2500 m) with the energy required being feed by Portuguese electricity supply mix and burning of diesel.

The sensitivity analysis reveals that the increase of the load for most of the impact categories can be somewhat linear with the injection depth.

As the share of CO_2eq emissions avoided are higher than the shares of emissions associated with transportation and injection phases, it can be concluded that the overall CCS system modelled for CPP considering pipeline transportation results in a mitigation of GWP of powerplant's operation.

Figure 44 shows the relativized results for ship without cooling, ship with cooling and pipeline transportation with injection at 1650 m.

It is possible to conclude that ship transportation for a great amount of hydrates slurry is unfeasible, even without the cooling system: besides, highly compromising other impact categories, especially when a cooling system is required, the overall balance for GWP is positive, which means that the processes of transport and storage emit more CO_2eq than the avoided emissions.

Figure 45 shows the relativized results of the LCA of CPP with pipeline transportation for onshore and offshore injection at 1650 m, with a sensitivity analysis to the grid quality used for transportation, injection wells commissioning and injection of hydrates slurry. It does also present the results relativized to the reference scenario.

It can be concluded that the overall performance of HGtS retrofitting CPP can benefit from the use of a less carbon intensive grid. Loads of some impact categories increase for CCS operation.

In Table 38 is possible to read the absolute values of the load for each impact category for best and worse performed pipeline scenario: storage injection at 800 m and electricity supplied by Norwegian grid mix and storage injection at 2500 m and electricity supplied by Portuguese grid mix, respectively. These results were obtained by disregarding the process of 'avoided emissions. It is also presented the variation within these CCS scenarios and the reference operation scenario (without HGtS retrofitting). Some of those variations can also be visualised in Figure 45, that presents the load of each scenario for the heaviest impact categories.

The mitigation potential of GWP ranges between 50 and 69 % with respect to the reference scenario. All the remaining impact categories are penalized, although some of them as abiotic depletion, ODP, photochemical oxidation, acidification and eutrophication score residual penalties (in absolute terms).

Although previous studies concluded that the construction of powerplants have a residual impact in relation to its operation, one must keep in mind that as the construction of powerplants was not considered but the construction of the pipelines and the drilling of the wells was, those variations are somewhat overestimated, as the load of impacts related to the reference scenarios should be in fact higher. However, the absolute differences between CCS scenarios and reference scenario are not compromised, as the load of powerplant construction would be equally scored for both scenarios.

The impact categories presenting heavier relative increases are the ones with marginal loads. For CPP, the most significant impacts variation is presented at last in Figure 46 and are mainly associated to the energy required for transportation and the steel required for pipelines.

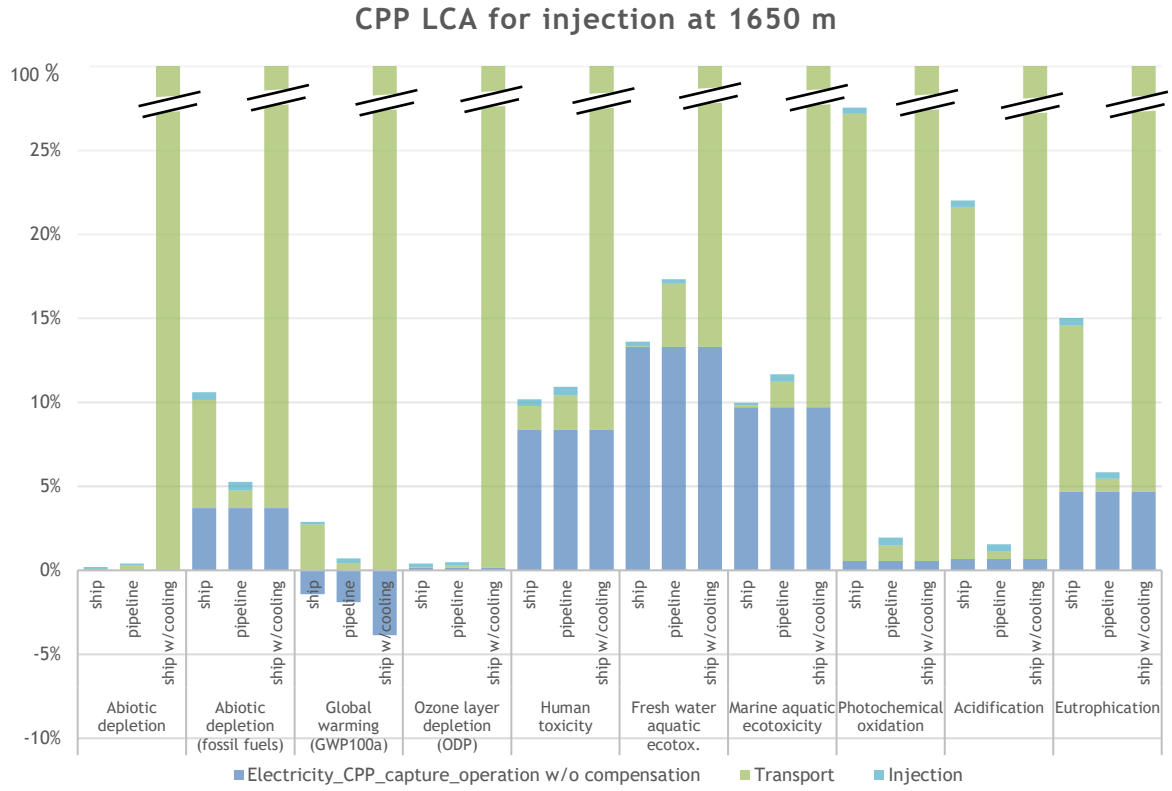

Figure 44 - Relativized results of the LCA for CPP with HGtS retrofitting with different means of transportation: bulk ship transportation without cooling system (ship); bulk ship transportation with cooling system (ship w/cooling) and pipeline (both onshore and offshore). The model comprises offshore injection for ship transportation and onshore and offshore injection for pipeline scenario. The injection depth is at 1650 m for the three scenarios.

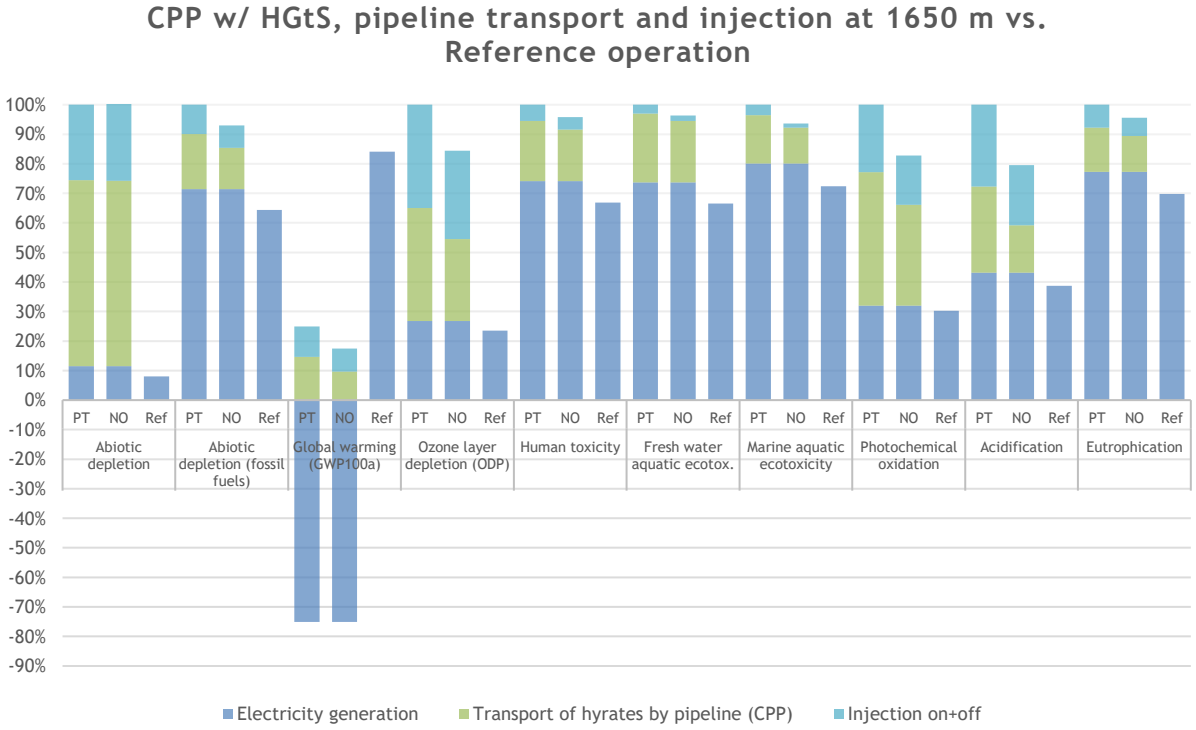

Figure 45 - Relativized results of the LCA modelled for three scenarios of CPP operation. Two CCS scenarios with pipeline transportation for onshore and offshore injection at 1650 m with a sensitivity analysis to the quality of the grid used for transport and onshore injection – Norwegian (NO) and Portuguese (PT) – and another scenario without HGtS retrofitting – reference scenario (Ref).

Table 38 - Load for reference operation scenario, worst and best CCS scenarios for CPP, and the variation between these and the reference scenario.

Impact Category	Unit	Reference Scenario	Best case scenario		Worst case scenario	
Abiotic depletion	kg Sb eq	4.61E-05	4.98E-04	+979%	6.47E-04	+1304%
Abiotic depletion (fossil fuels)	MJ	1.10E+04	1.53E+04	+39%	1.79E+04	+62%
Global warming (GWP100a)	kg CO2 eq	1.01E+03	3.12E+02	-69%	5.00E+02	-50%
Ozone layer depletion (ODP)	kg CFC-11 eq	8.56E-06	2.53E-05	+196%	4.22E-05	+393%
Human toxicity	kg 1,4-DB eq	3.46E+02	4.84E+02	+40%	5.29E+02	+53%
Fresh water aquatic ecotox.	kg 1,4-DB eq	3.28E+02	4.70E+02	+43%	4.99E+02	+52%
Marine aquatic ecotoxicity	kg 1,4-DB eq	1.25E+06	1.61E+06	+28%	1.75E+06	+40%
Photochemical oxidation	kg C2H4 eq	5.63E-02	6.59E+00	+149%	6.80E+00	+265%
Acidification	kg SO2 eq	1.64E+00	1.40E-01	+80%	2.06E-01	+189%
Eutrophication	kg PO4--- eq	2.30E+00	2.94E+00	+32%	4.74E+00	+48%

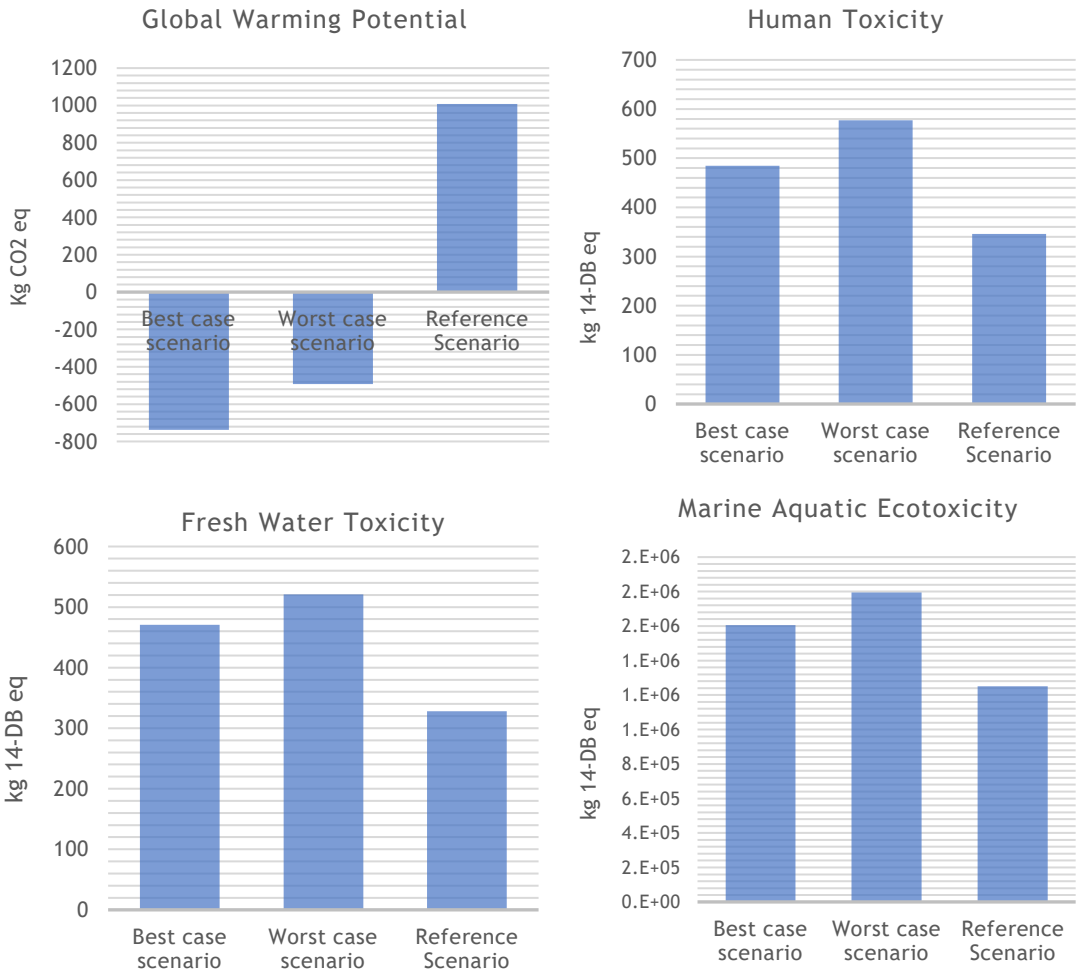

Figure 46 - Loads for best and worst CCS scenario with pipeline transportation and the reference scenario for: GWP, human toxicity, fresh water toxicity and marine aquatic ecotoxicity.

4.4.5 Full LCA: NGPP

4.4.5.1 Scenarios with offshore injection

Figure 47 shows the relativization of impacts loads for the scenarios with pipeline transport and offshore storage with a sensitivity analysis to the injection depth. The electricity supply used to model these scenarios was the electricity mix in Portugal.

Unlike, CPP, for NGPP, the impact categories with higher contribution of transportation and injection phases to the overall load are the ones with higher score: human toxicity, fresh water and marine aquatic ecotoxicity. This occurs do to the fact that these impact categories scores much less than CPP for plants operation (Figures 35 and 42), so that the increased loads of the downstream processes, besides being lower than the ones scored for CPP as further analysed, represent a higher share of the overall performance.

The sensitivity analysis reveals that the increase of the load for most of the impact categories can be somewhat linear with the injection depth.

Although the amount of emissions avoided from NGPP are much lower than the ones avoided in CPP, since the energy required for transport the mass of hydrates formed is also lower, the share of CO_2eq emissions avoided is much higher than the shares of emissions associated with transportation and injection phases. Thus, it can be concluded that the overall CCS system modelled for NGPP considering pipeline transportation and offshore storage results in a mitigation of GWP of powerplant's operation.

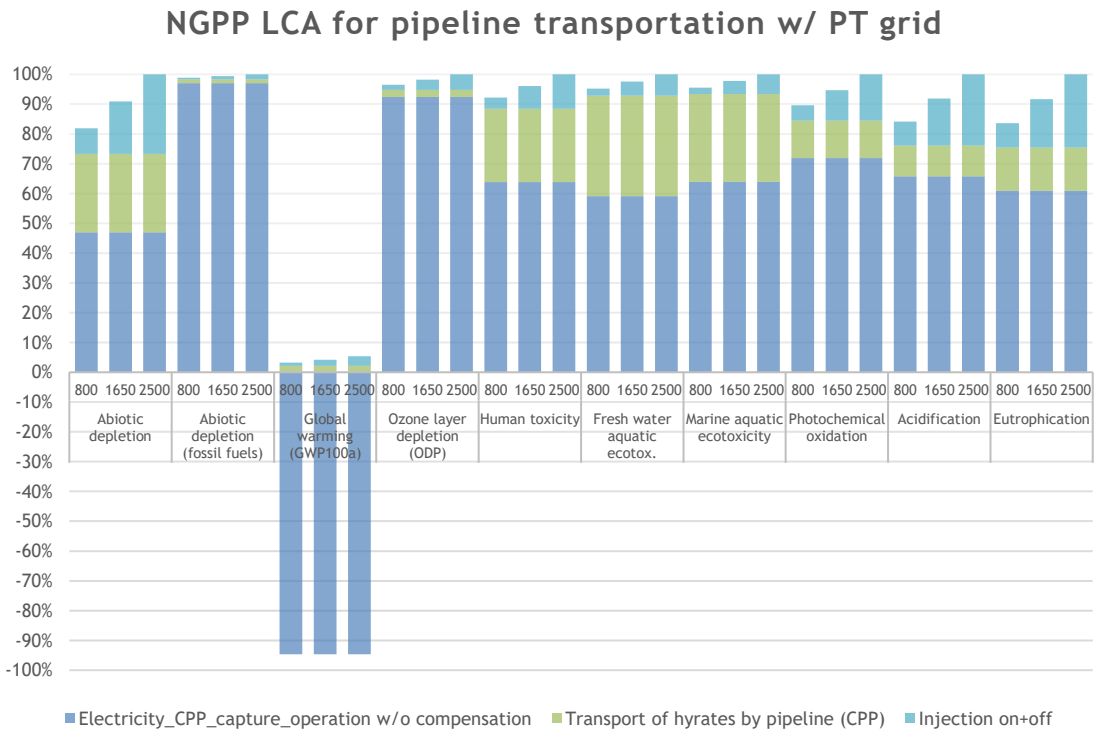

Figure 47 - Relativized results of the LCA for NGPP with HGtS retrofitting, pipeline transportation of hydrates slurry for offshore injection at different depths (800 m, 1650 m and 2500 m) with the energy required being feed by Portuguese electricity.

Figure 48 shows the relativized results for ship without cooling, ship with cooling and pipeline transportation with injection at 1650 m.

Figure 49 shows the relativized results of the LCA of NGPP with pipeline transportation for offshore injection at 1650 m, with a sensitivity analysis to the grid quality used for transportation. It does also present the results relativized to the reference scenario.

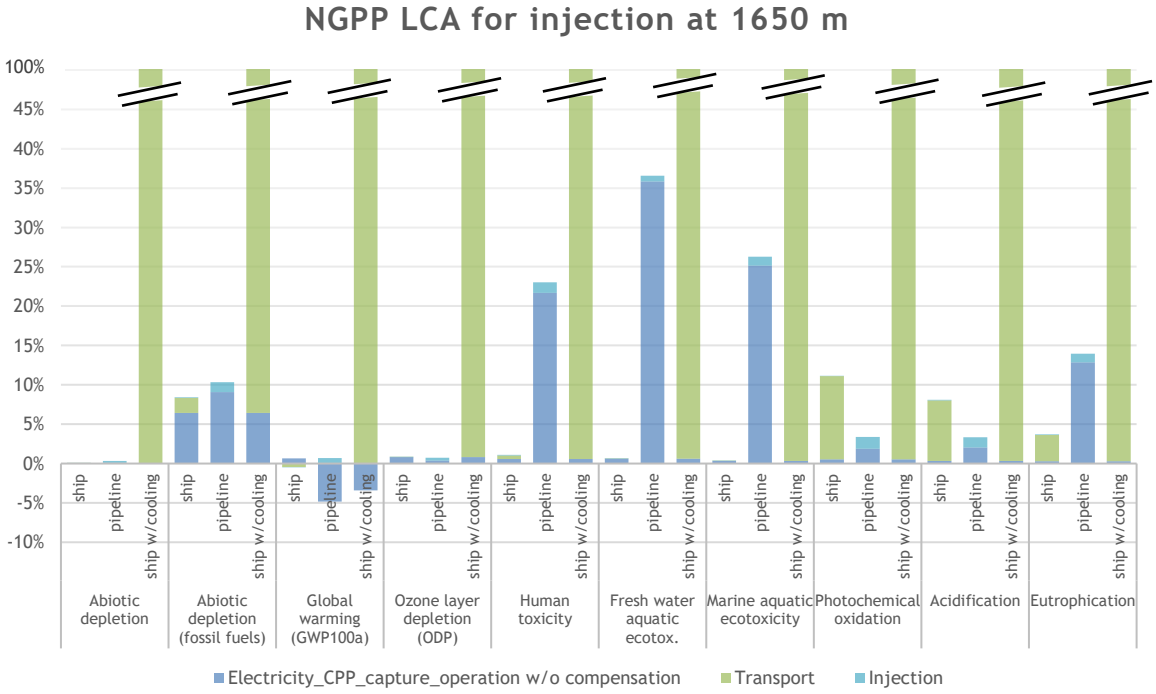

Figure 48 - Relativized results of the LCA for NGPP with HGtS retrofitting with different means of transportation: bulk ship transportation without cooling system (ship); bulk ship transportation with cooling system (ship w/cooling) and pipeline (both onshore and offshore). The model comprises offshore injection for ship transportation and onshore and offshore injection for pipeline scenario. The injection depth is at 1650 m for the three scenarios.

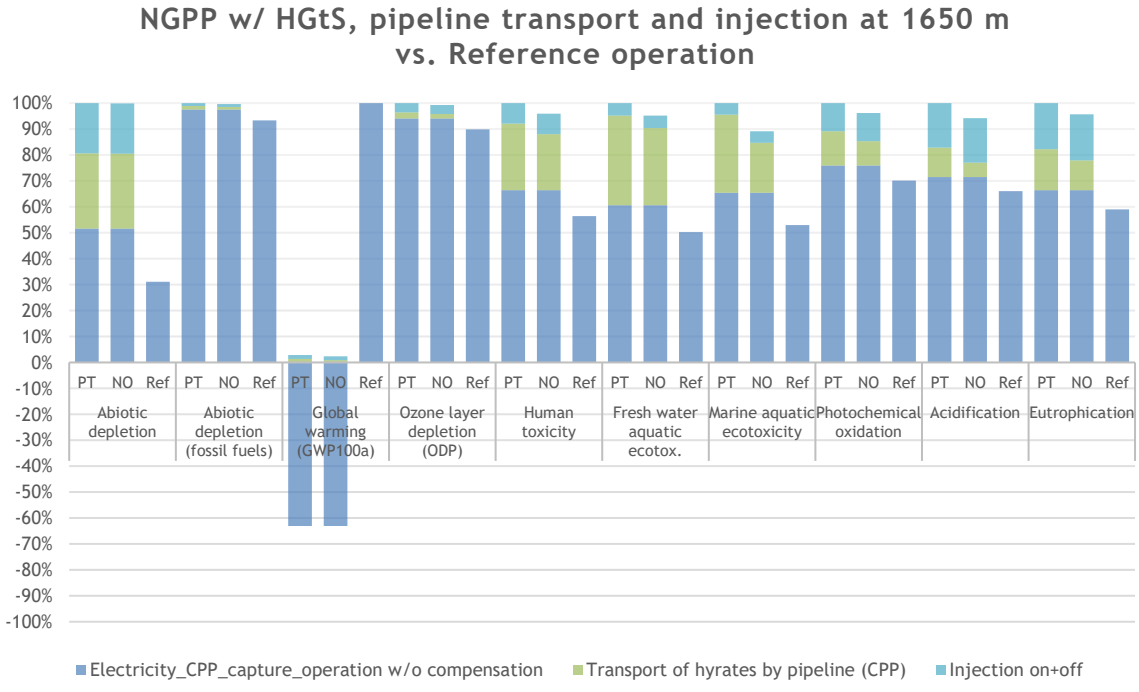

Figure 49 - Relativized results of the LCA modelled for three scenarios of NGPP operation. Two CCS scenarios with pipeline transportation for offshore injection at 1650 m with a sensitivity analysis to the quality of the grid used for transport and offshore storage.

For NGPP, transportation via ship remains compromised for the positive balance for the GWP, as well as, due to the significant increase of the load for other environmental categories. Therefore, based on the results obtained, it is expected that for somewhat short distances, the

transport of CO_2 to storage sites via ship presents higher environmental burdens than the transport via pipeline.

From Figure 49, it is concluded that the overall performance of HGtS retrofitting CPP can benefit from the use of a less carbon intensive grid, although those burdens decrease being less effective when compared to CPP. The loads of every impact category increase for CCS operation, weight exception of GWP.

In Table 39 is possible to read the absolute values of the load for each impact category for best and worst performed pipeline scenarios (with disregard of avoided emissions): storage injection at 800 m and electricity supplied by Norwegian grid mix and storage injection at 2500 m and electricity supplied by the Portuguese grid mix, respectively. The variation within these CCS scenarios and the reference operation scenario (without HGtS retrofitting) may be over penalized due the fact that powerplants construction was not considered, which diminishes the load of reference scenario. Some of these variations can also be visualised in Figure 50, that presents the load of each scenario for the heaviest impact categories.

The mitigation of GWP for NGPP in relation to the reference scenario ranges between 76 and 77 %. All the other impact categories are slightly penalized in absolute terms with exception for Marine Aquatic Ecotoxicity.

Table 39 - Load for reference operation scenario, worst and best CCS scenarios (NGPP with offshore injection), and the variation between these and the reference scenario.

Impact Category	Unit	Reference Scenario	Best case scenario		Worst case scenario	
Abiotic depletion	kg Sb eq	1.48E-05	4.26E-05	+188%	5.21E-05	+253%
Abiotic depletion (fossil fuels)	MJ	7.82E+03	8.31E+03	+6%	8.43E+03	+8%
Global warming (GWP100a)	kg CO2 eq	4.61E+02	1.04E+02	-77%	1.13E+02	-76%
Ozone layer depletion (ODP)	kg CFC-11 eq	1.99E-05	2.16E-05	+9%	2.25E-05	+13%
Human toxicity	kg 1,4-DB eq	8.17E+00	1.33E+01	+63%	1.51E+01	+84%
Fresh water aquatic ecotox.	kg 1,4-DB eq	4.86E+00	8.97E+00	+84%	9.91E+00	+104%
Marine aquatic ecotoxicity	kg 1,4-DB eq	1.36E+04	2.23E+04	+64%	2.62E+04	+93%
Terrestrial Ecotoxicity	kg 1,4-DB eq	7.20E-02	1.41E-01	+95%	1.50E-01	+108%
Photochemical oxidation	kg C2H4 eq	1.46E-02	1.89E-02	+30%	2.20E-02	+51%
Acidification	kg SO2 eq	2.46E-01	3.19E-01	+30%	4.05E-01	+65%
Eutrophication	kg PO4--- eq	4.93E-02	7.25E-02	+47%	9.10E-02	+85%

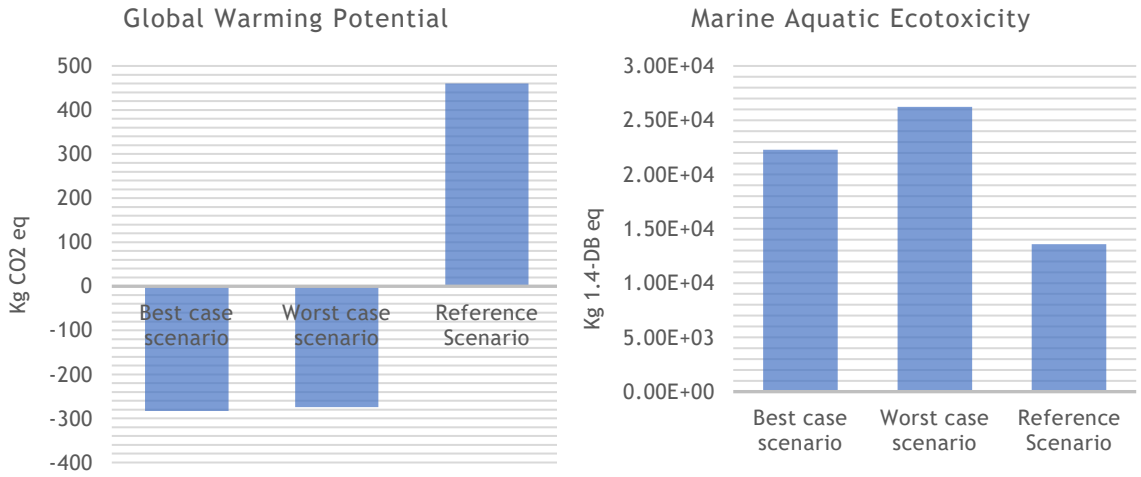

Figure 50 - Loads for best and worst CCS scenario with pipeline transportation and the reference scenario for: GWP, and marine aquatic ecotoxicity.

Figure 51 shows the results of the sensitivity analysis of the operation rate of the powerplant. The less sensitive impact categories to the downstream processes are the fossil fuels depletion, GWP and ODP. As the energy consumption per MWh of electricity produced remains approximately the same within the different scenarios these burdens do not fluctuate significantly, however, the performance (per MWh of electricity produced and supplied to the grid) is somewhat better for increased operation rates.

The energy consumption for transport and storage of CO_2 is dependent on the captured amount, thus it remains approximately constant within the different scenarios, however as the burdens related to construction (allocated to a year of operation) increase (when normalized to the functional unit) for lower utilization rates of the powerplant, the impact categories more sensitive to transport and storage phases, present an increase of burdens load with the decrease of powerplants activity.

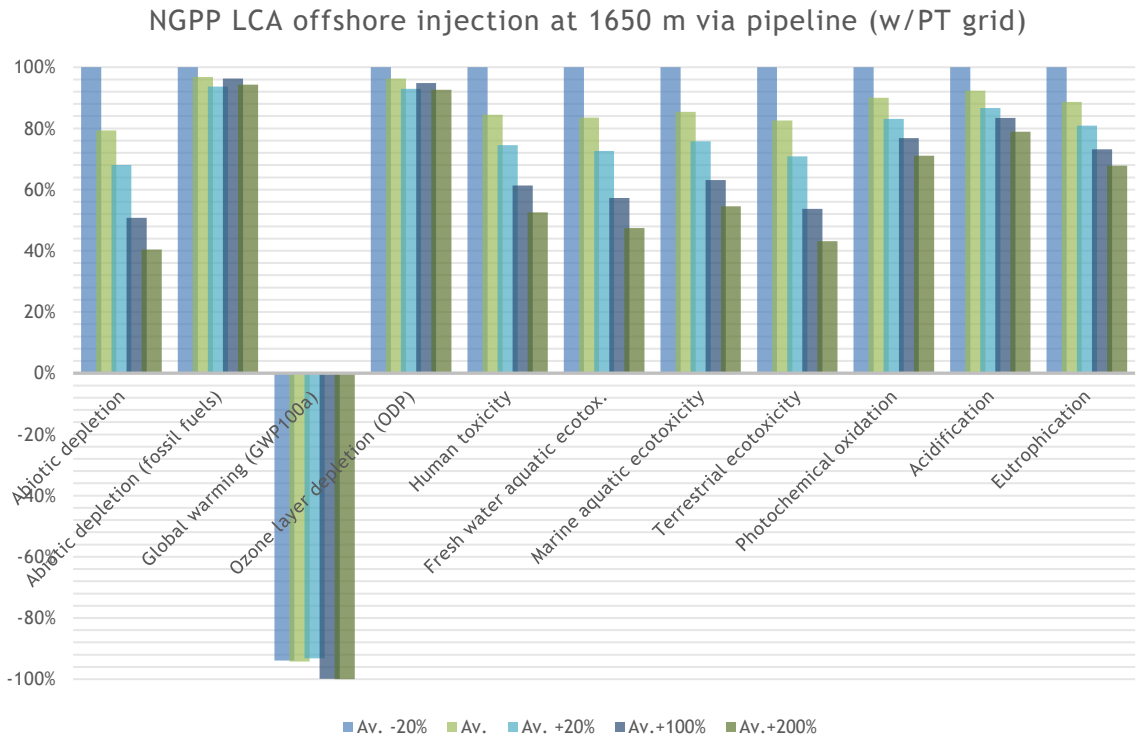

Figure 51 - Results of the LCA for NGPP with HGtS retrofiting, pipeline ransportation and offshore storage for several utilization rates of Ribatejo powerplant.

4.4.5.2 Scenarios with onshore injection

Figure 52 shows the relativization of impacts burdens for the scenarios with pipeline transport and onshore storage with a sensitivity analysis to the injection depth. The electricity supply used to model these scenarios was the electricity mix in Portugal.

As the transport does not require any pressurization besides an initial boosting, feed by the plant itself, its contribution to the overall burdens decreased in relation to the offshore storage scenarios. The injection is supported on the electricity grid, thus the system remains sensitive to it quality, as shown in Figure 53.

These scenarios result in even fewer environmental burdens, regarding HGtS retrofitting in NGPP with offshore storage (see Table 40), with exception for marine ecotoxicity for the 'wort-case' scenario, which increase in mainly related to the over consumption of electricity grid (PT) for the injection process. Although, energy consumption for the downstream processes being

lower than offshore storage scenarios, the GWP mitigation for the 'worst-case' scenario have slightly reduced to -74 %, for the same reason marine ecotoxicity increased.

Data available regarding the operational conditions for this onshore storage clusters unveils the injection of these amounts of hydrates. According to [66], hydrates formed by NGPP, could only be injected for lower utilization rates, until a maximum about 3500 hours of full load operation.

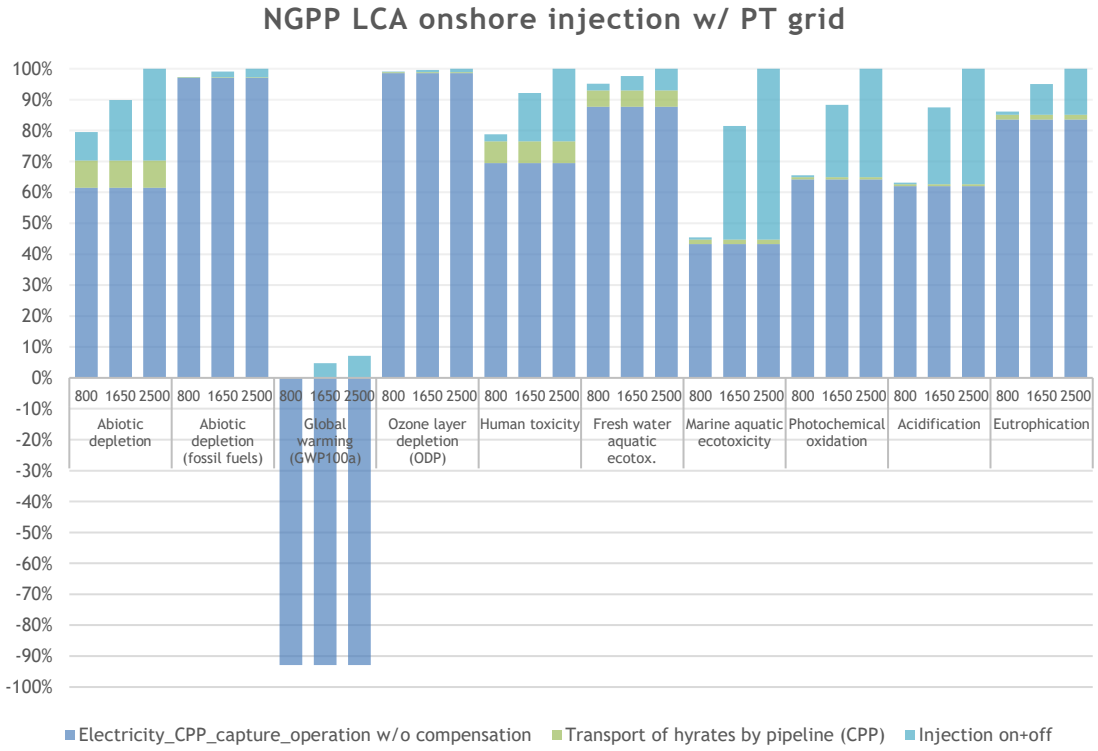

Figure 52 - Relativized results of the LCA for NGPP with HGtS retrofitting, pipeline transportation of hydrates slurry for onshore injection at different depths (800 m, 1650 m and 2500 m) with the energy required being feed by Portuguese electricity.

Table 40 – Environmental loads for reference operation scenario, worst and best CCS scenarios (NGPP with onshore injection), and the variation between these and the reference scenario.

Impact Category	Unit	Reference Scenario	Best case scenario		Worst case scenario	
Abiotic depletion	kg Sb eq	1.48E-05	3.16E-05	+114%	3.97E-05	+169%
Abiotic depletion (fossil fuels)	MJ	7.82E+03	8.20E+03	+5%	8.43E+03	+8%
Global warming (GWP100a)	kg CO2 eq	4.61E+02	9.62E+01	-79%	1.18E+02	-74%
Ozone layer depletion (ODP)	kg CFC-11 eq	1.99E-05	2.09E-05	+5%	2.11E-05	+6%
Human toxicity	kg 1,4-DB eq	8.17E+00	1.09E+01	+33%	1.38E+01	+69%
Fresh water aquatic ecotox.	kg 1,4-DB eq	4.86E+00	6.36E+00	+31%	6.69E+00	+37%
Marine aquatic ecotoxicity	kg 1,4-DB eq	1.36E+04	1.76E+04	+30%	3.88E+04	+185%
Terrestrial Ecotoxicity		7.20E-02	8.61E-02	+20%	1.02E-01	+41%
Photochemical oxidation	kg C2H4 eq	1.46E-02	1.61E-02	+11%	2.46E-02	+69%
Acidification	kg SO2 eq	2.46E-01	2.71E-01	+10%	4.29E-01	+75%
Eutrophication	kg PO4--- eq	4.93E-02	5.71E-02	+16%	6.63E-02	+35%

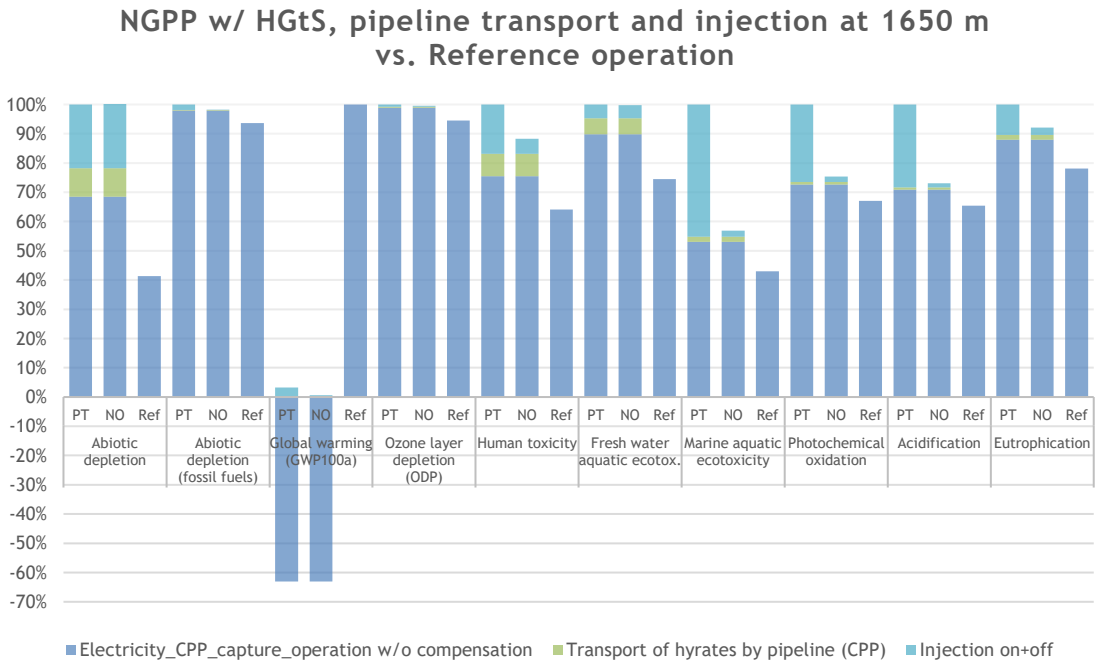

Figure 53 - Relativized results of the LCA modelled for three scenarios of NGPP operation. Two CCS scenarios with pipeline transportation for onshore injection at 1650 m with a sensitivity analysis to the quality of the grid used onshore storage.

4.4.6 CPP vs NGPP: 'cradle to grave'

Figure 54 shows the relativized impacts for each category, split into plants operation, transportation and storage phases for NGPP and CPP operating at distinct utilization rates, yet to producing the same amount of electricity for being supplied to the grid if the HGtS unit wanot in operation (without accounting it energy penalty). The transport is performed by pipeline, both onshore and offshore, to offshore injection sites at 1650 m of depth.

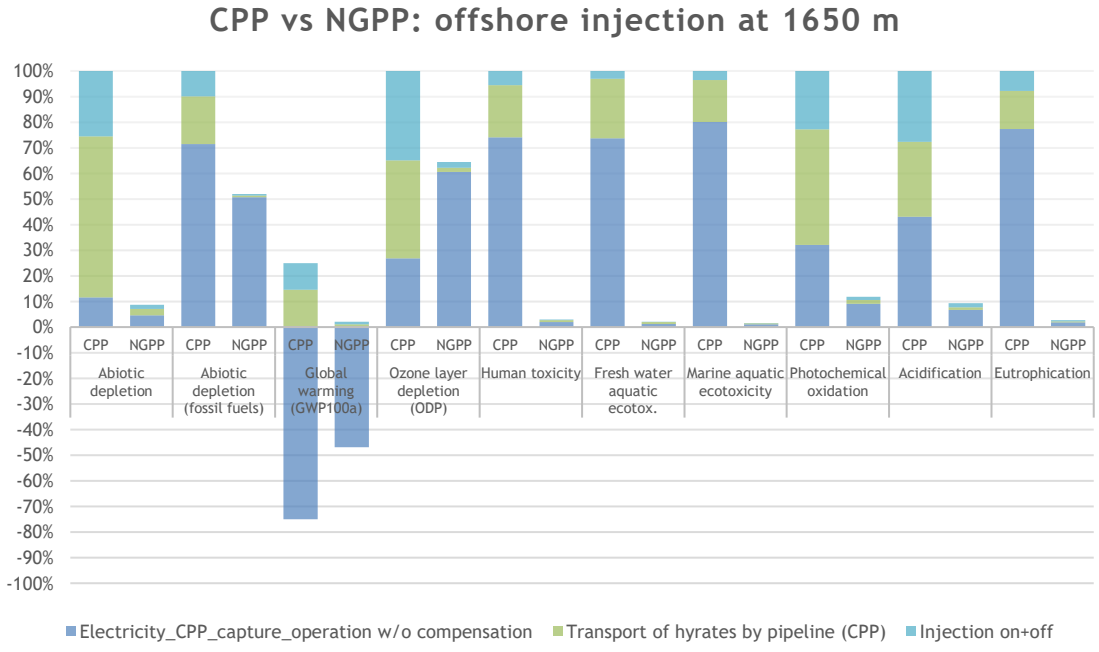

Figure 54 - Relativization of impact loads for CPP and NGPP for the scenarios with pipeline transportation and offshore injection at 1650 (using PT grid as electricity source for downstream processes).

Despite the fact that the mitigation of GWP for NGPP in relation to its reference scenario was better than the one achieved for CPP, the total CO_2eq emissions avoided by HGtS retrofitting in CPP are higher than the ones avoided in NGPP.

Even having a higher operating load than the NGPP, for the CPP, the transport and injection of CO_2 hydrates in slurry state by pipeline have a larger contribution to the overall system load than in the case of the NGPP, for all impact categories. On the one hand, the flow of slurry transported is much larger, on the other, the distance travelled is about double.

The following table shows the relationship between the load of each impact category resulting from the pipeline transportation for both plants, divided by t(CO2)km. Table 42 shows the load of each impact category resulting from the injection step (at 1650 m) for both plants, normalized to the mass of CO_2 injected.

Table 41 - Results obtained from pipeline transport step normalized to the mass of CO_2 transported and distance travelled.

Normalization of transportation impacts to tkm

	CPP	NGPP	
tonnes(CO2)/y*km	**8.65E+09**	**1.71E+09**	
Impact category	**load/tkm**	**load/tkm**	**NGPP/CPP**
Abiotic depletion	3.05E-07	6.26E-08	21%
Abiotic depletion (fossil fuels)	2.70E+00	5.06E-01	19%
Global warming (GWP100a)	1.48E-01	2.96E-02	20%
Ozone layer depletion (ODP)	1.18E-08	2.36E-09	20%
Human toxicity	8.92E-02	1.69E-02	19%
Fresh water aquatic ecotox.	9.73E-02	1.53E-02	16%
Marine aquatic ecotoxicity	2.38E+02	3.52E+01	15%
Terrestrial ecotoxicity	1.77E-03	2.76E-04	16%
Photochemical oxidation	7.10E-05	1.25E-05	18%
Acidification	1.05E-03	1.91E-04	18%
Eutrophication	4.16E-04	6.01E-05	14%

Table 42 - Results obtained for storage step normalized to the mass of CO2 injected.

Normalization of storage impacts to tonnes of CO_2

	CPP	NGPP	
tonnes(CO2)/y	**2.22E+07**	**9.47E+06**	
Impact category	**load/t**	**load/t**	**NGPP/CPP**
Abiotic depletion	4.83E-05	7.52E-06	16%
Abiotic depletion (fossil fuels)	5.62E+02	7.53E+01	13%
Global warming (GWP100a)	4.08E+01	5.36E+00	13%
Ozone layer depletion (ODP)	4.20E-06	6.44E-07	15%
Human toxicity	9.37E+00	9.43E-01	10%
Fresh water aquatic ecotox.	4.92E+00	3.82E-01	8%
Marine aquatic ecotoxicity	2.04E+04	9.33E+02	5%
Terrestrial ecotoxicity	4.75E-02	5.34E-03	11%
Photochemical oxidation	4.83E-05	7.52E-06	16%
Acidification	5.62E+02	7.53E+01	13%
Eutrophication	4.08E+01	5.36E+00	13%

Regarding the performance of the HGtS retrofitting on CPP, the overload of energy inputs and inherent to the pipeline construction phase are not reduced to the levels presented by NGPP, when normalized by the kg of CO_2 transported and km of distance travelled. The same happens with the injection phase, for the impacts allocated to the mass of CO2 injected per year.

According to the results obtained, it can be concluded that the penalisation of other environmental burdens besides GWP due to downstream processes of HGtS retrofit is heavier for plants with higher rates of atmospheric emissions, even when those burdens are normalized by the functional unit (MWh produced and supplied to the grid), by the mass of CO_2 transported, and by the distance of pipeline transport.

However, the mitigation potential of the GWP is greater for heavier emitting plants, such as CPP. From an overall process point of view, and taking into account that the absolute load of most impact categories has not been greatly aggravated relative to the reference electricity generation processes (without HGtS), the GWP mitigation potential for the CPP may make up the worse performance of transport and injection processes. LCA using site specific characterization factors could add value to support decision making.

4.4.7 Uncertainty analysis: Monte Carlo simulations

Figure 55 and 56 show the 95 % confidence intervals for the impact's characterization i.e. uncertainties levels for the CPP and NGPP, respectively, which were obtained through Monte Carlo analysis simulated on SimaPro. The high uncertainties verified for CPP unveils the exact characterization of some environmental burdens for the whole system, expected considering the results obtained for reference scenario. The most accurate impact categories are GWP and fossil fuels depletion. It should be mentioned that the high range for the 95 % confidence interval is mainly sourced in background data uncertainties.

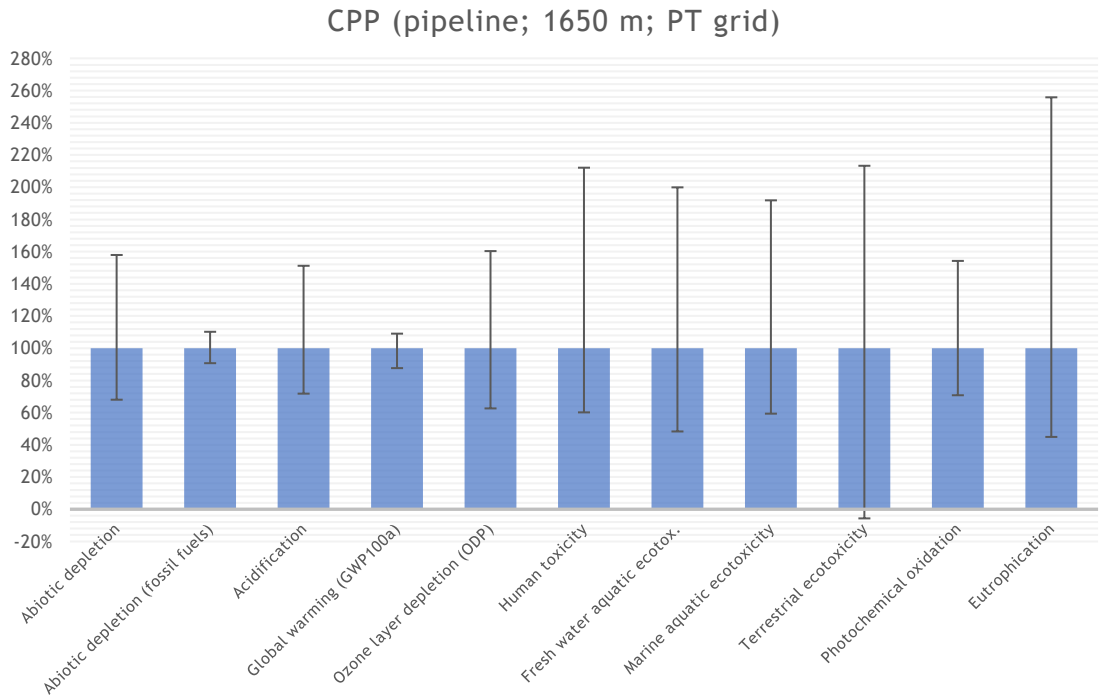

Figure 55 - Monte Carlo results for the 95 % confidence interval of each impact category, for CPP. These results were obtained for the CCS scenario with pipeline transportation to onshore and offshore storage at 1650 m using PT grid.

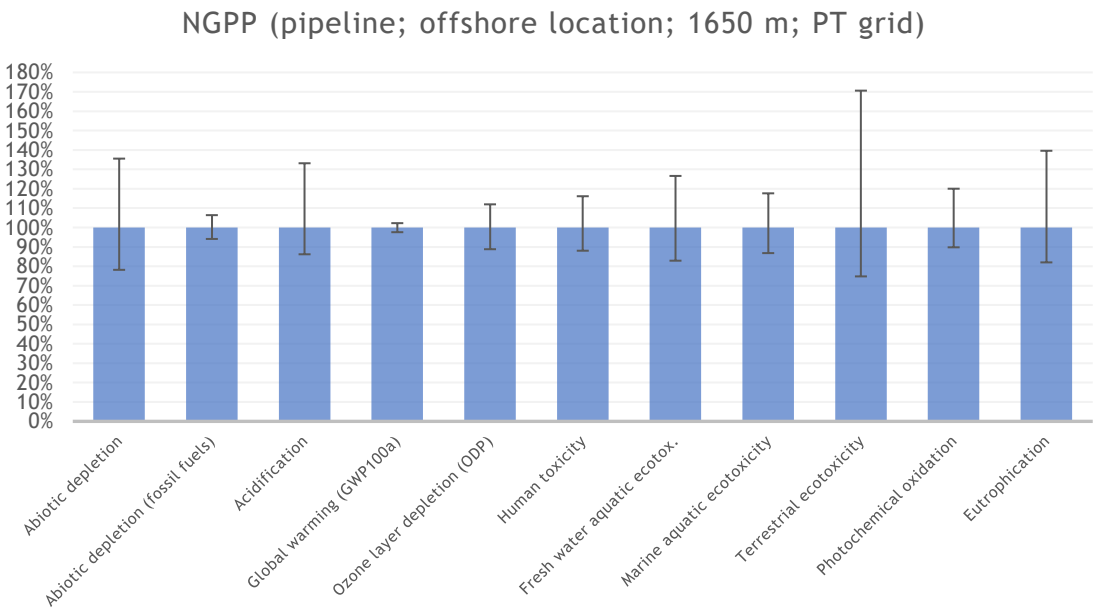

Figure 56 - Monte Carlo results for the 95 % confidence interval of each impact category, for NGPP. These results were obtained for the CCS scenario with pipeline transportation to offshore storage at 1650 m using PT grid.

The results of Monte Carlo simulations as well as other results extracted from SimaPro software, regarding both 'cradle to gate' and 'cradle to grave' approach can be found in Appendix XI.

Chapter 5

Conclusions

The fulfilment and development of the proposed LCA was a rather complex task, involving the acquisition of several data and the structuring of logistically feasible operating networks for both powerplants. Yet, the goals were accomplished:

1. HGtS retrofitting fossil fuel-based powerplants is an effective measure for reducing the GWP associated to the combustion processes by reducing their load.
2. For CPP the mitigation under a 'cradle to gate' approach is 89 % (considering no energy penalty compensation) and under a 'cradle to grave' approach is 50 % for the 'worst-case scenario' and 69 % for the 'best-case scenario'. For NGPP the mitigation under a 'cradle to gate' approach is 79 % and under a 'cradle to grave' approach is about 76 %.
3. The most penalized impact categories are related to human toxicity and ecotoxicity, related to energy consumption in downstream processes and pipeline and wells commissioning. Yet, under the approach of 'cradle to gate', by considering only the trade-offs of HGtS operation, the penalization is rather residual.
4. The key trade-offs are related to the energy consumption required for transport and injection, which can be significantly improved by the evolution for a cleaner grid, for which the use of HGtS can contribute. The additional energy required for transporting and injecting the water contributes to the penalization of both processes.
5. Although CPP achieved a higher GWP mitigation potential in absolute terms, it reveals higher penalization rates on other impact categories due to the higher fluxes of hydrates produced per MWh of electricity supplied to the grid. NGPP achieved better relative mitigation potential under the approach of 'cradle to grave'.
6. Regarding NGPP, the overall performance of HGtS retrofit improves for increased plant's utilization rates, especially for the impact categories more sensitive to transport and storage processes.
7. According to the results, ship transportation compromises the GWP mitigation of the overall system. Pipeline transport, on the turn, revealed itself to be sustainably feasible.

The main limitations of the assessment are related to data on which the storage scenarios were supported, especially related to the injection rates - determined based on available data for upper sediments and considering supercritical CO_2 instead of CO_2 hydrates in slurry state -, to the values used for pressures variation into the reservoir and to the leakage rates inherent to downstream processes. The use of background data on CPP scenarios increased the uncertainty ranges of most of the impact categories, which makes it difficult to characterize the exact burdens associated to those systems.

Recommendations

To better characterize the impact categories regarding CPP system, more quality data should be added instead of using average background data available in Ecoinvent libraries.

Regarding the storage modelling, a deeper site study to accurate thermodynamic and geophysical characteristics of the system should be performed, providing a better assessment of the risk and different pathways for CO_2 and other gases leakage. A sensitivity analysis to

estimate the impact of different operational parameters on leakage rates could be useful to set up the operational conditions of hydrates injection.

For a broader approach to the energy sector, a consequential analysis of the performance of HGtS retrofitting current powerplants operating in Portugal, within a wider timeframe could add relevant information to the benefits and trade-offs of its performance for the overall energy production mix.

Although, HGtS technology presents a high potential for outperforming other separation technologies based on its low energy penalty (9 % for CPP and 3-4 % for NGPP) and on their ability to eliminate air emissions (under plants frontiers), the overload of energy consumption during transport and injection due to the mass of water, can compromise the overall performance. Thus, the study could be modelled for other capture/separation technologies to provide the same basis operation for a comparison study.

Similar studies could also be applied to the Energy Intensive Industries with special focus on cement industry in Portugal, which is able of using the CO_2 captured in their own processes creating a basis for a circular economy while contributing to the mitigation of the GWP inherent to their processes.

The scope of the LCAs applied to this technology should also comprise the economic dimension, as an essential aspect for supporting decision making.

References

[1] P.R. Shukla, J. Skea, R. Slade, R. van Diemen, E. Haughey, J. Malley, M. Pathak, J. Portugal Pereira. (2019). Technical Summary. In: Climate Change and Land: an IPCC special report on climate change, desertification, land degradation, sustainable land management, food security, and greenhouse gas fluxes in terrestrial ecosystems.

[2] Edenhofer O., R. Pichs-Madruga, Y. Sokona, S. Kadner, J. C. Minx, S. Brunner, S. Agrawala, G. Baiocchi, I. A. Bashmakov, G. Blanco, et al. (2014). Technical Summary. In: Climate Change 2014: Mitigation of Climate Change. Contribution of Working Group III to the Fifth Assessment Report of the Intergovernmental Panel on Climate Change.

[3] Jos G.J. Olivier, Gre Janssens-Maenhout, Marilena Muntean, Jeroen A.H.W. Peters. (2016), Trends in Global CO_2 Emissions; 2016 Report. The Hague: PBL Netherlands Environmental Assessment Agency; Ispra: European Commission, Joint Research Centre.

[4] Leung D., Caramanna G., Maroto-Valer M. (2014), An overview of current status of carbon and storage technologies. Renewable and Sustainable Energy Reviews 39 (2014) 426-443.

[5] Ritchie H., Roser M. (2019), CO2 and Greenhouse Gas Emissions. Our World in Data. Available: https://ourworldindata.org/co2-and-other-greenhouse-gas-emissions

[6] Lindsey R. (2020), Climate change: atmospheric carbon dioxide. NOAA; Climate.gov. Available: https://www.climate.gov/news-features/understanding-climate/climate-change-atmospheric-carbon-dioxide

[7] Jackson RB., Le Quéré C., Andrew RM., Canadell J. G., Korsbakken J.I., Liu Z., Peters G.P., Zheng B., Friedlingstein P. (2019), Global Energy Growth Is Outpacing Decarbonization; A special report for the United Nations Climate Action Summit September 2019. Australia: Global Carbon Project, International Project Office.

[8] IEA (2020). *Global CO2 emissions in 2019*, IEA, Paris. Available: https://www.iea.org/articles/global-co2-emissions-in-2019

[9] Garcia, M. (2020), CCUS and energy intensive industries (EIIs). IEAGHG, International Energy Agency Greenhouse Gases. Available: https://ieaghg.org/files/2020-IP05_CCUS_and_Energy_Intensive_Industries_EIIs.pdf

[10] IEA, (2017), Energy and Technologies Perspectives 2017. Catalysing Energy Technology Transformations. OECD: International Energy Agency.

[11] Metz, B., Davidson, O., De Coninck, H., Loos, M., Meyer, L., Intergovernmental Panel on Climate Change, (2005), "IPCC Special Report on Carbon Dioxide Capture and Storage.". New York, NY, USA.

[12] IPCC, Masson-Delmotte, V., P. Zhai, H.-O. Pörtner, D. Roberts, J. Skea, P.R. Shukla, A. Pirani, W. Moufouma-Okia, C. Péan, R. Pidcock, S. Connors, J.B.R. Matthews, Y. Chen, X. Zhou, M.I. Gomis, E. Lonnoy, T. Maycock, M. Tignor, and T. Waterfield (eds.) (2018), Summary for Policymakers. In: Global Warming of 1.5°C. An IPCC Special Report on the impacts of global warming of 1.5°C above pre-industrial levels and related global greenhouse gas emission pathways, in the context of strengthening the global response to the threat of climate change, sustainable development, and efforts to eradicate poverty.

[13] M. E. Boot-Handford, J. C. Abanades, E. J. Anthony, M. J. Blunt, S. Brandani, N. Mac Dowell, J. R. Fern´andez, M.-C. Ferrari, R. Gross, J. P. Hallett, R. S. Haszeldine, P. Heptonstall, A. Lyngfelt, Z. Makuch, E. Mangano, R. T. J. Porter, M. Pourkashanian, G.

T. Rochelle, N. Shah, J. G. Yao, P. S. Fennell. (2014), Carbon Capture and storage update. Energy & Environmental Science, 2014, 7, 130. DOI: 10.1039/c3ee42350f.

[14] Sutter D., Werner M., Zappone A., Mazzotti M. (2013), 'Developing CCS into a realistic option in a country's energy strategy. Zurich, Switzrland: Energy Procedia 37, 6562-6570, 2013. DOI: 10.1016/j.egypro.2013.06.588

[15] IEA (2019), World Energy Model; Scenario analysis of future energy trends. International Energy Agency. Available: https://www.iea.org/reports/world-energy-model/sustainable-development-scenario

[16] Global CCS Institute, (2019), The Global Status of CCS: 2019. Australia.

[17] IEA (2009). World Energy Outlook 2009. Paris, France. ISBN: 978 92 64 06130 9.

[18] IEA, (2017), Energy and Technologies Perspectives 2017. Catalysing Energy Technology Transformations. OECD: International Energy Agency.

[19] Burnard K. (2020), The role and value of CCS in different national contexts. International Energy Agency, IEAGHG.

[20] Global CCS Institute (2018), CORE; Facilities Database. Available: https://co2re.co/FacilityData

[21] McCulloch S., (2016), 20 years of Carbon Capture and Storage; Accelerating future deployment. Paris, France: International Energy Agency.

[22] BloombergNEF (2020), Sector Coupling in Europe: Powering Decarbonization; Potential and Policy Implications of Electrifying the Economy.

[23] MIT (2016), Sleipner Fact Sheet: Carbon Dioxide Capture and Storage Project. USA: Carbon Capture & Sequestration Technologies – Massachusetts Institute of Technology.

[24] IEA (2019), Putting CO_2 to Use; Creating value from emissions. Paris, France.

[25] P.R. Shukla, J. Skea, R. Slade, R. van Diemen, E. Haughey, J. Malley, M. Pathak, J. Portugal Pereira. (2019). Technical Summary. In: Climate Change and Land: an IPCC special report on climate change, desertification, land degradation, sustainable land management, food security, and greenhouse gas fluxes in terrestrial ecosystems.

[26] Dowell N. M., Fennell P., Shah N., Maitland G. (2017), 'The role of CO2 capture and utilization in mitigating climate change'. Nature Clim Change 7, 243-249 (2017). https://doi.org/10.1038/nclimate3231

[27] Koytsoumps E., Christian Bergins, Emmanouli Kakaras. (2018). The CO_2 economy: review of CO_2 capture and reuse technologies. The Journal of Supercritical Fluids 132 (2018) 3-16. https://doi.org/10.1016/j.supflu.2017.07.029

[28] Herzog, H., Golomb, D., (2014), Carbon capture and storage from fossil fuel use. Encyclopedia of Energy, vol. 1. 1-11.

[29] Zou L., Sun Y., Che S. et al. (2017), Porous Polymers for Post-Combustion Carbon Capture, Advanced Materials vol. 29, Issue 31. https://doi.org/10.1002/adma.201700229

[30] Wang Y. Zhao L. Otto A. et al. (2017), A review paper of post-combustion CO_2 capture technologies from coal-fired power plants. Energy Procedia vol. 114, July 2017, 650-665. https://doi.org/10.1016/j.egypro.2017.03.1209

[31] Open Data Soft (2016). 'World Power Plants Database – analyse' (X axis 'Type' and without 'break down series' setting). Available: https://datasource.kapsarc.org/explore/dataset/world-power-plants-list

[32] Czarnota R. Knapik E., Wojnarowski P. et al. (2019) Carbon Dioxide Separation Technologies. Arch. Min. Sci. 64 (2019) 3, 487-498. DOI 10.24425/ams.2019.129364

[33] Korren, 2010.

[34] Lockwood T. (2017). A comparative review of next-generation carbon capture technologies for coal-fired power plant. Energy Procedia 114 (2017) 2658-2670. https://doi.org/10.1016/j.egypro.2017.03.1850

[35] Liang Z., Rongwong W., Liu H., et al. (2015). Recent progress and new developments in post-combustion carbon-capture technology with amine-based solvents. Int. Journal of Greenhouse Gas Control 40 (2015) 9 26-54. https://doi.org/10.1016/j.ijggc.2015.06.017

[36] Koytsoumps E., Christian Bergins, Emmanouli Kakaras. (2018). The CO_2 economy: review of CO_2 capture and reuse technologies. The Journal of Supercritical Fluids 132 (2018) 3-16. https://doi.org/10.1016/j.supflu.2017.07.029

[37] Cuéller-Franca R., Azapagic A. (2015). Carbon capture, storage and utilisation technologies: A critical analysis and comparison of their life cycle environmental impacts. Journal of CO2 Utilization 9 (2015) 3 82-102. https://doi.org/10.1016/j.jcou.2014.12.001

[38] Riboldi L., Bolland O., Overview on Pressure Swing Adsorption (PSA) as CO_2 capture technology: state-of-art, limits and potentials. Energy Procedia 114 (2017) 2390-2400. https://doi.org/10.1016/j.egypro.2017.03.1385

[39] Jing Li, Hedong Zhang, Zuopeg Gao, Jie Fu, Weyna Ao, Jianjun Dai. CO_2 capture with chemical looping combustion of gaseous fuels: an overview. Energy&fuels 31 (2017) 4 3475-3524. https://doi.org/10.1021/acs.energyfuels.6b03204

[40] Juan Adanez, Albert Abad et al. Progress in chemical-looping combustion and reforming technologies. Progress in energy and combustion science 38 (2012) 215–282. https://doi.org/10.1016/j.pecs.2011.09.001

[41] Erlach B, Schmidt M, Tsatsaronis B. Comparison of carbon capture IGCC with pre-combustion decarbonisation and with chemical-looping combustion. Energy 2011;36:3804–15. https://doi.org/10.1016/j.energy.2010.08.038

[42] APA (2020). National Invntory Report 2020 Portugal. Amadora, Lisboa: Agência Portuguesa do Ambiente.

[43] Song, Chunfeng et al. Cryogenic-based CO_2 capture technologies: state-of-art developments and current challenges. Renewable and Sustainable Energy Reviews 101 (2019) 265-278. https://doi.org/10.1016/j.rser.2018.11.018

[44] Martin J. Tuinier, Martin van Sint Annaland. Biogas purification using cryogenic packed-bed technology. Ind. Eng. Chem. Res. 2012, 51, 15, 5552-5558. https://doi.org/10.1021/ie202606g

[45] Baxter, L., Baxter, A., & Burt, S. (2009). Cryogenic CO2 capture as a cost-effective CO2 capture process. In *International Pittsburgh Coal Conference*.

[46] Clodic, D., El Hitti, R., Younes, M., Bill, A., & Casier, F. (2005). CO2 capture by anti-sublimation: Thermo-economic process evaluation. In *4th annual conference on carbon capture and sequestration* (pp. 2-5). Alexandria: National Energy Technology Laboratory.

[47] Fazlollahi, F., Bown, A., Ebrahimzadeh, E., & Baxter, L. L. (2015). Design and analysis of the natural gas liquefaction optimization process-CCC-ES (energy storage of cryogenic carbon capture). *Energy*, *90*, 244-257. https://doi.org/10.1016/j.energy.2015.05.139

[48] Song, C., Liu, Q., Ji, N., Deng, S., Zhao, J., Li, Y., ... & Li, H. (2018). Alternative pathways for efficient CO2 capture by hybrid processes—a review. *Renewable and Sustainable Energy Reviews*, *82*, 215-231. https://doi.org/10.1016/j.rser.2017.09.040

[49] He, Junnan; Liu, Yinan; et al. (2017). A literature research on the performance evaluation of hydrate-based CO_2 capture and separation process. Energy Procedia 105, 4090-4097. https://doi.org/10.1016/j.egypro.2017.03.867

[50] Dashti, H., Yew, L. Z., & Lou, X. (2015). Recent advances in gas hydrate-based CO2 capture. *Journal of Natural Gas Science and Engineering*, *23*, 195-207. https://doi.org/10.1016/j.jngse.2015.01.033

[51] Costa, M. (2017). The NETmix Technology, Applied to Gas Hydrates Production: A Potential Solution to CCS. Porto, Portugal: *Associate Laboratory LSRE – LCM*.

[52] Li, R., Li, X. S., Chen, Z. Y., Zhang, Y., Xu, C. G., & Xia, Z. M. (2018). Anti-agglomerator of tetra-n-butyl ammonium bromide hydrate and its effect on hydrate-based CO2 capture. *Energies*, *11*(2), 399. https://doi.org/10.3390/en11020399

[53] Linga, P., Kumar, R., Lee, J. D., Ripmeester, J., & Englezos, P. (2010). A new apparatus to enhance the rate of gas hydrate formation: Application to capture of carbon dioxide. *International Journal of Greenhouse Gas Control*, *4*(4), 630-637.https://doi.org/10.1016/j.ijggc.2009.12.014

[54] Yang, M., Jing, W., Zhao, J., Ling, Z., & Song, Y. (2016). Promotion of hydrate-based CO2 capture from flue gas by additive mixtures (THF (tetrahydrofuran)+ TBAB (tetra-n-butyl ammonium bromide)). *Energy*, *106*, 546-553. https://doi.org/10.1016/j.energy.2016.03.092

[55] He, J., Liu, Y., Ma, Z., Deng, S., Zhao, R., & Zhao, L. (2017). A literature research on the performance evaluation of hydrate-based CO2 capture and separation process. *Energy Procedia*, *105*, 4090-4097. https://doi.org/10.1016/j.egypro.2017.03.867

[56] Engineering toolbox (2003). Critical temperatures and pressures for some common substances. Available: https://www.engineeringtoolbox.com/gas-critical-temperature-pressure-d_161.html

[57] Race, J. M., Wetenhall, B., Seevam, P. N., & Downie, M. J. (2012). Towards a CO 2 pipeline specification: defining tolerance limits for impurities. *Journal of Pipeline Engineering*, *11*(3).

[58] Chapoy, A., Burgass, R., Tohidi, B., Austell, J. M., & Eickhoff, C. (2011). Effect of common impurities on the phase behavior of carbon-dioxide-rich systems: Minimizing the risk of hydrate formation and two-phase flow. *SPE Journal*, *16*(04), 921-930. https://doi.org/10.2118/123778-PA

[59] Carneiro, J.; Boavida, D. (2013) 'Ktejo and COMET projects towards a CCS Roadmap in Portugal'. Expert Meeting – CCS in Portugal and Norway, Towards Future Cooperation 2013-2015. LNEG, Universidade de Évora.

[60] Vangkilde-Pedersen, T., Anthonsen, K. L., Smith, N., Kirk, K., van der Meer, B., Le Gallo, Y., ... & Dalhoff, F. (2009). Assessing European capacity for geological storage of carbon dioxide–the EU GeoCapacity project. *Energy Procedia*, *1*(1), 2663-2670. https://doi.org/10.1016/j.egypro.2009.02.034

[61] Directive 2009/31/EC (2009) 'On geological storage of carbon dioxide'. European Parliament and of the Council of 23 April 2009 and Regulation (EC) No 1013/2006.

[62] Rochelle, C. A., Camps, A. P., Long, D., Milodowski, A., Bateman, K., Gunn, D., ... & Rees, J. (2009). Can CO2 hydrate assist in the underground storage of carbon dioxide?. *Geological Society, London, Special Publications*, *319*(1), 171-183. https://doi.org/10.1144/SP319.14

[63] Observatório da Energia, DGEG, ADENE. (2019). Energia em Números - Edição 2019. Portugal. ISBN: 978-972-8646-76-9.

[64] Bernardo J. PNEC 2030 – Plano Nacional da Energia e Clima – Sessão de Apresentação. Directorate General for Energy and Geology. (2019)

[65] APA (2019). Plano Nacional Energia e Clima 2021-2030 (PNEC 2030). Portugal: APA.

[66] Fundação da Ciência e Tecnologia, Laboratório Nacional da Energia e Geologia, Universidade de Évora. (2015) Captura e armazenamento de CO2 em Portugal; uma ponte para uma economia de baixo carbono. Portugal.

[67] EDP, (2009-2018). Declaração ambiental; central termoelétrica de Sines. Portugal: EDP – gestão da produção de energia S.A.

[68] EDP, (2008-2018). Declaração ambiental; central termoelétrica do Ribatejo. Portugal: EDP – gestão da produção de energia S.A.

[69] Net4Co2. (2020). 'Mission'. Available: https://www.net4co2.pt/p130-mission--en

[70] Net4CO2. (2020). 'Technology; CO2 Capture'. Available: https://www.net4co2.pt/p138-co2-capture-en

[71] LSRE-LCM. (2009) NETmix – A novel network static mixer and reactor. Available: https://lsre-lcm.fe.up.pt/projects/24

[72] Lopes, José; Dias, Madalena; et al. (2013). 'The NETmix recator: pressure drop measurements and 3D CFD modelling'. Chemical Engineering Research and Design nr.91: 2250-2258. DOI: 10.1016/j.cherd.2013.07.014

[73] ISO 14040:2006(E)

[74] ISO 14044:2006 (E)

[75] Marx J., Schreiber A., Zapp P., Fr Hake J. (2010). Environmental Evaluation of CCS using Life Cycle Assessment (LCA). Paris, France: IEAGHG.

[76] Sathre, R., Chester, M., Cain, J., & Masanet, E. (2012). A framework for environmental assessment of CO2 capture and storage systems. *Energy*, *37*(1), 540-548. https://doi.org/10.1016/j.energy.2011.10.050

[77] Schreiber, A., Zapp, P., Markewitz, P., & Vögele, S. (2010). Environmental analysis of a German strategy for carbon capture and storage of coal power plants. *Energy Policy*, *38*(12), 7873-7883. https://doi.org/10.1016/j.enpol.2010.09.006

[78] Volkart, K., Bauer, C., & Boulet, C. (2013). Life cycle assessment of carbon capture and storage in power generation and industry in Europe. *International Journal of Greenhouse Gas Control*, *16*, 91-106. https://doi.org/10.1016/j.ijggc.2013.03.003

[79] Wildbolz, C. (2007). Life cycle assessment of selected technologies for CO2 transport and sequestration. *Swiss Federal Institute of Technology*.

[80] Andersson, V., Kv, A., & Haines, M. (2005). Gas hydrates for deep ocean storage of CO2-Novel technology for utilising hydrates for transport of CO2. In *Greenhouse Gas Control Technologies 7* (pp. 1487-1492). Elsevier Science Ltd. https://doi.org/10.1016/B978-008044704-9/50169-5

[81] Drauker, L. C., James III PhD, R. E., Bromiley, R., & Skone, T. J. (2010). *Life Cycle Analysis: Existing Pulverized Coal (EXPC) Power Plant* (No. DOE/NETL-403/110809). NETL.

[82] Goedkoop M., Oele M., Leijting J., et al. (2016). Introduction to LCA with SimaPro. The Netherlands: PRé Consultants.

[83] Schori S., Frischkenecht R., (2012). Life Cycle Inventory of Natural Gas Supply. Swiss Federal Office of Energy SFOE: ESU-services Ltd

[84] Faist Emmenegger M., Del Duce A., Moreno Ruiz E., Brunner F., (2017). Update of the European natural gas supply chains. Zürich, Switzerland: Ecoinvent.

[85] EDP (2018). Central Termoelétrica de Sines; Processos tecnológicos/operações unitárias envolvidos. Portugal: EDP S.A.

[86] Clavreul, J., Guyonnet, D., & Christensen, T. H. (2012). Quantifying uncertainty in LCA-modelling of waste management systems. *Waste Management*, *32*(12), 2482-2495. https://doi.org/10.1016/j.wasman.2012.07.008

[87] DGEG, (2019). Energia em Portugal – annual reports (2013, 2014, 2015, 2016, 2019). Directorate General of Energy and Geology, Portugal.

[88] Safaei A., Freire F., Henggeler Antunes C., (2015). Life-Cycle Greenhouse Gas Assessment of Nigerian Liquefied Natural Gas Addressing Uncertainty. Environmental Science & Technology (3949-3957).

[89] Eni (2020). Environment and territory – Gas flaring and gas venting. Available: http://www.eniscuola.net/en/argomento/natural-gas1/environment-and-territory1/gas-flaring-and-gas-venting/

[90] Dieken, D. (1998). Gas turbine fire protection. *Power Engineering*, *102*(4), 44-48.

[91] Faist Emmenegger M., Del Duce A., Zah R. (2015). Update and extension of the inventory data for energy gases. Federal Office for the Environment (FOEN): Quantis.

[92] Meili C., Jungbluth N., Annaheim J., (2018). Life cycle inventories of crude oil extraction. Switzerland: ESU-services Ltd, Schaffhausen.

[93] Faist Emmenegger M., Moreno Ruiz E. (2018). Ecoinvent 3.6 dataset documentation; natural gas production, liquefied – RME. Ecoinvent Centre.

[94] Brito A., Alves J., Lopes F., (2019). 'De onde vem a energia que move o país – Energia do Futuro.' Portugal: Público, REN. Available: https://www.publico.pt/2019/11/12/infografia/onde-vem-energia-move-pais-384%20

[95] Countries of the world (2017). North Africa Pipelines map - Crude Oil (petroleum) pipelines - Natural Gas pipelines - Products pipelines. Available: https://theodora.com/pipelines/north_africa_oil_gas_products_pipelines_map.html

[96] Ouki M., (2019). Algerian Gas in Transition: domestic transformation and changing gas export potential. The Oxford Institute for Energy Studies, University of Oxford.

[97] Sea Routes. Available: https://www.searoutes.com/routing?speed=13&panama=true&suez=true&kiel=true&rivers=block&roads=block

[98] Faist Emmenegger M., Del Dulce A., Zah R (2019). Ecoinvent 3.6 dataset documentation; Transport, pipeline, onshore, long distance, natural – DZ. Ecoinvent Centre.

[99] APA (2017). Licença Ambiental nº. 667/0.0/2017; EDP – Gestão da Produção de Energia, S.A. Amadora, Portugal: Agência Portuguesa do Ambiente.

[100] Carras J., Franklin P., IPCC, (2006). Guidelines for National Greenhouse Gas Inventories – Coal mining. Chapter 4: Fugitive emissions.

[101] EPA (2019) Colombia Coal Mine, Methane Market Study. EPA Publication No: 430R19002.

[102] Eurostat database (2020). Your key to European statistics - Imports of solid fossil fuels by partner country (nrg_ti_sff). Available: https://ec.europa.eu/eurostat/data/database

[103] Eurostat (2019). Energy production and imports. Available: https://ec.europa.eu/eurostat/statistics-explained/index.php/Energy_production_and_imports#The_EU_and_its_Member_States_are_all_net_importers_of_energy

[104] Greeshma U., Annalakshmi S. (2015) Artificial Neural Network. International Journal of Scientific & Engineering Research, vol.6, Issue 4.

[105] Andrew T. (2017) 'The mostly complete chart of Neural Networks, explained'. Towards data science. Available: https://towardsdatascience.com/the-mostly-complete-chart-of-neural-networks-explained-3fb6f2367464

[106] missinglink.ai (2020). '7 Types of Neural Network Activion Functions: How to choose?' Available: https://missinglink.ai/guides/neural-network-concepts/7-types-neural-network-activation-functions-right/

[107] Sines (2020) 'Factos e Números'. Available: http://www.sines.pt/pages/310

[108] Ecoinvent (2012). Ecoinvent 3.6 dataset documentation: tap water production, conventional treatment – Europe without Switzerland.

[109] Hatakeyama T., Aida E., Yokomori T. et al. (2009). Fire extinction using carbon dioxide hydrate. Industrial & Engineering Chemistry Research, n.°48 (4083-4087). https://doi.org/10.1021/ie8019533

[110] Metz, B., Davidson, O., De Coninck, H., Loos, M., Meyer, L., Intergovernmental Panel on Climate Change, (2005), "Chapter: Transport; IPCC Special Report on Carbon Dioxide Capture and Storage.". New York, NY, USA.

[111] IPMA (2020). Temperatura média do solo a 5 cm (observações nas estações automáticas). Available: https://www.ipma.pt/pt/agrometeorologia/mapas/diario/index.jsp?page=dts5_co.xml

[112] Hirschberg, S., Wiemer, S., & Burgherr, P. (Eds.). (2014). *Energy from the Earth: Deep Geothermal as a Resource for the Future?* (Vol. 62). vdf Hochschulverlag AG.

[113] Metz, B., Davidson, O., De Coninck, H., Loos, M., Meyer, L., Intergovernmental Panel on Climate Change, (2005), "Chapter: Transport; IPCC Special Report on Carbon Dioxide Capture and Storage.". New York, NY, USA.

[114] Tian, L., Yang, Z., Jung, B., Joodaki, S., Erlström, M., Zhou, Q. and Niemi, A. (2016). Integrated 13 simulations of CO2 spreading and pressure response in the multilayer saline aquifer of South Scania 14 Site, Sweden. Greenhouse Gas Sci Technol, 6: 531–545. doi:10.1002/ghg.1583.

[115] Eurogas (2015). Eurogas Statistical Report 2015.

[116] Oers L., Guinée J. (2016). The abiotic depletion potential: Background, Updates, and Future.

[117] Heijungs, R., Kleijn, R., 2001. Numerical approaches towards life cycle interpretation – five examples. International Journal of Life Cycle Assessment 6, 141–148. https://doi.org/10.1007/BF02978732

[118] USGS – U.S. Geological Survey. World Coal Quality Inventory. Available: https://www.usgs.gov/centers/eersc/science/world-coal-quality-inventory.

[119] Senior C.L., Zeng T., Che J., Ames M.R., Saforim A.F. et al. (2000) Distribution of trace elements in selected pulverized coals as a function of particle size and density. Fuel Processing Technology 63 (215-241) https://doi.org/10.1016/S0378-3820(99)00098-3

[120] EIA (2019). U.S. Electric Power Annual 2018 (Table 7.3. Average quality of fossil fuel receipts for the electric power industry). USA: Energy Information Administration.

[121] Odunayo, A.R., Omoniyi P., Leslie P., Olorunfemi O. (2016). Comparative chemical and trace element composition of coal samples from Nigeria and South Africa. American Journal of Innovative Research and Applied Sciences. ISSN 2429-5396.

[122] Borken-Kleefed J. (2012). Default transport data per commodity group for the US and EU27 – Methodology and notes for Ecoinvent. Ecoinvent. Switzerland: Ecoinvent Centre.

[123] Sari, Osmann; Hu, Jin; Eicher, Sara; Egolf, P. W.; and Homsy, Paul, (2008). Thermo-Physical and Flow Properties of CO2 Hydrate Slurry. *International Refrigeration and Air Conditioning Conference*. Paper 990.

[124] Matmatch (2020). 'ASTM A516 Grade 70'. Available: https://matmatch.com/materials/tjci001-a516-gr-70-steel

[125] Engineering toolbox (2010). Densities of Common Materials. Available: https://www.engineeringtoolbox.com/density-materials-d_1652.html

[126] Prospector (2020). Polyurethane (PUR) Typical Properties Generic PUR, unspecified. Available: https://plastics.ulprospector.com/generics/45/c/t/polyurethane-pur-properties-processing

Figliozzi M. A. (2017). Lifecycle modelling and assessment of unmanned aerial vehicles (drones) CO2e. Transport and Environment (vol. 57, pages 251-261). https://doi.org/10.1016/j.trd.2017.09.011

Appendixes

Appendix I – Pedigree Matrix

The figure below represents the Pedrigree Matrix scores attributed to data, as geometric standard deviation, based on the choice of the six criteria. The figure was taken from SimaPro user manual.

Score:	1	2	3	4	5
1 Reliability	Verified data based on measurements	Verified data partly based on assumptions OR non-verified data based on measurements	Non-verified data partly based on qualified estimates	Qualified estimate (e.g. by industrial expert); data derived from theoretical information (stoichiometry, enthalpy, etc.)	Non-qualified estimate
	1.00	1.05	1.10	1.20	1.50
2 Completeness	Representative data from all sites relevant for the market considered over an adequate period to even out normal fluctuations	Representative data from >50% of the sites relevant for the market considered over an adequate period to even out normal fluctuations	Representative data from only some sites (<<50%) relevant for the market considered OR >50% of sites but from shorter periods	Representative data from only one site relevant for the market considered OR some sites but from shorter periods	Representativeness unknown or data from a small number of sites AND from shorter periods
	1.00	1.02	1.05	1.10	1.20
3 Temporal correlation	Less than 3 years of difference to our reference year	Less than 6 years of difference to our reference year	Less than 10 years of difference to our reference year	Less than 15 years of difference to our reference year	Age of data unknown or more than 15 years of difference to our reference year
	1.00	1.03	1.10	1.20	1.50
4 Geographical correlation	Data from area under study	Average data from larger area in which the area under study is included	Data from smaller area than area under study, or from similar area	Data from area with slightly similar produc-tion conditions	Data from unknown OR distinctly different area (north America instead of Middle East, OECD-Europe instead of Russia)
	1.00	1.001	1.02	1.05	1.10
5 Further technological correlation	Data from enterprises, processes and materials under study (i.e. identical technology)	Data from processes and materials under study (i.e. identical technology) but from different enterprises	Data on related processes or materials but same technology. OR data from processes and materials under study but from different technology	Data on related processes or materials but different technology. OR data on laboratory scale processes and same technology	Data on related processes or materials but on laboratory scale of different technology
	1.00	1.05	1.20	1.50	2.00

Figure I-1 - Pedrigree Matrix on SimaPro. Source: [82].

Appendix II – Natural gas imports by Portugal

Table II-1 shows data of natural gas imports by Portugal in Nm^3 gathered from annual reports of Directorate General of Energy and Geology 'Energia em Portugal' [87]. Table II-2 presents the share of each exporter with the last three columns showing the average shares between 2011 and 2018, 2016 and 2018 and the shares used to model natural gas supply chain scenarios for the current study, respectively.

Table II-1 - Data of natural gas imports by Portugal from 2011 until 2016 and 2018 in Nm^3. Source: [87].

Imports in Nm3	2011	2012	2013	2014	2015	2016	2018
Norway			199913	59892	79680		78000
USA						98032	465000
Unspecified countries	406264	203600	535262	587557	77	1078037	618000
Qatar		155434	261422	515821	223875	406444	642000
Argelia	1814369	1981018	2048181	2262450	2322636	2461980	1471000
Nigeria	2719030	1756930	997069	264687	1165650	900681	2241000
Egypt		102453	69619				5515000
Spain					898523		
Trinidad e Tobago	73938	62733	167563	88550			
Total	4939663	4273373	4174199	3857970	4778991	4945174	11030000

Table II-2 - Data of natural gas imports by Portugal from 2011 until 2016 and 2018 in percentage share and the result share used to model supply chain in the last column.

Imports in %	2011	2012	2013	2014	2015	2016	2018	Av. 11-18	Av. 16-18	Result
Norway	0%	0%	5%	2%	2%	0%	1%	1%	0%	**0%**
USA	0%	0%	0%	0%	0%	2%	4%	1%	3%	**0%**
Unspecified countries	8%	5%	13%	15%	0%	22%	6%	10%	14%	**10%**
Qatar	0%	4%	6%	13%	5%	8%	6%	6%	7%	**5%**
Argelia	37%	46%	49%	59%	49%	50%	13%	43%	32%	**40%**
Nigeria	55%	41%	24%	7%	24%	18%	20%	27%	19%	**25%**
Egypt	0%	2%	2%	0%	0%	0%	50%	8%	25%	**20%**
Spain	0%	0%	0%	0%	19%	0%	0%	3%	0%	**0%**
Trinidad e Tobago	0%	2%	2%	4%	2%	0%	0%	1%	0%	**0%**

Appendix III – Natural gas supply chain sub-processes

Natural gas production at Nigeria

Table III-1 shows the LCI for natural gas production at Nigeria from a combined process with crude oil. The dataset presented is already entirely allocated to natural gas production. The allocation was based on LHV. In the original report [92], the share for allocation considering low heating value and the mass reported for each product corresponds to 75 % and 25 % for crude oil and natural gas, respectively, with exception for some features which were only allocated to crude oil production as the water consumption.

Table III-1 - Life cycle inventory for natural gas production at Nigeria. Source: ESU-services database [92].

Production of natural gas (combined with oil) at Nigeria		**4E+10**	**m3**		
	Sub-compartiment	*Atribution*	*Unit*	*Distribution*	*SD*2*
Resources					
Gas, natural/m3 'Enerdata 2016'	in ground	4E+10	m3	Lognormal	1.24
Inputs from tecnosphere: Materials/fuels					
Chemicals inorganic, at plant/GLO S 'Generic value from Jungbluth 2007 calculated for 15% instead of 3% enhanced oil recovery.'		0.000138	kg	Lognormal	1.6
Chemicals organic, at plant/GLO S 'Generic value from Jungbluth 2007 calculated for 15% instead of 3% enhanced oil recovery.'		0.000106	kg	Lognormal	1.6
Transport, lorry >16t, fleet average/RER S 'Standard distance 600km'		3.35E-05	tkm	Lognormal	2.34
Transport, freight, rail/RER S 'Standard distance 600km'		0.000146	tkm	Lognormal	2.34
Well for exploration and production, onshore/GLO/I S 'Jungbluth 2007'		1.06E-06	m	Lognormal	3.01
Production plant crude oil, onshore/GLO/I S 'Questionnaire'		3.13E-11	p	Lognormal	3.23
Platform, crude oil, offshore/OCE/I U 'Questionnaire'		1.04E-11	p	Lognormal	3.23
Transport, crude oil pipeline, onshore/RER S 'Jungbluth 2007'		1.74E-09	tkm	Lognormal	3.23
Inputs from tecnosphere: Electricity/heat					
Diesel, burned in diesel-electric generating set/GLO S 'Calculation based on literature'		0	MJ	Lognormal	2.06
Electricity, low voltage, production RER, at grid/RER S 'IOGP 2016'		0.0031	kWh	Lognormal	2.06
Heavy fuel oil, burned in industrial furnace 1MW, non-modulating/RER S 'IOGP 2016'		0	MJ	Lognormal	2.06
Sweet gas, burned in gas turbine, production/MJ/NO S 'IOGP 2016'		0.355	MJ	Lognormal	2.06

Natural gas, vented {GLO}| natural gas venting from petroleum/natural gas production | Alloc Def, S 'Generic value according to IEA 2017'		0.00365	m3	Lognormal	10.1
Natural gas, sweet, burned in production flare/m3/GLO S 'World Bank 2017'		0.000134	m3	Lognormal	1.22

Emissions to air

Methane, bromotrifluoro-, Halon 1301 'assuming 20% halon compared to Jungbluth 2007'	low. pop.	7.28E-10	kg	Lognormal	1.5
Methane, trifluoro-, HFC-23 'assuming 80% HFC-23 compared to Jungbluth 2007'	low. pop.	2.9E-09	kg	Lognormal	1.59

Emissions to water

Oils, unspecified 'IOGP 2016'	river	6.45E-07	kg	Lognormal	1.83
BOD5, Biological Oxygen Demand 'Extrapolation for sum parameter'	river	2.03E-06	kg	Lognormal	1.84
COD, Chemical Oxygen Demand 'Extrapolation for sum parameter'	river	2.03E-06	kg	Lognormal	1.84
DOC, Dissolved Organic Carbon 'Extrapolation for sum parameter'	river	5.58E-07	kg	Lognormal	1.84
TOC, Total Organic Carbon 'Extrapolation for sum parameter'	river	5.58E-07	kg	Lognormal	1.84
AOX, Adsorbable Organic Halogen as Cl 'Extrapolation for sum parameter'	river	6.65E-12	kg	Lognormal	1.84
Nitrogen 'Extrapolation for sum parameter'	river	4.98E-10	kg	Lognormal	1.84
Sulphur 'Extrapolation for sum parameter'	river	1.73E-09	kg	Lognormal	1.84
Oils, unspecified 'IOGP 2016'	ocean	2.8E-06	kg	Lognormal	1.83
BOD5, Biological Oxygen Demand 'Extrapolation for sum parameter'	ocean	8.8E-06	kg	Lognormal	1.84
COD, Chemical Oxygen Demand 'Extrapolation for sum parameter'	ocean	8.8E-06	kg	Lognormal	1.84
DOC, Dissolved Organic Carbon 'Extrapolation for sum parameter'	ocean	2.42E-06	kg	Lognormal	1.84
TOC, Total Organic Carbon 'Extrapolation for sum parameter'	ocean	2.42E-06	kg	Lognormal	1.84
AOX, Adsorbable Organic Halogen as Cl 'Extrapolation for sum parameter'	ocean	2.88E-11	kg	Lognormal	1.84
Nitrogen 'Extrapolation for sum parameter'	ocean	2.16E-09	kg	Lognormal	2.29
Sulphur 'Extrapolation for sum parameter'	ocean	7.48E-09	kg	Lognormal	2.29

Emissions to soil

Oils, unspecified 'IOGP 2016'		8.75E-06	kg	Lognormal	1.83

Waste to treatment

Low active radioactive waste/CH S 'Jungbluth 2007'	5E-10	m3	Lognormal	3.3
Disposal, municipal solid waste, 22.9% water, to municipal incineration/CH S 'Shell 2001'	9.08E-05	kg	Lognormal	1.31

Liquefied natural gas production at Nigeria

Table III-2 presents the LCI for liquefication of natural gas at Nigeria based on data from the process of 'production of liquefied natural gas, Nigeria' in ecoinvent libraries, adjusted however to include the process described above for natural gas production.

Table III-2 - Life cycle inventory for liquefied natural gas production at Nigeria.

Production of liquefied natural gas at Nigeria		**0.987**	**m^3**		
	Sub-compartiment	*Atribution*	*Unit*	*Distribution*	*SD*2*
Inputs from tecnosphere: Materials/fuels					
Natural gas processing plant {GLO}| production | Alloc Def, S Estimation for infrastructure.		7.89E-13	p	Lognormal	1.76
Natural gas, burned in gas motor, for storage/DZ S Based in a gas consumption rate of 10,3% and the LHV of DZ natural gas (38,5 MJ/m3).		3.97	MJ	Lognormal	1.02
Production of natural gas, combined with oil (Nigeria) Allocation based on LHV. The volumes are in PTN.		0.987	m^3	Lognormal	2.34
Transport, natural gas, onshore pipeline, long distance. DZ /S Standard distance of 100 km for 75 % of the natural gas being produced (onshore production), considering a density of 0.78 kg/m^3. Pedigree matrix: (5;na;na;na;na)		0.577	tkm	Lognormal	1.5
Waste to treatment					
Waste, natural gas sweet, for burning at production flare {GLO} BAsed on flaring rate of 0.5% and the LHV of RME natural gas (37.5MJ/m3).					

Liquefied natural gas production at Egypt

Table III-3 presents the LCI for liquefication of natural gas at Egypt based on data from the process of 'production of liquefied natural gas, Algeria' in ecoinvent libraries.

Table III-3 - Life cycle inventory for liquified natural gas production at Egypt.

Production of liquefied natural gas at Egypt		**0.987**	**m^3**		
	Sub-compartiment	*Atribution*	*Unit*	*Distribution*	*SD*2*
Inputs from tecnosphere: Materials/fuels					
Natural gas processing plant {GLO}| production | Alloc Def, S Estimation for infrastructure.		7.89E-13	p	Lognormal	1.76
Natural gas, burned in gas motor, for storage/DZ S Based in a gas consumption rate of 10,3% and the LHV of DZ natural gas (38,5 MJ/m3).		3.97	MJ	Lognormal	1.02
Natural gas, at production/DZ S		0.987	m^3	Lognormal	1.11

Transport, natural gas, onshore pipeline, long distance. DZ /S	0.7699	tkm	Lognormal	1.5
Standard distance of 100 km considering a density of 0.78 kg/m³. Pedigree matrix: (5;na;na;na;na)				

Waste to treatment

Waste, natural gas sweet, for burning at production flare {GLO}
BAsed on flaring rate of 0.5% and the LHV of RME natural gas (37.5MJ/m3).

Liquefied natural gas production at Qatar

Table III-4 presents the LCI for liquefication of natural gas at Qatar based on data from the process of 'production of liquefied natural gas, Region of Middle East' available in ecoinvent 3.6 dataset documentation.

Table III-4 - Life cycle inventory for liquefied natural gas prodcution at Qatar.

Production of liquefied natural gas at Qatar (RME)		**0.962**	**m³**		
	Sub-compartiment	*Atribution*	*Unit*	*Distribution*	*SD*2*
Inputs from tecnosphere: Materials/fuels					
Natural gas processing plant {GLO}| production | Alloc Def, S		7.89E-13	p	Lognormal	1.76
Estimation for infrastructure.					
Natural gas, burned in gas motor, for storage/GLO S		3.86	MJ	Lognormal	1.02
Based on a gas consumption rate of 10.3% and the LHV of RME natural gas (37.5 MJ/m3).					
Natural gas, high pressure {RoW}| natural gas production | Alloc Def, S		0.962	m³	Lognormal	1.11
Scaled to LHV of ecoinvent v3. [Activity link to "natural gas production, GLO" introduced for v3.5 to connect directly to a supplying activity and thereby also avoiding supply from markets for natural gas (high pressure) in which evaporation might contribute].					
Transport, natural gas, onshore pipeline, long distance. DZ /S		0.7504	tkm	Lognormal	1.5
Standard distance of 100 km considering a density of 0.78 kg/m³. Pedigree matrix: (5;na;na;na;na)					
Waste to treatment					

Waste to treatment

Waste, natural gas sweet, for burning at production flare {GLO}	0.188	MJ
BAsed on flaring rate of 0.5% and the LHV of RME natural gas (37.5MJ/m3).		

Onshore pipeline transport on RER, w/o DE+NL+RU

The LCI used to model the process of onshore pipeline transportation of the natural gas in Spain and Portugal was adapted from Ecoinvent 3.6 documentation and is described in Table III-5. The purpose for modelling it was due the fact that [91] had reported an update value for leakage rates for Western Europe.

Table III-543 - Life cycle inventory for the natural gas transportation by onshore pipelines in western Europe.

Transport, pipeline onshore, natural gas {RER w/o DE+NL+RU}		**1**	**tkm**		
	Sub-compartiment	*Atribution*	*Unit*	*Distribution*	*SD*2*
Inputs from tecnosphere: Materials/fuels					
Natural gas, high pressure {ES}| market for | Alloc Def, S		0.000237	m3	Lognormal	1.06
Pipeline, natural gas, long distance, low capacity, onshore/GLO/I S		2.38E-09	km	Lognormal	1.04
Inputs from tecnosphere: Electricity/heat					
Electricity, medium voltage {RoW}| natural gas, burned in gas turbine, for compressor station | Alloc Def, S		0.0725	kWh	Lognormal	1.75
Emissions to water					
Butane	low. pop.	4.75E-07	kg	Lognormal	1.43
Carbon dioxide, fossil	low. pop.	1.42E-06	kg	Lognormal	1.11
Ethane	low. pop.	6.18E-06	kg	Lognormal	1.43
Mercury	low. pop.	2.37E-12	kg	Lognormal	2.27
Methane, bromochlorodifluoro-, Halon 1211	low. pop.	2.24E-08	kg	Lognormal	1.22
Methane, chlorodifluoro-, HCFC-22	low. pop.	6.93E-08	kg	Lognormal	1.22
Methane, fossil	low. pop.	0.000166	kg	Lognormal	1.43
NMVOC, non-methane volatile organic compounds, unspecified origin	low. pop.	2.38E-07	kg	Lognormal	1.47
Propane	low. pop.	1.42E-06	kg	Lognormal	1.43
Final waste flow					
Oil waste		1.16E-06	kg	Lognormal	1.43

Natural gas supply chain results analysis and comparison with RER average processes

The following table shows the environmental load for each impact category related to 1 m^3 of 'natural gas at use on NGPP', modelled in the current assessment, and the same results for the 'natural gas at use in European Region (RER)', an average process available in Ecoinvent libraries. The last one, accounts for a major share in all impact categories. Due the fact that 24 % of the NG consumed in Europe comes from Russian federation, longer distances along pipelines network, which results in more consumption of raw materials, more leakages and emissions, could explain such differences. As a matter of fact, Figure 1 represents the allocation of each impact category within the sub-processes involved, and as one may observe, the transport of natural gas via pipeline (which is also presented in the processes of LNG production in Qatar, Egypt and Nigeria, along a standard length of 100 km) scores a load for each of them. Moreover, the process modelled accounts the update for the leakage rate reported in [91], from 0.026 % per 1000 km to 0.019 %. The network of pipelines modelled for Spain and Portugal (with the leakage rate of 0.019 %) represents 103 % of the network length modelled for Algerian pipelines and yet, the GWP load for NG transportation (related to methane emissions) is 4 % lower. Besides, the NG produced in Russian Federation is sour [83], which implies higher environmental loads on processing steps, especially regarding categories related to toxicity and ecotoxicity. GWP would be highly penalized if flaring occurs, however, in [83] is reported that, natural gas in Russian Federation is mainly explored from gas fields, instead of being explored in combination with crude oil, thus flaring is unlikely.

Table 44 - Scores for each impact category of NG supply chain.

Impact category	Unit	Natural gas at use on NGPP 1 m^3	Natural gas at use in RER 1 m^3	RER/NGPP
Abiotic depletion	kg Sb eq	7.09E-08	1.76E-07	248%
Abiotic depletion (fossil fuels)	MJ	4.64E+01	4.65E+01	100%
Global warming (GWP100a)	kg CO2 eq	5.29E-01	5.38E-01	102%
Ozone layer depletion (ODP)	kg CFC-11 eq	1.17E-07	4.08E-07	348%
Human toxicity	kg 1,4-DB eq	4.71E-02	1.04E-01	220%
Fresh water aquatic ecotox.	kg 1,4-DB eq	2.81E-02	8.67E-02	308%
Marine aquatic ecotoxicity	kg 1,4-DB eq	7.80E+01	2.92E+02	375%
Terrestrial ecotoxicity	kg 1,4-DB eq	4.17E-04	6.46E-04	155%
Photochemical oxidation	kg C2H4 eq	8.61E-05	2.00E-04	232%
Acidification	kg SO2 eq	1.45E-03	2.81E-03	194%
Eutrophication	kg PO4--- eq	2.50E-04	5.08E-04	203%

Besides the differences in pipeline transport, longer distances of LNG transportation through maritime routes, could also explain the higher environmental load of NG at use in RER, as maritime routes can be longer: from Middle East and North Africa until the most important maritime ports in Europe located in North Sea.

However, the impacts are also a function of the mass transported and the, besides the amount the European consumption of NG sourced in Middle East (8 %) being somewhat similar to the proportion simulated for NGPP (5 %), NG sourced in Nigeria and North Africa (20 %) is far less than the amounts sourced in Russian Federation and Europe together (78 %), which transportation occurs mainly via pipeline. Besides, a significant part of the NG sourced in North Africa (12 %) is also transported by pipeline. This can also be supported on the fact that the less penalised impact categories – GWP and Eutrophication - are the ones with a major contribution of LNG transportation in the supply chain modelled (Figure III-1).

GWP is the less penalised impact category. Figure III-1 shows that the processes which represent a major contribute to the GWP for the supply chain modelled, are the transport of LNG in a freight ship and liquified natural gas production in Egypt and Nigeria. Besides, the explained relation with LNG transportation, natural gas flaring is an activity inherent to the NG exploration in Nigeria and is responsible for freeing significant amounts of CO_2 equivalent emissions.

In Figure III-2, one can also conclude that the allocation of each impact category to the different sub-processes is especially different for Ozone Layer Depletion (ODP), for which the major contributors are transport of NG by pipeline and LNG production in Egypt. The emissions of CFC equivalents during pipeline transportation are mainly related to the emission of Halons 1211, 1301 and HCFC-22. Those emissions are associated to leakages on refrigeration systems [83] and the use of Halon 1301 for fire control during flaring processes that may occur for reducing methane when venting is needed for safety reasons [90] and also during natural gas production.

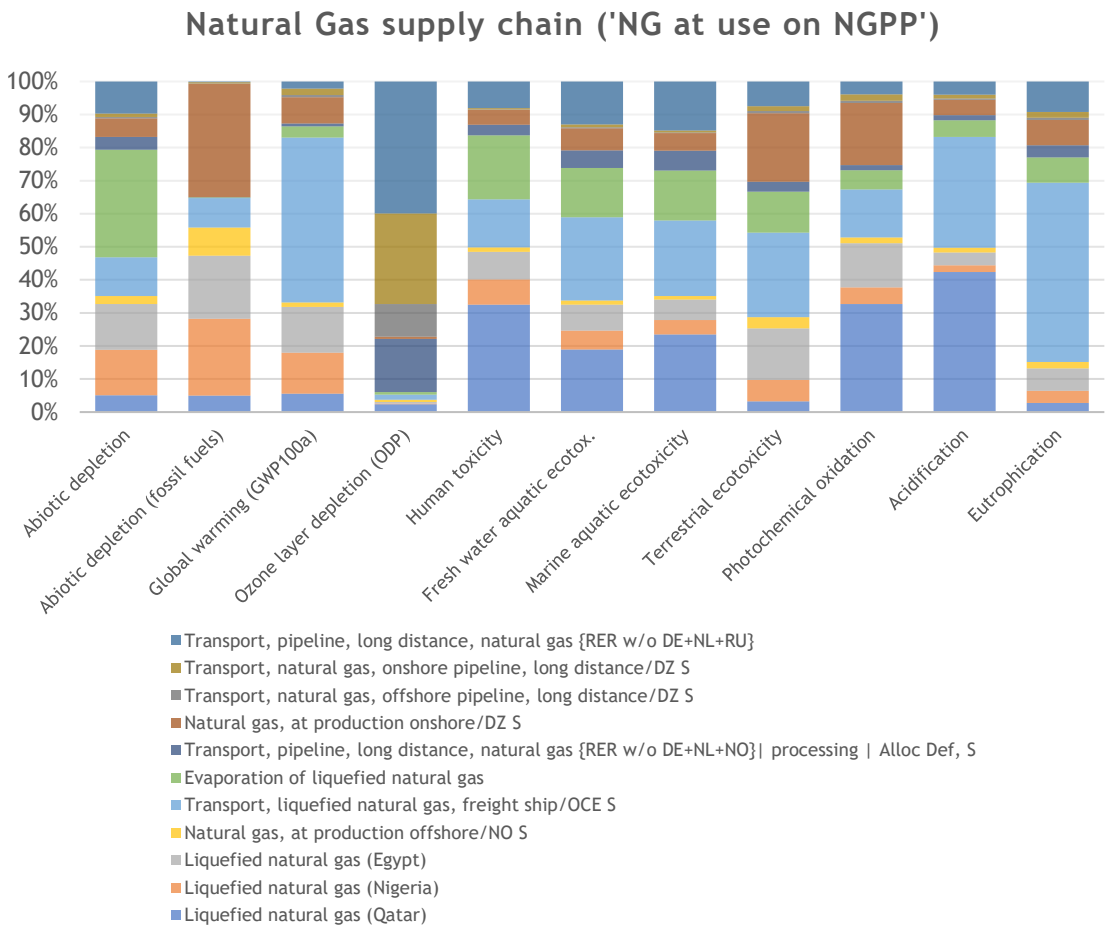

Figure III-1 - Impacts characterization within the different sub-processes of natural gas supply chain modelled in the current assessment, representing the 'Natural gas at use on NGPP'.

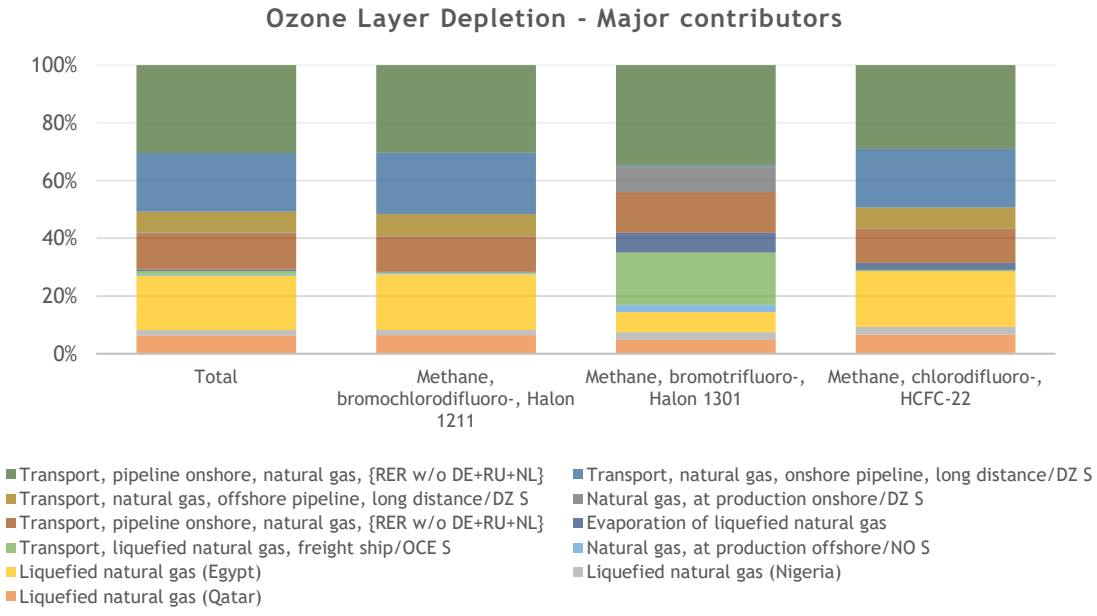

Figure III-2 - Characterization of ozone layer depletion (ODP) in NG supply chain.

Appendix IV – Distances for natural gas transportation

In the following table the distances for pipeline transportation from Algeria to Portugal are presented and the estimated distances for maritime routes from Qatar and Nigeria to Portugal [97] are also shown. The data for pipelines length was taken from Theodora database [95] and some missing data was estimated on google maps with measuring tool, while reproducing the pipeline network presented in Figures 1 and 2. The distances for maritime routes was also measured on Google Earth based on typical trading routes between the countries and reported in [97] (Figure 3 and 4).

Assumptions

1. Some pipeline lengths and marine routes were estimated by measuring on Google Earth.
2. For Qatar, Egypt and Nigeria (to the 75 % of offshore production), a standard distance of 100 km was considered, between processing plants and liquefication plants in seashore.
3. To model the supply chain from Algeria to Portugal, Hassi R'Mel was assumed as the field in which the imported NG is produced, as it is the most important field in Algeria [96].

Table IV-1 - Distances for pipeline and freight ship transporattion of natural gas.

Mean of transport.	Location	Start Point	End Point	Distance (km)	Source
Pipeline	Argelia	Hassi R'Mel	Arzew	440	estimated distance
		Arzew	Beni Saf	110	estimated distance
	Argelia - Spain	Beni Saf	Almeria	200	[81]
	Spain	Almeria	Cordoba	280	estimated distance
		Cordoba	Campo Major	191	[81]
	Spain-Portugal	Campo Maior	Leiria	219	[81]
	Portugal	Leiria	Lisboa (Carregado)	85	estimated distance
		Total distance from Algeria		1525	calculated
		Sines	Lisboa (Carregado)	209	[81]
Freight ship	Qatar,Egypt-Portugal	Dohra	Sines	11000	estimated distance
	Nigeria-Portugal	Nigeria	Sines	6500	estimated distance
	Unspecified offshore production			5000	standard distance
		Total distance by ship		22000	calculated

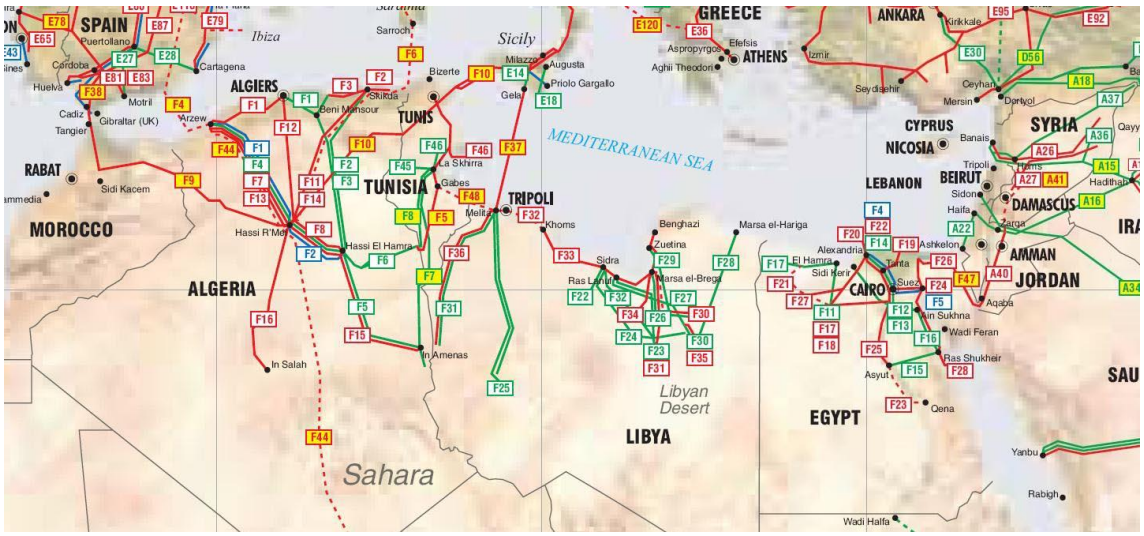

Figure IV-1 - Pipelines network for natural gas (red), and oil (green) transport in North Africa countries. Source: Theodora database [95].

Figure IV-2 - Pipelines network for natural gas (red), oil (green) and products (blue) transport and supply in Portugal and Spain. Source: Theodora database [95].

Figure IV-3 - The itinerary for maritime route from Nigeria to Portugal on google maps.

Figure IV-4 - The itinerary for maritime route from Qatar and Egypt to Portugal on google maps.

Appendix V – Natural gas powerplant data processing

The data used to estimate raw materials consumption and emissions was supported on a series of annual historical data (from 2008 to 2018) taken from environmental reports published by EDP, SA under EMAS industrial ecology certification program. Table 1 shows the raw data gathered from such reports.

Table V-1 - Raw data gathered from EDP's environmental reports.

		2008	2009	2010	2011	2012	2013	2014	2015	2016	2017	2018
Generated energy	MWh	7648987	5965231	3206573	1151870	251246	242661	250031	782890	1706822	2637446	2420079
Energy consumption	MWh	168459	147627	104957	5261	22068	20323	21216	35364	58800	78310	74260
Inputs												
Fuel (NG)	Nm3	1244101265	986634351	537568382	195472733	44373886	44273267	47108678	135023926	292109	443543	400216
Fuel (gasóleo)	ton	7.3	5.6	4.6	4.7	4.7	5.1	4.7	5.3	5.3	5.2	3.4
Hydrochloric acid	kg	1681840	1501300	544120	176050	62290	24660	99570	127350	285180	538900	401300
Sodium hypochlorite	kg	867310	828890	421830	181790	90030	50410	95040	291330	447480	555220	413200
Iron chloride	kg	20600	16500	31300	23760	11700	1300	0	0			
Ammonia	kg	9753	10091	8423	3978	1485	495	1540	3042	6156	6156	3078
Sodium hidroxide	kg	6300	19600	30000	20000	6000	0	12000	6000	10500	16500	12000
Hydrazine	kg	380	720	1380	540	1680	960	0	0			
Carbohydrazide	kg						2200	0	400			
Water	m3	5448591	4441602	2433423	908833	247103	238652	254879	627615	2194926	3634831	3372303
(Tejo river)										2047546	3464860	3354069
(groundwater)										147380	169971	18234
Outputs												
Gasuous emissions												
NOx	ton	4325	2929	382	173	36	29	26	91	181	285	307
CO	ton	116	139	26	9	4	9	16	18	20	26	15
PTS	kg	17190	7570	0.1	4.1	0.08	1.2	0.3	3.3	16.1	1.6	12.5
COVs	kg	234838	98671	14969.00	1338.00	141.00	2.90	6.80	13.80	17.80	62.00	51.40
CO2	ton	2131189	2698034	1167341	426648	95502	96209	100451	290989	626115	945110	869142
Effluents	m3	7281418	5262137	2566387	959197	255302	220047	241668	438649	837512	1478689	1550265
pH	sorence	7.5	7.5	7.44	7.63	7.74	7.53	7.67	7.68	7.78	7.6	7.6
Ammoniacal nitrogen	mg NH4/L	1.33	1.16	1.74	1.75	0.75	0.65	0.65	1.08	0.86	1.61	0.61
Total nitrogen	mg N/L	3.04	3.23	3.33	2.53	1.99	1.9	2.1	2.72	2.78	3.80	0.88
Biological oxygen demand	mg O2/L	3.34	6.76	4.13	4.61	5.19	3.48	2.7	2.48	3.53	6.03	2.33
Chemical oxygen demand	mg O2/L	23.65	25.18	23.92	19.03	18.93	17.72	14.93	17.37	21.23	29.65	7.21
Residual chlorine free	mg Cl/L	0.09	0.07	0.07	0.091	0.05	0.05	0.05	0.05	0.04	0.01	0.03
Residual chlorine total	mg Cl/L	0.26	0.13	0.13	0.12	0.08	0.07	0.1	0.06	0.09	0.06	0.05
Total phosphorus	mg P/L	1.4	0.55	0.33	0.26	0.34	0.23	0.96	0.26	0.23	0.18	0.10
Oils and fats	mg/L	0.39	0.55	0.66	0.82	0.15	0.3	0.25	0.29	0.62	0.80	0.65
Hydrocarbons	mg/L	0.3	0.41	0.45	0.53	0.06	0.1	0.25	0.16	0.39	0.63	0.28
Detergents	mg LAS/L	0.03	0.05	0.05	0.05	0.03	0.03	0.03	0.03	0.03	0.42	0.21
Total suspended solids (105ºC)	mg/L		31	14.8	10.5	10.77	6.13	5.6	6.37	10.02	0.05	0.02

		2008	2009	2010	2011	2012	2013	2014	2015	2016	2017	2018
						Outputs						
Wastes	kg	161287	184847	250071	66395	110234	37276	29664	103165	118043	110851	604487
Hazardous waste	kg	11339	21317	20886	3675	5924	3826	10784	5955	50405	14560	41910
Non-hazardous waste	kg	149948	163530	229185	62720	104310	33450	18880	97210	67638	96292	562577
Valorised (recycle+recovery)	kg	60021	147052	229776	59815	106204	33506	28304	101965	69394	49891	60364

The data processing comprised four main steps:

1. Identify raw materials which use was discontinued (iron chlronide, hydrazine and carbohydrazide) and if any eventual unit/process modification could interfere with powerplant's emissions.
2. Identifying missing values or values that shouldn't be used for predicting models' due processes paradigm changes.
3. Estimate the missing values.
4. Verify the quality of different standard regressions available in Excel between the total electricity produced with each parameter (for the emissions the correlations were verified in concentration and in total emitted mass).
5. Verify the ratio between the average for the parameters with a R squared bellow 0.8 with the standard deviation (sample).
6. Decide which method should be applied for predicting both raw materials consumption and process emissions.

The results from each step of the aforementioned procedure:

1. Iron chlorine, hydrazine and carbohydrazide were discontinued. Therefore, they were disregarded from the study. No events which could affect operations emissions were reported. However, in the last document from 2018, it is reported that some sampling anomalies on the wastewater monitoring system were identified which were preventing the normal operation of the analyser. The emission data that could be affected by such anomalies corresponds to the missing values (at yellow) for the years of 2017 and 2018.
2. The missing values are highlighted in yellow. The emissions of NOx and CO in 2008 and 2009 were reported in mass flux instead of total emitted mass, which demanded some auxiliary calculations, explained bellow. Unlikely other reports, some emissions in the wastewater for the years of 2017 and 2018 were not reported in the final effluent. Instead the concentration of each parameter was reported for wastewater from different sources, but the flow was not specified. The average of specific emissions (emission per MWh produced) from 2008 to 2016 was used to calculate these missing values.
3. *NOx and CO emissions*
   To estimate NOx and CO total emitted mass, the average of flow rate calculated for PTS and COV's emissions was assumed. Table 2 shows the data gathered from 2008 and 2009 annual reports and the further calculations. FF1, FF2 and FF3 are three sampling points in the same chimney through which the flue gas follows and frees from NG turbine after crossing the recovery boiler.

   Wastewater emissions
   After calculating the annual emitted mass, the values were divided by the power generated in each year. The average obtained for each parameter was used to calculate the emissions in kg for the missing years. The results are presented in Table 3.

Table V-2 - Calculation method to estimate missing values for NOx and CO emissions in 2008 and 2009.

Raw data									
		2008				2009			
		NOx	CO	PTS	COV	NOx	CO	PTS	COV
FF1	mg/Nm3	37.60	1.00	0.10	1.60	37.50	1.70	0.10	1.20
FF2	mg/Nm3	31.40	0.60	0.12	1.60	31.10	1.00	0.10	0.75
FF3	mg/Nm3	20.70	0.80	0.15	1.50	19.70	1.50	0.10	0.45
Mean	mg/Nm3	29.90	0.80	0.12	1.57	29.43	1.40	0.10	0.80
Mass	kg	-	-	17190	234838	-	-	7570	98671
Gas flow rate (Nm3/y) = Total emitted mass (kg/y) / Concentration (mg/Nm3) x 10^6									
Volume	Nm3			1.39E+11	1.50E+11			7.57E+10	1.23E+11
Average	Nm3			1.45E+11				9.95E+10	
Total emitted mass (kg/y) = Concentration (mg/Nm3) x Volume (Nm3/y) x 10^-6									
Mass	kg	4.32E+06	1.16E+05			2.93E+06	1.39E+05		

Table V-3 - Calculation method to estimate the missing values of wastewater emissions (2017 and 2018)

Effluents		**2008**	**2009**	**2010**	**2011**	**2012**	**2013**	**2014**	**2015**	**2016**	**Mean**	**SD**	**Error**
Ammoniacal nitrogen	kg/MWh	1.27E-03	1.02E-03	1.39E-03	1.46E-03	7.62E-04	5.89E-04	6.28E-04	6.05E-04	4.22E-04	9.05E-04	3.88E-04	43%
Total nitrogen	kg/MWh	2.89E-03	2.85E-03	2.67E-03	2.11E-03	2.02E-03	1.72E-03	2.03E-03	1.52E-03	1.36E-03	2.13E-03	5.62E-04	26%
Biological oxygen demand	kg/MWh	3.18E-03	5.96E-03	3.31E-03	3.84E-03	5.27E-03	3.16E-03	2.61E-03	1.39E-03	1.73E-03	3.38E-03	1.49E-03	44%
Chemical oxygen demand	kg/MWh	2.25E-02	2.22E-02	1.91E-02	1.58E-02	1.92E-02	1.61E-02	1.44E-02	9.73E-03	1.04E-02	1.66E-02	4.62E-03	28%
Total phosphorus	kg/MWh	2.48E-04	1.15E-04	1.04E-04	9.99E-05	8.13E-05	6.35E-05	9.67E-05	3.36E-05	4.42E-05	9.84E-05	6.24E-05	63%
Oils and fats	kg/MWh	1.33E-03	4.85E-04	2.64E-04	2.17E-04	3.45E-04	2.09E-04	9.28E-04	1.46E-04	1.13E-04	4.49E-04	4.14E-04	92%
Hydrocarbons	kg/MWh	3.71E-04	4.85E-04	5.28E-04	6.83E-04	1.52E-04	2.72E-04	2.42E-04	1.62E-04	3.04E-04	3.56E-04	1.79E-04	50%
Detergents	kg/MWh	2.86E-04	3.62E-04	3.60E-04	4.41E-04	6.10E-05	9.07E-05	2.42E-04	8.96E-05	1.91E-04	2.36E-04	1.37E-04	58%
Total suspended solids (105ºC)	kg/MWh	2.86E-05	4.41E-05	4.00E-05	4.16E-05	3.05E-05	2.72E-05	2.90E-05	1.68E-05	1.47E-05	3.03E-05	1.03E-05	34%

4. Results are shown in Table 5.
5. Results are shown in Table 5.
6. Results are shown in Table 5.

Some parameters (pH, ammoniacal nitrogen and chlorine free) were disregarded from the study as they were not model in SimaPro simulations. The column 'Prediction method' presents the method chosen to model/predict parameters values for each operation scenario simulated in SimaPro. All parameters were correlated to the generated power and all the tendency functions obtained with R squares above 0.80 were used. Diesel consumption and detergents concentration in the final effluent were almost constant along the time series, so that an average value was used equally for all scenarios instead. Some values were highly affecting correlations quality and were excluded (outliers). With the exception for carbon dioxide, outliers correspond to values which were calculated as an attempt to estimate the missing values. Figure 1 shows the linear tendency for carbon dioxide before (at grey) and after (at

red) outlier exclusion. It can be observed that coefficient increases only 4 percent points but the R squared gets significantly better.

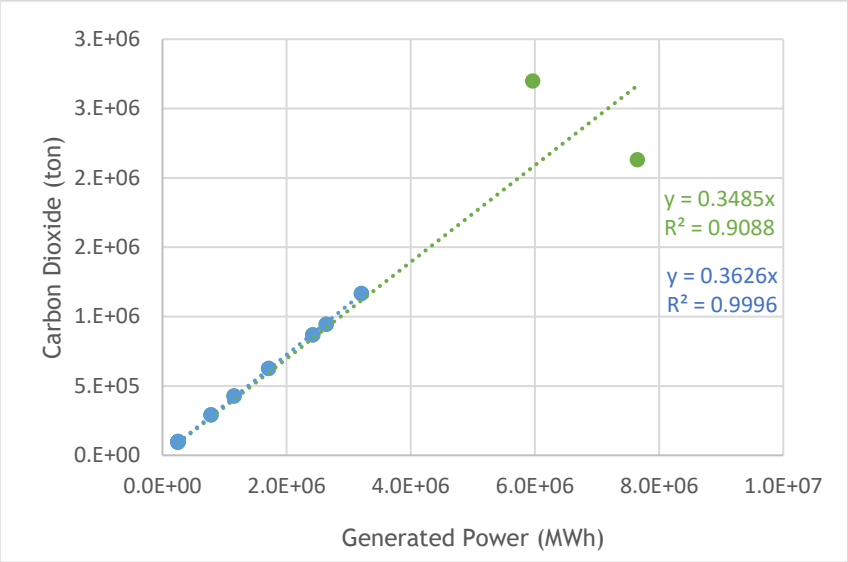

Figure V-1 - Linear regression functions to express the correlation between carbon dioxide emissions (ton) with generated power (MWh) before the exclusion of the outliers 2008 and 2009, at grey, and after, at dark red.

Determination of utilization rates

Utilization rates were important intermediary variables for data processing, as through its values is possible to estimate the number of hours the plants were operating, and in return calculate emissions flows from total emitted mass and vice-versa.

Unlike, Sines Powerplant reports, in the ones for Ribatejo, data regarding the utilization rate of plant was not provided. The utilization rates for Ribatejo were assumed to be the theorical ones, considering the operation at full load. Theoretically, the amount of electricity produced by a powerplant is obtained from its installed power, through the following expression:

$$Electricity\ capacity\ (MWh)\ =\ Installed\ power\ (MW) \times 365 \times 24$$

Then, the utilization rate is obtained through the ration between electricity produced and the electricity capacity. However, some mismatches may occur between theoretical and actual values as power groups (3 for Ribatejo powerplant) may not be simultaneously working.

Table V-4 - Results for predicting the values for each parameter for the operation scenarios tested on the simulations.

Parameter	*Unit*	*Prediction method*	*R^2*	*Mean*	*STD(av.)[18] SEE(reg.)*	*ERROR (STD/mean)*	*Outleirs excluded*
Energy consumption	MWh	Polynomial[19]	0.9405		5198		
			Inputs				
Fuel (NG)	Nm3	Linear	0.9996		29424412		
Fuel (gasóleo)	ton	Average		5.082	0.938	18%	
Hydrochloric acid	kg	Polynomial	0.9801		28480		
Sodium hypochlorite	kg	Polynomial	0.9235		43690		
Ammonia	kg	Polynomial	0.8716		524.5		
Sodium hidroxide	kg	Average		12627	8441	67 %	
Water	m3	Polynomial	0.9265		177592		
			Outputs				
Gasuous emissions							
NOx	ton	Polynomial	0.9795		65.5		2008,2009
CO	ton	Polynomial	0.8491		6.3		
PTS	kg	Polynomial[20]	0.9874		293.4		
COVs	kg	Polynomial[21]	0.9864		4172.7		
CO2	ton	Linear	0.9996		92925.4		2008,2009
Effluents	m3	Polynomial	0.9933		75030		
Total nitrogen	kg	Polynomial	0.9931		535.2		2017, 2018
Biological oxygen demand	kg	Linear	0.8408		1736.3		2017, 2018
Chemical oxygen demand	kg	Polynomial	0.994		3767.1		2017, 2018
Residual chlorine total	kg	Exponential[22]	0.9161		52.2		
Total phosphorus	kg	Exponential	0.9364		186.7		2017, 2018
Oils and fats	kg	Polynomial	9616		103.3		2017, 2018
Hydrocarbons	kg	Linear	0.9607		69.1		2017, 2018
Detergents	mg/L	Average		0.03667	0.010	27 %	2017, 2018
Total suspended solids (105ºC)	mg/L	Polynomial[23]	0.8919				2017, 2018
Wastes	kg	Average		117183	67571	58%	2018
Hazardous waste, unspecified treatment	kg	Average of proportion of total produced waste (10 %)					
Hazardous waste, recovery	kg	Average of proportion of total produced waste (5 %)					
Non-hazardous waste, unspecified treatment	kg	Average of proportion of total produced waste (20 %)					
Non-hazardous waste, recovery	kg	Average of proportion of total produced waste (65 %)					

[18] Standard deviation for sample sizes.
[19] This correlation does not cross the intersection (y=a*x+b). Parameter 'b' can be interpreted as the surplus energy required for each starting batch.
[20] For a range of energy produced generated negative values. For the scenarios ?? the minimum value reported in the original dataset was used.
[21] (9)
[22] Does not cross intersection.
[23] Does not cross intersection.

Table V-5 - Entries for Ribatejo (NG) powerplant LCI among different operation scenarios.

		Averg. (2016-2018)	Averg. (2016-2018) - 20%	Averg. (2016-2018) +20%	Aver. +40 %	Aver. +60 %	Aver. +80 %	Aver. +100 %	Aver. +200 %	Comparison base
Energy	GWh	2255	1804	2706	3157	3608	4059	4510	6764	8713
Utilization rate	%	22%	18%	26%	31%	35%	39%	44%	66%	85%
Functioning hours	h	1917	1534	2301	2684	3068	3451	3835	5752	7409
CO2 flow	ton/h	426	426	426	426	426	426	426	426	426
Reference Flows										
Generated energy	MWh	2.26E+06	1.80E+06	2.71E+06	3.16E+06	3.61E+06	4.06E+06	4.51E+06	6.76E+06	8.71E+06
Energy Consumption (by powerplant operation)	MWh	6.90E+04	5.68E+04	8.03E+04	9.09E+04	153998.658	153991.168	153992.168	153993.168	153994.168
Consumption by HGtS unit opeartion	MWh	83474	66797	100195	116872	133593	150271	166991	250465	322618
Balance w/capture	MWh	2171526	1737203	2605805	3040128	3474407	3908729	4343009	6513535	8390382
Hydrate formed	ton	6456161	5166276	7749414	9039299	10332552	11622437	12915690	19371851	24952373
Inputs										
Fuel (NG)	Nm3	3.71E+08	2.97E+08	4.46E+08	5.20E+08	5.94E+08	6.68E+08	7.43E+08	1.11E+09	1.43E+09
Fuel (gasóleo)	ton	5.08E+00	6.08E+00	7.08E+00	8.08E+00	9.08E+00	1.01E+01	1.11E+01	1.21E+01	1.31E+01
Hydrochloric acid	kg	4.23E+05	3.32E+05	5.18E+05	6.15E+05	7.16E+05	8.21E+05	9.28E+05	1.51E+06	2.09E+06
Sodium hypochlorite	kg	4.51E+05	3.69E+05	5.29E+05	6.02E+05	6.72E+05	7.38E+05	8.00E+05	1.05E+06	1.18E+06
Ammonia	kg	5.97E+03	4.94E+03	6.92E+03	7.79E+03	8.58E+03	9.29E+03	9.91E+03	1.18E+04	1.18E+04
Sodium hidroxide	kg	1.26E+04	1.26E+04	1.26E+04	1.26E+04	1.26E+04	1.26E+04	1.26E+04	1.26E+04	1.26E+04
Water	m3	2.49E+06	2.05E+06	2.89E+06	3.25E+06	3.59E+06	3.89E+06	4.16E+06	5.02E+06	5.10E+06
(from river)	m3	2.36E+06	1.95E+06	2.74E+06	3.09E+06	3.41E+06	3.69E+06	3.95E+06	4.77E+06	4.85E+06
(from ground)	m3	1.24E+05	1.03E+05	1.44E+05	1.63E+05	1.79E+05	1.94E+05	2.08E+05	2.51E+05	2.55E+05
Water (to HGtS)	ton	5638719	4512151	6768227	7894794	9024303	10150870	11280379	16919097	21793045
Thermal fluid	ton	60776								

	ton/y	6078								
Outputs										
Gasuous emissions										
NOx	ton	3.00E+02	1.67E+02	4.70E+02	6.76E+02	9.19E+02	1.20E+03	1.51E+03	3.64E+03	6.22E+03
CO	ton	2.76E+01	2.13E+01	3.44E+01	4.15E+01	4.91E+01	5.71E+01	6.54E+01	1.13E+02	1.63E+02
PTS	kg	0.08	0.08	0.08	5.14E+02	1.24E+03	2.13E+03	3.18E+03	1.09E+04	2.08E+04
COVs	kg	2.90	2.90	6.59E+03	1.62E+04	2.83E+04	4.28E+04	5.98E+04	1.81E+05	3.35E+05
CO2	ton	8.18E+05	6.54E+05	9.81E+05	1.14E+06	1.31E+06	1.47E+06	1.64E+06	2.45E+06	3.16E+06
Effluents	m3	1.51E+06	1.16E+06	1.89E+06	2.29E+06	2.71E+06	3.16E+06	3.63E+06	6.36E+06	9.21E+06
Nitrogen ammoniacal	kg	2.23E+03	1.75E+03	2.73E+03	3.24E+03	3.77E+03	4.31E+03	4.87E+03	7.92E+03	1.09E+04
Total nitrogen	kg	5.02E+03	3.93E+03	6.14E+03	7.31E+03	8.52E+03	9.77E+03	1.11E+04	1.81E+04	2.50E+04
Biological oxygen demand	kg	9.25E+03	7.40E+03	1.11E+04	1.29E+04	1.48E+04	1.66E+04	1.85E+04	2.77E+04	3.57E+04
Chemical oxygen demand	kg	3.73E+04	2.91E+04	4.60E+04	5.51E+04	6.46E+04	7.45E+04	8.48E+04	1.42E+05	2.01E+05
Residual chlorine free	kg	8.58E+01	6.21E+01	1.13E+02	1.43E+02	1.76E+02	2.13E+02	2.53E+02	5.01E+02	7.82E+02
Residual chlorine total	kg	9.02E+01	6.88E+01	1.18E+02	1.55E+02	2.03E+02	2.66E+02	3.49E+02	1.35E+03	4.34E+03
Total phosphorus	kg	3.37E+02	2.57E+02	4.42E+02	5.79E+02	7.60E+02	9.96E+02	1.30E+03	5.05E+03	1.62E+04
Oils and fats	kg	1.25E+03	1.02E+03	1.48E+03	1.69E+03	1.90E+03	2.11E+03	2.30E+03	3.14E+03	3.71E+03
Hydrocarbons	kg	6.77E+02	5.41E+02	8.12E+02	9.47E+02	1.08E+03	1.22E+03	1.35E+03	2.03E+03	2.61E+03
Detergents	kg	55.45	42.57	69.23	83.90	99.47	115.93	133.29	233.48	338.15
Total suspended solids (105ºC)	kg	1.24E+04	8.99E+03	1.68E+04	2.23E+04	2.94E+04	3.82E+04	4.94E+04	1.53E+05	3.43E+05
Wastes	kg	117183.4	117183.4	117183.4	117183.4	117183.4	117183.4	117183.4	117183.4	117183.4
Hazardous waste	kg	17577.51	17577.51	17577.51	17577.51	17577.51	17577.51	17577.51	17577.51	17577.51
unspecified treatment	kg	11718.34	11718.34	11718.34	11718.34	11718.34	11718.34	11718.34	11718.34	11718.34
recovery	kg	5859.17	5859.17	5859.17	5859.17	5859.17	5859.17	5859.17	5859.17	5859.17
Non-hazardous waste	kg	99605.89	99606.89	99607.89	99608.89	99609.89	99610.89	99610.89	99610.89	99610.89
unspecified treatment	kg	23436.68	23436.68	23436.68	23436.68	23436.68	23436.68	23436.68	23436.68	23436.68
recovery	kg	76169.21	76169.21	76169.21	76169.21	76169.21	76169.21	76169.21	76169.21	76169.21

Appendix VI – Sines powerplant data processing

The following table presents the raw data extracted from EDP's environmental reports from 2009 to 2018, representing the annual inventory of raw materials consumed, energy balance, atmospheric emissions, wastewater emissions and solid waste and by-products generated.

The methodology applied to process the raw dataset is the same as the one applied for natural gas powerplant (referred in the previous appendix). The identification of discontinued raw materials consumption and other disregarded values as well as the method to estimate the missing values is further described.

Table VI-1 - Raw data gathered from environmental reports from EDP about Sines powerplant operation. The values highlighted in red were disregarded. The values highlighted in yellow were estimated. The values highlighted in blue are calculated directly from the report data.

		2009	2010	2011	2012	2013	2014	2015	2016	2017	2018
Availability					93.00%	91.70%	96.80%	98.47%	91.69%	94.00%	94.40%
Use		85.63%	47.88%	66.87%	83.00%	77.00%	87.00%	93.23%	78.00%	91.30%	78.40%
Generated Energy	GWh	9516	5322	7432	9317	8567	8739	10341	8704	10117	8695
Turbines energy	GWh	17	10	11	17	13	13	16	16	12	8
Energy consumption	GWh	647	432	553	669	624	592	678	651	702	660
Raw material consumption											
Coal	ton	3191695	1 823 921	2 636 539	3 283 424	3069645	3189496	3700442	3204724	3611892	3227111
Fueloil	ton	7785	9794	9069	6676	6217	5100	3648	6284	3116	6563
Oil	ton	88	339	179	110	5	1518	0	164	6	37
Propane	ton	25	23	21	40	16	18	17	12	0	0
Limestone	ton	101449	56739	71687	86245	78183	68508	82196	59106	77299	71807
Hydrochloric acid	ton	1 509	1045	1252	1613	1503	1520	1713	2003	2039	467
Ammonia hydroxide	ton	0.003	1	8950	14039	14798	17893	20783	19060	22780	16542
Calcium hydroxide	ton	89	135	155	197	210	160	247	340	363	271
Sodium hydroxide	ton	880	751	859	1025	1025	1111	953	1340	1463	24
Iron (III) chloride	ton	4	7	14	21	22	30	27	14	21	26
TMT-15	ton	1.1	0	10	12	18	22	9	4	9	11
Polyelectrolyte	ton	3.3	4	7	12	15	24	14	12	10	10
Aluminum sulfate	ton	18	9	9	10	9	10	6	3	3	6
Hydrazine hydrate	ton	8	-	-	-	-	-	-	-	-	-
Carbohydrazide	ton	-	9	9	4	4	2	2	0	0	0
Hidrogen	m3	11 549	12320	6787	12813	21771	14784	16016	13886	20451	25872
Oils	ton	13	34	35	16	40	35	37	26	13	42
Carbon Dioxide	ton	58	16	10	22	24	19	18	28	37	17
Solvents	ton	1	1	1	2	2	2	1	1.4	0.6	0.8
Industrial water	m3	2237033	1667002	1960456	2909828	2269807	2092413	2350458	2249049	2464606	2243395
Industrial water	m3										
Drinkable water	m3	16086	21104	14759	36099	22307	15740	13342	13864	13265	11150
Drinkable water	m3										
Outputs											
Gasuous emissions											
SO2	ton	5713	2379	2998	3795	4045	3871	4856	3474	4343	3812
NOx	ton	17680	7613	4730	3833	4624	4461	5516	4564	5303	4069

NOx	ton	4934	2759							
Particles	ton	195	100	286	178	44	35	16	19	39	70
				69							
fluorinated compounds	ton	79	20	40	46	35	45	32	40	54	33
chlorinated compounds	ton	33	12	8	22	26	29	44	46	96	69
CO2	ton	7706253	4438198	6251550	7785589	7184113	7398654	8683899	7316936	8396291	7432821
CO	ton	889	495	1289	1600	3683	297	265	571	413	611
COV	ton	13	5	9	11	90	65	36	85	170	184
Heavy metals	ton	16	1	2	2	5	8	2	8	10	7
Effluents											
Desulphurisation effluent	**m3**	**82313**	**185012**	**265788**	**368130**	**293893**	**252556**	**235965**	**195479**	**216915**	**199254**
pH	sorensen	8.20	8.60	8.40	8.5	8.50	8.50	8.50	8.70	8.60	8.70
temperature	ºC	32.40	29.70	31.30	33.7	31.90	30.50	30.50	29.10	29.10	21.10
Cr(XI)	mg/l	0.01	6.70	14.80	0.03	0.03	21.00	0.017	0.01	0.01	0.01
COD	mg/l O2	135.00	79.10	73.10	67.5	55.20	69.80	88.30	85.50	99.50	109.30
K+	mg/l	32.00	23.60	22.10	21.9	22.40	30.50	40.80	46.70	49.10	70.30
Sulphates	mg/l	1352.00	1365.30	1317.00	1366	1776.00	1617.00	2654.30	3661.00	3288.50	1564.00
Sulphites	mg/l	1.00	0.30	0.50	0.5	0.50	0.50	0.50	0.50	0.50	0.37
Sulphides	mg/l	0.02	0.02	0.01	0.02	0.01	0.01	0.01	0.02	0.01	0.01
Total suspended solids	mg/l	34.00	12.20	26.20	16.4	9.10	14.50	37.90	21.90	22.30	38.95
Al	mg/l	3.0E-01	1.9E-01	2.3E-01	0.238	2.5E-01	3.3E-01	4.1E-01	2.5E-01	2.5E-01	1.9E-01
Ar (total)	mg/l	5.0E-03	5.0E-03	3.0E-03	0.003	3.0E-03	3.0E-03	3.0E-03	3.0E-03	3.0E-03	1.1E-02
Cd	mg/l	1.0E-03	1.0E-03	1.0E-03	0.001	1.0E-03	1.0E-03	4.0E-03	2.2E-02	1.0E-02	1.0E-03
Pb (total)	mg/l	4.0E-03	6.0E-03	3.0E-03	0.188	2.6E-01	4.2E-01	2.0E-02	2.0E-02	2.0E-02	2.0E-03
Cu (total)	mg/l	6.0E-03	1.7E-02	3.5E-02	0.03	2.0E-02	2.5E-02	5.0E-03	7.0E-03	5.0E-03	4.0E-03
Cr (total)	mg/l	4.0E-03	7.0E-03	1.7E-02	0.048	3.6E-02	2.4E-02	2.3E-02	2.2E-02	9.0E-03	3.0E-03
Fe (total)	mg/l	2.5E-01	3.3E-01	1.2E-01	0.267	3.8E-01	1.7E-01	3.4E-01	2.4E-01	3.1E-01	1.8E-01
Mg	mg/l	691.00	468.50	614.00	380.5	512.50	670.00	768.00	650.00	885.50	958.80
Hg (total)	mg/l	1.0E-03	1.7E-02	9.0E-03	0.041	3.4E-02	2.7E-02	7.0E-02	2.3E-02	1.4E-02	4.0E-03
Ni (total)	mg/l	1.0E-01	2.4E-02	5.0E-02	0.145	6.5E-02	5.0E-02	6.0E-02	2.0E-01	2.4E-01	7.9E-02
Vanadium	mg/l	1.0E-02	6.5E-02	3.1E-01	0.3	3.3E-01	3.5E-01	3.5E-01	3.5E-01	3.5E-01	3.5E-01
Zn (total)	mg/l	1.9E-02	3.3E-02	8.0E-03	0.01	2.3E-02	8.0E-03	2.6E-02	3.1E-02	3.0E-02	8.0E-03
Domestic and chemical effluent	**m3**	**561925**	**210437**	**335590**	**395560**	**366393**	**286524**	**191088**	**404131**	**241874**	**135939**
pH	sorensen	7.70	7.42	7.50	7.6	7.20	7.70	7.70	7.60	8.00	8.30
BOD	mg/l	2.20	1.36	1.40	1.6	2.60	2.62	2.33	3.19	2.29	2.60
COD	mg/l	58.00	24.52	20.00	26.9	28.00	25.80	24.70	28.27	27.85	26.90
Total suspended solids	mg/l	21.00	8.57	10.80	8.5	12.00	10.40	13.70	10.77	5.65	6.20
Mineral oils	mg/l	0.40	0.23	0.11	0.06	0.06	0.25	0.25	0.26	0.59	0.30
Oils and fats	mg/l	0.50	0.31	0.16	0.12	0.17	0.35	0.25	0.38	0.69	0.50
N ammoniacal	mg/l	1.30	0.27	0.57	0.78	1.39	3.30	1.78	3.64	2.93	2.10
N total	mg/l	44.00	5.93	3.97	3.35	5.61	6.93	4.39	4.94	4.73	3.60
F	mg/l	0.90	2.36	1.71	0.71	0.19	0.39	0.17	0.22	0.19	0.30
NO3	mg/l	168.00	21.55	12.50	7.5	11.51	10.90	7.93	4.23	7.15	4.70
SO4	mg/l	744.00	403.00	261.20	313.1	352.70	286.60	274.90	295.00	313.92	286.40

Pb (total)	mg/l	6.0E-03	3.0E-03	3.0E-03	0.076	1.0E-01	9.0E-02	2.0E-02	2.0E-02	2.0E-02	3.0E-03
Fe (total)	mg/l	6.7E-02	2.7E-01	1.4E-01	0.077	1.0E-01	9.0E-02	7.0E-02	2.4E-01	5.9E-02	5.4E-02
Hg (total)	mg/l	8.0E-03	3.0E-03	1.0E-03	0.001	4.0E-04	4.0E-04	4.0E-04	1.0E-03	4.0E-04	4.0E-04
Vanadium	mg/l	9.6E-02	2.3E-01	3.1E-01	0.367	3.3E-01	3.5E-01	3.5E-01	3.5E-01	3.5E-01	3.5E-01
Zn (total)	mg/l	3.4E-02	4.7E-02	1.4E-02	0.029	1.9E-02	3.0E-02	6.0E-02	4.0E-02	2.4E-02	1.2E-02
Cr (total)	mg/l	4.0E-03	3.0E-03	3.0E-03	0.002	2.0E-03	2.0E-03	2.0E-03	3.0E-03	2.0E-02	2.0E-03
Al	mg/l	5.7E-01	4.6E-01	4.5E-01	0.442	5.8E-01	6.9E-01	9.1E-01	2.9E-01	7.3E-01	7.8E-01
Ar (total)	mg/l	8.0E-03	2.0E-03	3.0E-03	0.003	3.0E-03	3.0E-03	3.0E-03	3.0E-03	3.0E-03	2.0E-03
Cu (total)	mg/l	6.0E-03	1.0E-02	2.0E-02	0.02	2.2E-02	2.0E-02	2.0E-03	2.0E-03	2.0E-03	2.0E-03
Mn (total)	mg/l	1.1E+00	1.6E-01	1.1E-01	0.043	4.5E-02	5.0E-02	9.0E-02	7.3E-02	3.5E-02	3.4E-01
Ni (total)	mg/l	4.7E-02	3.3E-02	5.0E-02	0.055	5.0E-02	5.0E-02	1.0E-02	1.3E-02	3.0E-03	3.0E-03
Waste (in storage)	ton	227266	126789	85650	176378	81914	58659	59968	43907	27213	7663
Waste (in storage) corrected	ton	17695	92701	59272	146254	45856	20475	16503	12907	27213	7663
Hardazous wastes	ton	649	1235	1050	2276	2038	3239	1846	1991	1408	1571
Hazardous waste	%	0%	1%	1%	1%	2%	6%	3%	5%	5%	21%
Non-hardazous wastes	ton	226617	125553	84600	174102	79876	55420	58122	41916	25805	6092
Non-hardazous wastes corrected	ton	17046	100390	58222	143978	43818	17236	14657	10916	25805	6092
Non-hazardous waste	%	100%	99%	99%	99%	98%	94%	97%	95%	95%	79%
Waste (out storage)	ton	182570	262454	107461	240568	94220	64225	113789	105199	33206	24245
Valorised	ton	129590	222711	19033	86773	20779	6656	67197	101057	28572	21745
Valorised waste corrected	ton	42854	222711								
Valorised waste	%	71%	85%	18%	36%	22%	10%	59%	96%	86%	90%
Fly ash (in landfill)	ton	12980	9063	39768	121039	34884	15616	759	980	684	0
By-products											
Coal slag (in landfill)	ton	36750	25163	26378	30124	36058	38184	43465	0	1945	0
Coal slag (out landfill)	ton		45532	4160	71481	1786	1460	24486	61112	0	20463
Coal slag (sold)	ton	0	0	0	0	0	0	0	0	0	35712
Coal slag produced	ton	36750	25163	26378	30124	36058	38184	43465	31000	37322	15249
Fly ash (in storage)	ton	0	0	0	0	0	94197	63958	60947	53076	25006
Fly ash (out storage)	ton	0	0	0	0	0	0	0	190025	30389	51687
Fly ash (sold)	ton	333308	171187	194541	189870	216619	292271	306312	273919	268494	259547
Fly ash produced	ton	333308	171187	194541	189870	216619	386468	370270	144841	291181	232866
Gympsum (in landfill)	ton	86085	8925	1023	7291	6184	2	0	0	0	3908
Gympsum (out landfill)	ton	0	98734	0	0	16695	4182	32048	435	0	0
Gympsum (sold)	ton	86736	0	113342	72420	118752	181924	168870	109785	139613	121880
Gympsum produced	ton	172821	8925	114365	79711	108241	177744	136822	109350	139613	125788
Water recirculated from ocean	ton	1.2E+09	7.28E+08	9.93E+08	1155308760	1119362400	1175298000	1234322640	113985200	121936300	112886880
Cl (monthly average)	mg/L	0.14	0.11	0.16	0.12	0.11	0.14	0.15	0.14	0.16	0.14

Missing values determination and other calculations

Utilization rates

The utilization rates for 2009, 2010 and 2011 were not reported. However, their estimation was necessary for calculate some emissions reported in kg/h in tonnes. Therefore, the linear regression obtained when utilization rates are correlated with the electricity generated in the plant (Figure 1) was used to calculate the missing values.

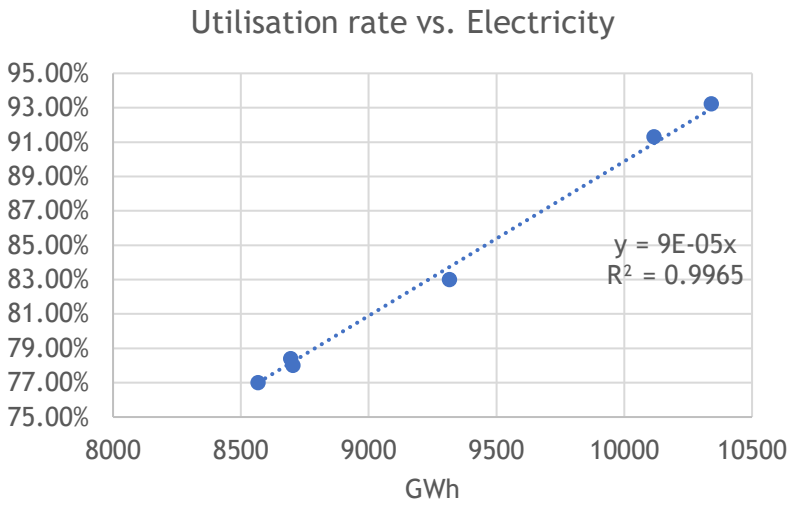

Figure VI-1 - Linear regression obtained for utilization rate vs. electricity generated by the plant.

Ammonia hydroxide, Oils and Solvents

In inventory from 2009, ammonia hydroxide, oils and solvents consumption were reported in a volume basis. For the conversion, the densities considered are represented in the table below.

Table VI-2 - Density for the substances for which volume data was reported instead of being a mass basis.

Substance	*Unit*	*Density (T=20ºC, P=1 atm)*	*Source*
Ammonia hydroxide	*Kg/m³*	*4016*	*Engineering toolbox*
Oils	*Kg/m³*	*925*	*Engineering toolbox*
Solvents	*Kg/m³*	*1014*	*Engineering toolbox (assumed a density similar to water)*

Nitrogen oxides, particles emissions, industrial and drinkable water

The denitrification unit for flue gas treatment was installed in 2011. Therefore, nitrogen oxide emissions reported in 2009 and 2010 are not representative of the current operation. On the other hand, during unit's construction, the sampling system for particles measuring was affected causing an overestimation of particles emissions in that year (2011).

With the main purpose of using these historical data for designing a predicting model for the annual input/output inventory, the emissions for both parameters was estimated based on the average of the specific emission values (tonnes of NO_x emitted per GWh of electricity generated and tonnes of particles emitted per GWh of electricity generated, respectively).

The high consumption of both industrial and drinkable water in 2012 was associated to events of broken pipes reported. With the purpose of remove such external factors from the normal

materials and/or substances inventory, the values used for predicting were also calculated using average specific values for both parameters.

Table VI-3 - Estimated values for nitrogen oxides, particles emissions and industrial and drinkable water consumption.

	Nox ton/GWh	Particles ton/GWh	Industrial water m^3/GWh	Drinkable water m^3/GWh
2009		2.049E-02	235.0812	1.6904
2010		1.879E-02	313.2285	3.9654
2011	6.364E-01		263.7858	1.9859
2012	4.114E-01	1.910E-02		
2013	5.397E-01	5.136E-03	264.9477	2.6038
2014	5.105E-01	4.005E-03	239.4339	1.8011
2015	5.334E-01	1.547E-03	227.2950	1.2902
2016	5.244E-01	2.183E-03	258.3926	1.5928
2017	5.242E-01	3.855E-03	243.6104	1.3112
2018	4.680E-01	8.051E-03	258.0098	1.2823
Mean	5.185E-01	9.240E-03	255.9761	1.9470
		Missing values		
	ton	**ton**	**m^3**	**m^3**
2009	4934			
2010	2759			
2011		68.67		
2012			2384929	18140

Fluorinated (F^-) and chlorinated (Cl^-) compounds, heavy metals, carbon monoxide (CO) and volatile organic compounds (VOCs) emissions

The emissions for Fluorinated (F^-) and chlorinated (Cl^-) compounds, heavy metals, carbon monoxide (CO) and volatile organic compounds (VOCs) are reported in mass concentration. The table below shows the reported data.

Table VI-4 - Atmospheric emissions in kg per hour reported in []. Heavy metals emissions from 2014 to 2018 is calculated as the sum of the Metals I, II and III. The emissions of hydrogen sulphide (H_2S) were disregarded from the study, as its emissions are only reported for 3 years.

kg/h		Chimney 1			Chimney 2	
		1st test	2nd tes	3rd test	1st test	2nd tes
2009	CO	43	36		120	38
	VOCs	1.1	0		1.7	0.6
	Heavy metals	3.696	0.3		0.12	0.156
	F-	5.94	4.8		5.9	4.36
	Cl-	1.1	2		0.6	5.1
2010	CO	25	60		118	33
	VOCs	0	0		0	2.6
	Heavy metals	0.11	0.05		0.05	0.06
	F-	2.2	1.2		4.7	1.6
	Cl-	1.5	0.9		1.8	1.4
2011	CO	21	28		73	84
	COV	0.6	10		0.7	3.7
	F-	3.6	3.9		3.7	2.3
	Cl-	2.1	<2.6		0.7	<3.2
	Heavy metals	0.24	0.31		0.18	0.35
2012	CO	273	12		27	128
	VOCs	1.2	0.12		1.6	0.12
	Heavy metals	0.1	0.14		0.1	0.2
2013	CO	746	68		273	5
	VOCs	2.7	8.3		3.4	12.4
	Heavy metals	0.081	0.353		0.403	0.709
	H2S		0.022			0.024

	Metals I		0.018			0.05
	Metals II		0.162			0.505
	Metals III		0.173			0.154
2014	CO	43			25	10
	VOCs	3.5			3.6	10
	Heavy metals	0.922			0.9	0.26
	H2S	1			1	0.066
	Metals I	0.032			0.044	0.015
	Metals II	0.443			0.321	0.108
	Metals III	0.447			0.535	0.137
2015	CO	19	16	46	1	10
	VOCs	1.8	1.8	3.1	1.6	2.8
	Heavy metals	0.162	0.227	0.087	0.151	0.106
	H2S	0.015	0.019	0.038	0.01	0.047
	Metals I	0.03	0.027	0.026	0.033	0.023
	Metals II	0.132	0.2	0.061	0.118	0.083
	Metals III	0.104	0.131	0.239	0.098	0.158
2016	CO	25	87		27	28
	VOCs	5.6	6.8		6.6	5.8
	Heavy metals	0.636	0.546		0.775	0.491
	Metals I	0.063	0.049		0.06	0.051
	Metals II	0.319	0.247		0.315	0.083
	Metals III	0.254	0.25		0.4	0.357
2017	CO	32	25.3		26	20
	VOCs	8.5	12.9		16.2	4.8
	Heavy metals	0.37	0.59		0.84	0.64
	Metals I	0.05	0.05		0.03	0.06
	Metals II	0.13	0.24		0.58	0.32
	Metals III	0.19	0.3		0.23	0.26
2018	CO	12	99		38	29
	VOCs	1.1	21		4	27.4
	Heavy metals	0.374	0.379		0.525	0.692
	Metals I	0.054	0.046		0.059	0.041
	Metals II	0.116	0.044		0.302	0.315
	Metals III	0.204	0.289		0.164	0.336

The total amount of emissions per year was calculated by the following expression:

$$Emissions\ (ton/y) = \left(C_{chimney1}\ (kg/h) + C_{chimney2}\ (kg/h)\right) \times 10^{-3} \times\ hours\ of\ operation\ (h/y)$$

Where, $C_{chimney1}$ and $C_{chimney2}$ corresponds to the average of the concentrations reported for chimneys 1 and 2, respectively.

The hours of operation were calculated by the following expression:

$$hours\ of\ operation\ (h/y)\ =\ utilization\ rate \times 365 \times 24$$

The results are presented in table XX, highlighted in blue.

Effluent emissions

The total amount of pollutants emitted per year through effluents from TL 8 (domestic) and TL 9 (chemical and rainwater potentially contaminated) were calculated by the following expression:

$$M\ pollutant\ (ton/y) = C\ pollutant\ (mg/L) \times effluent\ volume\ (m^3/y) \times 10^{-3}$$

Where M pollutant is the total emitted mass of each chemical compound per year, C pollutant is the reported concentration for each of them. The amounts obtained for each effluent were then summed. The results are presented in table below.

Table 45 - Emissions for ocean by desulphurisation, chemical and domestic effluents in tonnes.

		9	10	11	12	13	14	15	16	17	18
Cr(XI)	ton	8.23E-01	1.24E+03	3.93E+03	5.45E+03	8.23E+00	5.30E+03	4.01E+00	2.74E+00	1.08E+00	9.96E-01
COD	ton	4.37E+04	1.98E+04	2.47E+04	3.48E+04	2.65E+04	2.50E+04	2.56E+04	2.81E+04	2.83E+04	2.54E+04
K+	ton	2.63E+03	4.37E+03	5.87E+03	8.14E+03	6.58E+03	7.70E+03	9.63E+03	9.13E+03	1.07E+04	1.40E+04
Sulphates	ton	5.29E+05	3.37E+05	4.19E+05	5.88E+05	6.51E+05	4.91E+05	6.79E+05	8.35E+05	7.89E+05	3.51E+05
Sulphites	ton	8.23E+01	5.55E+01	1.33E+02	1.84E+02	1.47E+02	1.26E+02	1.18E+02	9.77E+01	1.08E+02	7.37E+01
Sulphides	ton	1.23E+00	3.70E+00	2.66E+00	3.68E+00	2.94E+00	1.52E+00	1.18E+00	3.52E+00	1.08E+00	9.96E-01
Total suspended solids	ton	1.46E+04	4.06E+03	9.83E+03	1.39E+04	7.07E+03	6.64E+03	1.16E+04	8.63E+03	6.20E+03	8.60E+03
Al	ton	3.47E+02	1.31E+02	1.78E+02	2.59E+02	2.87E+02	2.80E+02	2.71E+02	1.65E+02	2.31E+02	1.45E+02
Ar (total)	ton	4.91E+00	1.35E+00	1.59E+00	2.29E+00	1.98E+00	1.62E+00	1.28E+00	1.80E+00	1.38E+00	2.46E+00
Cd	ton	8.23E-02	1.85E-01	2.66E-01	3.68E-01	2.94E-01	2.53E-01	9.44E-01	4.30E+00	2.17E+00	1.99E-01
Pb (total)	ton	3.70E+00	1.74E+00	1.59E+00	2.29E+00	1.12E+02	1.32E+02	8.54E+00	1.20E+01	9.18E+00	8.06E-01
Cu (total)	ton	3.87E+00	5.25E+00	1.46E+01	2.08E+01	1.39E+01	1.20E+01	1.56E+00	2.18E+00	1.57E+00	1.07E+00
Cr (total)	ton	2.58E+00	1.93E+00	5.32E+00	7.44E+00	1.13E+01	6.63E+00	5.81E+00	5.51E+00	6.79E+00	8.70E-01
Fe (total)	ton	5.82E+01	1.18E+02	6.78E+01	9.76E+01	1.49E+02	6.87E+01	9.34E+01	1.44E+02	8.15E+01	4.32E+01
Mg	ton	5.69E+04	8.67E+04	1.63E+05	2.26E+05	1.51E+05	1.69E+05	1.81E+05	1.27E+05	1.92E+05	1.91E+05
Hg (total)	ton	4.58E+00	3.78E+00	2.66E+00	3.71E+00	1.01E+01	6.93E+00	1.66E+01	4.90E+00	3.13E+00	8.51E-01
Ni (total)	ton	3.46E+01	1.14E+01	2.66E+01	3.82E+01	3.74E+01	2.70E+01	1.61E+01	4.34E+01	5.28E+01	1.61E+01
Vanadium	ton	5.48E+01	6.11E+01	1.66E+02	2.39E+02	2.18E+02	1.89E+02	1.49E+02	2.10E+02	1.61E+02	1.17E+02
Zn (total)	ton	2.07E+01	1.60E+01	5.85E+00	8.48E+00	1.37E+01	1.06E+01	1.76E+01	2.22E+01	1.23E+01	3.23E+00
N total	ton	2.47E+04	1.25E+03	1.06E+03	1.57E+03	2.06E+03	1.99E+03	8.39E+02	2.00E+03	1.14E+03	4.89E+02
F	ton	5.06E+02	4.97E+02	4.54E+02	6.76E+02	6.96E+01	1.12E+02	3.25E+01	8.89E+01	4.60E+01	4.08E+01
NO3	ton	9.44E+04	4.53E+03	3.32E+03	4.94E+03	4.22E+03	3.12E+03	1.52E+03	1.71E+03	1.73E+03	6.39E+02
Mn (total)	ton	6.32E+02	3.39E+01	3.00E+01	4.47E+01	1.65E+01	1.43E+01	1.72E+01	2.95E+01	8.47E+00	4.62E+01
BOD	ton	1.24E+03	2.86E+02	3.72E+02	5.54E+02	9.53E+02	7.51E+02	4.45E+02	1.29E+03	5.54E+02	3.53E+02
Mineral oils	ton	2.25E+02	4.84E+01	2.92E+01	4.35E+01	2.31E+01	7.16E+01	4.78E+01	1.05E+02	1.43E+02	4.08E+01
Oils and fats	ton	2.81E+02	6.52E+01	4.25E+01	6.33E+01	6.27E+01	1.00E+02	4.78E+01	1.54E+02	1.67E+02	6.80E+01

Waste and by-products generation

Coal slag and gypsum were redefined as a by-product in 2017 and December of 2010, respectively. Therefore, with the attempt to correct historical data for the prediction model,

the amounts of waste that enters in storage, and the non-hazardous waste produced for the years from 2009 to 2016 were corrected, by the subtraction of the amounts of coal slag produced for the series from 2010 to 2016 and both amounts of coal slag and gypsum for 2009.

It is worth to mention that the amount of valorised waste does not refer necessarily to the parcel of produced waste in that year that is valorised, as the waste can be stored for long periods to be correctly classified.

By-products production is only reported for 2009, for the remaining it was determined by an indirect calculation method:

- Coal slag produced is the coal slag that got in landfill during the years it was consider a waste instead of a by-product and starting in 2018, it is the sum of slag that goes to storage landfill with the amount that is directly sold. There are however some inconsistency in the results for 2016 and 2017. EDP reported that starting in 2015, significant amounts of slag would start being removed from the landfill with the attempt to reduce the environmental liability of the landfill, which capacity was full in the end of 2017. For those years, the values used for further prediction modelling

were calculated through the polynomial regression obtained for coal slag produced vs. electricity generated (from 2009 to 2015 – Figure 2). The waste scenarios will be modelled considering the current waste flows.

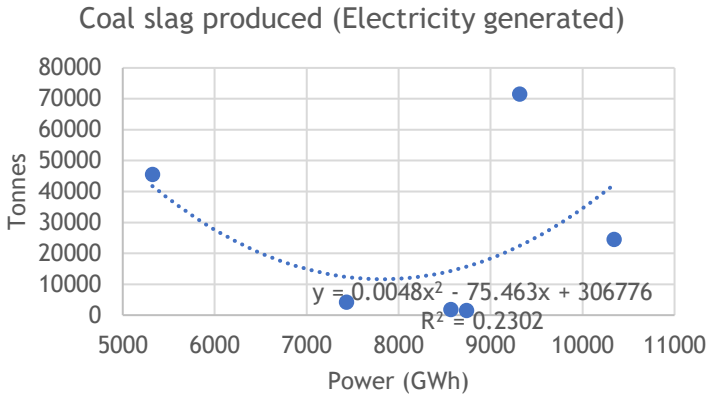

Figure VI-2 - Polynomial regression for coal slag produced as a function of electricity generated from 2009 to 2015.

- Fair fly ash produced (valorised) is the sum of ash that goes to storage warehouse in each year with the amount that is directly sold.
- Gypsum produced is the sum of gypsum that goes to storage landfill in each year with the amount that is directly sold.

Regressions and predicting model

As already mentioned, unlike natural gas powerplant, only a few features provide good regressions (with R-squared > 0.8). The reason for this could be linked to the variability of coal composition within the years, factor of major impact on emissions [14, 75-78]. Therefore, an ANN was designed to predict waste and by-products generation, atmospheric emissions (except CO_2, which linear regression provides an R-squared of 0.9920), wastewater emissions (with exception for: Cr (VI) because it presents a high variability which could increase the noise in the model; and oils and fats as their concentration is more or less regular and are not related to coal composition). The other features omitted from the predicting model were:

- The energy penalty from plants operation because its linear regression with the electricity generated has an R-squared of 0.9107;
- Fuels and industrial water consumption because their linear and polynomial regressions with the electricity generated by the plant ranges between 0.7640 (for diesel) to 0.9689 (for coal);
- Other raw material consumption, which is somewhat random for the cases of oils, solvents, carbon dioxide and drinkable water, and most of them do not represent a close relation to any of the inputs given in the model (coal composition and electricity generated). Moreover, a model with only 10 samples is more sensible to data noise, so there was an effort to minimize the number of features into the model;
- The chlorine emitted by the recirculated ocean water in the steam system because it is almost constant.

The construction of the model is detailed in subsection 3.3. and Appendix VII. The results obtained were not satisfying to be used for predicting emissions which turns the sensitivity analysis for electricity generated in the powerplant unfeasible.

Even using direct data from inventories of years with different utilization rates, since the difference between the produced electricity ranges does not reflect any pattern between the quantities of raw materials consumed and the emissions, this sensitivity analysis would be impracticable.

Conclusion

For coal powerplant instead of predicting input/output inventories for different operation scenarios for producing LCA results sensible to the amount of electricity produced, the LCA was based on the historical data. The amount of electricity generated in the years of 2014, 2016 and 2018 were almost equivalent with the average value of 8713 GWh and a standard deviation of 23 GWh (about 0.27 %). However, as expected from the results of regressions, raw materials consumption and emissions can vary significantly. An average scenario using data from these three years was modelled and the standard deviation of each parameter was used to estimate the uncertainties on the results by considering that the variation within the data for each parameter is described by a normal distribution. The operation scenario initially defined to serve the comparison between coal powerplant and natural gas powerplant of 5 GWh was, by consequence, redefined for 8713 GWh.

Appendix VII – Coal composition

The annual average of coal composition is a weighted average of the main components of coal according to national hard coal supply mix. For that purpose, data regarding coal composition on the main exporters was carried out. The dataset presented in Table 1 shows the data found in literature and it results from the average of the content of coal samples from several different exploitation sources in each country. Table 2 show the share of imports by country for the time series considered in the study. Table 4 show the results for coal composition in each year calculated by the following expression applied for each parameter:

$$Content\ of\ x = \sum_{i=1}^{10} Import\ Share_{\ i} \times Average\ Content_{\ i}$$

where, content of x represents the content of a single parameter in coal composition and index i represents each main exporter considered.

The table below shows the raw importing share.

Table VII-1 - Imports of bituminous coal by Portugal per exporter country, in tonnes.

	Imports in tones									
	2009	**2010**	**2011**	**2012**	**2013**	**2014**	**2015**	**2016**	**2017**	**2018**
Canada										45342
Russia	68000	39000	10566	10923	11091	315	5097		296672	70931
USA	1064000	609000	784632	1123679	506971	301077	125627	85021	740426	691971
Spain			10397	11496	99	7355	6326	9299	311	266
Colombia	1834000	1297000	2856538	4016301	3533860	4021220	5469060	4719584	4509885	3683792
South Africa	1654000	483000			164418	162425		320485	163355	
Saudi Arabia					163049					
Ukraine			11689		19110	83781				
Norway	240000	217000	82281	14518						
Venezuela	110000									
Non specified country						6625	9201	7062	0	
total	4970000	2645000	3756103	5176917	4398598	4582798	5615311	5141451	5710649	4492302
Source	Eurostat database [103]		DGEG, 'Energia em Portugal' [87]						Eurostat database [103]	

The data for coal composition was mainly gathered from World Coal Inventory Quality Inventory Data. The datasets had some missing values, that were filled with data from other sources. However, good quality data regarding the properties of coal produced in Russia, Spain, Saudi Arabia and Venezuela was not found, besides, as Canada, these countries have small importing shares. Therefore, these countries are disregarded, and their shares were equally divided per the other. The same database does not provide information about the coal produced in USA. That data was also gathered from other sources.

Table VII-2 - Imports share of bituminous coal by Portugal, per country. For each year the right column represents the share used for calculations. The increment (Δ) is added to each share highlighted in colours, and results from the the disivion of the total share of not considered countries (Russia, Spain, Saudi Arabia, Venezuela) and non specified countries for the number of the countries considered in each year.

Imports in %

	2009		2010		2011		2012		2013		2014		2015		2016		2017		2018	
Canada	0.00%		0.00%		0.00%		0.00%		0.00%		0.00%		0.00%		0.00%		0.00%		1.0%	
Russia	1.37%		1.47%		0.28%		0.21%		0.25%		0.01%		0.09%		0.00%		5.20%		1.6%	
USA	21.41%	22.30%	23.02%	23.39%	20.89%	21.03%	21.71%	21.85%	11.53%	12.52%	6.57%	6.65%	2.24%	2.42%	1.65%	1.76%	12.97%	14.7%	15.4%	16.7%
Spain	0.00%		0.00%		0.28%		0.22%		0.00%		0.16%		0.11%		0.18%		0.01%		0.0%	
Colombia	36.90%	37.80%	49.04%	49.40%	76.05%	76.19%	77.58%	77.73%	80.34%	81.33%	87.75%	87.82%	97.40%	97.58%	91.79%	91.90%	78.97%	80.7%	82.0%	83.3%
South Africa	33.28%	34.18%	18.26%	18.63%	0.00%		0.00%		3.74%	4.7%	3.54%	3.62%	0.00%		6.23%	6.34%	2.86%	4.6%	0.0%	
Saudi Arabia	0.00%		0.00%		0.00%		0.00%		3.71%		0.00%		0.00%		0.00%		0.00%		0.0%	
Ukraine	0.00%		0.00%		0.31%	0.45%	0.00%		0.43%	1.42%	1.83%	1.91%	0.00%		0.00%		0.00%		0.0%	
Norway	4.83%	5.72%	8.20%	8.57%	2.19%	2.33%	0.28%	0.42%	0.00%		0.00%		0.00%		0.00%		0.00%		0.0%	
Venezuela	2.21%		0.00%		0.00%		0.00%		0.00%		0.00%		0.00%		0.00%		0.00%		0.0%	
Non specified country	0.00%		0.00%		0.00%		0.00%		0.00%		0.14%		0.16%		0.14%		0.00%		0.0%	
Increment (Δ)	0.90%		0.37%		0.140%		0.14%		0.99%		0.08%		0.18%		0.11%		1.73%		1.30%	

The components selected are the ones which chemical elements are presented in the emissions reported by EDP [67].

Table VII-3 - Dataset used to estimate the composition and calorific value of coal used in Sines powerplant.

Country	LAB2 NITROGEN IN % ON AS-RECEIVED BASIS	LAB2 SULFUR IN % ON AS-RECEIVED BASIS	CALORIFIC VALUE IN MJ PER kg ON AS-RECEIVED BASIS	LAB2 SULFATE SULFUR IN % ON AS-RECEIVED BASIS	LAB1 ASH YIELD AT 525 (C) IN % ON AS-DETERMINED BASIS	LAB1 SiO_2 OF ASH IN % ON AS-DETERMINED BASIS	LAB1 Al_2O_3 OF ASH IN % ON AS-DETERMINED BASIS	LAB1 CaO OF ASH IN % ON AS-DETERMINED BASIS	LAB1 MgO OF ASH IN % ON AS-DETERMINED BASIS	LAB1 Na_2O OF ASH IN % ON AS-DETERMINED BASIS	LAB1 K_2O OF ASH IN % ON AS-DETERMINED BASIS	LAB1 Fe_2O_3 OF ASH IN % ON AS-DETERMINED BASIS	LAB1 TiO_2 OF ASH IN % ON AS-DETERMINED BASIS	LAB1 P_2O_5 OF ASH IN % ON AS-DETERMINED BASIS	LAB1 SO_3 OF ASH IN % ON AS-DETERMINED BASIS
Columbia	1.53	0.97	30.28	0.05	6.19	48.22	32.55	2.12	0.99	0.47	0.47	7.29	1.75	0.48	3.95
USA	1.18	3.6		0.04	10.26	44.38	17.35	4	0.85	0.63	1.8	19.8	0.91	0.12	4.62
Ukraine	1.48	2.65	30.10	0.19	14.23	34.19	14.09	3.89	0.95	0.82	1.25	29.82	0.45	0.66	3.46
Norway	1.34	1.93	25.90	0.08	9.70	18.22	11.98	13.14	3.99	5.47	0.68	16.67	0.68	1.17	8.51
South Africa	1.16	0.5	20.526	0.05	9.44	16.90	11.40	0.18	0.12	0.14	0.62	0.37	0.44	0.28	2.62

Country	LAB1 Al IN % ON DRY, WHOLE-COAL BASIS	LAB1 Mg IN % ON DRY, WHOLE-COAL BASIS	LAB1 K IN % ON DRY, WHOLE-COAL BASIS	LAB1 Fe IN % ON DRY, WHOLE-COAL BASIS	LAB1 P IN % ON DRY, WHOLE-COAL BASIS	LAB1 S IN % ON DRY, WHOLE-COAL BASIS	LAB1 Cd IN PPM ON DRY, WHOLE-COAL BASIS	LAB1 Cr IN PPM ON DRY, WHOLE-COAL BASIS	LAB1 Cu IN PPM ON DRY, WHOLE-COAL BASIS	LAB1 Hg IN PPM ON DRY, WHOLE-COAL BASIS	LAB1 Ni IN PPM ON DRY, WHOLE-COAL BASIS	LAB1 Pb IN PPM ON DRY, WHOLE-COAL BASIS	LAB1 V IN PPM ON DRY, WHOLE-COAL BASIS	LAB1 Zn IN PPM ON DRY, WHOLE-COAL BASIS
Columbia	1.02	0.038	0.026	0.464	0.011	0.755	0.16	10.87	16.19	0.07	10.44	3.06	29.57	15.31
USA	1.42	0.142	0.131	1.04	0.033	1.47	0.16	13.75	16.00	0.10	14.00	11.00	22	58.93
Ukraine	1.28	0.08	0.253	1.993	0.019	2.767	0.07	18.90	19.57	3.71	17.53	8.07	31.22	16.54
Norway	0.5	0.221	0.064	1.158	0.047	1.438	0.42	28.72	3.47	0.13	24.28	2.57	17.38	29.87
South Africa	2.88	0.228	0.179	0.544	0.053	0.92	0.16	53.20	32.80	0.16	20.60	7.02	54.70	38.6

USA

Year	2008	2009	2010	2011	2012	2013	2014	2015	2016	2017	2018
Average MJ per kg	23.14	23.03	22.89	22.71	22.49	22.47	22.59	22.41	22.37	22.20	22.18

Data Source
[99]
[100]
Estimated.
[101]
[102]

Table VII-4 - Composition and calorific value estimated for coal in each year of the period considered in the study.

Year	LAB2 NITROGEN IN % ON AS-RECEIVED BASIS	LAB2 SULFUR IN % ON AS-RECEIVED BASIS	CALORIFIC VALUE IN MJ PER kg ON AS-RECEIVED BASIS	LAB2 SULFATE SULFUR IN % ON AS-RECEIVED BASIS	LAB1 ASH YIELD AT 525 (C) IN % ON AS-DETERMINED BASIS	LAB1 SiO_2 OF ASH IN % ON AS-DETERMINED BASIS	LAB1 Al_2O_3 OF ASH IN % ON AS-DETERMINED BASIS	LAB1 CaO OF ASH IN % ON AS-DETERMINED BASIS	LAB1 MgO OF ASH IN % ON AS-DETERMINED BASIS	LAB1 Na_2O OF ASH IN % ON AS-DETERMINED BASIS	LAB1 K_2O OF ASH IN % ON AS-DETERMINED BASIS	LAB1 Fe_2O_3 OF ASH IN % ON AS-DETERMINED BASIS	LAB1 TiO_2 OF ASH IN % ON AS-DETERMINED BASIS	LAB1 P_2O_5 OF ASH IN % ON AS-DETERMINED BASIS	LAB1 SO_3 OF ASH IN % ON AS-DETERMINED BASIS
2009	1.32	1.45	19.94	0.05	8.41	34.94	20.75	2.51	0.83	0.68	0.83	8.25	1.06	0.37	3.91
2010	1.36	1.58	21.01	0.05	8.05	38.91	23.29	3.14	1.05	0.87	0.83	9.73	1.22	0.42	4.25
2011	1.46	1.57	23.89	0.05	7.25	46.95	28.83	2.61	0.98	0.53	0.77	10.49	1.54	0.41	4.10
2012	1.45	1.55	23.65	0.05	7.09	47.25	29.14	2.58	0.97	0.52	0.76	10.07	1.57	0.41	4.12
2013	1.47	1.30	26.02	0.05	6.96	46.05	29.38	2.29	0.93	0.48	0.66	8.85	1.57	0.43	3.97
2014	1.49	1.16	27.91	0.05	6.73	46.56	30.42	2.21	0.95	0.47	0.58	8.30	1.63	0.45	3.94
2015	1.52	1.03	29.55	0.05	6.29	48.13	32.18	2.17	0.99	0.47	0.50	7.60	1.73	0.47	3.97
2016	1.50	0.99	29.13	0.05	6.47	46.17	30.94	2.03	0.94	0.45	0.50	7.07	1.66	0.46	3.88
2017	1.46	1.34	25.38	0.05	6.94	46.22	29.34	2.31	0.93	0.48	0.67	8.81	1.57	0.42	3.99
2018	1.47	1.41	25.23	0.05	6.87	47.58	30.01	2.44	0.97	0.49	0.69	9.38	1.61	0.42	4.06

Year	LAB1 Al IN % ON DRY, WHOLE-COAL BASIS	LAB1 Mg IN % ON DRY, WHOLE-COAL BASIS	LAB1 K IN % ON DRY, WHOLE-COAL BASIS	LAB1 Fe IN % ON DRY, WHOLE-COAL BASIS	LAB1 P IN % ON DRY, WHOLE-COAL BASIS	LAB1 S IN % ON DRY, WHOLE-COAL BASIS	LAB1 Cd IN PPM ON DRY, WHOLE-COAL BASIS	LAB1 Cr IN PPM ON DRY, WHOLE-COAL BASIS	LAB1 Cu IN PPM ON DRY, WHOLE-COAL BASIS	LAB1 Hg IN PPM ON DRY, WHOLE-COAL BASIS	LAB1 Ni IN PPM ON DRY, WHOLE-COAL BASIS	LAB1 Pb IN PPM ON DRY, WHOLE-COAL BASIS	LAB1 V IN PPM ON DRY, WHOLE-COAL BASIS	LAB1 Zn IN PPM ON DRY, WHOLE-COAL BASIS	LAB1 Al IN % ON DRY, WHOLE-COAL BASIS
2009	1.72	0.14	0.10	0.66	0.03	1.01	0.17	27.00	21.10	0.11	15.50	6.16	35.77	33.83	1.72
2010	1.42	0.11	0.08	0.67	0.03	1.01	0.18	20.96	18.15	0.10	14.35	5.61	31.43	31.10	1.42
2011	1.11	0.06	0.05	0.62	0.02	0.96	0.16	11.75	16.17	0.16	11.42	4.85	27.96	24.58	1.11
2012	1.11	0.06	0.05	0.59	0.02	0.91	0.16	11.58	16.10	0.08	11.28	4.79	27.86	24.90	1.11
2013	1.16	0.06	0.05	0.56	0.02	0.88	0.16	13.33	16.99	0.13	11.46	4.31	29.82	21.88	1.16
2014	1.12	0.05	0.04	0.53	0.01	0.85	0.16	12.75	16.85	0.14	11.18	3.83	30.00	19.08	1.12
2015	1.03	0.04	0.03	0.48	0.01	0.77	0.16	10.94	16.19	0.07	10.53	3.25	29.38	16.37	1.03
2016	1.14	0.05	0.04	0.48	0.01	0.78	0.16	13.61	17.24	0.08	11.15	3.45	31.03	17.56	1.14
2017	1.16	0.06	0.05	0.55	0.02	0.87	0.16	13.24	16.93	0.08	11.43	4.41	29.61	22.79	1.16
2018	1.09	0.06	0.04	0.56	0.01	0.87	0.16	11.35	16.16	0.07	11.04	4.39	28.30	22.60	1.09

Appendix VIII – Artificial Neural Network for predicting emissions on Sines powerplant

The algorithm designed for creating both ANN models (feed-forward and k-fold) for predicting the emissions on a mass basis resulting from Sines powerplant operation is presented below. The code was written on Python 3 using Keras, a deep learning application programming interface, available on the library of Tensorflow, one of the most developed machine learning platforms.

Feed-forward ANN:

1. Import of libraries
```
import numpy as np
from sklearn import preprocessing
import tensorflow as tf
from tensorflow import keras
from sklearn import metrics
from sklearn.model_selection import KFold
from tensorflow.keras.models import Sequential
from tensorflow.keras.layers import Dense, Activation
```
2. Import of learning dataset
```
data=np.loadtxt('dataset_wo_cr.csv',delimiter=',')
unscaled_inputs=data[:,0:30]
unscaled_targets=data[:,30:64]
```
3. Data pre-processing
```
scaled_inputs = preprocessing.scale(unscaled_inputs)
scaled_targets=preprocessing.scale(unscaled_targets)
samples_count=scaled_inputs.shape[0]
train_samples_count=int(0.6*samples_count)
validation_samples_count=int(0.2*samples_count)
test_samples_count=samples_count-train_samples_count-validation_samples_count
train_inputs=scaled_inputs[:train_samples_count]
train_targets=scaled_targets[:train_samples_count]
validation_inputs=scaled_inputs[train_samples_count:train_samples_count+valida
tion_samples_count]
validation_targets=scaled_targets[train_samples_count:train_samples_count+vali
dation_samples_count]
test_inputs=scaled_inputs[train_samples_count+validation_samples_count:]
test_targets=scaled_targets[train_samples_count+validation_samples_count:]
print(np.sum(train_targets),   train_samples_count,   np.sum(train_targets)   /
train_samples_count)
print(np.sum(validation_targets),                    validation_samples_count,
np.sum(validation_targets) / validation_samples_count)
print(np.sum(test_targets),    test_samples_count,    np.sum(test_targets)    /
test_samples_count)
np.savez('coal_data_mass_train', inputs=train_inputs, targets=train_targets)
np.savez('coal_data_mass_validation',                inputs=validation_inputs,
targets=validation_targets)
np.savez('coal_data_mass_test', inputs=test_inputs, targets=test_targets)
```
4. ANN model design
```
npz=np.load('coal_data_mass_train.npz')
train_inputs = npz['inputs'].astype(np.float)
train_targets = npz['targets'].astype(np.float)
npz = np.load('coal_data_mass_validation.npz')
validation_inputs, validation_targets = npz['inputs'].astype(np.float),
npz['targets'].astype(np.float)
npz = np.load('coal_data_mass_test.npz')
test_inputs, test_targets = npz['inputs'].astype(np.float),
npz['targets'].astype(np.float)
```

```
input_size = 30
output_size = 33
hidden_layer_size = 2
model = tf.keras.Sequential([
    tf.keras.layers.Dense(hidden_layer_size,input_shape=(30,),
activation='relu'),
    tf.keras.layers.Dense(hidden_layer_size, activation='relu'),
    tf.keras.layers.Dense(output_size, activation='linear')
])

model.compile(optimizer='adam', loss='mean_absolute_error',
metrics=['MeanAbsoluteError','mse'])

batch_size = 10
max_epochs = 20
callback=tf.keras.callbacks.EarlyStopping(patience=3)
model.fit(train_inputs,
          train_targets,
          batch_size=10,
          epochs=max_epochs,
          verbose=2,
          callbacks=[callback],
          validation_data=(validation_inputs, validation_targets)
          )
test_loss= model.evaluate(test_inputs, test_targets)

OUT: 2/2 [==============================] - 0s 1ms/sample - loss: 0.7086 -
mean_absolute_error: 0.7086 - mean_squared_error: 0.7577
```

5. Import the input dataset for predicting emissions for four different scenarios: 5000 GWh (5K); 7338 GWh (AVminus – average between 2016 and 2018 minus 20 %); 9172 GWh (AV – average between 2016 and 2018); 11006 GWh (AVplus - average between 2016 and 2018 plus 20 %). For all scenarios the same composition of coal is used (average between 2016 and 2018).

```
in_data=np.loadtxt('sines_predicting.csv',delimiter=',')
av_x=in_data[0,:]
avplus_x=in_data[1,:]
avminus_x=in_data[2,:]
fivek_x=in_data[3,:]
   6.  Prediction
av_y=model.predict(av_x[None,:])
print(av_y)
avplus_y=model.predict(avplus_x[None,:])
print(avplus_y)
avminus_y=model.predict(avminus_x[None,:])
print(avminus_y)
fivek_y=model.predict(fivek_x[None,:])
print(fivek_y)
```

K-Fold cross validation ANN:

1. (equal to feed-forward model)
2. (equal to feed-forward model)
3. ANN model design

```
kf = KFold(5)
fold = 0
for train, test in kf.split(x):
    fold+=1
       oos_y = []
```

```
       oos_pred = []
    print(f"Fold #{fold}")
    x_train = x[train]
    y_train = y[train]
    x_test = x[test]
    y_test = y[test]

    input_size = 30
    output_size = 33
    hidden_layer_size = 2
    model = Sequential()
    model.add(Dense(hidden_layer_size, activation='relu'))
    model.add(Dense(hidden_layer_size, activation='relu'))
    model.add(Dense(output_size, activation='linear'))
    model.compile(optimizer='adam',loss='mean_absolute_error',
metrics=['MeanAbsoluteError'])
    model.fit(x_train,y_train,validation_data=(x_test,y_test),verbose=2,epochs=20)
    pred = model.predict(x_test)
    oos_y.append(y_test)
    oos_pred.append(pred)
    # Measure this fold's RMSE
    score = np.sqrt(metrics.mean_absolute_error(pred,y_test))
    print(f"Fold score (RMSE): {score}")
```

4. (equal to 5. in feed-forward model)

The dataset used to train the model based on estimated data (for coal composition – inputs) and historical data (for electricity generated – input – and emissions – targets) is shown in the tables below, with the average and standard deviation for populations (used in python by default) which were used to scale the dataset. The inputs for predicting and the results obtained for each operation scenarios (5k, AVminus, AV, AVplus) are also shown in tables 1 and 2, respectively. The coal composition in a mass basis and calorific value in GJ was obtained by applying the following expressions (coal consumed is obtained by its linear regression with electricity generated):

$$Composition\ parameters\ (tonnes)\ = \frac{composition\ parameters\ (\%)}{100} \times\ coal\ consumed\ (tonnes)$$

$$Calorific\ value\ (GJ) = \ Calorific\ value\ (MJ/kg) \times coal\ consumed\ (tonnes)$$

$$Composition\ parameters\ (kg)\ =\ composition\ parameteres\ (ppm) \times\ coal\ consumed\ (tonnes) \times 10^{-3}$$

TableVIII- 1 - Dataset with model inputs for learning step. Source: DGEG [87], EUROSTAT [102], coal composition [118-121], EDP [67]

Inputs dataset for learning

Feature		2009	2010	2011	2012	2013	2014	2015	2016	2017	2018	μ	Σ
Power	GWh	9.52E+03	5.32E+03	7.43E+03	9.32E+03	8.57E+03	8.74E+03	1.03E+04	8.70E+03	1.01E+04	8.70E+03	8.68E+03	1.37E+03
N	Ton	4.20E+04	2.49E+04	3.84E+04	4.77E+04	4.51E+04	4.76E+04	5.64E+04	4.81E+04	5.28E+04	4.75E+04	4.51E+04	8.25E+03
Sulfur	Ton	4.63E+04	2.88E+04	4.13E+04	5.09E+04	4.00E+04	3.70E+04	3.83E+04	3.17E+04	4.83E+04	4.55E+04	4.08E+04	6.77E+03
Calorific value	MJ	6.37E+07	3.83E+07	6.30E+07	7.76E+07	7.99E+07	8.90E+07	1.09E+08	9.34E+07	9.17E+07	8.14E+07	7.87E+07	1.88E+07
Sulfate in Sulfur	Ton	1.55E+03	9.00E+02	1.33E+03	1.55E+03	1.54E+03	1.65E+03	1.84E+03	1.59E+03	1.73E+03	1.54E+03	1.52E+03	2.43E+02
Ash Yeld	Ton	2.68E+05	1.47E+05	1.91E+05	2.33E+05	2.14E+05	2.15E+05	2.33E+05	2.07E+05	2.51E+05	2.22E+05	2.18E+05	3.16E+04
SiO2	Ton	1.12E+06	7.10E+05	1.24E+06	1.55E+06	1.41E+06	1.49E+06	1.78E+06	1.48E+06	1.67E+06	1.54E+06	1.40E+06	2.93E+05
Al2O3 of ash	Ton	6.62E+05	4.25E+05	7.60E+05	9.57E+05	9.02E+05	9.70E+05	1.19E+06	9.92E+05	1.06E+06	9.69E+05	8.89E+05	2.08E+05
CaO of ash	Ton	8.01E+04	5.74E+04	6.88E+04	8.47E+04	7.03E+04	7.05E+04	8.02E+04	6.51E+04	8.34E+04	7.86E+04	7.39E+04	8.42E+03
MgO of ash	Ton	2.66E+04	1.92E+04	2.57E+04	3.20E+04	2.86E+04	3.03E+04	3.66E+04	3.00E+04	3.37E+04	3.13E+04	2.94E+04	4.55E+03
Na2O of ash	Ton	2.16E+04	1.59E+04	1.40E+04	1.72E+04	1.46E+04	1.51E+04	1.74E+04	1.44E+04	1.72E+04	1.59E+04	1.63E+04	2.11E+03
K2O of ash	Ton	2.65E+04	1.51E+04	2.03E+04	2.50E+04	2.01E+04	1.85E+04	1.86E+04	1.62E+04	2.43E+04	2.24E+04	2.07E+04	3.61E+03
Fe2O3 of ash	Ton	2.63E+05	1.78E+05	2.77E+05	3.31E+05	2.72E+05	2.65E+05	2.81E+05	2.27E+05	3.18E+05	3.03E+05	2.71E+05	4.21E+04
TiO2 of ash	Ton	3.37E+04	2.22E+04	4.06E+04	5.14E+04	4.81E+04	5.19E+04	6.42E+04	5.31E+04	5.67E+04	5.21E+04	4.74E+04	1.15E+04
P2O5 in ash	Ton	1.19E+04	7.64E+03	1.09E+04	1.33E+04	1.32E+04	1.45E+04	1.75E+04	1.48E+04	1.52E+04	1.36E+04	1.33E+04	2.55E+03
SO3 in ash	Ton	1.25E+05	7.75E+04	1.08E+05	1.35E+05	1.22E+05	1.26E+05	1.47E+05	1.24E+05	1.44E+05	1.31E+05	1.24E+05	1.88E+04
Al	Ton	5.47E+04	2.58E+04	2.92E+04	3.63E+04	3.56E+04	3.57E+04	3.81E+04	3.67E+04	4.21E+04	3.51E+04	3.69E+04	7.31E+03
Mg	Ton	4.36E+03	2.07E+03	1.63E+03	2.02E+03	1.86E+03	1.68E+03	1.50E+03	1.66E+03	2.24E+03	1.79E+03	2.08E+03	7.90E+02
K	Ton	3.32E+03	1.50E+03	1.41E+03	1.61E+03	1.52E+03	1.37E+03	1.06E+03	1.20E+03	1.75E+03	1.40E+03	1.61E+03	5.97E+02
Fe	Ton	2.11E+04	1.23E+04	1.64E+04	1.95E+04	1.72E+04	1.70E+04	1.77E+04	1.54E+04	2.00E+04	1.81E+04	1.75E+04	2.37E+03
P	Ton	1.03E+03	4.93E+02	4.21E+02	5.24E+02	4.86E+02	4.51E+02	4.27E+02	4.50E+02	5.84E+02	4.74E+02	5.34E+02	1.72E+02
S	Ton	3.22E+04	1.84E+04	2.52E+04	3.00E+04	2.70E+04	2.70E+04	2.86E+04	2.49E+04	3.13E+04	2.82E+04	2.73E+04	3.73E+03
Cd	Kg	5.53E+02	3.30E+02	4.19E+02	5.28E+02	4.86E+02	5.04E+02	5.91E+02	5.11E+02	5.76E+02	5.15E+02	5.01E+02	7.33E+01
Cr	Kg	8.62E+04	3.82E+04	3.10E+04	3.80E+04	4.09E+04	4.07E+04	4.05E+04	4.36E+04	4.78E+04	3.66E+04	4.44E+04	1.46E+04
Cu	Kg	6.73E+04	3.31E+04	4.26E+04	5.29E+04	5.22E+04	5.37E+04	5.99E+04	5.53E+04	6.11E+04	5.22E+04	5.30E+04	9.11E+03
Hg	Kg	3.49E+02	1.78E+02	4.24E+02	2.50E+02	3.96E+02	4.59E+02	2.59E+02	2.41E+02	2.81E+02	2.40E+02	3.08E+02	8.84E+01
Ni	Kg	4.95E+04	2.62E+04	3.01E+04	3.70E+04	3.52E+04	3.57E+04	3.90E+04	3.57E+04	4.13E+04	3.56E+04	3.65E+04	5.91E+03
Pb	Kg	1.97E+04	1.02E+04	1.28E+04	1.57E+04	1.32E+04	1.22E+04	1.20E+04	1.11E+04	1.59E+04	1.42E+04	1.37E+04	2.64E+03
V	Kg	1.14E+05	5.73E+04	7.37E+04	9.15E+04	9.15E+04	9.57E+04	1.09E+05	9.94E+04	1.07E+05	9.13E+04	9.30E+04	1.61E+04
Zn	Kg	1.08E+05	5.67E+04	6.48E+04	8.18E+04	6.72E+04	6.09E+04	6.06E+04	5.63E+04	8.23E+04	7.29E+04	7.11E+04	1.52E+04

Table VIII - 2 - Dataset of model output/targets for supervised learning: atmospheric emissions at yellow, effluent emissions at blue and solid waste and by-products at white. Source: EDP [67].

Targets dataset for learning

Feature		2009	2010	2011	2012	2013	2014	2015	2016	2017	2018	μ	σ
SO2	ton	5.71E+03	2.38E+03	3.00E+03	3.80E+03	4.05E+03	3.87E+03	4.86E+03	3.47E+03	4.34E+03	3.81E+03	3.93E+03	8.80E+02
Nox	ton	4.93E+03	2.76E+03	4.73E+03	3.83E+03	4.62E+03	4.46E+03	5.52E+03	4.56E+03	5.30E+03	4.07E+03	4.48E+03	7.48E+02
Particles	ton	1.95E+02	1.00E+02	6.87E+01	1.78E+02	4.40E+01	3.50E+01	1.60E+01	1.90E+01	3.90E+01	7.00E+01	7.65E+01	6.01E+01
CO	ton	8.89E+02	4.95E+02	1.29E+03	1.60E+03	3.68E+03	2.97E+02	2.65E+02	5.71E+02	4.13E+02	6.11E+02	1.01E+03	9.81E+02
COV	ton	1.28E+01	5.45E+00	8.90E+00	1.11E+01	9.04E+01	6.52E+01	3.62E+01	8.47E+01	1.70E+02	1.84E+02	6.68E+01	6.26E+01
Heavy metals	ton	1.60E+01	5.66E-01	1.58E+00	1.96E+00	5.21E+00	7.93E+00	2.35E+00	8.36E+00	9.76E+00	6.76E+00	6.05E+00	4.51E+00
COD	ton	4.37E+04	1.98E+04	2.47E+04	3.48E+04	2.65E+04	2.50E+04	2.56E+04	2.81E+04	2.83E+04	2.54E+04	2.82E+04	6.28E+03
K+	ton	2.63E+03	4.37E+03	5.87E+03	8.14E+03	6.58E+03	7.70E+03	9.63E+03	9.13E+03	1.07E+04	1.40E+04	7.87E+03	3.09E+03
Sulphates	ton	5.29E+05	3.37E+05	4.19E+05	5.88E+05	6.51E+05	4.91E+05	6.79E+05	8.35E+05	7.89E+05	3.51E+05	5.67E+05	1.64E+05
Sulphites	ton	8.23E+01	5.55E+01	1.33E+02	1.84E+02	1.47E+02	1.26E+02	1.18E+02	9.77E+01	1.08E+02	7.37E+01	1.13E+02	3.58E+01
Sulphides	ton	1.23E+00	3.70E+00	2.66E+00	3.68E+00	2.94E+00	1.52E+00	1.18E+00	3.52E+00	1.08E+00	9.96E-01	2.25E+00	1.10E+00
Total suspended solids	ton	1.46E+04	4.06E+03	9.83E+03	1.39E+04	7.07E+03	6.64E+03	1.16E+04	8.63E+03	6.20E+03	8.60E+03	9.11E+03	3.23E+03
Al	ton	3.47E+02	1.31E+02	1.78E+02	2.59E+02	2.87E+02	2.80E+02	2.71E+02	1.65E+02	2.31E+02	1.45E+02	2.29E+02	6.79E+01
Ar (total)	ton	4.91E+00	1.35E+00	1.59E+00	2.29E+00	1.98E+00	1.62E+00	1.28E+00	1.80E+00	1.38E+00	2.46E+00	2.07E+00	1.02E+00
Cd	ton	8.23E-02	1.85E-01	2.66E-01	3.68E-01	2.94E-01	2.53E-01	9.44E-01	4.30E+00	2.17E+00	1.99E-01	9.06E-01	1.28E+00
Pb (total)	ton	3.70E+00	1.74E+00	1.59E+00	2.29E+00	1.12E+02	1.32E+02	8.54E+00	1.20E+01	9.18E+00	8.06E-01	2.83E+01	4.71E+01
Cu (total)	ton	3.87E+00	5.25E+00	1.46E+01	2.08E+01	1.39E+01	1.20E+01	1.56E+00	2.18E+00	1.57E+00	1.07E+00	7.69E+00	6.69E+00
Cr (total)	ton	2.58E+00	1.93E+00	5.32E+00	7.44E+00	1.13E+01	6.63E+00	5.81E+00	5.51E+00	6.79E+00	8.70E-01	5.42E+00	2.89E+00
Fe (total)	ton	5.82E+01	1.18E+02	6.78E+01	9.76E+01	1.49E+02	6.87E+01	9.34E+01	1.44E+02	8.15E+01	4.32E+01	9.21E+01	3.37E+01
Mg	ton	5.69E+04	8.67E+04	1.63E+05	2.26E+05	1.51E+05	1.69E+05	1.81E+05	1.27E+05	1.92E+05	1.91E+05	1.54E+05	4.88E+04
Hg (total)	ton	4.58E+00	3.78E+00	2.66E+00	3.71E+00	1.01E+01	6.93E+00	1.66E+01	4.90E+00	3.13E+00	8.51E-01	5.73E+00	4.35E+00
Ni (total)	ton	3.46E+01	1.14E+01	2.66E+01	3.82E+01	3.74E+01	2.70E+01	1.61E+01	4.34E+01	5.28E+01	1.61E+01	3.04E+01	1.26E+01
Vanadium	ton	5.48E+01	6.11E+01	1.66E+02	2.39E+02	2.18E+02	1.89E+02	1.49E+02	2.10E+02	1.61E+02	1.17E+02	1.56E+02	5.96E+01
Zn (total)	ton	2.07E+01	1.60E+01	5.85E+00	8.48E+00	1.37E+01	1.06E+01	1.76E+01	2.22E+01	1.23E+01	3.23E+00	1.31E+01	5.90E+00
N total	ton	2.47E+04	1.25E+03	1.06E+03	1.57E+03	2.06E+03	1.99E+03	8.39E+02	2.00E+03	1.14E+03	4.89E+02	3.71E+03	7.02E+03
F	ton	5.06E+02	4.97E+02	4.54E+02	6.76E+02	6.96E+01	1.12E+02	3.25E+01	8.89E+01	4.60E+01	4.08E+01	2.52E+02	2.37E+02
NO3	ton	9.44E+04	4.53E+03	3.32E+03	4.94E+03	4.22E+03	3.12E+03	1.52E+03	1.71E+03	1.73E+03	6.39E+02	1.20E+04	2.75E+04
Mn (total)	ton	6.32E+02	3.39E+01	3.00E+01	4.47E+01	1.65E+01	1.43E+01	1.72E+01	2.95E+01	8.47E+00	4.62E+01	8.72E+01	1.82E+02
BOD	ton	1.24E+03	2.86E+02	3.72E+02	5.54E+02	9.53E+02	7.51E+02	4.45E+02	1.29E+03	5.54E+02	3.53E+02	6.79E+02	3.47E+02
Fly ash (in landfill)	ton	1.30E+04	9.06E+03	3.98E+04	1.21E+05	3.49E+04	1.56E+04	7.59E+02	9.80E+02	6.84E+02	0.00E+00	2.36E+04	3.52E+04
Coal slag produced	ton	3.68E+04	2.52E+04	2.64E+04	3.01E+04	3.61E+04	3.82E+04	4.35E+04	3.10E+04	3.73E+04	1.52E+04	3.20E+04	7.75E+03
Fly ash produced	ton	3.33E+05	1.71E+05	1.95E+05	1.90E+05	2.17E+05	3.86E+05	3.70E+05	1.45E+05	2.91E+05	2.33E+05	2.53E+05	8.19E+04
Gypsum produced	ton	1.73E+05	8.93E+03	1.14E+05	7.97E+04	1.08E+05	1.78E+05	1.37E+05	1.09E+05	1.40E+05	1.26E+05	1.17E+05	4.58E+04

Table VIII - 3 - Inputs dataset for predicting emissions for the 4 scenarios tested. For each scenario, the right column is the result from standardization by Z-score method (Z=(x-μ)/σ) applied in python on pre-processing step.

Inputs dataset for predicting

Input features		5k		AVminus		AV		AVplus	
Generated Energy	GWh	5.00E+03	-2.68E+00	7.34E+03	-9.76E-01	9.17E+03	3.63E-01	1.10E+04	1.70E+00
N	ton	2.64E+04	-2.26E+00	3.87E+04	-7.68E-01	4.84E+04	4.07E-01	5.81E+04	1.58E+00
Sulfur	ton	2.22E+04	-2.75E+00	3.26E+04	-1.21E+00	4.07E+04	-1.14E-02	4.89E+04	1.19E+00
Calorific value	GJ	4.74E+07	-1.66E+00	6.96E+07	-4.86E-01	8.70E+07	4.38E-01	1.04E+08	1.36E+00
Sulfate in Sulfur	ton	8.64E+02	-2.70E+00	1.27E+03	-1.04E+00	1.59E+03	2.63E-01	1.90E+03	1.57E+00
Ash Yeld	ton	1.21E+05	-3.08E+00	1.77E+05	-1.30E+00	2.21E+05	9.99E-02	2.65E+05	1.50E+00
SiO2	ton	8.32E+05	-1.93E+00	1.22E+06	-6.03E-01	1.53E+06	4.40E-01	1.83E+06	1.48E+00
Al2O3 of ash	ton	5.37E+05	-1.69E+00	7.88E+05	-4.85E-01	9.85E+05	4.63E-01	1.18E+06	1.41E+00
CaO of ash	ton	4.03E+04	-3.99E+00	5.91E+04	-1.75E+00	7.39E+04	3.13E-03	8.87E+04	1.76E+00
MgO of ash	ton	1.69E+04	-2.76E+00	2.48E+04	-1.02E+00	3.09E+04	3.36E-01	3.71E+04	1.70E+00
Na2O of ash	ton	8.44E+03	-3.74E+00	1.24E+04	-1.87E+00	1.55E+04	-4.09E-01	1.86E+04	1.06E+00
K2O of ash	ton	1.11E+04	-2.65E+00	1.63E+04	-1.21E+00	2.04E+04	-8.18E-02	2.45E+04	1.05E+00
Fe2O3 of ash	ton	1.50E+05	-2.88E+00	2.21E+05	-1.21E+00	2.76E+05	1.02E-01	3.31E+05	1.41E+00
TiO2 of ash	ton	2.88E+04	-1.62E+00	4.22E+04	-4.49E-01	5.28E+04	4.69E-01	6.33E+04	1.39E+00
P2O5 in ash	ton	7.76E+03	-2.16E+00	1.14E+04	-7.34E-01	1.42E+04	3.82E-01	1.71E+04	1.50E+00
SO3 in ash	ton	7.10E+04	-2.82E+00	1.04E+05	-1.06E+00	1.30E+05	3.32E-01	1.56E+05	1.72E+00
Al	ton	2.02E+04	-2.29E+00	2.96E+04	-9.97E-01	3.70E+04	1.55E-02	4.45E+04	1.03E+00
Mg	ton	1.01E+03	-1.36E+00	1.48E+03	-7.63E-01	1.85E+03	-2.96E-01	2.22E+03	1.72E-01
K	ton	7.70E+02	-1.41E+00	1.13E+03	-8.11E-01	1.41E+03	-3.37E-01	1.70E+03	1.36E-01
Fe	ton	9.47E+03	-3.38E+00	1.39E+04	-1.51E+00	1.74E+04	-4.07E-02	2.08E+04	1.43E+00
P	ton	2.67E+02	-1.55E+00	3.92E+02	-8.28E-01	4.90E+02	-2.59E-01	5.88E+02	3.10E-01
S	ton	1.50E+04	-3.30E+00	2.20E+04	-1.42E+00	2.75E+04	5.08E-02	3.30E+04	1.53E+00
Cd	kg	2.85E+02	-2.96E+00	4.18E+02	-1.14E+00	5.22E+02	2.85E-01	6.27E+02	1.71E+00
Cr	kg	2.27E+04	-1.49E+00	3.33E+04	-7.57E-01	4.17E+04	-1.85E-01	5.00E+04	3.88E-01
Cu	kg	2.99E+04	-2.54E+00	4.39E+04	-1.00E+00	5.49E+04	2.06E-01	6.59E+04	1.41E+00
Hg	kg	1.35E+02	-1.95E+00	1.98E+02	-1.24E+00	2.48E+02	-6.75E-01	2.97E+02	-1.15E-01
Ni	kg	2.00E+04	-2.80E+00	2.93E+04	-1.22E+00	3.67E+04	2.49E-02	4.40E+04	1.27E+00
Pb	kg	7.28E+03	-2.43E+00	1.07E+04	-1.14E+00	1.34E+04	-1.30E-01	1.60E+04	8.82E-01
V	kg	5.29E+04	-2.49E+00	7.76E+04	-9.59E-01	9.70E+04	2.47E-01	1.16E+05	1.45E+00
Zn	kg	3.74E+04	-2.22E+00	5.49E+04	-1.07E+00	6.87E+04	-1.63E-01	8.24E+04	7.42E-01

TableVIII - 4 - Results obtained from feed-forward ANN predictions. For each scenario, the results obtained directly by the model are standardized and presented at left.

Results obtained from predicting

Targets		5k		AVminus		AV		AVplus	
SO2	ton	4.0E+03	8.5E-02	3.9E+03	2.4E-02	4.1E+03	1.6E-01	4.5E+03	6.3E-01
Nox	ton	4.6E+03	1.5E-01	4.5E+03	5.0E-02	4.7E+03	2.5E-01	5.2E+03	9.5E-01
Particles	ton	8.4E+01	1.2E-01	7.9E+01	4.0E-02	8.9E+01	2.0E-01	1.2E+02	7.7E-01
CO	ton	8.6E+02	-1.5E-01	9.7E+02	-4.4E-02	7.9E+02	-2.3E-01	1.5E+02	-8.8E-01
COV	ton	7.6E+01	1.4E-01	6.9E+01	4.1E-02	8.0E+01	2.1E-01	1.2E+02	8.3E-01
Heavy metals	ton	5.9E+00	-3.5E-02	6.0E+00	-1.3E-02	5.8E+00	-4.5E-02	5.3E+00	-1.6E-01
COD	ton	2.8E+04	-9.5E-02	2.8E+04	-3.3E-02	2.7E+04	-1.8E-01	2.4E+04	-6.9E-01
K+	ton	7.7E+03	-6.8E-02	7.8E+03	-2.5E-02	7.5E+03	-1.3E-01	6.3E+03	-4.9E-01
Sulphates	ton	5.9E+05	1.4E-01	5.7E+05	4.0E-02	6.0E+05	2.1E-01	7.0E+05	8.3E-01
Sulphites	ton	1.1E+02	-9.4E-02	1.1E+02	-2.7E-02	1.1E+02	-1.8E-01	8.8E+01	-6.9E-01
Sulphides	ton	2.1E+00	-9.7E-02	2.2E+00	-2.8E-02	2.0E+00	-1.9E-01	1.4E+00	-7.4E-01
Total suspended solids	ton	8.6E+03	-1.6E-01	9.0E+03	-4.6E-02	8.3E+03	-2.5E-01	5.9E+03	-9.8E-01
Al	ton	2.4E+02	1.4E-01	2.3E+02	4.6E-02	2.4E+02	2.0E-01	2.8E+02	7.5E-01
Ar (total)	ton	2.1E+00	-8.9E-03	2.1E+00	-4.6E-03	2.1E+00	1.6E-02	2.1E+00	7.4E-02
Cd	ton	9.8E-01	5.9E-02	9.3E-01	1.6E-02	1.1E+00	1.1E-01	1.5E+00	4.4E-01
Pb (total)	ton	2.4E+01	-8.5E-02	2.7E+01	-2.9E-02	2.1E+01	-1.5E-01	2.0E+00	-5.6E-01
Cu (total)	ton	8.0E+00	4.0E-02	7.8E+00	1.5E-02	8.0E+00	4.2E-02	8.7E+00	1.5E-01
Cr (total)	ton	5.9E+00	1.5E-01	5.5E+00	4.4E-02	6.2E+00	2.6E-01	8.3E+00	1.0E+00
Fe (total)	ton	9.7E+01	1.3E-01	9.4E+01	4.3E-02	9.8E+01	1.8E-01	1.1E+02	6.7E-01
Mg	ton	1.5E+05	-3.1E-03	1.5E+05	-4.7E-03	1.5E+05	-3.4E-02	1.5E+05	-1.2E-01
Hg (total)	ton	5.1E+00	-1.5E-01	5.5E+00	-4.8E-02	4.7E+00	-2.3E-01	2.0E+00	-8.5E-01
Ni (total)	ton	3.2E+01	1.7E-01	3.1E+01	5.3E-02	3.3E+01	2.4E-01	4.2E+01	9.1E-01
Vanadium	ton	1.5E+02	-1.5E-01	1.5E+02	-4.5E-02	1.4E+02	-2.6E-01	9.6E+01	-1.0E+00
Zn (total)	ton	1.3E+01	1.4E-02	1.3E+01	6.1E-03	1.3E+01	-1.5E-02	1.3E+01	-6.8E-02
N total	ton	3.0E+03	-1.1E-01	3.5E+03	-3.5E-02	2.7E+03	-1.4E-01	-5.5E+01	-5.4E-01
F	ton	2.7E+02	9.0E-02	2.6E+02	3.1E-02	2.9E+02	1.5E-01	3.9E+02	5.7E-01
NO3	ton	1.4E+04	6.2E-02	1.2E+04	1.5E-02	1.4E+04	6.8E-02	1.9E+04	2.7E-01
Mn (total)	ton	9.8E+01	5.9E-02	9.0E+01	1.6E-02	1.1E+02	1.1E-01	1.7E+02	4.3E-01
BOD	ton	6.8E+02	-4.5E-03	6.8E+02	-4.9E-03	6.7E+02	-2.8E-02	6.5E+02	-9.5E-02
Fly ash (in landfill)	ton	2.2E+04	-5.8E-02	2.3E+04	-1.6E-02	1.9E+04	-1.3E-01	5.6E+03	-5.1E-01

For all scenarios the same coal composition was given as input, thus it was expected a slight increase or even decrease of emissions with the increase of electricity generated by the plant, in a regular behaviour. However, results describe irregular and hyperbolic behaviours for most of the emissions. The reason may be linked to an overfitting of the models to the original dataset, which is common for models trained with small sample sizes (with less than 100 samples). While overfitting, the model will reduce the loss function, improving its precision and accuracy but compromising its predictive power for other input datasets. None of the models were good enough for predicting emissions. Hence, their use was disregard and the sensitivity analysis to different operation scenarios (corresponding to different utilization rates or electricity produced) was not performed for Sines powerplant.

Figure 1 shows the results obtained by the k-fold ANN used for predicting emissions under different operation scenarios i.e. producing different ranges of electricity annually.

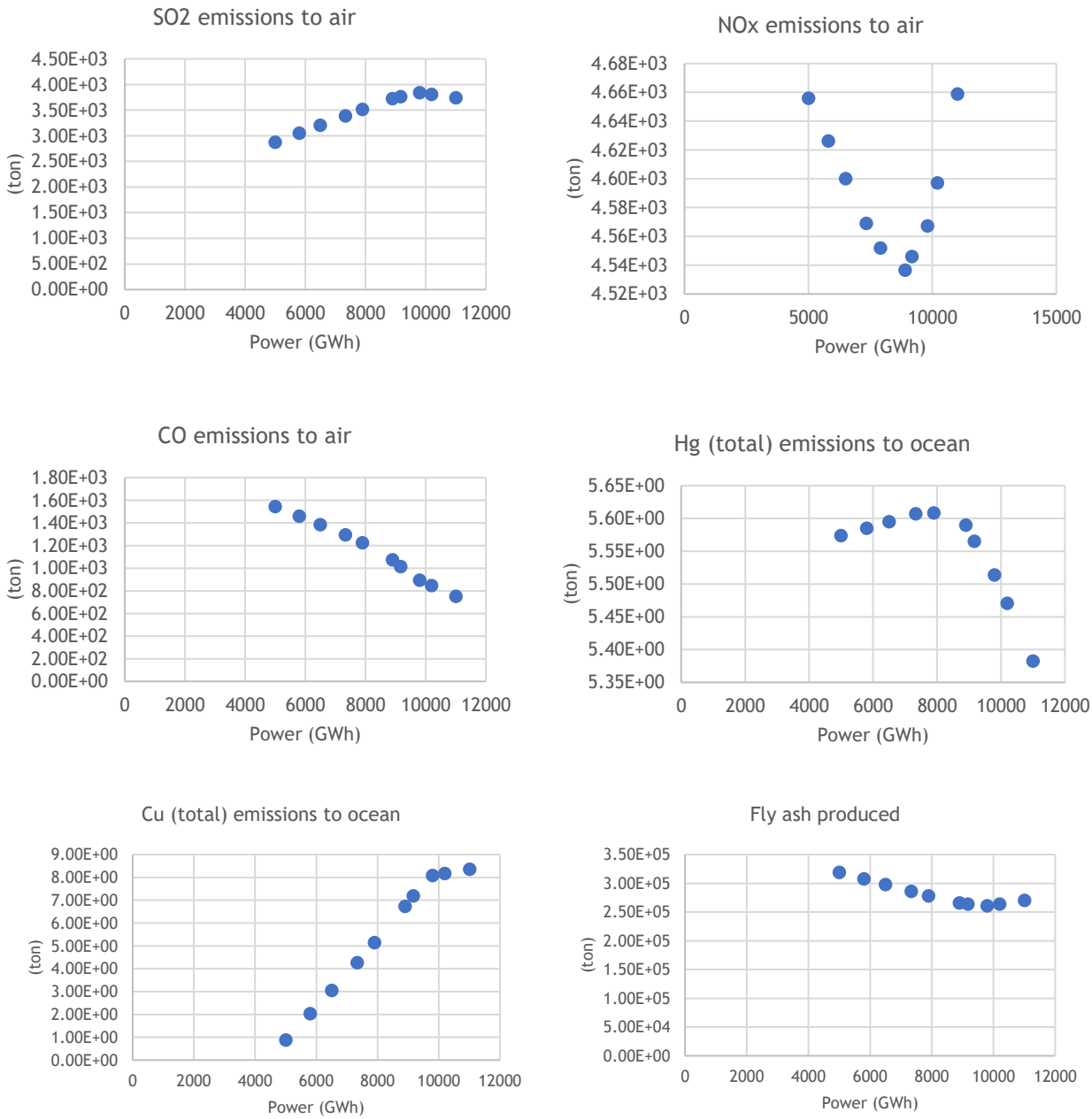

Figure VIII - 1 - Representation of some of the results obtained for different operation scenarios by the ANN modelled.

Appendix IX – HGtS operation data provided by Net4CO_2

The data provided by Net4CO_2, regarding the operation of HGtS unit is presented in the table below. The parameters are calculated based on the input of CO_2 flow rate, based on theoretical relations, simulations and one experimental parameter obtained from tests on laboratory scale units.

Table IX - 1 - Raw data regarding HGtS unit's operation.

Process description		***Sines (2014)***	***Sines (2016)***	***Sines (2018)***	***Ribatejo***
Water Input	ton/h	6697	7387	7465	2941
CO2 Input	ton/h	971	1071	1082	426
Thermal fluid #1 (ethylene glycol 27%)	ton/h	117692	129822	131205	51696
Thermal fluid #2 (ethylene glycol 35%)	ton/h	20674	22804	23047	9081
Hydrate formed	ton/h	2911	3211	3245	1279
Total slurry formed	ton/h	7667	8458	8548	3368
Netmix Reactor	MW	308.5	340.3	343.9	135.5
Gas Compressor	MW	16.4	18.1	18.3	7.2
Water Pump	MW	9.0	9.9	10.1	4.0
CO2 Pump	MW	0.9	1.0	1.0	0.4
Transport Pump	MW	0.0	0.0	0.0	0.0
Gas Pre-Cooler HeatEx	MW	8.8	9.8	9.9	3.9
Gas InterCooler HeatEx	MW	24.5	27.0	27.3	10.8
Gas After-Cooler HeatEx	MW	91.5	101.0	102.0	40.2
Water HeatEx	MW	62.7	69.2	69.9	27.5
Recirculation Pump 1	MW	3.6	4.0	4.0	1.6
Recirculation Pump 2	MW	1.1	1.2	1.2	0.5
Refrigeration Chiller 1	MW	54.8	60.5	61.1	24.1
Refrigeration Chiller 2	MW	13.2	14.6	14.8	5.8

Appendix X – Materials requirement of pipeline commissioning for transportation of hydrate slurry

In this section the process from which the materials requirements have resulted is presented. Table 1 shows pipelines parameters and their source. Figure 1 presents the cross section design of the pipeline assumed for the current assessment. Table 1 represents the results of intermediary calculations step-be-step and the final results for the requirement of polyurethane, steel and sand as well as the tonnes-km for materials supply chain, based on standard distances found in Ecoinvent documentation [122] and materials density.

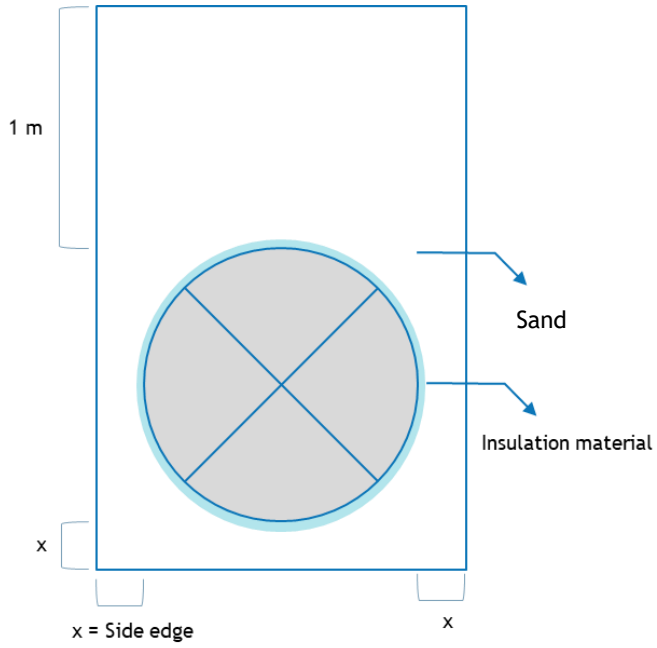

Figure 1 - Cross section of onshore pipeline.

Table 1 - Onshore pipeline parameters.

Pipelines parameteres			**Source**
material		C-steel (A516 Grade 70)	
wall thickness	mm	35	Function of c-steel corrosion by CO2 hydrates slurry (about 1mm/y) [123]
yield strength	MPa	485	[124]
density	kg/m3	7850	[124]
Buried depth	mm	1000	Recommeded by IPCC [111].
Side edges	mm	200	
Sand density	kg/m3	1730	[125]
Lifetime	years	25	[79]
Insulation material		Polyurethane	
Insulation material density	kg/m3	1.25	[126]

The inner diameter of the pipelines and the thickness of the insulation material are outputs from the simulations performed on Aspen, by Net4CO_2. As the use of Unmanned Aerial Vehicle

such as drones for surveying, mapping and infrastructure inspection is becoming more and more frequent, instead of modelling helicopters patrol as it is typically performed for pipelines process [79,113]. It was assumed that per year, the time spend of monitoring per km is about 1 hour and the energy consumed per hour was taken from [127], a 'Lifecycle modeling and assessment of unmanned aerial vehicles (drones)'. The leakage rate of CO_2 was assumed to be half of the leakage rate of natural gas leakages on western European pipeline networks, as its gasification besides slow, is rather unlikely as long as the thermodynamic conditions remain within the expected. The leakage rate of the remaining species is assumed to be the same (this assumption was based on [79]).

Table 2 - Materials requirement for pipelines commissioning and other relevant parameters for LCI.

		Ribatejo	Sines	*Source*
I. Pipelines sizing				
Inner diameter	mm	762	1067	
Outer diameter	mm	797	1102	
II. Heat Loss from Pipelines				
Thickness of insulation material	mm	76	76	
Volume of insulation material p/km	m3	208	281	
Mass of insulation material p/km	kg	261	352	[126]
III. C-Steel requirement				
Pipeline volume p/km	m3	499	953	
Required material p/km	m3	43	60	
Required material p/km	kg	336414	467958	
Plus factor of 3%	%	0	0	For valves, flanges, ect. [79]
Required material p/km with surcharge	kg	346506	481997	[125]
III. Sand requirement				
X	m	1	2	
Y	m	1000	1000	
Z	m	2	2	
Total volume occupied by the trench (p/km)	m3	2899	4058	
Volume of sand (p/km)	m3	2674	3665	
Mass of sand (p/km)	ton	4626	6341	[125]
IV. Transport distances for materials supply chain (by truck/lorry 16-32 t)				[122]
Gravel and crushed stone (72)	tkm	298958	386715	72 km
Plastic and rubbbers	tkm	50	68	193 km
Articles of base metal (34)	tkm	193697	269436	559 km
Total	tkm	492705	656219	824 km
V. Energy required for monitoring by drone				
Annually number of hours per km	h	1		Assumption
Electricity consumption per hour	Wh	21.6		[127]
VI. Leakage rate				
Leakage rate of NG per 1000 km	%	0.019		[84,79]
Carbon dioxide and carbon monoxide	%	0.0095		
Other emissions	%	0.019		

Appendix XI – Raw results

The results obtained from SimaPro software are presented in the current appendix.

Table 1 shows the results obtained for the approach of 'cradle to gate' for the three scenarios modelled: without compensation; downstream compensation with Norwegian grid; downstream compensation with Portuguese grid. The last column refers to reference scenario. The following tables show the results for the 'cradle to grave' approach.

Table XI-1 - Results for NGPP and CPP for 'Cradle to gate' approach.

Natural Gas Power Plant: 'cradle to gate'					
Electricity	**MWh**	**7771842**	**8078000**	**8078000**	**8078000**
Categoria de impacte	Unit	Electricity_NGPP_capture_operation	Electricity_NGPP_capture_operation w/ NO grid	Electricity_NGPP_capture_operation w/ PT grid	Electricity_NGPP_reference_operation
Abiotic depletion	kg Sb eq	1.90E+02	1.90E+02	1.90E+02	1.19E+02
Abiotic depletion (fossil fuels)	MJ	6.36E+10	6.36E+10	6.36E+10	6.32E+10
Global warming (GWP100a)	kg CO2 eq	-2.26E+09	-2.26E+09	-2.26E+09	3.72E+09
Ozone layer depletion (ODP)	kg CFC-11 eq	1.62E+02	1.62E+02	1.62E+02	1.61E+02
Human toxicity	kg 1,4-DB eq	7.47E+07	7.47E+07	7.48E+07	6.60E+07
Fresh water aquatic ecotox.	kg 1,4-DB eq	4.56E+07	4.56E+07	4.56E+07	3.93E+07
Marine aquatic ecotoxicity	kg 1,4-DB eq	1.30E+11	1.30E+11	1.31E+11	1.10E+11
Terrestrial ecotoxicity	kg 1,4-DB eq	6.16E+05	6.16E+05	6.17E+05	5.82E+05
Photochemical oxidation	kg C2H4 eq	1.23E+05	1.23E+05	1.23E+05	1.18E+05
Acidification	kg SO2 eq	2.07E+06	2.07E+06	2.07E+06	1.98E+06
Eutrophication	kg PO4--- eq	4.31E+05	4.31E+05	4.31E+05	3.98E+05
Electricity	MWh	7771842	7771842	7771842	8078000

Coal Power plant: 'cradle to gate'					
Electricity	MWh	7324431	8078000	8078000	8078000
Categoria de impacte	Unit	Electricity_CPP_capture_operation (comp. NO)	Electricity_CPP_capture_operation (PT)	Electricity_CPP_capture_operation w/o compensation	Electricity_CPP_reference_operation
Abiotic depletion	kg Sb eq	4.93E+02	5.04E+02	4.78E+02	3.73E+02
Abiotic depletion (fossil fuels)	MJ	8.96E+10	9.58E+10	8.96E+10	8.90E+10
Global warming (GWP100a)	kg CO2 eq	-6.59E+09	-6.13E+09	-6.59E+09	8.14E+09
Ozone layer depletion (ODP)	kg CFC-11 eq	7.20E+01	1.02E+02	7.15E+01	6.92E+01
Human toxicity	kg 1,4-DB eq	2.81E+09	2.93E+09	2.81E+09	2.79E+09
Fresh water aquatic ecotox.	kg 1,4-DB eq	2.66E+09	2.75E+09	2.66E+09	2.65E+09
Marine aquatic ecotoxicity	kg 1,4-DB eq	1.01E+13	1.07E+13	1.01E+13	1.01E+13
Terrestrial ecotoxicity	kg 1,4-DB eq	3.30E+07	3.35E+07	3.30E+07	3.29E+07
Photochemical oxidation	kg C2H4 eq	4.37E+05	5.90E+05	4.36E+05	4.55E+05
Acidification	kg SO2 eq	1.34E+07	1.75E+07	1.34E+07	1.32E+07
Eutrophication	kg PO4--- eq	1.86E+07	1.93E+07	1.86E+07	1.85E+07

Table XI-2 - Results for CPP for approach 'cradle to grave' using Norwegian grid.

CPP w/NO grid			800 m of injection				1650 m of injection				2500 m of injection			
Categoria de impacte	Unidade	Totalt	Electricity_CPP_capture_operation w/o compensation	Transport of hyrates by pipeline (CPP)	Injection on+off, h=800 (coal)	Totalt	Electricity_CPP_capture_operation w/o compensation	Transport of hyrates by pipeline (CPP)	Injection on+off, h=1650 (coal)	Totalt	Electricity_CPP_capture_operation w/o compensation	Transport of hyrates by pipeline (CPP)	Injection on+off, h=2500 (coal)	
Abiotic depletion	kg Sb eq	3645.769	484.0172	2630.713	531.0387	4206.98763	484.0172	2630.713	1092.257	8892.71	484.01725	2630.713	5777.979	
Abiotic depletion (fossil fuels)	MJ	1.12E+11	8.96E+10	1.76E+10	4.78E+09	1.1665E+11	8.96E+10	1.76E+10	9.47E+09	1.25E+11	8.9599E+10	1.76E+10	1.82E+10	
Global warming (GWP100a)	kg CO2 eq	-5.4E+09	-6.6E+09	8.46E+08	3.46E+08	-5060681496	-6.6E+09	8.46E+08	6.86E+08	-4.4E+09	-6593262180	8.46E+08	1.39E+09	
Ozone layer depletion (ODP)	kg CFC-11 eq	185.6781	71.54846	73.91364	40.21598	225.13522	71.54846	73.91364	79.67312	297.5857	71.5484619	73.91364	152.1236	
Human toxicity	kg 1,4-DB eq	3.55E+09	2.81E+09	6.61E+08	79027978	3630624883	2.81E+09	6.61E+08	1.61E+08	4.04E+09	2808455489	6.61E+08	5.69E+08	
Fresh water aquatic ecotox.	kg 1,4-DB eq	3.45E+09	2.66E+09	7.53E+08	31634026	3480386465	2.66E+09	7.53E+08	64465887	3.66E+09	2662601061	7.53E+08	2.47E+08	
Marine aquatic ecotoxicity	kg 1,4-DB eq	1.18E+13	1.01E+13	1.53E+12	8.5E+10	1.1849E+13	1.01E+13	1.53E+12	1.73E+11	1.22E+13	1.0145E+13	1.53E+12	5.55E+11	
Terrestrial ecotoxicity	kg 1,4-DB eq	48265966	33000416	14857015	408534.5	48685159.5	33000416	14857016	827728.1	50718459	33000415.8	14857015	2861028	
Photochemical oxidation	kg C2H4 eq	1013942	436071.6	463578.2	114291.9	1126584.67	436071.6	463578.2	226934.9	140113	436071.594	463578.2	501482.9	
Acidification	kg SO2 eq	21565593	13377213	4994509	3193870	24689546.2	13377213	4994509	6317823	30059284	13377213.4	4994509	11687562	
Eutrophication	kg PO4--- eq	22269855	18603955	2911894	754006.1	23010373.4	18603955	2911894	1494524	24479039	18603954.7	2911894	2963190	

Table XI-3 - Results for CPP for approach 'cradle to grave' using Portuguese grid.

PT grid			800 m of injection				1650 m of injection				2500 m of injection			
Categoria de impacte	Unidade	Totalt	Electricity_CPP_capture_operation w/o compensation	Transport of hyrates by pipeline (CPP)	Injection on+off, h=800 (coal)	Totalt	Electricity_CPP_capture_operation w/o compensation	Transport of hyrates by pipeline (CPP)	Injection on+off, h=1650 (coal)	Totalt	Electricity_CPP_capture_operation w/o compensation	Transport of hyrates by pipeline (CPP)	Injection on+off, h=2500 (coal)	
Abiotic depletion	kg Sb eq	3645.769	3.67E+03	4.84E+02	2.64E+03	5.42E+02	4.20E+03	4.84E+02	2.64E+03	1.07E+03	8.91E+03	4.84E+02	2.64E+03	
Abiotic depletion (fossil fuels)	MJ	1.12E+11	1.24E+11	8.96E+10	2.34E+10	1.07E+10	1.25E+11	8.96E+10	2.34E+10	1.25E+10	1.35E+11	8.96E+10	2.34E+10	
Global warming (GWP100a)	kg CO2 eq	-5.4E+09	-4.52E+09	-6.59E+09	1.28E+09	7.91E+08	-4.41E+09	-6.59E+09	1.28E+09	9.06E+08	-3.61E+09	-6.59E+09	1.28E+09	
Ozone layer depletion (ODP)	kg CFC-11 eq	185.6781	2.42E+02	7.15E+01	1.02E+02	6.89E+01	2.67E+02	7.15E+01	1.02E+02	9.33E+01	3.46E+02	7.15E+01	1.02E+02	
Human toxicity	kg 1,4-DB eq	3.55E+09	3.77E+09	2.81E+09	7.72E+08	1.92E+08	3.79E+09	2.81E+09	7.72E+08	2.08E+08	4.23E+09	2.81E+09	7.72E+08	
Fresh water aquatic ecotox.	kg 1,4-DB eq	3.45E+09	3.63E+09	2.66E+09	8.42E+08	1.23E+08	3.61E+09	2.66E+09	8.42E+08	1.09E+08	3.82E+09	2.66E+09	8.42E+08	
Marine aquatic ecotoxicity	kg 1,4-DB eq	1.18E+13	1.28E+13	1.01E+13	2.06E+12	6.28E+11	1.27E+13	1.01E+13	2.06E+12	4.52E+11	1.31E+13	1.01E+13	2.06E+12	
Terrestrial ecotoxicity	kg 1,4-DB eq	48265966	4.92E+07	3.30E+07	1.53E+07	8.97E+05	4.94E+07	3.30E+07	1.53E+07	1.05E+06	5.15E+07	3.30E+07	1.53E+07	
Photochemical oxidation	kg C2H4 eq	1013942	1.32E+06	4.36E+05	6.14E+05	2.69E+05	1.36E+06	4.36E+05	6.14E+05	3.11E+05	1.66E+06	4.36E+05	6.14E+05	
Acidification	kg SO2 eq	21565593	2.98E+07	1.34E+07	9.06E+06	7.35E+06	3.10E+07	1.34E+07	9.06E+06	8.60E+06	3.70E+07	1.34E+07	9.06E+06	
Eutrophication	kg PO4--- eq	22269855	2.37E+07	1.86E+07	3.60E+06	1.46E+06	2.41E+07	1.86E+07	3.60E+06	1.86E+06	2.57E+07	1.86E+07	3.60E+06	

Table XI-4 - Results for CPP for ship scenarios

CPP			Ship without cooling (1650 m)				Ship with cooling system (1650 m)			
Categoria de impacte	Unidade	TotalI	Electricity_CPP_capture_operation w/o compensation	Transport of hyrates by pipeline (CPP)	Injection on+off, h=800 (coal)	TotalI	Electricity_CPP_capture_operation w/o compensation	Transport of hyrates by pipeline (CPP)	Injection on+off, h=1650 (coal)	TotalI
Abiotic depletion	kg Sb eq	3645.769	1.05E+06	4.84E+02	1.04E+06	1.05E+03	1.98E+03	4.84E+02	4.44E+02	1.05E+03
Abiotic depletion (fossil fuels)	MJ	1.12E+11	2.42E+12	8.96E+10	2.32E+12	1.10E+10	2.57E+11	8.96E+10	1.56E+11	1.10E+10
Global warming (GWP100a)	kg CO2 eq	-5.4E+09	1.57E+11	-6.59E+09	1.63E+11	7.81E+08	6.79E+09	-6.59E+09	1.26E+10	7.81E+08
Ozone layer depletion (ODP)	kg CFC-11 eq	185.6781	4.61E+04	7.15E+01	4.59E+04	9.39E+01	1.86E+02	7.15E+01	2.08E+01	9.39E+01
Human toxicity	kg 1,4-DB eq	3.55E+09	3.36E+10	2.81E+09	3.06E+10	1.34E+08	3.42E+09	2.81E+09	4.74E+08	1.34E+08
Fresh water aquatic ecotox.	kg 1,4-DB eq	3.45E+09	2.00E+10	2.66E+09	1.73E+10	5.40E+07	2.72E+09	2.66E+09	5.71E+06	5.40E+07
Marine aquatic ecotoxicity	kg 1,4-DB eq	1.18E+13	1.05E+14	1.01E+13	9.43E+13	1.32E+11	1.04E+13	1.01E+13	1.49E+11	1.32E+11
Terrestrial ecotoxicity	kg 1,4-DB eq	48265966	1.83E+08	3.30E+07	1.49E+08	7.61E+05	3.43E+07	3.30E+07	4.95E+05	7.61E+05
Photochemical oxidation	kg C2H4 eq	1013942	7.67E+07	4.36E+05	7.60E+07	2.71E+05	2.11E+07	4.36E+05	2.04E+07	2.71E+05
Acidification	kg SO2 eq	21565593	1.99E+09	1.34E+07	1.97E+09	7.66E+06	4.38E+08	1.34E+07	4.17E+08	7.66E+06
Eutrophication	kg PO4--- eq	22269855	3.99E+08	1.86E+07	3.78E+08	1.77E+06	5.99E+07	1.86E+07	3.95E+07	1.77E+06

Table XI-5 - Results from Monte Carlo simulation on CPP designed model (pipeline transport and injection at 1650 m)

Impact Category	Unidade	Média	Mediana	SD	CV	2,5%	97,5%	SEM
Abiotic depletion	kg Sb eq	4.16E+03	3.94E+03	1.01E+03	2.43E+01	2.83E+03	6.58E+03	3.20E+01
Abiotic depletion (fossil fuels)	MJ	1.25E+11	1.25E+11	6.16E+09	4.93E+00	1.13E+11	1.38E+11	1.95E+08
Acidification	kg SO2 eq	3.08E+07	2.95E+07	6.49E+06	2.11E+01	2.21E+07	4.66E+07	2.05E+05
Eutrophication	kg PO4--- eq	2.40E+07	2.03E+07	1.37E+07	5.71E+01	1.08E+07	6.13E+07	4.33E+05
Fresh water aquatic ecotox.	kg 1,4-DB eq	3.61E+09	3.18E+09	1.89E+09	5.23E+01	1.74E+09	7.21E+09	5.97E+07
Global warming (GWP100a)	kg CO2 eq	-4.42E+09	-4.44E+09	2.42E+08	-5.47E+00	-4.82E+09	-3.87E+09	7.65E+06
Human toxicity	kg 1,4-DB eq	3.73E+09	3.32E+09	1.58E+09	4.25E+01	2.24E+09	7.91E+09	5.01E+07
Marine aquatic ecotoxicity	kg 1,4-DB eq	1.27E+13	1.17E+13	4.49E+12	3.54E+01	7.53E+12	2.43E+13	1.42E+11
Ozone layer depletion (ODP)	kg CFC-11 eq	2.67E+02	2.55E+02	6.66E+01	2.50E+01	1.67E+02	4.28E+02	2.11E+00
Photochemical oxidation	kg C2H4 eq	1.36E+06	1.30E+06	2.83E+05	2.09E+01	9.59E+05	2.09E+06	8.96E+03
Terrestrial ecotoxicity	kg 1,4-DB eq	4.98E+07	4.98E+07	2.68E+07	5.39E+01	-2.83E+06	1.06E+08	8.49E+05

Table XI-6 - Results for NGPP for approach 'cradle to grave' using Norwegian grid and considering offshore injection.

NGPP - NO grid (offshore)			800 m of injection				1650 m of injection				2500 m of injection			
Categoria de impacte	Unidade	Totalt	Electricity_CPP_capture_operation w/o compensation	Transport of hyrates by pipeline (CPP)	Injection on+off, h=800 (coal)	Totalt	Electricity_CPP_capture_operation w/o compensation	Transport of hyrates by pipeline (CPP)	Injection on+off, h=1650 (coal)	Totalt	Electricity_CPP_capture_operation w/o compensation	Transport of hyrates by pipeline (CPP)	Injection on+off, h=2500 (coal)	
Abiotic depletion	kg Sb eq	3645.769	3.31E+02	1.90E+02	1.06E+02	3.46E+01	3.67E+02	1.90E+02	1.06E+02	7.12E+01	4.04E+02	1.90E+02	1.06E+02	
Abiotic depletion (fossil fuels)	MJ	1.12E+11	6.46E+10	6.36E+10	6.26E+08	3.61E+08	6.49E+10	6.36E+10	6.26E+08	7.14E+08	6.53E+10	6.36E+10	6.26E+08	
Global warming (GWP100a)	kg CO2 eq	-5.4E+09	-2.20E+09	-2.26E+09	3.27E+07	2.56E+07	-2.17E+09	-2.26E+09	3.27E+07	5.08E+07	-2.15E+09	-2.26E+09	3.27E+07	
Ozone layer depletion (ODP)	kg CFC-11 eq	185.6781	1.68E+02	1.62E+02	2.88E+00	3.08E+00	1.71E+02	1.62E+02	2.88E+00	6.10E+00	1.74E+02	1.62E+02	2.88E+00	
Human toxicity	kg 1,4-DB eq	3.55E+09	1.03E+08	7.47E+07	2.43E+07	4.40E+06	1.08E+08	7.47E+07	2.43E+07	8.93E+06	1.13E+08	7.47E+07	2.43E+07	
Fresh water aquatic ecotox.	kg 1,4-DB eq	3.45E+09	6.97E+07	4.56E+07	2.24E+07	1.78E+06	7.16E+07	4.56E+07	2.24E+07	3.62E+06	7.34E+07	4.56E+07	2.24E+07	
Marine aquatic ecotoxicity	kg 1,4-DB eq	1.18E+13	1.73E+11	1.30E+11	3.84E+10	4.36E+09	1.78E+11	1.30E+11	3.84E+10	8.84E+09	1.82E+11	1.30E+11	3.84E+10	
Terrestrial ecotoxicity	kg 1,4-DB eq	48265966	1.09E+06	6.16E+05	4.51E+05	2.51E+04	1.12E+06	6.16E+05	4.51E+05	5.06E+04	1.14E+06	6.16E+05	4.51E+05	
Photochemical oxidation	kg C2H4 eq	1013942	1.47E+05	1.23E+05	1.52E+04	8.88E+03	1.56E+05	1.23E+05	1.52E+04	1.76E+04	1.65E+05	1.23E+05	1.52E+04	
Acidification	kg SO2 eq	21565593	2.48E+06	2.07E+06	1.60E+05	2.51E+05	2.72E+06	2.07E+06	1.60E+05	4.97E+05	2.98E+06	2.07E+06	1.60E+05	

Eutrophication	kg PO4--- eq	22269855	5.63E+05	4.31E+05	7.42E+04	5.82E+04	6.20E+05	4.31E+05	7.42E+04	1.15E+05	6.79E+05	4.31E+05	7.42E+04

Table XI-7 - Results for NGPP for approach 'cradle to grave' using Norwegian grid and considering onshore injection.

NGPP - NO grid (onshore)			800 m of injection				1650 m of injection				2500 m of injection		
Categoria de impacte	Unidade	Totalt	Electricity_CPP_capture_operation w/o compensation	Transport of hyrates by pipeline (CPP)	Injection on+off, h=800 (coal)	Totalt	Electricity_CPP_capture_operation w/o compensation	Transport of hyrates by pipeline (CPP)	Injection on+off, h=1650 (coal)	Totalt	Electricity_CPP_capture_operation w/o compensation	Transport of hyrates by pipeline (CPP)	Injection on+off, h=2500 (coal)
Abiotic depletion	kg Sb eq	3645.769	245.5579	189.978	27.04677	28.53308	282.601562	189.978	27.04677	65.57676	316.2841	189.978041	27.04677
Abiotic depletion (fossil fuels)	MJ	1.12E+11	6.37E+10	6.36E+10	1.34E+08	31068930	6.3797E+10	6.36E+10	1.34E+08	93239240	6.38E+10	6.357E+10	1.34E+08
Global warming (GWP100a)	kg CO2 eq	-5.4E+09	-2.3E+09	-2.3E+09	722127.4	2836917	-2236194613	-2.3E+09	722127.4	2078451	-2.2E+09	-2257701251	722127.4
Ozone layer depletion (ODP)	kg CFC-11 eq	185.6781	162.5576	161.7978	0.509741	0.250044	162.865668	161.7978	0.509741	0.558127	163.1525	161.7978	0.509741
Human toxicity	kg 1,4-DB eq	3.55E+09	84741879	74743173	7572345	2426361	87441352.3	74743173	7572345	5125834	90079461	74743173.2	7572345
Fresh water aquatic ecotox.	kg 1,4-DB eq	3.45E+09	49458512	45558812	2789114	1110586	50654706.7	45558812	2789114	2306781	51842440	45558812	2789114
Marine aquatic ecotoxicity	kg 1,4-DB eq	1.18E+13	1.37E+11	1.3E+11	4.23E+09	2.38E+09	1.3979E+11	1.3E+11	4.23E+09	5.08E+09	1.42E+11	1.3047E+11	4.23E+09
Terrestrial ecotoxicity	kg 1,4-DB eq	48265966	669359.6	616450.9	41275.61	11633.06	685824.859	616450.9	41275.61	28098.35	700241.1	616450.897	41275.61

Photochemical oxidation	kg C2H4 eq	1013942	125504.2	122874.6	1487.633	1141.97	127350.072	122874.6	1487.633	2987.823	128880.5	122874.616	1487.633
Acidification	kg SO2 eq	21565593	2103614	206714	20578.74	15888.81	2129428.1	206714	20578.74	41703.17	2150787	2067146.19	20578.74
Eutrophication	kg PO4--- eq	22269855	444049.3	430782	8012.154	5255.088	451176.459	430782	8012.154	12382.27	457532.8	430782.033	8012.154

Table XI-8 - Results for NGPP for approach 'cradle to grave' using Portuguese grid and considering offshore injection.

NGPP - PT grid (offshore)			800 m of injection				1650 m of injection				2500 m of injection		
Categoria de impacte	Unidade	Totalt	Electricity_CPP_capture_operation w/o compensation	Transport of hyrates by pipeline (CPP)	Injection on+off, h=800 (coal)	Totalt	Electricity_CPP_capture_operation w/o compensation	Transport of hyrates by pipeline (CPP)	Injection on+off, h=1650 (coal)	Totalt	Electricity_CPP_capture_operation w/o compensation	Transport of hyrates by pipeline (CPP)	Injection on+off, h=2500 (coal)
Abiotic depletion	kg Sb eq	3645.769	8	1.90E+02	1.07E+02	3.46E+01	3.68E+02	1.90E+02	1.07E+02	7.12E+01	4.05E+02	1.90E+02	1.07E+02
Abiotic depletion (fossil fuels)	MJ	1.12E+11	6.48E+10	6.36E+10	8.63E+08	3.61E+08	6.51E+10	6.36E+10	8.63E+08	7.14E+08	6.55E+10	6.36E+10	8.63E+08
Global warming (GWP100a)	kg CO2 eq	-5.4E+09	-2.18E+09	-2.26E+09	5.05E+07	2.56E+07	-2.16E+09	-2.26E+09	5.05E+07	5.08E+07	-2.13E+09	-2.26E+09	5.05E+07
Ozone layer depletion (ODP)	kg CFC-11 eq	185.6781	1.69E+02	1.62E+02	4.02E+00	3.08E+00	1.72E+02	1.62E+02	4.02E+00	6.10E+00	1.75E+02	1.62E+02	4.02E+00
Human toxicity	kg 1,4-DB eq	3.55E+09	1.08E+08	7.47E+07	2.88E+07	4.40E+06	1.12E+08	7.47E+07	2.88E+07	8.93E+06	1.17E+08	7.47E+07	2.88E+07
Fresh water aquatic ecotox.	kg 1,4-DB eq	3.45E+09	7.33E+07	4.56E+07	2.60E+07	1.78E+06	7.52E+07	4.56E+07	2.60E+07	3.62E+06	7.71E+07	4.56E+07	2.60E+07

Marine aquatic ecotoxicity	kg 1,4-DB eq	1.18E+13	1.95E+11	1.30E+11	6.00E+10	4.36E+09	1.99E+11	1.30E+11	6.00E+10	8.84E+09	2.04E+11	1.30E+11	6.00E+10
Terrestrial ecotoxicity	kg 1,4-DB eq	48265966	1.11E+06	6.16E+05	4.70E+05	2.51E+04	1.14E+06	6.16E+05	4.70E+05	5.06E+04	1.16E+06	6.16E+05	4.70E+05
Photochemical oxidation	kg C2H4 eq	1013942	1.53E+05	1.23E+05	2.13E+04	8.88E+03	1.62E+05	1.23E+05	2.13E+04	1.76E+04	1.71E+05	1.23E+05	2.13E+04
Acidification	kg SO2 eq	21565593	2.64E+06	2.07E+06	3.26E+05	2.51E+05	2.89E+06	2.07E+06	3.26E+05	4.97E+05	3.14E+06	2.07E+06	3.26E+05
Eutrophication	kg PO4--- eq	22269855	5.91E+05	4.31E+05	1.02E+05	5.82E+04	6.48E+05	4.31E+05	1.02E+05	1.15E+05	7.07E+05	4.31E+05	1.02E+05

Table XI-9- Results for NGPP for approach 'cradle to grave' using Portuguese grid and considering onshore injection.

NGPP - PT grid (onshore)			800 m of injection				1650 m of injection				2500 m of injection		
Categoria de impacte	Unidade	Totalt	Electricity_CPP_capture_operation w/o compensation	Transport of hyrates by pipeline (CPP)	Injection on+off, h=800 (coal)	Totalt	Electricity_CPP_capture_operation w/o compensation	Transport of hyrates by pipeline (CPP)	Injection on+off, h=1650 (coal)	Totalt	Electricity_CPP_capture_operation w/o compensation	Transport of hyrates by pipeline (CPP)	Injection on+off, h=2500 (coal)
Abiotic depletion	kg Sb eq	3645.769	245.5546	189.978	27.04677	28.52976	277.6164261	189.978	27.04677	60.59162	308.797	189.9780408	27.04677
Abiotic depletion (fossil fuels)	MJ	1.12E+11	6.37E+10	6.36E+10	1.34E+08	318046 79	64903503613	6.36E+10	1.34E+08	1.2E+09	6.55E+10	63569502576	1.34E+08
Global warming (GWP100a)	kg CO2 eq	-5.4E+09	-2.3E+09	-2.3E+09	722128.4	289912 4	-2142625085	-2.3E+09	722127.4	1.14E+08	-2.1E+09	-2257701251	722128.4
Ozone layer depletion (ODP)	kg CFC-11 eq	185.6781	162.558	161.7978	0.509741	0.250466	163.4994025	161.7978	0.509741	1.191861	164.1043	161.7978002	0.509741
Human toxicity	kg 1,4-DB eq	3.55E+09	84749602	74743173	7572345	243408 4	99058625.64	74743173	7572345	16743108	1.08E+08	74743173.19	7572345

Fresh water aquatic ecotox.	kg 1,4-DB eq	3.45E+09	49458571	45558812	2789114	1110645	50742583.45	45558812	2789114	2394657	51974421	45558812.03	2789114	
Marine aquatic ecotoxicity	kg 1,4-DB eq	1.18E+13	1.37E+11	1.3E+11	4.23E+09	2.46E+09	2.45724E+11	1.3E+11	4.23E+09	1.11E+11	3.02E+11	1.30473E+11	4.23E+09	
Terrestrial ecotoxicity	kg 1,4-DB eq	48265966	669398.9	616450.9	41275.61	11672.41	745011.8138	616450.9	41275.61	87285.31	789133.5	616450.8966	41275.61	
Photochemical oxidation	kg C2H4 eq	1013942	125532	122874.6	1487.633	1169.709	169073.4719	122874.6	1487.633	44711.22	191544.5	122874.6161	1487.633	
Acidification	kg SO2 eq	21565593	2104136	206714 6	20578.75	16411.31	2915350.529	206714 6	20578.74	827625.6	3331157	2067146.192	20578.75	
Eutrophication	kg PO4--- eq	22269855	444074.9	430782	8012.155	5280.71	489715.5287	430782	8012.154	50921.34	515414.3	430782.033	8012.155	

Table XI-10 - Results for NGPP for approach 'cradle to grave' for scenarios with bulk ship transportation.

NGPP			Ship without cooling (1650 m)				Ship with cooling system (1650 m)			
Categoria de impacte	Unidade	TotalI	Electricity_CPP_capture_operation w/o compensation	Transport of hyrates by pipeline (CPP)	Injection on+off, h=800 (coal)	TotalI	Electricity_CPP_capture_operation w/o compensation	Transport of hyrates by pipeline (CPP)	Injection on+off, h=1650 (coal)	TotalI
Abiotic depletion	kg Sb eq	3645.769	445983.1	189.978	16.74594	445705.1	71.22013	331.8597	189.978	16.74594
Abiotic depletion (fossil fuels)	MJ	1.12E+11	9.87E+11	6.36E+10	30838501	9.23E+11	7.14E+08	8.33E+10	6.36E+10	30838501
Global warming (GWP100a)	kg CO2 eq	-5.4E+09	6.18E+10	-2.3E+09	2332483	6.4E+10	50813506	-6.7E+08	-2.3E+09	2332483
Ozone layer depletion (ODP)	kg CFC-11 eq	185.6781	19778.68	161.7978	0.183776	19610.6	6.097927	170.6017	161.7978	0.183776
Human toxicity	kg 1,4-DB eq	3.55E+09	1.3E+10	74743173	4670438	1.29E+10	8931142	1.46E+08	74743173	4670438
Fresh water aquatic ecotox.	kg 1,4-DB eq	3.45E+09	7.43E+09	45558812	1705236	7.38E+09	3622211	51579612	45558812	1705236

Marine aquatic ecotoxicity	kg 1,4-DB eq	1.18E+13	4.04E+13	1.3E+11	2.54E+09	4.02E+13	8.84E+09	1.6E+11	1.3E+11	2.54E+09
Terrestrial ecotoxicity	kg 1,4-DB eq	48265966	64165594	616450.9	25283.62	63473257	50603.03	752530.9	616450.9	25283.62
Photochemical oxidation	kg C2H4 eq	1013942	23455134	122874.6	827.3892	23313820	17612.14	2620462	122874.6	827.3892
Acidification	kg SO2 eq	21565593	6.56E+08	2067146	11139.33	6.54E+08	496890.2	53182783	2067146	11139.33
Eutrophication	kg PO4--- eq	22269855	1.44E+08	430782	4648.662	1.44E+08	115110.5	5347956	430782	4648.662

Table XI-11 - NGPP: Sensitivity analysis to the utilization rate of the power plant.

Categoria de impacte	Unidade	Av. (16-18) -20%	Av. (16-18)	Av. (16-18) +20%	Av. (16-18) +40%	Av. (16-18) +60%	Av. (16-18) +80%	Av. (16-18) +100%	Av. (16-18) +200%
Abiotic depletion	kg Sb eq	8.23E+01	8.78E+01	9.65E+01	1.04E+02	1.12E+02	1.19E+02	1.27E+02	1.65E+02
Abiotic depletion (fossil fuels)	MJ	1.41E+10	1.76E+10	2.10E+10	2.45E+10	2.79E+10	3.14E+10	3.48E+10	5.21E+10
Global warming (GWP100a)	kg CO2 eq	-4.83E+08	-6.07E+08	-7.30E+08	-8.54E+08	-9.78E+08	-1.10E+09	-1.23E+09	-1.84E+09
Ozone layer depletion (ODP)	kg CFC-11 eq	3.57E+01	4.45E+01	5.33E+01	6.21E+01	7.09E+01	7.97E+01	8.85E+01	1.32E+02
Human toxicity	kg 1,4-DB eq	2.10E+07	2.44E+07	2.84E+07	3.21E+07	3.59E+07	3.97E+07	4.34E+07	6.22E+07
Fresh water aquatic ecotox.	kg 1,4-DB eq	1.24E+07	1.44E+07	1.69E+07	1.92E+07	2.15E+07	2.39E+07	2.62E+07	3.78E+07
Marine aquatic ecotoxicity	kg 1,4-DB eq	3.78E+10	4.33E+10	5.03E+10	5.68E+10	6.34E+10	6.99E+10	7.64E+10	1.09E+11
Terrestrial ecotoxicity	kg 1,4-DB eq	1.48E+05	1.79E+05	2.13E+05	2.45E+05	2.78E+05	3.11E+05	3.44E+05	5.07E+05
Photochemical oxidation	kg C2H4 eq	2.95E+04	3.59E+04	4.25E+04	4.90E+04	5.55E+04	6.21E+04	6.86E+04	1.01E+05
Acidification	kg SO2 eq	4.92E+05	5.98E+05	7.10E+05	8.20E+05	9.30E+05	1.04E+06	1.15E+06	1.70E+06
Eutrophication	kg PO4--- eq	9.91E+04	1.18E+05	1.40E+05	1.61E+05	1.82E+05	2.03E+05	2.24E+05	3.39E+05

Table XI-12 - Results of Monte Carlo Simulations for NGPP scenario with pipeline transportation and offshore storage at 1650 m.

Categoria de impacte	Unidade	Média	Mediana	SD	CV	2,5%	97,5%	SEM
Abiotic depletion	kg Sb eq	366.9727	358.344	52.63754	14.34372	286.8946	497.4126	1.664545
Abiotic depletion (fossil fuels)	MJ	6.52E+10	6.52E+10	2.1E+09	3.226529	6.14E+10	6.94E+10	66553994
Acidification	kg SO2 eq	2898498	2790492	368156.7	12.70164	2498407	3859279	11642.14
Eutrophication	kg PO4--- eq	650922.8	624912.3	102950.8	15.81612	533859.3	908654.6	3255.589
Fresh water aquatic ecotox.	kg 1,4-DB eq	75287331	74057232	8271615	10.98673	62412134	95320665	261571.4
Global warming (GWP100a)	kg CO2 eq	-2.2E+09	-2.2E+09	26077862	-1.21034	-2.2E+09	-2.1E+09	824654.4
Human toxicity	kg 1,4-DB eq	1.13E+08	1.12E+08	7915617	7.018467	99291873	1.31E+08	250313.8
Marine aquatic ecotoxicity	kg 1,4-DB eq	2E+11	1.98E+11	1.55E+10	7.735432	1.74E+11	2.35E+11	4.89E+08
Ozone layer depletion (ODP)	kg CFC-11 eq	172.1025	172.0097	10.0598	5.845234	152.8379	192.6774	0.318119
Photochemical oxidation	kg C2H4 eq	162457	159397.6	12723.84	7.83213	145862	194985.5	402.3633
Terrestrial ecotoxicity	kg 1,4-DB eq	1147862	1061602	303581	26.4475	858371.6	1958357	9600.073